The Effects of Physical Activity on Hip Development

A dissertation submitted to the University of Oxford in partial fulfilment of the requirements for the degree of

Doctor of Philosophy in Musculoskeletal Sciences

Scott James Fernquest

Worcester College

2019

Abstract

In recent decades the sports opportunities available to young athletes has risen significantly. The effect of such high levels of physical exertion on the developing skeleton is largely unknown. Retired football players have significantly greater rates of hip osteoarthritis than control groups, and a higher prevalence of morphological abnormalities known to predispose to future osteoarthritis, such as cam morphology, acetabular dysplasia and retroversion, and varus leg alignment. Cam morphology is likely acquired during adolescence, and dysplasia and leg alignment develop from birth throughout childhood and adolescence. High activity is a recognised risk factor for the development of these morphologies. However, their aetiology is insufficiently understood to recommend intervention. The aim of this thesis is to explore the impact of high levels of activity during adolescence on the development of the skeletally immature hip and knee. This is achieved via a longitudinal prospective observational cohort study in elite level footballers and age matched controls age 9-18 years.

The first three studies in this thesis investigate the effect of activity on hip morphology and leg alignment. The results provide strong evidence that elite level football and high activity during adolescence significantly influences skeletal development in these areas. High activity individuals are more likely to develop cam morphology, dysplastic and retroverted acetabula, and varus leg alignment. The most significant effects appear to occur between 11 and 14 years of age. At present, it is not possible to recommend intervention such as activity modification due to our limited understanding of aetiology, and the cardiovascular benefits of exercise are likely to outweigh potentially detrimental effects on morphology. However, high activity individuals between the ages of 11 and 14 years likely represent a high-risk cohort warranting surveillance for early joint failure.

The effect of exercise on cartilage in weight bearing joints in young healthy individuals is poorly understood. The final study in this thesis uses compositional MRI to determine the effect of high activity on cartilage composition during youth. The results suggest that elite level footballers and individuals with high activity levels may have differing cartilage composition and architecture to low activity individuals during adolescence.

Funding Bodies

NIHR Oxford Biomedical Research Unit

Osteoarthritis Research UK

Acknowledgements

I would like to dedicate this thesis to my parents. Without their lifelong inspiration, significant sacrifices, and endurance of financial hardships my higher education journey would not have been possible. I would also like to express the deepest gratitude to my significant other for her unwavering support during long evenings spent in the MRI scanning suite and ability to create culinary masterpieces without her sous chef.

A sincerest thank you is offered to my supervisor Professor Sion Glyn-Jones for his comprehensive and invaluable academic support. To my other supervisor Mr Antony Palmer, whose mentorship and guidance has profoundly impacted my life and career for almost a decade, I can only apologise for being a constant drain on your limited reserves. An unpayable debt will always be owed to Mr Joseph Ryan for teaching a seventeen year old state school student from South Wales an invaluable lesson in 'why not?'

This thesis would not have been possible without the kind support of Southampton Football Club, and in particular Mo Gimpel and Richard Birchall. I would also like to thank all of the research volunteers and their families for sacrificing their time to participate in these studies. A number of colleagues dedicated vast amounts of their resources and energy to ensure the success of these research projects. The generosity of time displayed by Claudio Pereira was a constant source of amazement and I often reflect on his impeccable bedside manner.

Finally, I hugely value all of the friendships I have been fortunate to develop during my research. These colleagues made it a pleasure to work in the Botnar Research Centre.

Abbreviations

Aa	Anterior Acetabular Cartilage
Af	Anterior Femoral Cartilage
ALDFA	Anatomical Lateral Distal Femoral Angle
ALDTA	Anatomical Lateral Distal Tibial Angle
AMPTA	Anatomical Medial Proximal Tibial Angle
AOR	Anterior Offset Ratio
AP	Anteroposterior
ASa	AnteroSuperior Acetabular Cartilage
ASf	AnteroSuperior Femoral Cartilage
AUC	Area Under the Curve
BMI	Body Mass Index
CEA	Centre Edge Angle
CT	Computerised Tomography
dGEMRIC	Delayed Gadolinium Enhanced MRI of Cartilage
FABER	Flexion Abduction External Rotation
FADIR	Flexion Adduction Internal Rotation
FAI	Femoroacetabular Impingement
FAIM	Femoroacetabular Impingement MRI Study
FTA	Fibrochondroosseous Tissue Area
HKA	Hip Knee Angle
HTE	Horizontal Toit Externe

ICC	Intra/Inter Class Correlation
JLCA	Joint Line Congruence Angle
LPFA	Lateral Proximal Femoral Angle
LDFPhyA	Lateral Distal Femoral Physis Angle
MLDFA	Mechanical Lateral Distal Femoral Angle (mLDFA)
MLDTA	Mechanical Lateral Distal Tibial Angle
MMPTA	Mechanical Medial Proximal Tibial Angle
MNSA	Mean Neck Shaft Angle
MPFA	Medial Proximal Femoral Angle
MPTPhyA	Medial Proximal Tibial Physis Angle
MRI	Magnetic Resonance Imaging
NICE	National Institute for Health and Care Excellence
OA	Osteoarthritis
Pa	Posterior Acetabular Cartilage
PAQ-A	Physical Activity Questionnaire for Adolescents
PAQ-C	Physical Activity Questionnaire for Children
PDFS	Proton Density Fat Saturation
Pf	Posterior Femoral Cartilage
PROMS	Patient Reported Outcome Measures
PSa	PosteroSuperior Acetabular Cartilage
PSF	PosteroSuperior Femoral Cartilage
RCT	Randomised Controlled Trial
ROC	Receiver Operating Characteristic

ROI	Region of Interest
SAa	SuperoAnterior Acetabular Cartilage
SAf	SuperoAnterior Femoral Cartilage
SD	Standard Deviation
SDD	Smallest Detectable Difference
Spa	SuperoPosterior Acetabular Cartilage
SPf	SuperoPosterior Femoral Cartilage
SUFE	Slipped Upper Femoral Epiphysis
TE	Echo Time
TR	Repetition Time
TSE	Turbo Spin Echo
WATSf	Water Selective (fluid)
WAVE	Water Selective Volume Excitation
WBR	Weight Bearing Ratio

Contents

Thesis Summary **24**

Chapter 1 Introduction and Literature Review **28**

1.1 Current Clinical Challenges **28**

1.2 Scope of Thesis **31**

1.3 Bone Development **32**

1.3.1 Long bones 32

1.3.2 Acetabulum 34

1.3.3 Factors Influencing Bone Development 37

1.3.4 Disorders of Bone Development 38

1.4 Effect of Physical Activity on Bone Development **61**

1.4.1 Effect of Physical Activity on the Proximal Femoral Physis: Cam Morphology 63

1.4.2 Effect of Physical Activity on the Acetabulum: Dysplasia and Retroversion 67

1.4.3 Effect of Physical Activity on Leg Alignment: Genu Varum 68

1.5 Cartilage Composition Development **73**

1.5.1 Cartilage Composition During Adolescence 73

1.5.2 Cartilage Composition 73

1.5.3 Evaluating Cartilage Composition 74

1.5.4 Effect of Activity on Cartilage Composition 76

1.6 Remaining Areas of Uncertainty **79**

1.7 Conclusions **86**

1.8 Thesis Aims and Objectives 88

Chapter 2 Methods: Femoroacetabular Impingement MRI Study (FAIM) 91

2.1 Abstract 91

2.2 Introduction 93

2.3 Aims 94

2.4 Ethical Approval 95

2.5 Study Design 95

2.5.1 Sample Age and Sex 95

2.5.2 Sample Size 96

2.5.3 Study Population 97

2.5.4 Inclusion and Exclusion Criteria 99

2.5.5 Baseline Recruitment 99

2.5.6 Patient and Public Involvement 101

2.5.7 Follow-up Recruitment 102

2.6 Questionnaire 104

2.6.1 Patient Demographics and Past Medical History 104

2.6.2 Activity Levels 105

2.7 Imaging Measures 106

2.7.1 Assessment of Femoral Head Morphology 106

2.7.2 Assessment of Acetabular Morphology 123

2.7.3 Assessment of Leg Alignment Morphology 137

2.7.4 Assessment of Cartilage Composition 148

2.8 MRI Protocol 151

2.8.1 3D Water Selective Fluid (WATSf) 151

2.8.2 3D Proton Density Fat Saturation (PDFS) 151

2.8.3 Water Selective Volume Excitation (WAVE) 152
2.8.4 Stacked T1 Weighted Turbo Spin Echo (TSE) Coronal Pelvis 152
2.8.5 T2 mapping 153
2.9 Reproducibility Studies of Imaging Measures 154
2.10 Cohort Characteristics 161
2.10.1 Activity Levels 164
2.10.2 BMI 166
2.10.3 Physeal Development 168
2.11 Statistical Analysis and Data Diagnostics 173
2.12 Discussion 174
2.13 Acknowledgement 178
Chapter 3 Femoral Head Morphology in Adolescence and the Effects of Activity 179
3.1 Abstract 179
3.2 Introduction 181
3.3 Aims 182
3.4 Methods 183
3.4.1 Study design 183
3.4.2 Population 183
3.4.3 Activity Levels 185
3.4.4 Imaging Protocol 185
3.4.5 Imaging Measures 186
3.4.6 Statistical Analysis 189
3.5 Results 191
3.5.1 Participant demographics 191

3.5.2 Risk Factors for Cam Development 193
3.5.3 Age of Cam Development 197
3.5.4 Location of Cam Development 202
3.5.5 Location of Cam Development 204
3.5.6 Predicting Cam Development 207
3.6 Discussion 212
3.6.1 Individuals at Risk of Cam Development 212
3.6.2 Age of Cam Development 213
3.6.3 Mechanism of Cam Development 214
3.6.4 Predicting Cam Development 215
3.6.5 Limitations 216
3.6.6 Conclusion 217
Chapter 4 Acetabular Morphology in Adolescence and the Effects of Activity 218
4.1 Abstract 218
4.2 Introduction 220
4.3 Aims 221
4.4 Methods 222
4.4.1 Study design 222
4.4.2 Population 222
4.4.3 Activity Levels 224
4.4.4 Imaging Protocol 224
4.4.5 Imaging Measures 225
4.5 Results 229
4.5.1 Participant demographics 229

4.5.2 Change in Acetabular Morphology with Age 230
4.5.3 Risk Factors for Abnormal Acetabular Morphology Development 242
4.5.4 Relationship Between Femoral and Acetabular Morphology 246
4.5.5 Predicting Abnormal Acetabular Morphology 247
4.6 Discussion 249
4.6.1 Change in Acetabular Morphology with Age 249
4.6.2 Risk Factors for Abnormal Acetabular Morphology 250
4.6.3 Effect of Femoral Morphology on Acetabular Morphology 252
4.6.4 Predicting Abnormal Acetabular Morphology 253
4.6.5 Limitations 253
4.6.6 Conclusion 254
Chapter 5 Leg Alignment in Adolescence and the Effects of Activity 255
5.1 Abstract 255
5.2 Introduction 257
5.3 Aims 258
5.4 Methods 259
5.4.1 Study design 259
5.4.2 Population 259
5.4.3 Activity Levels 261
5.4.4 Imaging Protocol 261
5.4.5 Imaging Measures 262
5.4.6 Statistical Analysis 266
5.5 Results 267
5.5.1 Participant demographics 267
5.5.2 Change in Leg Alignment with Age 268

5.5.3 Risk Factors for Varus Leg Alignment 275
5.5.4 Anatomical Associations with Varus Leg Alignment 278
5.5.5 Mechanism of Varus Knee Morphology Formation 281
5.5.6 Predicting Varus Leg Alignment 282
5.6 Discussion 283
5.6.1 Change in Leg Alignment with Age 283
5.6.2 Risk Factors for Varus Leg Alignment 284
5.6.3 Effect of Femoral Morphology on Leg Alignment 286
5.6.4 Mechanism of Varus Leg Alignment Development 287
5.6.5 Predicting Varus Leg Alignment 287
5.6.6 Limitations 288
5.6.7 Conclusion 288
Chapter 6 Cartilage Composition in Adolescence and the Effects of Activity 289
6.1 Abstract 289
6.2 Introduction 292
6.3 Aims 294
6.4 Methods 295
6.4.1 Study design 295
6.4.2 Population 295
6.4.3 Activity Levels 295
6.4.4 Imaging Protocol 297
6.4.5 Imaging Measures 297
6.4.6 Statistical Analysis 299
6.5 Results 300

6.5.1 Participant Demographics 300
6.5.2 Change in Cartilage Compositional with Age 301
6.5.3 Factors Affecting Cartilage Composition 309
6.5.4 Effect of Cam Morphology on Cartilage Composition 313
6.6 Discussion 314
6.6.1 Change in Cartilage Composition with Age 314
6.6.2 Factors Affecting Cartilage Composition 315
6.6.3 Effect of Cam Morphology on Cartilage Composition 317
6.6.4 Limitations 318
6.6.5 Conclusion 318
Chapter 7 Conclusions 319
7.1 Summary of Findings 319
7.2 Future Directions 328
7.2.1 Female athletes 328
7.2.2 The role of the Fibrochondroosseous Tissue Area 329
7.2.3 The mechanism of acetabular dysplasia formation 332
7.2.4 The mechanism of varus leg formation 333
7.2.5 Understanding compositional MRI values 334
7.2.6 Intervention 334
Bibliography 337

Figures

Figure 1-1 - Epiphyseal Cartilage, Articular cartilage, and Fibrochondroosseous Tissue in an 11 Year Old Elite Male Footballer....33

Figure 1-2 - Triradiate Cartilage at the Base of the Acetabulum in a 10 Year Old Elite Male Footballer. Axial Oblique View....35

Figure 1-3 - Triradiate Cartilage in a 10 Year Old Elite Male Footballer. Coronal View. 36

Figure 1-4 - MRI radial slices of a normal hip (A), a hip with cam morphology (B), and a hip with pincer morphology (C)....40

Figure 1-5 - 3D reconstructed models from a 4D dynamic hip CT scan in an individual with cam-type FAI showing the patient at rest (A) and impinging within a functional range of flexion (B). 41

Figure 1-6 - Anteroposterior radiograph of a hip with cam morphology (white arrow) and evidence of osteoarthritis (red arrow).....42

Figure 1-7 - Elite level football player age 11 years at baseline with soft tissue hypertrophy at the femoral head-neck junction (A) which preceded lateral epiphyseal extension and osseous cam morphology seen at follow-up aged 14 years (B)....45

Figure 1-8 - Anteroposterior radiograph of a hip with a normal femoral head coverage (A), and a hip with a reduced femoral head coverage showing evidence of mild dysplasia (B). 48

Figure 1-9 - Full leg length MRI scans in adolescent males showing varus leg alignment (A) and valgus leg alignment (B). Coronal view....56

Figure 1-10 - Development of the tibiofemoral angle in children during growth. 57

Figure 1-11 - Sagittal Compositional MRI Map of a Male Footballer....75

Figure 2-1: Anteroposterior radiographs with alpha angle measurement of a hip with normal morphology (A) and cam morphology (B)....107

Figure 2-2: Anteroposterior radiographs with triangular index ratio measurement of a hip with normal morphology (A) and cam morphology (B)....108

Figure 2-3: Anteroposterior radiographs with anterior offset ratio measurement of a hip with normal morphology (A) and cam morphology (B)....110

Figure 2-4: Superoanterior radial MRI planes in a participant with normal hip morphology (A-D) and cam morphology (E-F): 12 o'clock (A&E), 1 o'clock (B&F), 2 o'clock (C&G), and 3 o'clock (D&H). 113

Figure 2-5: Bone (A) and cartilage (B) alpha angle measurements at 3 o'clock in a ten year old male. 116
Figure 2-6: Lateral epiphyseal extension measurements at 1 o'clock position. 117
Figure 2-7: Appearances of an Open, Partially Closed, and Closed Physis on WATSf MRI Sequence 119
Figure 2-8: MRI radial slice in 12 year old male with significant fibrochondrooseous tissue hypertrophy at the femoral head-neck junction. Measurement of the alpha angle fails to account for the tissue mass. 120
Figure 2-9: Area of fibro-chondro-osseous tissue shown in an elite level football player at baseline age 12 years (A), with hierarchical partitioned terrain map overlaying the radial image (B) and user selection of the Fibrochondroosseous Tissue Area (C), and new bony cam morphology at follow-up age 15 years (D) 122
Figure 2-10: Anteroposterior radiographs with lateral centre edge angle measurement of a hip with normal morphology (A) and dysplasia (B) 124
Figure 2-11: Lateral radiographs with anterior Centre Edge Angle (CEA) measurement of a hip with normal morphology 125
Figure 2-12: Anteroposterior radiographs with femoral head extrusion index measurement of a hip with normal morphology (A) and dysplasia (B).....127
Figure 2-13: Anteroposterior radiographs with Horizontal Toit Externe angle measurement of a hip with normal morphology (A) and dysplasia (B).....128
Figure 2-14: Anteroposterior radiographs with acetabular index of depth to width measurement of a hip with normal morphology (A) and dysplasia (B).....129
Figure 2-15: Anteroposterior radiographs with normal acetabulum in anteversion (A) and acetabulum displaying cross-over sign suggesting retroversion (B).....133
Figure 2-16: Axial slice through a CT scan of the pelvis at the centre of the hip joint showing measurement of acetabular anteversion. The reference line is formed between the femoral head centres. 135
Figure 2-17: Full leg length weight bearing MRI of a 16 year old male showing Hip-Knee-Angle (HKA) and Weight-Bearing-Ratio (WBR) measures.....141
Figure 2-18: Full leg length weight bearing MRI of a 16 year old male showing Mean Neck Shaft Angle (MNSA), Medial Proximal Femoral Angle (MPFA), Lateral Proximal Femoral Angle (LPFA), Mechanical Lateral Distal Femoral Angle (mLDFA), Anatomical Lateral Distal Femoral Angle (aLDFA), Mechanical Medial Proximal Tibial Angle (mMPTA), Anatomical Medial Proximal Tibial Angle (aMPTA), Mechanical Lateral Distal Tibial Angle (mLDTA), and Anatomical Lateral Distal Tibial Angle (aLDTA) measures.....144

Figure 2-19: Full leg length weight bearing MRI of a16 year old male showing Joint Line Congruence Angle (JLCA), Medial Proximal Tibial Physis Angle (MPTPhyA), and Lateral Distal Femoral Physis Angle (LDFPhyA) measures. 146
Figure 2-20: Geographic Zones of Right Hip. The clockface zones are orientated such that 12 o'clock is the most superior aspect of the acetabulum and the 6 o'clock position represents the middle of the transverse ligament. Modified from Ilizaliturri et al 2008[281] 149
Figure 2-21: Example Regions of Interest (ROI) for T2 Segmentation. 150
Figure 2-22: Recruitment flowchart for study 162
Figure 2-23: Box and Whisker Plot of Physical Activity Questionnaire Score Versus Age at Baseline and Follow-up 165
Figure 2-24: Box and Whisker Plot of Physical Activity Questionnaire Score Versus Cohort at Baseline and Follow-up 165
Figure 2-25: Box and Whisker Plot of Body Mass Index Versus Age at Baseline and Follow-up 167
Figure 2-26: Box and Whisker Plot of Body Mass Index Versus Cohort at Baseline and Follow-up 167
Figure 2-27: Stage of Physeal Development at Baseline in Each Age group for Male Footballers 170
Figure 2-28: Stage of Physeal Development at Follow-up in Each Age group for Male Footballers 170
Figure 2-29: Stage of Physeal Development at Baseline in Each Age group for Male Controls 171
Figure 2-30: Stage of Physeal Development at Follow-up in Each Age group for Male Controls 171
Figure 2-31: Stage of Physeal Development at Baseline in Each Age group for Female Controls 172
Figure 2-32: Stage of Physeal Development at Follow-up in Each Age group for Female Controls 172
Figure 3-1 – Recruitment flowchart for study. 184
Figure 3-2 – Alpha angle in an elite level football player at baseline age 11 years (A) and at follow-up age 14 years (B). Change in alpha angle = 40 degrees. 186
Figure 3-3 – Lateral epiphyseal extension measurements at 1 o'clock position. Elite level football player at baseline aged 11 years with normal morphology (A) and at follow-up age 14 years (B). Change in lateral epiphyseal extension = 0.26 187
Figure 3-4 – Area of Fibrochondroosseous Tissue shown in an elite level football player at baseline age 12 years (A), with hierarchical partitioned terrain map overlaying the radial image and user selection of the Fibrochondroosseous Tissue Area (B). 188
Figure 3-5 – Change in Average Cartilage Alpha Angle in Individuals from the Elite Footballer Cohort, Male Controls, and Female Controls. Box and whisker plot. 193

Figure 3-6 – Change in Average Cartilage Alpha Angle in Individuals with a PAQ Score below 2, 2-3, 3-4, and above 4 at baseline. Box and whisker plot 194
Figure 3-7 – Change in Average Alpha Angle versus PAQ Score. Scatter plot with 95% Confidence Intervals. Coefficient 0.79, $R^2 = 0.62$, p = <0.001 195
Figure 3-8 – Change in average cartilage alpha angle with age for all participants. Age groups based on chronological age of participant at baseline. Box and whisker plot. Dashed line represents the alpha angle inter-observer SDD (4.22 degrees) 197
Figure 3-9 – Change in average cartilage alpha angle with age in male footballers. Age groups based on chronological age of participant at baseline. Box and whisker plot. Dashed line represents the alpha angle inter-observer SDD (4.22 degrees) 199
Figure 3-10 – Change in average cartilage alpha angle with age in male controls. Age groups based on chronological age of participant at baseline. Box and whisker plot. Dashed line represents the alpha angle inter-observer SDD (4.22 degrees) 199
Figure 3-11 – Change in average cartilage alpha angle with age in female controls. Age groups based on chronological age of participant at baseline. Box and whisker plot. Dashed line represents the alpha angle inter-observer SDD (4.22 degrees) 200
Figure 3-12 – Change in average cartilage alpha angle by physeal maturity. Box and whisker plot. Dashed line represents the alpha angle inter-observer SDD (4.22 degrees) 201
Figure 3-13 – Average Change in Alpha Angle by Position On Femoral Head-Neck Junction. Bar Chart..... 202
Figure 3-14 – Change in Lateral Epiphyseal Extension versus Change in Average Alpha Angle. Scatter plot with 95% Confidence Intervals. Coefficient=0.002, $R^2 = 0.060$, p=0.012 205
Figure 3-15 – Baseline Fibrochondroosseous Tissue Area versus Change in Average Alpha Angle. Scatter plot with 95% Confidence Intervals. Coefficient 4.09, $R^2 = 0.580$, p = 0.003 206
Figure 3-16 – ROC Curve for Examination Measures; Internal Rotation (AUC 0.61), and PAQ Score (AUC 0.62) 208
Figure 3-17 – ROC Curve for Imaging Measures; FTA (AUC 0.83), and average lateral epiphyseal extension (AUC 0.53) 209
Figure 3-18 – ROC Curve for Combined Measures; Baseline Examination Measures (AUC 0.66) and Baseline Imaging measures (AUC 0.84) 210
Figure 3-19 – ROC Curve for Combined Examination and Imaging Measures (AUC 0.85) 211
Figure 4-1 - Recruitment flowchart for study. 223

Figure 4-2 - Coronal Image from WAVE Sequence Illustrating Measurement of Lateral Centre Edge Angle. 225

Figure 4-3 - Sagittal Image from WAVE Sequence Illustrating Measurement of Anterior Centre Edge Angle 226

Figure 4-4 - Axial image from WAVE Sequence Illustrating Measurement of Angle of Anteversion 226

Figure 4-5 - Lateral CEA plotted against age for all participants from baseline and follow-up. Polynomial regression fit with 95% CI 231

Figure 4-6 - Anterior CEA plotted against age for all participants from baseline and follow-up. Polynomial regression fit with 95% CI 231

Figure 4-7 - Angle of anteversion plotted against age for all participants from baseline and follow-up. Polynomial regression fit with 95% CI 232

Figure 4-8 - Change in Lateral CEA with Age in All Individuals. Age groups based on chronological age of participant at baseline. Box and Whisker Plot. 236

Figure 4-9 - Change in Anterior CEA with Age in All Individuals. Age groups based on chronological age of participant at baseline. Box and Whisker Plot. 236

Figure 4-10 - Change in Anteversion with Age in All Individuals. Age groups based on chronological age of participant at baseline. Box and Whisker Plot. 237

Figure 4-11 - Change in Lateral CEA by Skeletal Maturity. Box and whisker plot 239

Figure 4-12 - Change in Anterior CEA by Skeletal Maturity. Box and whisker plot. 240

Figure 4-13 - Change in Anteversion by Skeletal Maturity. Box and whisker plot. 241

Figure 4-14 - Change in Lateral CEA by Cohort. Box and whisker plot. 242

Figure 4-15 - Change in Anterior CEA by cohort. Box and whisker plot. 243

Figure 4-16 - Change in Angle of Anteversion by Cohort. Box and whisker plot. 244

Figure 4-17 - Change in Lateral CEA versus Change in Average Alpha Angle. Scatter plot with 95% Confidence Intervals. Coefficient –0.114, $R^2 = 0.090$, $p = 0.014$ 246

Figure 4-18 - Change in Anterior CEA versus Change in Average Alpha Angle. Scatter plot with 95% Confidence Intervals. Coefficient = - 0.064, $R^2 = 0.020$, $p = 0.316$ 247

Figure 5-1 - Recruitment flowchart for study. 260

Figure 5-2 - Full leg length weight bearing MRI of a 16 year old male showing Hip-Knee-Angle (HKA) and Weight-Bearing-Ratio (WBR) measures. 263

Figure 5-3 - Full leg length weight bearing MRI of a 16 year old male showing Joint Line Congruence Angle (JLCA), Medial Proximal Tibial Physis Angle (MPTPhyA), and Lateral Distal Femoral Physis Angle (LDFPhyA) measures. 264
Figure 5-4 - Full leg length weight bearing MRI of a 16 year old male showing Mean Neck Shaft Angle (MNSA), Medial Proximal Femoral Angle (MPFA), Lateral Proximal Femoral Angle (LPFA), Mechanical Lateral Distal Femoral Angle (mLDFA), Anatomical Lateral Distal Femoral Angle (aLDFA), Mechanical Medial Proximal Tibial Angle (mMPTA), Anatomical Medial Proximal Tibial Angle (aMPTA), Mechanical Lateral Distal Tibial Angle (mLDTA), and Anatomical Lateral Distal Tibial Angle (aLDTA) measures. 265
Figure 5-5 - Hip Knee Angle (HKA) with Age for All Individuals. Age groups based on chronological age of participants at time of MRI scan. Box and whisker plot 270
Figure 5-6 - Hip Knee Angle (HKA) with age for elite footballers, male controls, and female controls. Polynomial regression fit with 95% CI. 272
Figure 5-7 - Hip Knee Angle (HKA) with Age for Male Footballers. Age groups based on chronological age of participants at time of MRI scan. Box and whisker plot 273
Figure 5-8 - Hip Knee Angle by Physeal Maturity. Box and whisker plot 274
Figure 5-9 - Hip Knee Angle by Cohort. Box and whisker plot. 275
Figure 5-10 - Hip Knee Angle in Skeletally Mature Individuals by Cohort. Box and whisker plot 276
Figure 5-11 - Hip Knee Angle Versus PAQ score in Skeletaly Mature Individuals. Linear regression fit with 95% CI 277
Figure 5-12 - Hip Knee Angle versus Weight Bearing Ratio. Linear regression fit with 95% CI 278
Figure 5-13 - Hip Knee Angle versus Medial Proximal Tibial Physis Angle. Linear regression fit with 95% CI 281
Figure 5-14 - ROC Curve for PAQ Score as a Predictor of Varus Leg Alignment (AUC 0.69) 282
Figure 6-1 - Recruitment flowchart for study. 296
Figure 6-2 - Regions of Interest (ROI) for T2 Segmentation. 298
Figure 6-3 – Acetabular Cartilage T2 Values with Age for All Individuals. Age groups based on chronological age of participants at time of MRI scan. Box and whisker plot 303
Figure 6-4 – Femoral Cartilage T2 Values with Age for All Individuals. Age groups based on chronological age of participants at time of MRI scan. Box and whisker plot 303
Figure 6-5 – Acetabular Cartilage T2 Values with Age for Elite Male Footballers. Age groups based on chronological age of participants at time of MRI scan. Box and whisker plot 307

Figure 6-6 – Acetabular Cartilage T2 Values by Physeal Maturity in All Individuals. Box and whisker plot308

Figure 6-7 – Acetabular Cartilage T2 Values by Cohort. Box and whisker plot 309

Figure 6-8 – Femoral Cartilage T2 Values by Gender. Box and whisker plot 310

Figure 6-9 – Acetabular Cartilage T2 Values by PAQ Score. Box and whisker plot 311

Figure 6-10 – Femoral Cartilage T2 Values by PAQ Score. Box and whisker plot 312

Tables

Table 2-1 - FAIM recruitment target at baseline 98

Table 2-2 - Cohort Demographics 163

Table 2-3 - Mean and Standard Deviation of Physical Activity Questionnaire (PAQ) 164

Table 2-4 - Mean and Standard Deviation of Body Mass Index (BMI) 166

Table 2-5 - Stage of Physeal Development by Age Group at Baseline. 168

Table 2-6 - Stage of Physeal Development by Age Group at Follow-up. 169

Table 3-1 - Cohort demographics 191

Table 3-2 - Mean Alpha Angle, Lateral Epiphyseal Extension, and Fibrochondroosseous Tissue Area at Baseline and Follow-up by Cohort and Age Group. 192

Table 3-3 - Predictors of change in average alpha angle. *Age and cohort as covariables. **Age, gender, and Physical Activity Questionnaire as covariables. ***Physeal maturity, gender, and Physical Activity Questionnaire as covariable 196

Table 3-4 - Change in average alpha angle with age by cohort 198

Table 3-5 - Change in alpha angle by position on femoral head-neck axis. *Age as a covariable 203

Table 3-6 - Multivariate regression analysis of lateral epiphyseal extension with alpha angle by position on femoral head-neck axis. Age, gender, and activity level as covariables 204

Table 3-7 - Multivariate regression analysis of Fibrochondroosseous Tissue Area with change in alpha angle by position on femoral head-neck axis. Age, gender, and activity level as covariables 206

Table 3-8 - ROC Area and Cut Off Values for Cam Morphology Development; Internal Rotation, PAQ Score, Fibrochondroosseous Tussie Area, Latersal Epiphyseal Extension, and Combined Variables 208

Table 4-1 - Cohort demographics 229

Table 4-2 - Mean Lateral and Anterior CEA, and Angle of Anteversion at Baseline and Follow-up by Cohort and Age Group. 230

Table 4-3 - Predictors of Change in Lateral CEA. *Age and cohort as covariables. **Age, gender and activity level as covariables. ***Physeal maturity, gender, and activity levels as covariables 233

Table 4-4 - Predictors of Change in Anterior CEA. *Age and cohort as covariables. **Age, gender and activity level as covariables. ***Physeal maturity, gender, and Physical Activity Questionnaire as covariables 234

Table 4-5 - Predictors of Change in Angle of Anteversion. *Age and cohort as covariables. **Age, gender and activity level as covariables. ***Physeal maturity, gender, and Physical Activity Questionnaire as covariables 235
Table 4-6 - Change in acetabular morphology and version with age by cohort. 238
Table 5-1 - Cohort demographics 267
Table 5-2 - Hip Knee Angle, Weight Bearing Ratio, and Medial Proximal Tibial Physeal Angle by Cohort and Age Group. 269
Table 5-3 - Predictors of change in Hip Knee Angle. *Age and cohort as covariables. **Age, gender and activity level as covariables. ***Physeal maturity, gender, and activity levels as covariables 271
Table 5-4 - Hip Knee Angle with Age by Cohort. Univariate Regression. 272
Table 5-5 - Hip Knee Angle Regression Analysis with Measures of Leg Alignment. Multivariate regression adjusting for age, gender and activity level. 280
Table 5-6 - ROC Area and Cut Off Values for Varus Leg Alignment Development; PAQ Score 282
Table 6-1 – Cohort Demographics 300
Table 6-2 – Acetabular Cartilage, Femoral Cartilage, and Anterosuperior Acetabular cartilage T2 Values by Cohort and Age Group. 302
Table 6-3 – Predictors of Acetabular Cartilage Values. *Age and cohort as covariables. **Age, gender and activity level as covariables. ***Physeal maturity, gender, and activity levels as covariables 304
Table 6-4 – Predictors of Femoral Cartilage Values. *Age and cohort as covariables. **Age, gender and activity level as covariables. ***Physeal maturity, gender, and activity levels as covariables 305
Table 6-5 – T2 cartilage value with Age by Cohort. Univariate Regression. 306
Table 6-6 – Effect of Cam Morphology on Anterosuperior Acetabular Cartilage Composition. *Age, gender, and activity level (PAQ Score) as covariables. 313

Thesis Summary

In recent decades the sports opportunities available to young athletes and the general population have risen significantly, with an increasing numbers of sports turning professional. International level of sport requires intense practice for a minimum of 10 years or 10,000 hours. The majority of this practice takes place during adolescence. Bone growth is dependent upon a number of factors, but is highly responsive to mechanical loading during adolescence. The effect of such high levels of physical exertion on the developing skeleton is largely unknown.

Retired football players have significantly greater rates of hip and knee osteoarthritis than control groups, and a higher prevalence of morphological abnormalities known to predispose to future osteoarthritis (OA), such as cam type Femoroacetabular Impingement (FAI) syndrome, acetabular dysplasia and retroversion, and varus leg alignment. These morphologies are believed to develop throughout childhood and during adolescence at around the time of physeal closure. It has been suggested that these abnormal morphologies develop secondary to repetitive trauma to the epiphyseal plate sustained through high activity levels that affects normal endochondral bone formation.

As acquired disorders it may be that these abnormal morphologies are preventable or modifiable. However, their aetiology is insufficiently understood to recommend intervention at this point. Preventative strategies are most likely to be effective when

addressing the underlying disease aetiology through risk factor modification or mitigation of their effect during the period of skeletal maturation of greatest susceptibility. However, contention exists over the age of genesis and risk factor profile for each morphology, and the quantitative impact of high activity levels.

These uncertainties limit the capabilities of clinicians to intervene in or monitor individuals at greatest risk of developing abnormal joint morphology at the necessary age. The cardiovascular benefits of exercise are likely to outweigh potentially detrimental effects on hip morphology. Nevertheless, individuals participating in high-level sports during youth represent a high-risk cohort that warrants further investigation.

The aim of this thesis was to explore the development of the skeletally immature hip, and leg alignment, and determine the impact of high activity levels during adolescence. This was achieved via a longitudinal prospective observational cohort study in elite level footballers and age matched controls age 9-18 years. The main findings of this thesis are:

1. Hip morphology undergoes the greatest change between 11 and 14 years of age.
2. Hip morphology and leg alignment development is significantly affected by elite level sport and high activity levels
3. Hip cartilage composition in adolescence is significantly affected by elite level sport and high activity levels

The first study in this thesis investigated the effect of activity on the development of the femoral head. The results provide strong evidence that high activity during adolescence promotes soft tissue hypertrophy and epiphyseal extension that gives rise to cam morphology. The effect of activity is quantifiable using the Physical Activity Questionnaire (PAQ) Score, with scores above 3 resulting in significantly greater change to femoral head morphology than scores below 3. The greatest change to femoral head morphology occurred in individuals aged 11-12 years, and no significant changes were seen after 14 years of age.

The second study in this thesis investigated the effect of activity on the development of the acetabulum. The results suggest that high activity during adolescence reduces lateral and anterior acetabular growth and anteversion such that elite footballers and individuals with high activity levels have significantly more dysplastic and retroverted acetabula. The greatest changes to lateral and anterior acetabular morphology occurred in individuals aged 11-12 years, and the greatest changes to anteversion occurred in individuals aged 13-14 years. The development of cam morphology appeared to be related to reduced lateral and anterior growth of the acetabulum.

The third study in this thesis investigated the effect of activity on the development of leg alignment. The results suggested that during adolescence leg alignment moves from valgus towards neutral. Elite footballers and individuals with high activity levels however developed varus alignment. The change from valgus to varus alignment appeared to take place age 14 to 15 years and is likely secondary to physiological adaption to load at the medial proximal tibial physis.

The final study in this thesis investigated the effect of activity on cartilage composition in adolescence. The results suggest that elite footballers and individuals with high activity levels have a different acetabular cartilage composition than controls. Cam morphology did not affect cartilage composition during adolescence.

Chapter 1 Introduction and Literature Review

1.1 Current Clinical Challenges

Osteoarthritis (OA) is the most common joint disease worldwide affecting an estimated 10% of males and 18% of females over 60 years of age[1]. OA treatment primarily consists of pain management in the early stages and joint arthroplasty for advanced disease[2-4]. Arthroplasty surgery is an extremely effective intervention in late symptomatic disease and relieves pain, restores function, and improves quality of life[5]. However, limitations include the possibility of surgical complications or persistent pain and stiffness, as well as the finite lifespan of prostheses[2,3,6]. There remains no effective treatment to address the morbidity experienced during early disease[7]. Given the ageing global population and increasing prevalence of osteoarthritis[8,9], disease prevention and the treatment of early OA represents a research priority.

Our current inability to develop effective preventative strategies for osteoarthritis stems from a number of sources, but primarily is a result of not being able to predict accurately which individuals will develop the disease. The aetiology of osteoarthritis is complex and multifactorial, but there has been progress on this front with better characterisation of risk factors. Varus or valgus alignment of the knee[10,11], acetabular dysplasia and retroversion[12-14], and cam morphology of the hip[15] are the most prevalent examples.

Preventative strategies are most likely to be effective when addressing the underlying disease aetiology through risk factor modification or mitigation of their effect. One

explanation offered for the failure of therapies aimed at preventing the development and progression of osteoarthritis to date has been the failure to recognise and address specific disease phenotypes responsible for joint failure[16]. However, the aetiology of cam morphology, acetabular dysplasia and retroversion, and varus leg alignment remains poorly understood.

Retired football players have significantly greater rates of hip osteoarthritis than control groups[17-19]. Elite sportspeople also show a higher prevalence of cam morphology, acetabular dysplasia and retroversion, and varus leg alignment[20,21], which are known to cause OA[10,22-28]. These morphologies are believed to develop throughout childhood and during adolescence at around the time of physeal closure[29-32] with high activity individuals being at particular risk[15,29,33]. Accordingly, adolescent elite level sportspeople likely represent a salient cohort of individuals in which to investigate the aetiology of risk factors for OA.

In recent decades the sports opportunities available to young athletes and the general population has risen significantly, with an increasing numbers of sports turning professional[34]. It has been suggested that to reach an international level of sport requires intense practice for a minimum of 10 years[35] or 10,000 hours[36,37]. The majority of this practice takes place during adolescence. Members of elite football academies follow an intense training programme from as early as eight years of age. The effect of such high levels of physical exertion on the developing skeleton is largely unknown, but intense sports training has been shown to result in pronounced adaptive skeletal changes in adolescence[38,39].

Bone growth is dependent upon genetic and environmental factors, but is also responsive to both physiological and mechanical factors during the adolescent years[40,41]. Skeletal growth at the epiphyseal plate is an active and dynamic process that responds to the level of load put through it[42,43]. Abnormal growth is likely secondary to repetitive trauma to the epiphyseal plate which affects normal endochondral bone formation[44].

As acquired disorders it may be that cam morphology, dysplasia, retroversion, and varus leg alignment are preventable or modifiable. However, their aetiology is insufficiently understood to recommend the timing or type of intervention at this point. Disagreement exists over the age of genesis of each disorder, how to define abnormal from normal morphological change, the mechanism by which each morphology develops, and the exact role that activity levels play in their development.

These uncertainties limit the capabilities of clinicians to intervene in or monitor individuals at greatest risk of developing abnormal joint morphology at the necessary age. The cardiovascular benefits of exercise are likely to outweigh potentially detrimental effects on hip morphology. Nevertheless, individuals participating in high-level sports during youth represent a high-risk cohort that warrants further investigation.

1.2 Scope of Thesis

This thesis focuses on the development of hip morphology and leg alignment during adolescence and the effect of high activity levels on this. This thesis starts with a literature review of our understanding of bone and joint development, the aetiology of femoral head, acetabular, and leg alignment disorders, and the impact of exercise on hip morphology, leg alignment, and cartilage composition.

1.3 Bone Development

1.3.1 Long bones

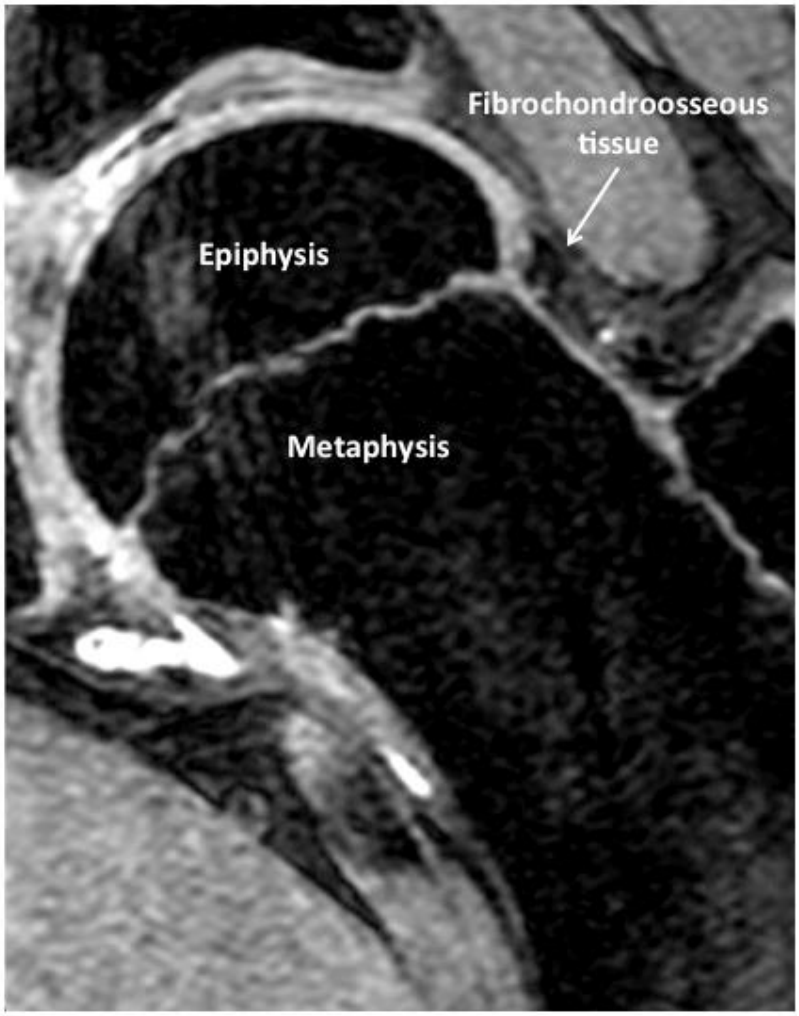
Long bones develop through endochondral ossification, where a pre-existing hyaline structure is replaced with bone, and intramembranous ossification, where bone is deposited directly upon the diaphysis. The first evidence of ossification is seen at eight weeks gestation within the centre of the diaphysis, denoted the primary ossification centre. Secondary ossification centres develop within the epiphysis approximately six months after birth. These ossification centres give rise to two zones of growth: i) The horizontal layer of cartilage that lies between the primary and secondary ossification centres called the physis. This is responsible for longitudinal bone growth[45-47]. ii) The spherical layer of cartilage that surrounds the secondary ossification centre that gives rise to transverse and spherical growth.

Epiphyseal cartilage lies beneath the articular cartilage and is responsible for shaping the articular surfaces. The epiphyseal growth plate can be divided into three main chondrocyte subpopulations: the resting, proliferating and hypertrophic chondrocytes[48]. Longitudinal bone growth is primarily achieved through the action of chondrocytes in the proliferative and hypertrophic zones of the growth plate[49]**.** Resting zone chondrocytes are recruited to start active proliferation and then undergo differentiation, hypertrophic differentiation, death, blood vessel invasion, and mineralization[45,50]**.**

The areas above and below the physis are known as the epiphysis and metaphysis respectively. The junction between the metaphysis and epiphysis is of particular interest

in the development of cam morphology, as this dictates the shape of the eventual head-neck junction[51-53]. In the immature hip there is a discrete circumferential fibrochondroosseous structure at this site that consists of the ossification groove of Ranvier and the perichondrial fibrous ring of La Croix. This structure is thought to be responsible for lateral expansion and structural support of the physis. The groove of Ranvier is a wedge of proliferative cells, whereas the ring of La Croix is an overlying fibrous band that is continuous with the metaphyseal periosteum[54] (Figure 1-1).

Figure 1-1 - Epiphyseal Cartilage, Articular cartilage, and Fibrochondroosseous Tissue in an 11 Year Old Elite Male Footballer



Lateral expansion has been linked to periosteal apposition driven by the process of osteoblast precursor proliferation[55], however there is some debate that growth in width may also be due to interstitial growth from the physis[56]. Since the physis is wider than the diaphysis, a process of funnelisation is required to maintain the diameter of the diaphysis as it increases in length. During this process osteoclasts resorb the peripheral metaphyseal bone shortly after it is produced[57].

1.3.2 Acetabulum

A combination of interstitial, endochondral, and appositional bone formation determines the growth and dimensions of the acetabulum[58-60]. During adolescence three secondary centers of ossification appear in the hyaline cartilage surrounding the acetabular cavity. This results in a triradiate acetabular cartilage complex that is interposed between the ossified ilium, ischium, and pubis. Similarly to long bones, this complex is composed of epiphyseal growth-plate cartilage adjacent to the ilium, ischium, and pubis[59]. The epiphysis of the pubis forms the anterior wall of the acetabulum and the epiphysis of the ilium forms part of the superior wall of the acetabulum. (Figure 1-2 and Figure 1-3)

Interstitial growth within the triradiate cartilage complex causes the hip socket to expand laterally during growth. The depth of the acetabulum increases as the result of interstitial growth, appositional growth at the periphery of the cartilage, and endochondral ossification at the acetabular margin[59]. Bone growth in the metaphysis adjacent to illium and pubis are responsible for increases in acetabular depth and width. Stunting of these growth plates in the achondroplastic child results in a narrow, shallow acetabulum and similar changes are seen when the triradiate growth plates are

destroyed by trauma or surgical intervention[59].

The concavity of the acetabulum is believed to develop in response to the presence of the spherical femoral head[61,62]. Unreduced congenital dislocations of the hip[17], and the removal of the femoral head in animal models[18], result in a reduced area and depth of the acetabular socket and atrophy and degeneration of the acetabular cartilage, whilst the triradiate epiphyseal growth plate cartilage remains normal. Closure of the triradiate cartilage is believed to take place by the age of fourteen years[63].

Figure 1-2 - Triradiate Cartilage at the Base of the Acetabulum in a 10 Year Old Elite Male Footballer. Axial Oblique View.

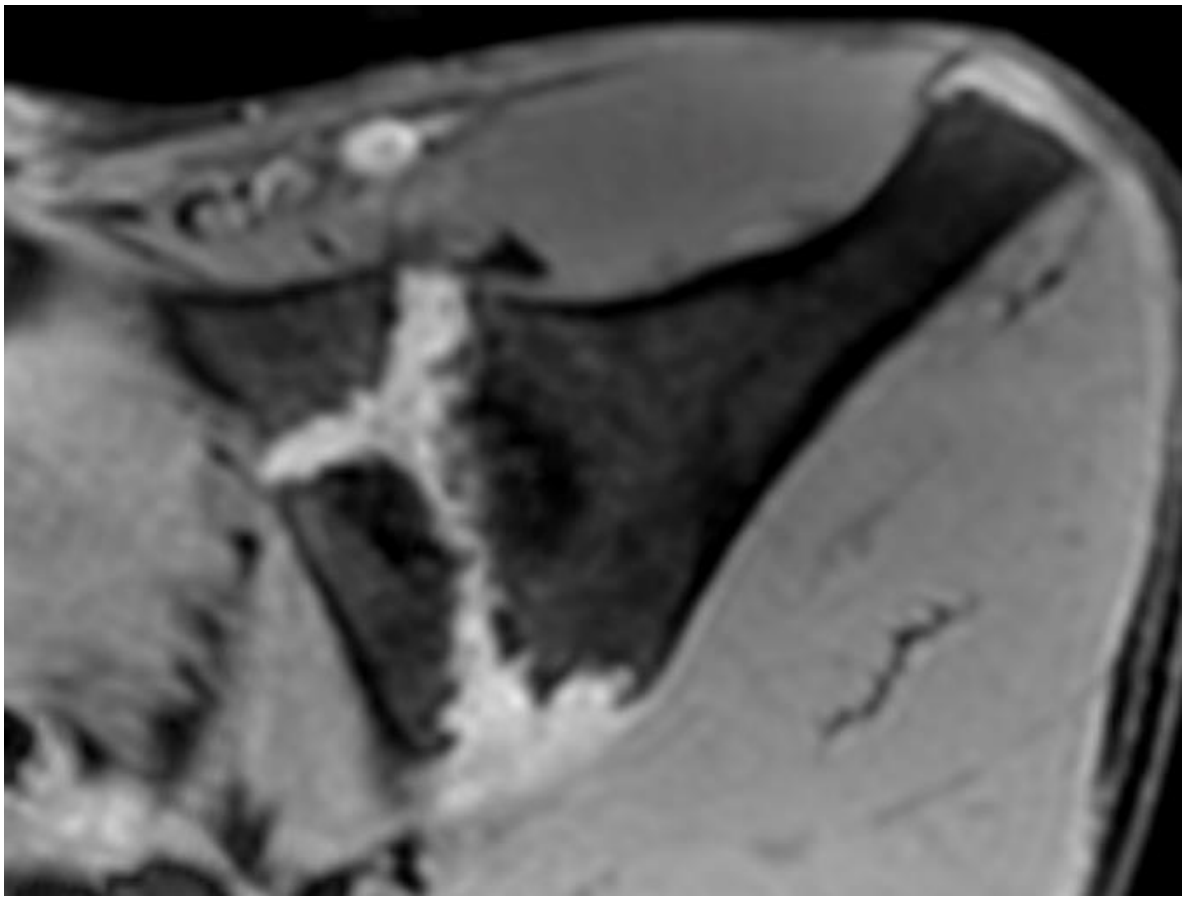


Figure 1-3 - Triradiate Cartilage in a 10 Year Old Elite Male Footballer. Coronal View.



1.3.3 Factors Influencing Bone Development

Bone growth is dependent upon genetic and environmental factors, but is also responsive to both physiological and mechanical factors during the adolescent years[40,41]. Bone growth and physeal closure during adolescence are orchestrated by a complex interaction between growth hormones and sex hormones which regulate chondrocyte proliferation and differentiation[64]. An intricate network of regulatory endocrine signals exist in this capacity including growth hormone, insulin-like growth factor I, glucocorticoid, thyroid hormone, oestrogen, androgen, vitamin D, and leptin[47]. These systemic hormones, along with locally produced peptide growth factors, act on growth plate chondrocytes to trigger changes in gene expression to induce chondrocyte proliferation and differentiation with resultant bone growth[46,47].

Mechanical loading is also recognised as a key factor for normal bone development. In adolescence bone is more responsive to loading. This might be due to peaks in nutrients, sex steroids, growth hormones, and insulin like growth factors[42]. Mechanical forces stimulate the synthesis of extracellular proteins which can affect the bone tissue's overall structure[65]. A feedback mechanism exists to ensure that longitudinal bone growth proceeds in the direction of the predominant mechanical forces[49] via chondrocyte mechanotransduction mediated through their primary cilium[66]. During maturation the individual epiphyses undergo central calcification, absorption of cartilage and endochondral ossification, which is impacted by the degree of local distortion secondary to mechanical load[67].

1.3.4 Disorders of Bone Development

1.3.4.1 Disorders of Proximal Femoral Physeal Development

Many genetic and endocrine conditions disrupt normal bone growth. The physis is also particularly susceptible to traumatic injury given that it lies between the rigid metaphysis and epiphysis. Injuries involving the physis account for between 15% and 30% of all skeletal injuries in children[68]. A resultant disruption to the epiphyseal circulation may inhibit physeal growth, or if the epiphysis is brought into direct contact with the metaphysis, a bone bridge may result.

Slipped Upper Femoral Epiphysis (SUFE) describes a condition where the femoral neck translates anteriorly and rotates externally relative to the femoral head through a cleavage line passing across the proliferative and hypertrophic zones of the physis. SUFE is the most common hip disorder affecting adolescents and the average age of presentation is 12 years for males and 11 years for females[69]. Although the majority of cases are deemed idiopathic, risk factors include those that reduce the resistance to shear, such as endocrine disorders, and those that increase stress across the femoral physis, such as femoral or acetabular retroversion[70]. More than 80% children diagnosed with SUFE are obese, and this probably reflects a combination of endocrine and mechanical factors[71].

SUFE predisposes to osteoarthritis[72-75]. In a study investigating the causes for end stage hip OA in individuals below 50 years of age SUFE represented the underlying aetiology in 9.5% of patients receiving hip arthroplasty[76]. In the same study 35.9% of individuals undergoing hip replacement before the age of 50 were found to have Femoroacetabular

Impingement (FAI) morphology[76].

1.3.4.2 Femoroacetabular Impingement

Femoroacetabular impingement results from abnormal contact between the proximal femur and acetabulum secondary to a loss of concavity at the femoral head-neck junction (cam morphology) or acetabular overcoverage of the femoral head (pincer morphology) (Figure 1-4). Whereas all hips impinge at the extremes of movement[77], this abnormal contact takes place within a functional range of movement[78] (Figure 1-5). Although cam and pincer morphology may co-exist, the two conditions are distinct[79] and give rise to different patterns of joint pathology[80].

Figure 1-4 - MRI radial slices of a normal hip (A), a hip with cam morphology (B), and a hip with pincer morphology (C)

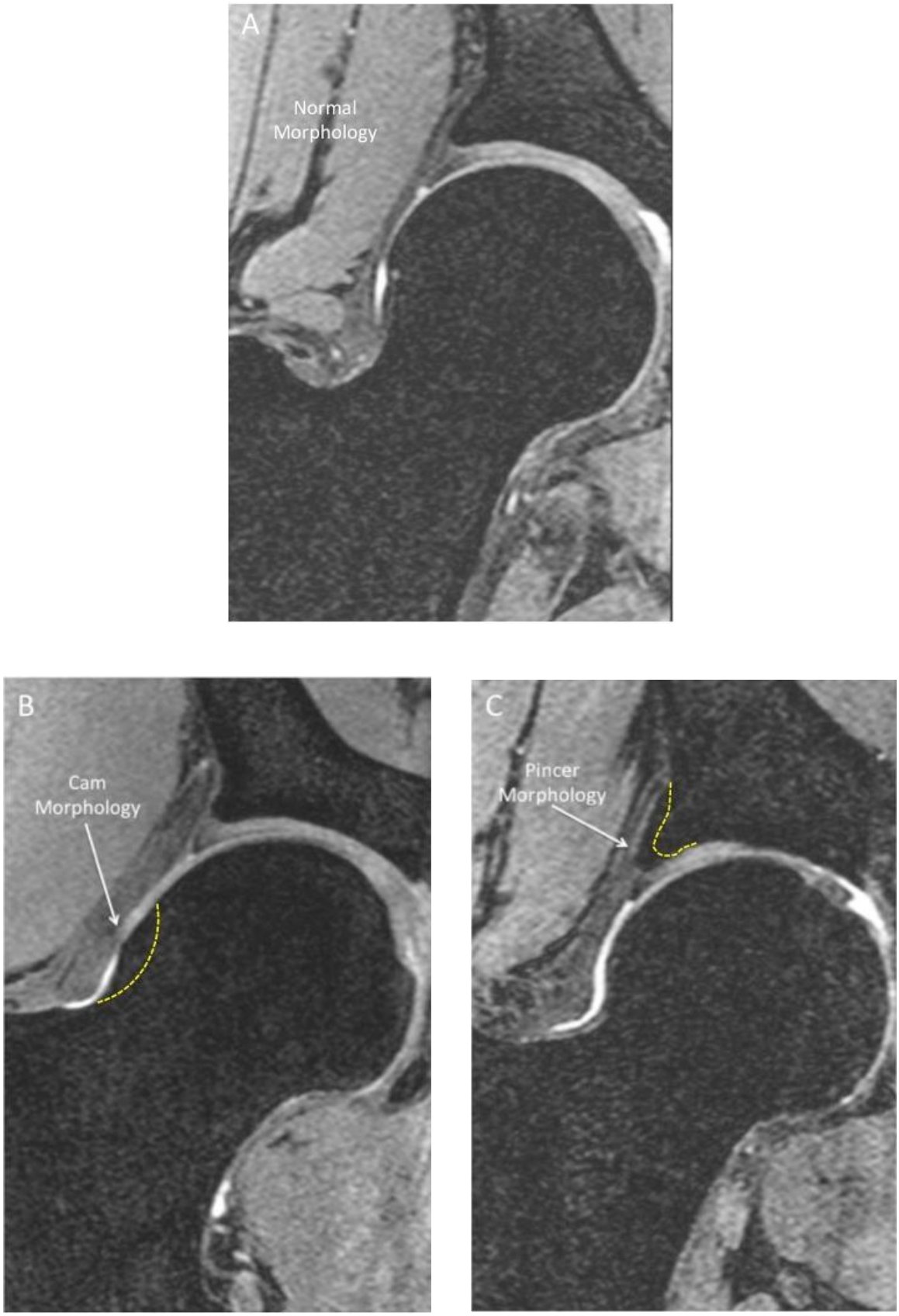
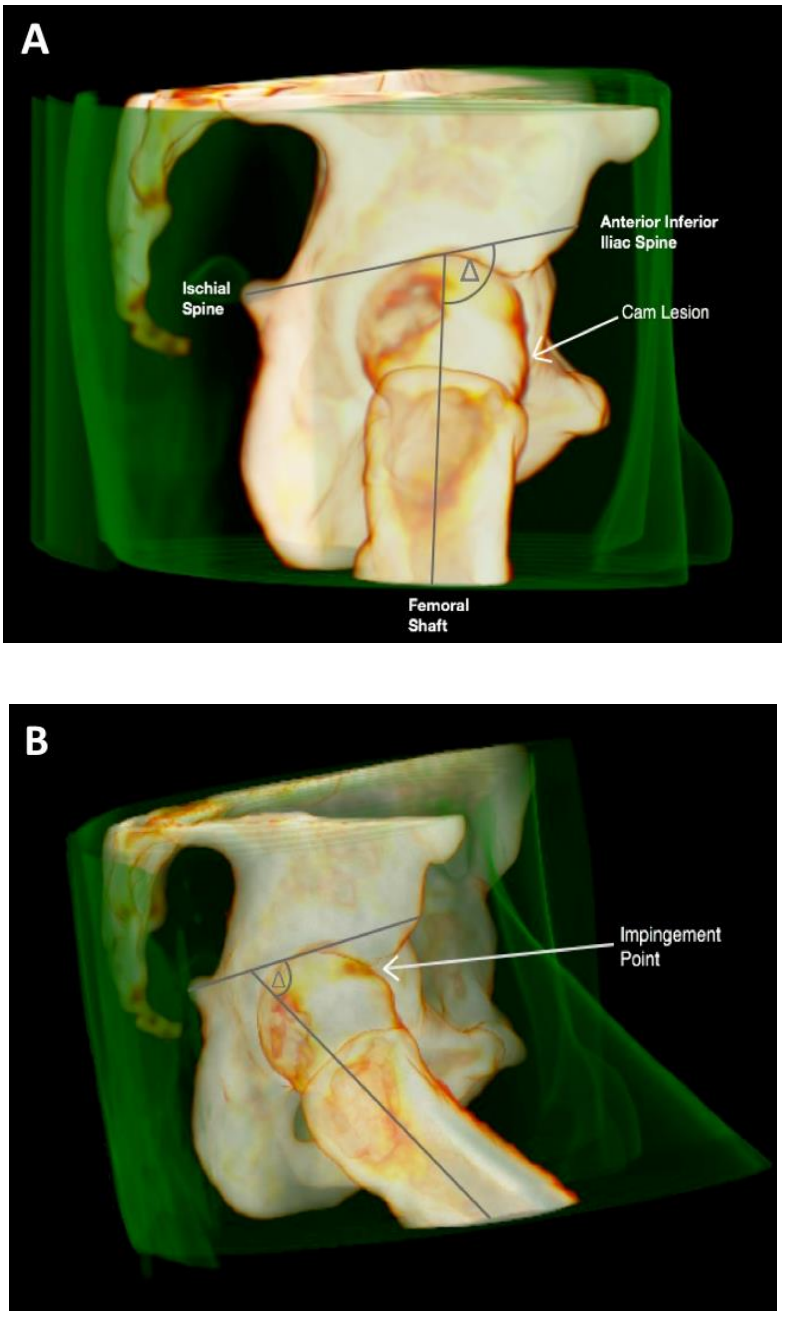


Figure 1-5 - 3D reconstructed models from a 4D dynamic hip CT scan in an individual with cam-type FAI showing the patient at rest (A) and impinging within a functional range of flexion (B).

In a normal hip, the concavity of the femoral head-neck junction allows an extensive range of hip movement without impingement of the femur against the acetabular rim. In cam morphology the loss of this concavity at the anterior and superior head-neck junction results in impaction of the femur against the acetabular rim when the hip moves into flexion and internal rotation. This results in damage to the labrum and may progress to involve the acetabular cartilage with development of osteoarthritis.



Images reproduced from:

- Fernquest S, Arnold C, Palmer A, et al. Osseous impingement occurs early in flexion in cam-type femoroacetabular impingement: a 4D CT model. Bone Joint J. 2017;99-B(4 Supple B):41-8.

Pincer morphology may be localised as with acetabular retroversion, or global as with coxa profunda or protrusio acetabuli[81]. It is associated with pain but appears to confer less risk for developing future osteoarthritis than cam morphology[82,83]. Cam morphology may result from conditions such as SUFE, or femoral neck fracture malunion, although the majority arise without apparent pre-existing hip disease[84]. Cam morphology represents a significant risk for developing hip pain[85] and osteoarthritis[22] (Figure 1-6).

Figure 1-6 - Anteroposterior radiograph of a hip with cam morphology (white arrow) and evidence of osteoarthritis (red arrow).

The aspherical femoral head impinges on the acetabulum on hip flexion and internal rotation leading to delamination of the acetabular cartilage from the underlying subchondral bone and the development of Osteoarthritis.



A recent systematic review concluded that it is not possible to determine the true prevalence of cam morphology in the general population or selected subgroups. This was primarily due to heterogeneous populations and differing diagnostic criteria, resulting in prevalence ranging from 5% to 75%, although cam morphology did appear consistently higher in males[86]. A cross-sectional study of 2081 skeletally mature young healthy adults found that 35% males and 10% females displayed cam morphology[87]. In a systematic review of asymptomatic populations of males and females the overall prevalence of cam morphology was 37%, but was 54.8% in athletes and 23.1% in the general population[88]. Sporting activity is a recognised but poorly-defined risk factor for hip osteoarthritis[89], and high activity levels during adolescence may promote the development of cam morphology[15,29,33].

A prospective study of the CHECK cohort consisting of 1002 volunteers with early symptomatic osteoarthritis revealed that cam morphology can confer up to a 10-fold increased risk of developing end-stage disease within five years[90]. These findings are supported by a prospective study of the Chingford cohort consisting of 1003 females recruited from the general population and followed for 20 years. Cam morphology was associated with both osteoarthritis and future hip arthroplasty[91]. It also conferred an increased risk of hip osteoarthritis progression in the Johnson County Osteoarthritis Project[92]. In these cohorts, the greater the size of the cam morphology, the greater the risk of developing osteoarthritis. A number of cross-sectional and case-control studies report a higher prevalence of cam morphology in individuals with radiographic osteoarthritis[93,94]. Causality is supported by the cartilage damage seen intra-operatively at the specific sites where impingement takes place[81,95]. Early osteoarthritis can be detected within the acetabulum of asymptomatic patients with cam morphology at the

point of impingement using compositional MRI techniques (delayed Gadolinium-Enhanced MRI of Cartilage)[96,97].

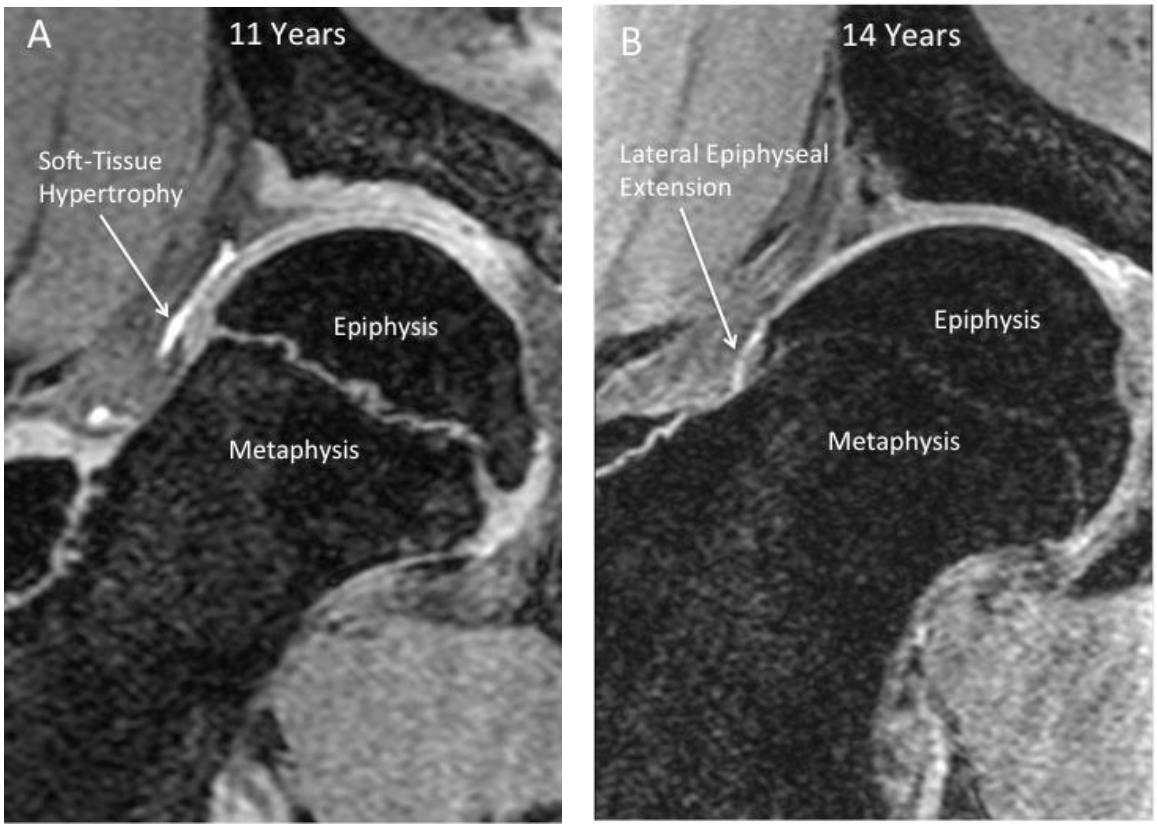
Despite the strong association between cam morphology and the development of osteoarthritis, the majority of individuals with this morphology will not develop osteoarthritis. Depending on cohort characteristics and the diagnostic criteria for cam morphology, the positive predictive value for future osteoarthritis is low, ranging from 6-25%, whereas the negative predictive value is high, ranging from 98-99%[15]. Whilst individuals with normal hip morphology are unlikely to develop osteoarthritis, cam morphology must be accompanied by other risk factors for osteoarthritis to develop. These risk factors may include acetabular morphology, the nature and magntiude of activity, or intrinsic susceptibility to hostile biomechanics.

The aetiology of cam morphology is poorly understood. Sub-clinical SUFE giving rise to a prominent femoral metaphysis has been a widely adopted theory for the development of cam morphology[72,98-101]. SUFE can be a cause of cam morphology and some authors propose that it may account for up to 44% of cases[99]. Moreover, the sex ratio of cam morphology is similar to that of SUFE[69]. However, the hypothesis that subclinical SUFE is the dominant aetiological factor for cam morphology has been brought into question by recent studies, such as the absence of posterior tilt on lateral hip radiographs of symptomatic patients with femoroacetabular impingement[102].

Epiphyseal extension along the anterosuperior femoral neck is an increasingly

recognised mechanistic phenomenon in individuals with cam morphology[102] and may represent a distinct pathology that gives rise to cam morphology (Figure 1-7). However, The relationship between epiphyseal extension and subsequent cam morphology is not well documented or understood[51-53]. Epiphyseal extension could be considered an adaptive rather than pathological process and finite element models of the hip show high mechanical stress on impact loading precisely where cam deformity most frequently develops[103]. Subtle morphological changes in physeal development have been reported in association with many sports[104], including the proximal humeral physis in baseball[105], suggesting activity levels may represent a key aetiological factor. Indeed, previous studies report athletes show greater epiphyseal extension than controls[53].

Figure 1-7 - Elite level football player age 11 years at baseline with soft tissue hypertrophy at the femoral head-neck junction (A) which preceded lateral epiphyseal extension and osseous cam morphology seen at follow-up aged 14 years (B)



The prevalence of cam morphology is constant throughout all age groups after physeal closure, suggesting it's a disorder of physeal growth[15,105,106]. Studies have therefore focused on morphological changes that take place around the time of physeal closure. Monazzam[30] et al performed a retrospective study of 225 abdominal CTs of patients aged 2 to 19 years with no known orthopaedic hip pathology. Alpha angles were measured at the 3 o'clock position and no cam morphology (alpha angle greater than 55 degrees) was evident between ages 4 and 10. After 10 years of age, an increasing number of individuals exhibited raised alpha angles. Bixby et al[107] performed a retrospective study of 132 patients who underwent CTs for abdominal pain aged 12 to 18 years. In all radial planes there was extension of the epiphysis away from the articular surface in patients with a closed compared with an open physis, consistent with normal growth. The prevalence and magnitude of cam morphology was greater in males than females.

Kienle[31] et al assessed changes in femoral morphology over 1 year in a prospective MRI study of 64 asymptomatic school pupils aged between 9 and 17. During the study period, there was no significant increase in alpha angle on radial slices. They found with physeal closure there was a decrease in alpha angle at the 1 o'clock position. Average alpha angle was higher in participants with an open physis compared with a closed physis. However, no individuals with an open physis had an alpha angle above 55 degrees compared with 8% individuals with a closed physis. This added further weight to the proposal that cam lesion morphology develops around the time of physeal closure. As found in the study by Bixby et al[107], the epiphysis extended away from the articular cartilage with increasing age until the physis closed. Extension was similar for both sides of the physis, consistent with normal growth. In contrast, Siebenrock et al described localised epiphyseal extension in the anterosuperior position as a cause of cam

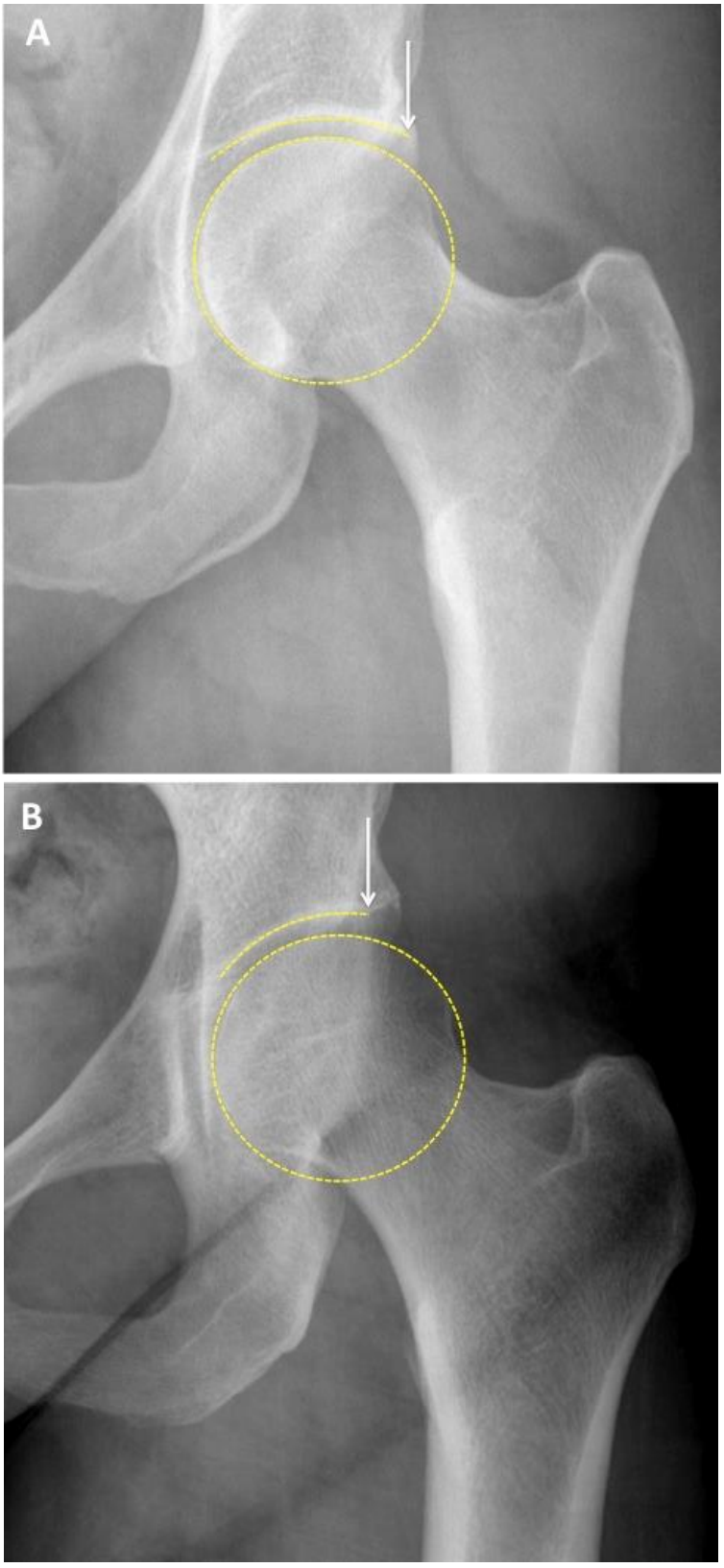
morphology in patients with femoroacetabular impingement[102].

1.3.4.3 Disorders of Acetabular Development

Epidemiologic studies indicate that osteoarthritis (OA) of the hip frequently occurs in the absence of OA in other large joints, suggesting that local factors are important in its pathogenesis[81,108-111]. It was therefore suggested that subclinical biomechanical factors might be important in the development of hip OA[24,112,113]. The predominant biomechanical mechanisms are FAI morphology, as previously mentioned, and abnormal acetabular morphology, such as acetabular dysplasia and acetabular retroversion. The aetiology of disorders of acetabular morphology have been well documented during early childhood but are poorly understood during adolescence.

Hip dysplasia describes a condition where there is reduced acetabular coverage of the femoral head[114] (Figure 1-8). Hip dysplasia is a result of misalignment between the femoral head and the acetabulum secondary to changes in their shape, size, and orientation. The site of deficient acetabular coverage of the femoral head historically is thought to be anterolateral[115]. This misalignment results in structural instability causing mechanical overloading of the acetabular rim during normal activities [116,117] with associated increased stresses in the cartilage. The stress placed on the joint cartilage in hip dysplasia can be beyond the physiologic level of tolerance[114] and left untreated can lead to labral-chondral damage and eventually arthritis[12-14]. Hip Dysplasia has been estimated to play a role in 20% to 40% of all hip osteoarthritis[23-25] and be present in 48% of those receiving hip arthroplasty surgery before the age of 50[76].

Figure 1-8 - Anteroposterior radiograph of a hip with a normal femoral head coverage (A), and a hip with a reduced femoral head coverage showing evidence of mild dysplasia (B).



The prevalence of hip dysplasia varies significantly depending on the population studied and the adopted diagnostic criteria. A general population cohort from Denmark consisting of 1332 asymptomatic males and 2288 asymptomatic females estimated the prevalence of dysplasia as 4.3% in males and 3.6% in females[93]. In the same cohort, the prevalence was found to range between 5.4% to 12.8% depending on the diagnostic criteria[118]. The absence of agreed diagnostic criteria is a significant limitation in all studies of hip morphology.

In the normal hip, the acetabular opening is inclined from the horizontal plane and anteverted from the sagittal plane[41]. Dysplastic hips are globally shallow, however the deficiency in coverage may be more pronounced in the anterolateral or posterolateral acetabulum, which may affect the relative degree of inclination and anteversion of the acetabulum[119].

An association between decreased acetabular anteversion and osteoarthritis was found as early as 1991 by Menke et al[120] and the prevalence of retroversion among patients with idiopathic hip osteoarthritis has been found to be 20% versus 5% among the general population[121]. Decreased acetabular anteversion was also found to be a major cause of hip pain and osteoarthritis in a study by Tönnis et al investigating the CTs of individuals presenting to hospital with hip pain[122]. Li et al[119] found retroversion of the acetabulum to be present in 40 of 232 developmental dysplastic hips and Mast et al[123] found retroversion to be as frequent as 87 in 235 developmental dysplastic hips. A high prevalence of retroverted acetabula has also been reported in patients with FAI[30,121]. A reduction of acetabular anteversion is likely to cause increased impingement of the

anterior acetabulum against the femoral head-neck junction with resultant cartilage damage in individuals with cam morphology without dysplasia.

Female sex, primiparity, breech position, and family history are known risk factors for hip dysplasia development during childhood[124-126]. Less is known about the impact of environmental factors on the development of abnormal acetabular morphology during adolescent skeletal maturation. Although high activity levels are a known risk factor for disorders of the developing femoral head such as cam morphology, the impact of high activity on acetabular development is largely unknown. However, femoral head disorders and disorders of the acetabulum are thought to be closely linked. Clohisy et al[76] showed that proximal femoral deformities were present in 92.6% of the 108 hips treated for symptomatic acetabular dysplasia in their study, with 72% of the hips having cam morphology. Much as the proximal femoral physis responding to stress or damage may result in SUFE [70] or cam morphology[102], similar events at the triradiate cartilage of the acetabulum during skeletal maturation may be responsible for disorders of acetabular morphology. It is accepted that acetabular concavity its dependent upon its interaction and articulation with the spherical femoral head[59,60]. It would follow that acetabular width and depth are also dependent upon the forces placed upon the acetabulum by the articulating femur. With skeletal maturity, the increase in alpha angle of the femoral head-neck junction[32] could possibly lead to increased pressure between femur and anterolateral acetabular wall. This may result in adaptation or reduced growth of the acetabular wall. However, further study is necessary in order to support this hypothesis.

Considerably less is known on acetabular development, and the changes taking place during adolescent skeletal growth, than is known on femoral head development and its associated disorders[127]. Although the prevalence of hip dysplasia and acetabular retroversion is well documented, the continued development of these morphologies after childhood is largely unknown. The majority of studies investigating acetabular development have been cross-sectional and retrospective using CT in poorly defined asymptomatic cohorts, and produced contrasting results[30,127-131].

Reikeras et al[131] evaluated the CT scans of 34 children with idiopathic increased acetabular anteversion aged 4 to 12 years, and 6 children with congenital dislocation of the hip aged 3 to 5 years. The main aim of the study was to determine if the degree of anteversion in the acetabulum and femoral neck were correlated. They reported that in individuals with an anteverted femoral neck there was minimal compensation in the degree of anteversion in the acetabulum. However, they also found no correlation between the degree of acetabular anteversion and age, suggesting that little change in acetabular anteversion takes place up to 12 years of age.

The finding that little change in acetabular anteversion takes place during skeletal growth was later reiterated in the work by Weinar et al[129]. Weinar et al[129] retrospectively evaluated the CT scans of 170 children aged 6 months to 17 years who had undergone investigation for intrabdominal pathology. In their study they also measured anterior and posterior femoral head coverage. They found the acetabulum deepens and becomes increasingly spherical until 13 years , after which no further change is seen. This correlated to the time of closure of the triradiate cartilage. They also reported that the closure of the triradiate cartilage occurs slighlty earlier in females than males, and that

the anterior Centre Edge Angle (CEA) decreased after 6 years of age. However, their study was limited in that the effect of pelvic tilt was not controlled for.

Kim et al[130] retrospectively analysed acetabular anteversion using CT scans of 39 hips from children and adults aged 3 to 33 years with dysplasia, and 27 hips from an age matched control population who had unilateral disease only. In agreement with the above studies they found no difference in the degree of acetabular anteversion between individuals below 15 years and over 15 years in the control cohort. However, individuals over 15 years of age with dysplasia had a significantly greater degree of acetabular anteversion than those under 15 years of age. This contradicted the findings of the earlier work above in suggesting that important changes in acetabular anteversion and femoral head coverage that could lead to future pathology may be taking place towards the end of skeletal maturation during adolescence.

More recent work has added weight to the findings of Kim et al[130] in suggesting that important morphological changes to acetabular version and femoral head coverage may be taking place towards the end of skeletal maturation. Monazzam et al[30] retrospectively analysed the CT scans of 225 asymptomatic pediatric and adolescent patients aged 2 to 19 years. They reported a significant increase in acetabular anteversion and femoral head coverage with age. Each year of age accounted for a 1 degree increase in lateral CEA and a 0.58 degree increase in anteversion. Indeed, no substantial differences of acetabular anteversion were seen until after 12 years of age, which may explain the lack of findings by Reikeras et al[131] whose oldest participant was 12 years of age.

Hingsammer et al[128] retrospectively evaluated CT images of 200 hips in 100 asymptomatic paediatric patients aged 9 to 18 years who had undergone investigation for abdominal pain. In their study acetabular anteversion and femoral head coverage was greater in individuals with a closed physis than in those with an open physis. They suggested that the increases in version and coverage were a result of growth of the posterior wall. Peterson et al[127] retrospectively analysed the CT scans 157 individuals aged 8 to 17 years who had presented to Accident and Emergency. They also reported an increase in acetabular version and surface area with age. They further suggested that females had significantly greater acetabular anteversion and tilt than males in all age groups.

It should be noted that all of the above studies were cross sectional and retrospective using CT to evaluate the skeletally immature hip. CT fails to elicit the true dimensions of the skeletally immature acetabulum because the cartilaginous portions of the acetabular wall are underrepresented. Moreover, the above studies used differing measurement methodologies. This may explain the contrasting findings as there is no consensus as to the level of the acetabulum at which version or anterior femoral head coverage can reproducibly be measured.

In an attempt to increase understanding of acetabular development Albers et al[132] used MRI to prospectively assess changes in acetabular anteversion and femoral head coverage in 65 asymptomatic children aged 7-16 years over a time period of 1 year. They determined the triradiate cartilage complex at each time point to be open or closed to create three groups; individuals with an open complex at baseline and follow-up (open-open), individuals with a closed complex at baseline and follow-up (closed-closed), and

individuals with an open complex at baseline and closed complex at follow-up (open-closed). They found acetabular anteversion significantly increased between time points in individuals in the open-closed group, but not in the open-open or closed-closed groups. In keeping with this finding, acetabular anterversion was significantly greater in individuals with a closed triradiate cartilage complex compared to those with an open complex. This supported the findings from previous retrospective CT based studies in suggesting that acetabular anteversion increases with age with the most significant changes taking place towards the end of skeletal maturation[30,128,130].

Contrary to findings from CT studies, Albers et al[132] found there to be no significant difference in femoral head coverage or acetabular depth between individuals with an open or closed triradiate cartilage complex. They also reported there to be no significant change in the degree of femoral head coverage or acetabular depth in either skeletally immature or skeletally mature groups. Based on these findings they suggested that acetabular depth and femoral head coverage remain relatively constant with advancing skeletal maturity, whereas acetabular version increases.

1.3.4.4 Disorders of Leg Alignment Development

An association has been found between varus leg alignment and cam morphology of the hip[133, 134]. As with abnormal femoral head and acetabular morphology, leg alignment is believed to develop throughout childhood and during adolescence as the distal femoral physis and proximal tibial physis mature[135]. This raises the possibility that leg alignment may impact hip joint development, or vice versa. Neutral mechanical leg alignment is the normal situation in healthy skeletally mature individuals, which leads to symmetrical mediolateral loading in the knee. However, as with the proximal femur in the development of cam morphology, there is a great responsiveness of bone to mechanical loading in the distal femur and proximal tibia at the knee[42]. The Hueter-Volkmann's law states that growth at the physis is retarded by increased compression, whereas reduced loading accelerates growth. Accordingly, any mismatch in load transfer between the medial and lateral sides of the knee during skeletal growth might result in abnormal leg alignment.

Genu varum describes the anatomical leg alignment of the knees being angled away from each other when the legs are straightened (varus alignment). Genu valgum describes the anatomical leg alignment of the knees being angled towards each other when the legs are straightened (valgus alignment) (Figure 1–9). In healthy children it has been demonstrated that leg alignment progresses from varus alignment in the infant to valgus alignment in early childhood then back towards varus alignment in adolescence[136-138] (Figure 1-10). The development of genu varum during late childhood is considered atypical[137,139] and may place adverse biomechanical stresses upon the cartilage[10]

Figure 1-9 - Full leg length MRI scans in adolescent males showing varus leg alignment (A) and valgus leg alignment (B). Coronal view.

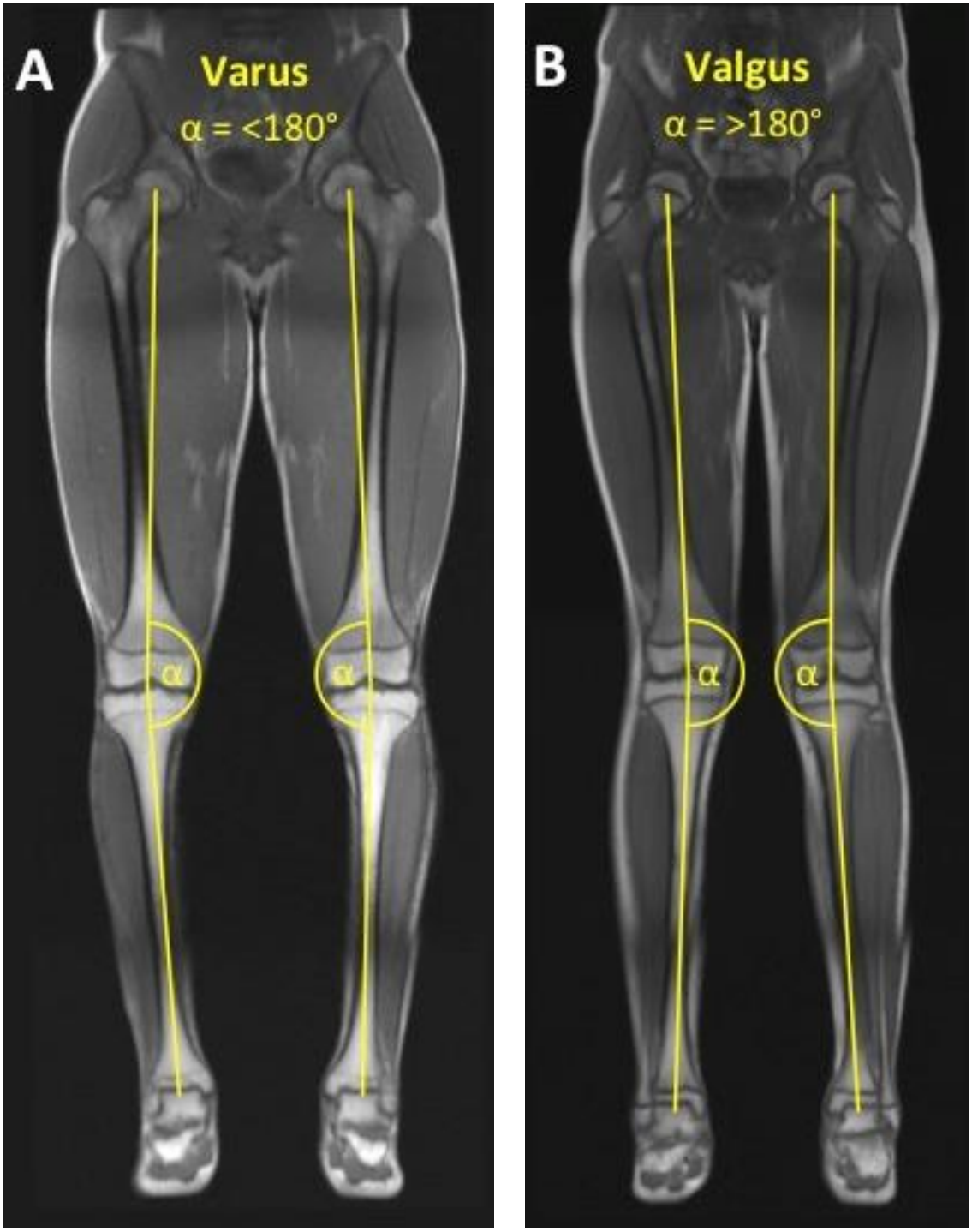
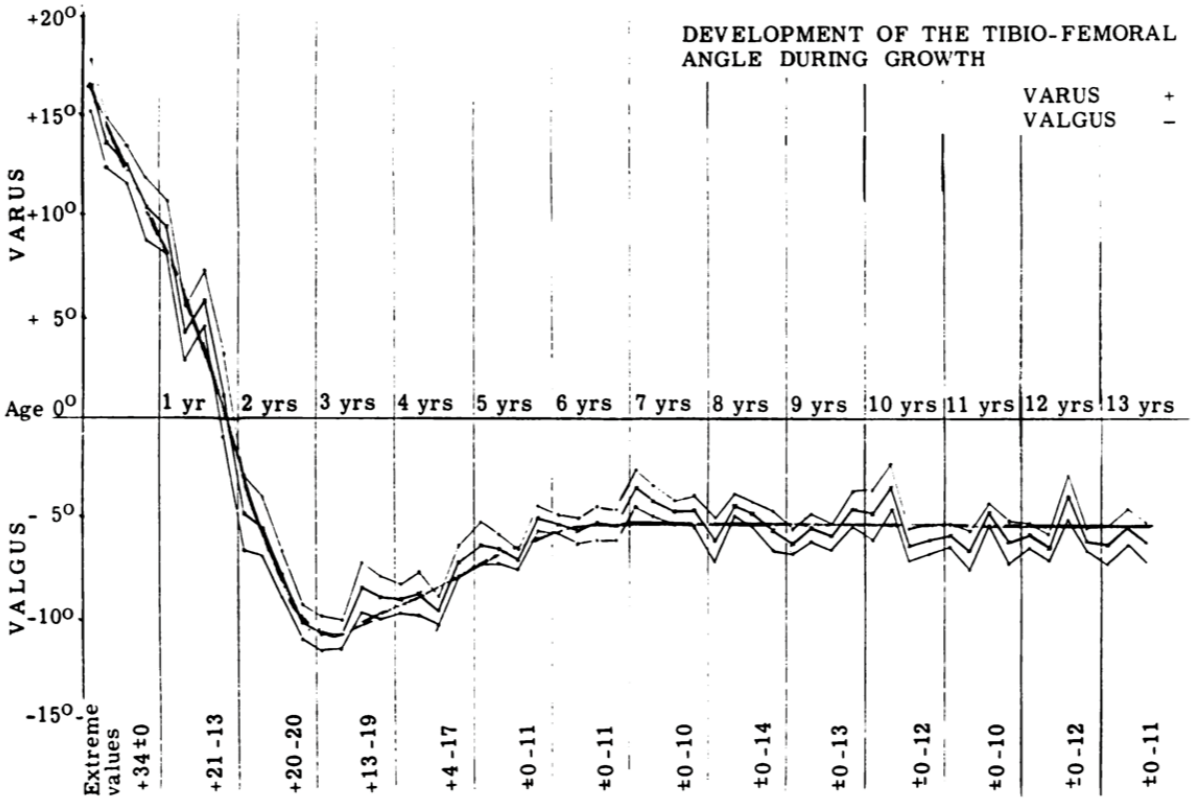


Figure 1-10 - Development of the tibiofemoral angle in children during growth.

The results are based on 1480 measurements of the tibiofemoral angle of children at different ages. The mean of the measurements is in the middle and on both sides of this is the error of the mean, which was an average of ± 4.4 degrees. The standard deviation was ± 8 degrees. Reproduced from Salenius and Vankka 1975[138]



Genu varum is one of the most common anatomical variations of musculoskeletal alignment[140]. Varus and valgus leg alignment can be physiological or pathological in nature. Physiological varus alignment is often due to an abnormal internal rotation of the tibia, while physiological valgus alignment is due to an abnormal external rotation. Both pathological varus and valgus alignment may be caused by systemic disorders such as nutritional rickets or bone metabolic diseases, bone dysplasia, asymmetric growth from unilateral trauma, infection, or neoplasm[140-142]. Although the physiological type of genu varum and genu valgum can improve with age, pathological genu varum and valgum tend to worsen with skeletal growth[141]. In a cohort of 250 asymptomatic adults aged 20 to 27 years the incidence of physiological varus leg alignment (3 degrees or more) was found to be 32% in males and 17% in females[143].

Varus leg alignment increases risk for the development of knee osteoarthritis[10,26-28] and is associated with higher tensions at the ACL[144,145], meniscal tears, patellofemoral pain syndrome[146-148], and shin splints[149]. Varus alignment is thought to predispose to knee OA as the line of weight bearing force shifts medially from the joint center intensifying the medial compartment load and creating a medial joint reaction force that can be three and a half times that of the lateral compartment[150]. Leg alignment is determined by both modifiable and non-modifiable parameters, which include gender[143,151], obesity[152], and athletic activity[135,153]. Rezende et al demonstrated that there was a positive correlation between degree of genu varum and anthropometric variables such as weight, height, and BMI[154]. Voloc et al reported that low levels of vitamin D increased the risk of genu varum[155]. Obesity is associated with greater valgus leg alignment in girls[152]. A higher incidence of knee OA and a higher prevalence of varus leg alignment exists in retired soccer players than a general population of the same age[20]. This would suggest that

activity levels play an important role in determining leg alignment. Indeed, further studies have shown that athletic activity is associated with greater varus leg alignment in boys[135,153].

It has been hypothesized that regular practicing of an intensive sport during adolescence may lead to a growth deformity[20]. The development of genu varum is thought to be secondary to biomechanical overloading of the proximal medial tibial physis[156-158]. The Hueter–Volkmann law suggests that increased pressure parallel to the axis of the epiphysis inhibits growth, whereas decreased pressure promotes it, and that changes in compressive forces cause asymmetrical growth of a joint[159,160]. The ''chondral modeling'' theory of Frost suggests that physiological loading stimulates growth, whereas loads outside this range, either higher or lower, will inhibit it[161]. Mechanical overload has been shown to play an important role in the development of genu varum, where restricted and asymmetric physeal growth due to excessive asymmetric loading led to progressive deformity[157]**.** This mechanism of varus alignment development would explain the high prevalence of genu varum in footballers as intensely playing football regularly exposes the knee joint to load and torque stresses that may affect the physis[146].

To elucidate the cause of tibia vara Cook et al[157] in 1983 used finite element analysis of the proximal tibia to investigate the stresses occuring in the physeal plate during one legged stance in 2 and 5 year old children. Stresses were calculated as a function of degree of varus and body weight. They found that increasing varus alignment resulted in increased stress in the medial tibial physis. They suggested that in a 5 year old child only 10 degrees of varus stress was required to retard growth at the medial physis. They

theorised that excessive asymmetrical loading of the medial physis may lead to restricted and asymmetrical physeal growth and result in varus leg alignment.

1.4 Effect of Physical Activity on Bone Development

Mechanical loading of the bone is important for normal epiphyseal plate physiology[42]. Skeletal growth at the epiphyseal plate is an active and dynamic process which responds to the level of load put through it[43]. Increased load through exercise has a healthy biomechanical function on the normal growth of the physis[42].

The immature skeleton is more responsive to the osteotrophic effect of exercise than the mature skeleton[47]**.** Indeed, intense training has been shown to result in pronounced adaptive skeletal changes in adolescence[38,39]. In recent decades the sports opportunities available to young athletes has increased[34]. Beyond the positive aspects sport brings, there exists the potential risk of overuse and injury to the musculoskeletal system[162].

Skeletally immature children who participate in extreme levels of sport participation can sustain repetitive trauma[44]. This repetitive trauma can cause the epiphyseal plate to widen. Laor et al[44] hypothesized that the metaphyseal vascular supply may become disrupted and affect the normal process of chondrocyte proliferation and differentiation that results in endochondral bone formation. This may result in the development of abnormal bone morphology.

Overt epiphyseal injuries are usually due to shearing, avulsion, or compressive forces due to either severe twisting or direct blows that can result in a disruption of the epiphyseal growth plate[38]. In young athletes as the bone stiffness increases and resistance to impact diminishes sudden overload may subject bone to either bow or

buckle[38]. Trauma may also result in swelling and hyperemia in the physeal area which may result in deformity[163]. It should be noted however, that on balance pursuing sports as leisure time activity has not been found to be harmful for children[164].

There is a lack of literature on the effect of inactivity and stress deprivation on the epiphyseal growth plate. Load-bearing tissue, such as articular cartilage, will atrophy in the absence of mechanical forces[165] but the response of the physis to reduced load is unknown. Further research should take into consideration what lack of exercise and lessened mechanical load bearing has on the function of the epiphyseal growth plate[42].

1.4.1 Effect of Physical Activity on the Proximal Femoral Physis: Cam Morphology

Sporting activity during adolescence is increasingly implicated in the development of cam morphology, although this was first noted in 1971[100]. There is an extremely high prevalence of cam morphology amongst elite athletes. Kapron[21] et al performed radiographs of 67 male collegiate American Football players and 78% displayed at least one sign of cam morphology. Studies have since looked at changes in hip morphology during adolescence in relation to activity levels. The hypothesis is that increased loading may result in a subclinical SUFE or physeal adaptation that leads to cam morphology.

Carsen et al[32] recruited 44 volunteers pre and post physeal closure. This asymptomatic cohort consisted of males aged 10-12 and 15-18, and females aged 8-10 and 14-18. No participant exhibited cam lesion morphology on MRI (alpha angle greater than 50.5 degrees at 3 o'clock) prior to physeal closure whereas 14% displayed cam morphology after physeal closure. The fact that alpha angles were higher after physeal closure is contrary to the CT study of Bixby et al[107] and highlights potential differences between cohorts, imaging modalities, and methods of measuring morphology. Daily activity levels were assessed using a validated questionnaire and found to be higher in participants with cam morphology, further supporting physeal loading as an aetiological factor.

Siebenrock et al investigated the development of cam morphology in male ice hockey[166] and basketball players[29,53]. MR imaging of 77 elite ice hockey players aged 9 to 36 years of age revealed cam morphology in 6% hips with an open physis and 56% of hips with a closed physis. This is consistent with the age of onset seen in other studies but with a

much higher prevalence compared with general population cohorts[31]. The difference in alpha angle between an open and closed physis was specific to the radial slice, with increases at the 1 and 2 o'clock positions and decreases at the 9 and 10 o'clock positions. The highest absolute values and greatest change was seen at 1 o'clock. Few studies have assessed symptoms and signs in relation to cam morphology, and a greater increase in anterosuperior alpha angle was seen in symptomatic compared with asymptomatic joints. There was also a statistically significant negative correlation between anterosuperior alpha angles and internal rotation. This raises the possibility of clinically identifying individuals that are developing cam morphology.

To further understand the effect of elite sports on hip development during skeletal immaturity, Siebenrock et al[29] recruited 37 male basketball players aged 9 to 25 and 38 age-matched non-athletic controls. MRI demonstrated that alpha angle was greatest at the 1 o'clock position for athletes but 12 o'clock for controls. Athletes had higher alpha angles throughout the anterosuperior quadrant both pre and post physeal closure, albeit this was more pronounced after closure. Considering pre and post physeal closure alpha angles within each group, there was no statistically significant change in any radial slice for the control group, but a significant increase at 12, 1, and 2 o'clock for the athletes. It is worth noting that there was no significant difference at 3 o'clock between athletes and controls given other studies have shown an increase in alpha angle at this position in general population cohorts[32]. Considering an alpha angle greater than 55 degrees in any plane, 9% of control hips displayed cam lesions compared with 89% of athlete hips. Later, Siebenrock[53] studied physeal changes in this cohort, excluding those above 22 years of age. Athletes had greater epiphyseal extension than control subjects in all positions both before and after physeal closure. However, this difference between

groups was smaller after physeal closure, contrary to expectation given cam deformity is thought to develop at the time of physeal closure. Interestingly, there was no difference in epiphyseal extension at the 1 o'clock position between athletes with an open and closed physis, even though alpha angle was highest at the 1 o'clock position. In the control group, there was greater epiphyseal extension in all positions after physeal closure, consistent with the studies of Monazzam[30] and Bixby[107]. A possible explanation is that epiphyseal extension takes place earlier in athletes. Overall the correlations between epiphyseal extension and alpha angle were not strong.

A sport attracting particular attention with respect to cam morphology pathogenesis is football, given it is the most widely played sport in the world. It is hypothesized that kicking places significant stress through the physis, which may affect hip development. The prevalence of cam morphology in football players remains unclear. Gerhandt et al[167] performed anteroposterior and frog-lateral radiographs on 96 elite male and female adult football players and found cam morphology in 68% males and 50% females. Using the same radiographic protocol, Johnson et al[168] compared hip morphology of 50 former elite football players with 50 control participants of both sexes and did not find a difference in the prevalence of cam morphology. Cam morphology was seen in 60% of male subjects and 56% male controls, and 36% female subjects and 32% of female controls. Such a high prevalence in the control group does bring the nature of this group into question.

Also using anteroposterior and frog-leg radiographs, Agricola et al[33] imaged 89 elite youth football players aged 12 to 19 and compared the morphology with control

radiographs from a database. Statistical Shape Modeling was used to automatically measure alpha angle and head-neck junction was graded qualitatively. They found that alpha angles exceeding 60 degrees were already evident at 12 years of age in both athletes and controls, suggesting that morphological changes may start prior to this age. Alpha angles above 60 degrees were present in 26% of football players and 17% of controls, which did not reach statistical significance. Cam morphology did not appear to be related to leg dominance and only limited data were available on activity levels of the control group. The authors followed up 63 of the football players with repeat imaging two years later[51]. The average alpha angle increased from 59.4 degrees at baseline to 61.3 degrees at follow-up. There was no change in the prevalence of cam morphology based on the alpha angle, but they did report qualitative changes consistent with the development of cam morphology. Whereas the work by Siebenrock et al[166] suggested that epiphyseal extension may precede cam formation, in this study the baseline measures of epiphyseal extension did not predict subsequent cam formation. The significance of epiphyseal extension therefore remains unclear. Nevertheless, in hips without cam morphology at baseline, reduced internal rotation did predict the development of cam morphology at follow-up, hence cartilaginous structures may be present at an early age that later ossify to become a cam deformity.

1.4.2 Effect of Physical Activity on the Acetabulum: Dysplasia and Retroversion

While a positive association has been shown between male gender and activity levels and the risk of cam morphology[32,33,51,52], the effect of these factors on acetabular morphology and version is unknown. There is a paucity of research with regards to the impact of factors such as elite level sport on acetabular development during adolescence. As football is thought to invoke significant stress across the proximal femoral physis[51] it is likely to affect the triradiate cartilage complex similarly. Further research is required in this area.

1.4.3 Effect of Physical Activity on Leg Alignment: Genu Varum

The development of abnormal varus leg alignment occurs during childhood and early adolescence[137,139] and is likely secondary to biomechanical overload at the medial tibial physis[156-158]. Accordingly, the majority of studies investigating the development of genu varum have focussed on the effect of sport on leg alignment during adolescence.

In 1985 Chantraine et al[20] examined the knee joints of 81 veteran footballer players aged 40 to 74 years. They observed that 73% of the cohort displayed a varus angulation. However, 47% of the cohort had undergone excision of at least one meniscus, and 56% had radiological osteoarthritis, both of which have been shown to cause genu varum[28,169]. Chantraine et al hypothesized that the high amount of medial load and torque stresses imposed on the knee joint during growth and adolescence, such as is observed in intensive practice of sports requiring cutting movements such as football[146], may contribute to the development of genu varum.

To determine the effect of football on leg alignment Yaniv et al[139] measured the intermalleolar distance in 106 male soccer players aged 10 to 21 years, and 68 age matched tennis players. They reported a significantly higher prevalence of varus leg alignment in football players compared to tennis players. They found that football players become significantly more varus after 13 years of age. They concluded that football in particular is a risk factor for genu varum, but that it may in fact be a protective mechanism. They suggested that as much as developmental genu varum plays a role in balance and stability during infancy[170], it may also do so in football in adolescence.

Witvrouw et al[153] expanded on the effect of soccer on leg alignment by measuring the intermalleolar distance in 336 male soccer players recruited from top level division teams, and 458 male non-soccer players aged 8-18 years. Similarly to Yaniv et al[139] they found a statistically significant increase in the degree of genu varum in both football players and non-football players from the age of 14. They reported that at the age of 16 to 18 years a significantly higher degree of genu varum was present in the football players compared to the non-football players. They concluded that intense football participation increases the degree of genu varum in males from the age of 16.

Thijs et al[135] measured the intermalleolar distance in 256 children aged 7 to 18 years who played sport (track and field, field hockey, basketball, volleyball, tennis, badminton, and squash) at least 3 hours a week and 256 children aged 7 to 18 years who played one hour of sport or less a week. They found that from the age of 13 years individuals who played sport had significantly more varus leg alignment than individuals who did not play sport. In both groups they found a change of leg alignment from valgus to varus at around 13 years of age. Based on the similarity of their findings to those of Witvrouw et al[153] and Yaniv et al[139] in football players, Thijs et al concluded that participation in load bearing sports in general, and not just football, may be significantly related to a greater varus alignment of the leg in adolescent boys.

Asadi et al[148] measured sports participation levels and the distances between the tibiofemoral joint line in 1500 males aged 10 to 18 years. Professional football players were defined as those who played football more than 6 hours a week. In agreement with the above studies[135,139,153], Asadi et al found the incidence of genu varum was

significantly higher in professional soccer players, and it was more prevalent in the 16-18 year age group than younger age groups. They further reported a statistically significant association between the number of sports practices and the prevalence of genu varum. Moreover, they reported that previous trauma to the knees and practicing in other sports with high load bearing activities led to an increase in the degree of genu varum. They concluded that higher incidence of genu varum in football players was due to the stress and load imposed on the knee joint.

The anatomical measures taken in the studies above provided evidence for the association between genu varum and sport, but could not provide any insight into the pathophysiology of the development of genu varum due to their lack of imaging. Moreover, anatomical measures taken by hand are more prone to error than imaging measures. Bellemans et al[143] performed full-leg length standing radiographs on 250 asymptomatic adults aged 20 to 27 years and retrospectively asked about activity levels during adolescence. They found individuals with increased sports activity during the second decade of life had more varus leg alignment. They also reported the main contributor to varus leg alignment was the medial proximal tibial angle.

Colyn et al[171] performed full-leg length standing radiographs on 100 asymptomatic male and 100 asymptomatic female participants aged between 20 and 27 years. Participants were retrospectively asked about their sports activity during adolescence in 3 age groups, 10-12, 13-14, 15-17 years in males, and 8-10, 11-12,1 13-15 years in females. They reported that males with high levels of athletic activity during adolescence were significantly more varus by approximately 2 degrees than males with low levels of

athletic activity during adolescence. In agreement with the findings of Yaniv et al[139], Colyn et al found that males who practiced football between 10–12 years and 15–17 years had more varus leg alignment than individuals who practiced other high activity sports in these age categories. They further reported that the medial proximal tibial angle was significantly lower in individuals who practiced high-activity sports during the age of 10–12 years compared to those who practiced low-activity sports during this age. Based on this finding, and in agreement with Bellemans et al[143], they suggested that genu varum was primarily determined by the medial proximal tibia.

Lahner et al[133] retrospectively analysed standing full leg radiographs of 80 symptomatic patients aged 18–60 years to determine if a relationship existed between leg alignment and cam morphology. They reported that individuals with significant varus or valgus leg alignment (defined as the distance from the weight bearing line to the centre of the knee being greater than 15mm in either direction) had significantly higher alpha angles than those with more neutral alignment, by 7.86 degrees. They found that 95.2% of individuals with significant varus or valgus leg alignment had cam morphology (alpha angle greater than 55 degrees). From these findings Lahner et al suggested that significant varus or valgus leg alignment may be a risk factor for the development of cam morphology.

To further elucidate whether disorders of leg alignment are associated with cam morphology Palmer et al[134] retrospectively analysed standing full leg length radiographs from 50 symptomatic patients and 20 controls, aged 25 to 80 years. They found that individuals requiring knee realignment surgery had a significantly higher prevalence of

cam morphology (alpha angle greater than 65 degrees) (57%) than both individuals requiring medial compartment knee replacement (40%) and controls (30%). They also report that individuals with varus leg alignment (defined as the medial proximal tibial angle being one standard deviation toward varus) were significantly more likely to have cam morphology than individuals with neutral or valgus alignment. Palmer et al concluded that individuals requiring surgery with varus leg alignment are more likely to experience epiphyseal disruption at both the proximal tibia and at the proximal femur during growth, which could be either congenital or acquired in origin.

1.5 Cartilage Composition Development

1.5.1 Cartilage Composition During Adolescence

How the composition of cartilage develops during adolescence is largely unknown and uninvestigated. Cam morphology may be evident from 14 years of age[52], and can cause changes to the composition of acetabular cartilage in asymptomatic adult patients who go on to develop radiographic osteoarthritis[97]. However, it is unknown when these changes first occur, or if cam morphology impacts cartilage composition development.

1.5.2 Cartilage Composition

Hyaline articular cartilage consists of chondrocytes embedded in an extracellular matrix that is comprised mainly of collagen in the form of a rigid meshwork of triple-helical fibrils, proteoglycans with chains of glycosaminoglycans (GAGs), cations, and water molecules[172,173]. The collagen fibres have a well-organized ultra-structure, which has been used as the basis to subdivide non-calcified cartilage into three histological zones[174,175]. Starting from the articular surface, these three zones are the superficial (tangential) zone where the fibres are mostly parallel to the surface, the transitional (intermediate) zone where the fibres are believed to be random, and the radial (deep) zone where the fibres are oriented perpendicularly to the surface. The earliest events in the development of osteoarthritis are thought to be compositional changes which precede structural changes; glycosaminoglycan (GAG) depletion and increased water content, followed by loss of collagen fibre orientation and decreased water content as disease advances[176]. These compositional changes reduce the ability of cartilage to resist deformation effectively and leave it more prone to damage[177].

1.5.3 Evaluating Cartilage Composition

Compositional Magnetic Resonance imaging (MRI) techniques are increasingly used as non-invasive surrogate markers of cartilage composition. They are capable of detecting discrete matrix alterations in cartilage that precede the development of OA[178]. A plethora of compositional sequences exist, however Delayed Gadolinium Enhanced Magnetic Resonance Imaging of Cartilage (dGEMRIC) and T2 mapping are arguably the most researched and widely used.

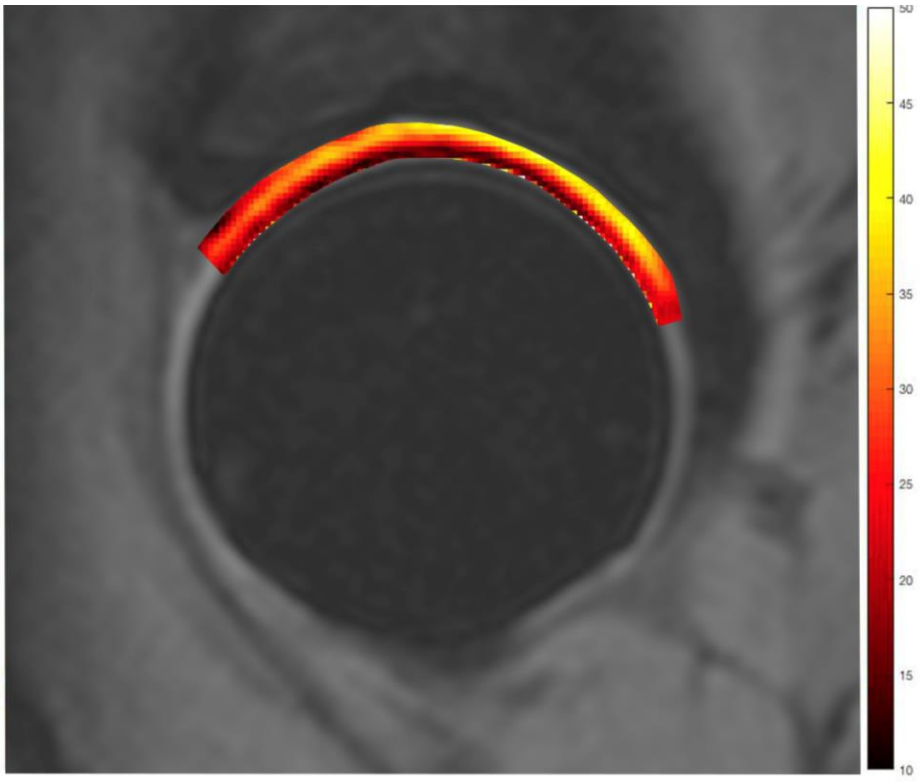
dGEMRIC of the hip is a well validated compositional MRI technique that indirectly measures cartilage glycosaminoglycan (GAG) content[179] . There is a strong correlation between in vivo dGEMRIC values and histological grade of early OA in the hip[180]. dGEMRIC is also capable of predicting disease progression in dysplasia[181] and femoracetabuar impingement (FAI) in the hip[97]. However, dGEMRIC requires the use intravenous gadolinium based contrast agents. This results in significant logistical issues due to the required delay between contrast administration and MRI acquisition. Moreover, these contrast agents are potentially nephrotoxic[182,183] and repeated use of linear gadolinium based contrast agents can result in gadolinium deposition in brain tissue[184]. Accordingly, non-contrast based cartilage-imaging techniques have been suggested to offer greater clinical applicability, such as T2 mapping.

T2 mapping is thought to be sensitive to the water content of cartilage and the integrity of the collagen network[185,186], but may also measure GAG content[187]. A correlation between T2 relaxation times and histological severity of early OA has been shown[188] and

T2 mapping has been found to enhance the ability to diagnose early osteoarthritis[189]. In contrast to dGEMRIC, T2 mapping does not require the use of a contrast agent and is available on all clinical scanners. T2 mapping has recently superseded dGEMRIC as the MRI sequence of choice for the assessment of cartilage composition. (Figure 1 – 11)

Compositional MRI is starting to gain traction as a useful tool in professional sport. It has is being used to identify athletes at risk of injury prior to the development of overt joint damage and in helping to determine time to return to play in a post-injury scenario[190]. For example, cartilage in patients with ACL reconstruction 6 months post surgery shows diminished quality (increased T2 values) and reduced in vivo resiliency to exercise induced deformation compared with controls[191], suggesting increased risk to damage.

Figure 1-11 - Sagittal Compositional MRI Map of a Male Footballer



1.5.4 Effect of Activity on Cartilage Composition

The effect of exercise on cartilage in weight bearing joints is poorly understood. Long term sporting activity is a recognized but poorly-defined risk factor for hip OA[89]. Acute biomechanical loading of cartilage is known to alter its composition transiently; for example, cartilage T2 values are elevated after running a marathon[192]. However, whether sustained exercise induces permanent changes in cartilage composition in healthy individuals is largely unknown. Healthy cartilage requires compressive loading from physical activity to develop normally and maintain form and function[193]. However, excessive loading resulting from high-intensity or long-duration exercise can lead to cartilage damage[194]. The nature and extent of changes to cartilage composition induced by exercise, and whether these are protective or predispose to OA, remains unclear.

Animal studies have suggested that physical exercise increases the GAG content in weight-bearing cartilage[195-198]. In the knee joint of dogs running 4 km/day for 15 weeks cartilage GAG content of the femoral condyles increased by 30% compared to sedentary controls[196]. Similarly, horses that were exercised 30 minutes a day, three times per week for a 6-week period increased the amount of newly synthesized proteoglycans in their cartilage compared to sedentary controls[198]. Moreover, load-bearing areas in adult animals have an increased GAG content whereas areas subjected to shear stress show different collagen orientation[199-201]. In vitro, cyclic compression of cartilage simulating walking markedly stimulates GAG synthesis[202]. It has been shown that enzymatic GAG depletion of cartilage decreases its indentation stiffness[203]. It has therefore been suggested that increased cartilage stiffness as a result of increased GAG levels is a functional means to withstand higher mechanical demands. During growth

chondrocytes are believed to develop different phenotypes by adapting to local functional requirements within the joint to produce GAG rich areas[204,205]. This would suggest that exercise during skeletal maturation might determine the cartilage composition of weight bearing joints.

Although animal models are necessary to study histological alterations in cartilage that result from exercise, they are poor models of human joint biomechanics. Muhlbauer et al[206] performed MR imaging on the right knee joints of nine male triathletes (10 hours training per week for at least 3 years) and nine inactive male volunteers (less than 1 hour of physical activity per week throughout life) aged 20 to 30 years. They found that triathletes exhibit no difference in mean or maximal cartilage thickness in the knee joint surfaces compared with physically inactive volunteers. They concluded that the level of physical activity has only a limited effect on the quantitative distribution of articular cartilage in the knee joint. Eckstein et al[207] performed MR imaging on the right knee joints of 18 male and female triathletes, and 18 inactive volunteers aged 20 to 30 years. They also found no difference in cartilage thickness; however, triathletes displayed somewhat larger knee joint surface areas. They proposed the potential reason for the lack of difference in cartilage thickness between athletes and controls is that beyond a certain thickness the cartilage is unable to receive adequate nutrition[208].

Tiderius et al[209] compared dGEMRIC values of femoral head cartilage in healthy volunteers aged 22 to 28 years with differing levels of exercise. They compared 9 elite level runners with 16 individuals who perform exercise twice weekly and 12 individuals who perform no regular exercise. They found dGEMRIC values were significantly

increased in elite level runners compared to individuals who perform regular exercise, who in turn had higher dGERMIC values than people who perform no regular exercise. They concluded that, similarly to animal models, human knee cartilage adapts to exercise by increasing the GAG content

Stehling et al[210] retrospectively analysed the T2 maps of patella cartilage and matching Physical Activity Scale scores from 120 asymptomatic subjects at risk of OA aged 45 to 55 years. They found that subjects with high activity levels had higher T2 values and a higher prevalence of cartilage lesions than subjects with lower activity levels. They concluded that T2 relaxation times in the knee might be a marker for internal joint derangement in terms of cartilage and meniscal lesions.

Roos et al[211] investigated the change in dGEMRIC values induced by a supervised exercise protocol versus no increase in exercise over a 4 month period in 30 subjects aged 35 to 50 years who had undergone partial medial meniscectomy 3-5 years previously. They found a significant improvement in dGEMRIC values in the exercise group compared to the control group, and a high correlation between dGEMRIC values and self reported change in physical activity. They concluded that compositional adaptation of cartilage via an increase in GAG content might occur over relatively short time intervals in response to exercise and mechanical loading.

Text modified from:

- Fernquest S, Palmer A, Gammer B, et al. Compositional MRI of the Hip: Reproducibility, Effect of Joint Unloading, and Comparison of T2 Relaxometry with Delayed Gadolinium-Enhanced Magnetic Resonance Imaging of Cartilage. Cartilage. 2019:1947603519841670. PMID: 30971110

1.6 Remaining Areas of Uncertainty

1.6.1.1 Cam Morphology

The studies discussed above provide valuable insight into the pathogenesis of cam morphology. However, the majority of these studies are limited by being poorly constructed, non-controlled, and measuring the bone as opposed to the cartilage alpha angle. Accordingly, many questions remain. It appears that cam deformities develop near the time of physeal closure, but it is not known at what age changes are first seen. Several studies report that no participants display cam morphology when the physis is open[31,32], however others report cam morphology as early as 10 years of age[29,30].

Distinguishing normal growth from pathological changes in morphology is a challenge. The alpha angle is a validated measure of femoral head asphericity that is used extensively in both research and clinical practice[212]. While most studies demonstrate increasing prevalence of cam morphology as skeletal maturity is reached, some studies demonstrate a fall in alpha angle with advancing age[31,107]. Alpha angles in the skeletally immature individuals must therefore be interpreted with caution[51].

All the studies discussed measure the bone alpha angle, however the ossification centre of the immature hip does not accurately reflect the shape of the cartilaginous femoral head. The bone alpha angle does not accurately measure femoral head shape until late in skeletal maturation. Cartilage alpha angles should therefore be used in child and adolescent cohorts (Chapter 2). Epiphyseal extension may offer a more valid assessment of hip development[102], but the relationship between epiphyseal extension and

subsequent cam morphology has not been strong in studies to date[51,53]. The ability to compare cohorts is severely limited by the different imaging modalities, methods of quantifying morphology, and thresholds for pathology.

There is increasing evidence that high activity levels during skeletal immaturity increase the risk of developing cam morphology. However, the nature of the activity that induces cam morphology remains unknown. Football is thought to invoke significant stress across the proximal femoral physis, particularly in the kicking leg, however morphology has not been shown to correlate with leg dominance[51]. Indeed, studies have not universally demonstrated an increased prevalence in footballers over control groups[168], although studies are frequently limited by small sample sizes and the confounding factor that a high proportion of the general population play football during youth. Furthermore, all studies to date performed in footballers have used radiography which lacks sensitivity for diagnosing cam morphology during adolescence[213].

To summarise, the most significant remaining areas of uncertainty are:

- The age at which cam morphology begins to develop
- The quantitative effect of exercise on the developing femoral head
- The mechanism of cam morphology of development

1.6.1.2 Acetabular Dysplasia and Retroversion

Prior studies have provided good insight into the development of the acetabulum during childhood, however many questions remain with regards to changes taking place during adolescence. It appears that changes in acetabular morphology may continue to take place until near the time of physeal closure, but these have been poorly categorised. Some studies report that changes only take place around the time of closure of the triradiate cartilage[132]. Other studies report changes in morphology occur throughout skeletal maturation[30,127]. Moreover, the nature of the changes to the acetabulum, and the extent to which they occur, are uncertain with contradictory evidence. Some studies report that acetabular anteversion increases with age[30,127,128,130,132], and other studies report no change in acetabular anteversion with age[129,131]. Some studies report femoral head coverage increases with age[30,128,129], and some report that no change in coverage occurs with age[132].

These uncertainties with regards to normal acetabular development stem form a lack of prospective studies of an adequate time frame in well-defined cohorts using MRI to evaluate the cartilaginous acetabular structures. The limited studies performed have mostly assessed the bony acetabulum during adolescence retrospectively using radiography[30,129,214-216]. Only a single prospective MRI study has taken place, and that only over 1 year in 65 individuals[132]. Knowledge of normal changes in acetabular version and femoral head coverage are vital as dysplasia is a known risk factor for hip osteoarthritis (OA)[23-25] and acetabular retroversion has been implicated in several pathologic hip processes and future hip OA[41,120,122,128]. However, distinguishing normal growth from pathological change is a challenge. The Centre Edge Angle (CEA) and Anteversion are validated measures of acetabular morphology[217]. However,

disagreement exists over pathological values for these measures[218] and the correct methodology of their measurement[41].

The studies discussed above have shown that high activity can influence the development of the proximal femoral physis and leg alignment, yet there is a paucity of research with regards to the impact of factors such as elite level sport on acetabular development. Acetabular concavity is dependent upon its interaction and articulation with the spherical femoral head[59,60]. A high prevalence of retroverted acetabula has been reported in patients with Femoroacetabular Impingement (FAI) [30,121]. However, the effect of the aspherical femoral head seen in cam-type FAI on the developing acetabulum is unclear.

To summarise, the most significant remaining areas of uncertainty are:

- How the morphology of the acetabulum changes with age during adolescence
- The effect of exercise on the developing acetabulum
- The effect of cam morphology on the developing acetabulum

1.6.1.3 Varus Leg Alignment

Valuable insight into the development of genu varum has been gained from the studies discussed above, yet a detailed understanding of its pathogenesis is currently limited by a lack of imaging studies performed during adolescence. It appears that leg alignment progresses from varus alignment in the infant to valgus alignment in early childhood and back to varus alignment in adolescence[136-138]. However the age at which genu varum develops is unclear with some studies stating genu varum appears at around 13-14 years of age[135,139,153], and others at 16 years of age[148]. These findings are based off anatomical measures taken by hand, which only assess external anatomy that may be heavily influenced by posture and measurement error, and fails to assess the true joint anatomy. The development of genu varum in relation to stage of skeletal maturity has yet to be investigated.

The development of genu varum has been suggested to be due to affected growth at the medial proximal tibial physis[157] resulting in a reduced medial proximal tibial angle[134,171]. However, Cook et al[157] only investigated the physis of children aged 2 and 5 years when genu varum development may continue into adolescence. Moreover, the medial proximal tibial physis has only been investigated in a skeletally mature population using radiography, which fails to adequately visualise the physis. The changes taking place at the medial proximal tibial physis in a skeletaly immature adolescent cohort have yet to be investigated. Accordingly, the mechanism of genu varum development remains largely unknown.

A number of variables have been found to influence leg alignment including

gender[143,151], obesity[152], and athletic activity[135,153]. Significant focus has been placed on the impact of sport on leg alignment, particularly the effect of playing football. However, in the prospective studies in sporting cohorts performed to date leg alignment has only been assessed using external measures[135,139,148,153]. Moreover, imaging studies have only used activity data retrospectively recalled from up to 17 years prior, introducing significant recall bias into their findings[143,171]. There are no imaging studies investigating the effect of activity on leg alignment in an adolescent cohort.

Evidence from skeletally mature cohorts would suggest there is an association between cam morphology and varus leg alignment[133,134]. However, due to the lack of imaging research in skeletally immature cohorts it is unknown whether the development of these morphologies happens concurrently or whether one of the morphologies may predispose to the other.

To summarise, the most significant remaining areas of uncertainty are:

- How leg alignment develops during adolescence
- The effect of activity on developing leg alignment
- The mechanism of varus leg alignment formation
- The relationship between cam morphology and varus leg alignment

1.6.1.4 Cartilage Composition

Results from previous studies have suggested that high activity may influence cartilage composition. However, these studies have been underpowered and in adult subjects only such that compositional changes in adolescent cartilage remain uninvestigated. Animal studies suggest that exercise results in increased GAG content in weight bearing joints[195-198], which may be an adaptive responsive to increase the stiffness of cartilage[203]. Compositional MRI studies in human adults have similarly shown that exercise induces increased GAG content[209-211]. However, chondrocytes are most responsive to load in producing GAG rich areas during skeletal growth[204,205], and the above studies were performed in adults only. As such the effect of exercise on developing cartilage composition in skeletally immature individuals is unknown.

Compositional MRI is capable of predicting progression to radiographic OA in adults with cam morphology based on reduced GAG content in the anterosuperior acetabular cartilage[97]. It is unknown when these changes first occur. Cam morphology may be evident from 14 years of age[52], but cartilage volume loss visible on radiographs may not be present for a number of decades[91]. The length of time prior to radiographic changes that cam morphology starts to cause compositional change remains uncertain.

To summarise, the most significant remaining areas of uncertainty are:

- How cartilage composition develops during adolescence
- The impact of activity on cartilage composition during adolescence
- If changes to cartilage composition secondary to cam moprhology are detectable during adolescence

1.7 Conclusions

Cam morphology, acetabular dysplasia and retroversion, and varus leg alignment are known risk factors for developing OA[24,112,113]. An in depth understanding of the period of adolescence where individuals are at risk of developing abnormal joint morphology, and the specific risk factors predisposing to this, may allow the development of a specific phenotype to inform intervention or monitoring. Early identification of at risk individuals could allow the management of OA in weight bearing joints to move towards prevention rather than treating advanced disease. However, a significant number of uncertainties remain regarding the aetiology and mechanism of formation of cam morphology, acetabular dysplasia and retroversion, and varus leg alignment.

The development of the above morphologies is believed to occur during childhood and into adolescence at around the time of physeal closure, but uncertainties remain over exact timings[29-32]. Elite level sport is a recognised but poorly defined risk factor for cam moprhology and varus leg alignment[20,21]. The effect of exercise during adolesence on the developing acetabulum is unknown. Further uncertainties surround the effect of exercise on cartilage composition.

There remains insufficient evidence to make suggestions upon the nature of any potential intervention, and the cardiovascular benefits of exercise are likely to outweigh potentially detrimental effects on hip morphology. However, individuals participating in high-level sports during youth represent a high-risk cohort that warrants further investigation.

Significant remaining areas of uncertainty are:

i) The age at which morphological changes associated with cam morphology, acetabular dysplasia and retroversion, and varus leg alignment begin and end
ii) The effect of high activity levels during adolescence on the development of cam morphology, acetabular dysplasia and retroversion, and varus leg alignment
iii) The mechanism of development of cam morphology, acetabular dysplasia and retroversion, and varus leg alignment
iv) The effect of high activity levels on cartilage composition during adolescence and when compositional changes associated with cartilage damage in cam morphology are first evident

1.8 Thesis Aims and Objectives

This thesis aims is to explore hip development using a high risk cohort, elite footballers, with specific emphasis on cam morphology, acetabular dysplasia and retroversion, leg alignment, and cartilage composition.

The following studies have been designed to address the remaining areas of uncertainty detailed above.

Chapter 2:

Aim: Define the methodology of the Femoroacetabular Impingement MRI Study (FAIM), evaluate different methods of quantifying hip and leg alignment morphology and cartilage composition, investigate the reproducibility of the imaging measures used in the study, and characterise the FAIM cohort.

To explore the effect of physical activity on hip and leg alignment development a cohort of elite level football players aged 9-18 years has been recruited and followed up over 3 years. Morphological and compositional measurements are described and applied to this cohort. Measurements that demonstrate the greatest validity and reproducibility in published literature to date are selected and adopted as outcome measures for individual studies within this thesis. Intra-observer and inter-observer reproducibility are evaluated for measurements performed within each study.

Chapter 3:

Aim: Characterise aetiological factors responsible for cam morphology development.

The aetiology of cam morphology remains uncertain, but studies suggest it may be associated with high activity levels during adolescence. This chapter investigates the timing of cam morphology development, its risk factors, and the mechanism of formation in a prospective longitudinal cohort study of elite level footballers and controls aged 9-18 years.

Chapter 4:

Aim: Investigate the effect of elite level sport on acetabular morphology development.

The effect of high activity levels on the developing acetabulum is largely unknown. This chapter investigates the timing of acetabular morphology development and the impact of high activity levels in a prospective longitudinal cohort study of elite level footballers and controls aged 9-18 years.

Chapter 5:

Aim: Characterise aetiological factors responsible for varus leg alignment development.

The aetiology of varus leg alignment remains uncertain, but studies suggest it may be associated with high activity levels during adolescence. This chapter investigates the timing of varus leg alignment development, its risk factors, and the mechanism of its formation in a cross-sectional cohort study of elite level footballs and controls aged 9-18 years.

Chapter 6:

Aim: Investigate the effect of elite level sport on cartilage composition in adolescence

The development of cartilage composition and the effect of exercise on cartilage composition remains uncertain. Studies suggest increased exercise levels may increase GAG content, but there is a paucity of research on the subject. This chapter investigates the effect of exercise on cartilage composition in a cross-sectional cohort study of elite level footballers and controls aged 9-18 years.

Chapter 2 Methods: Femoroacetabular Impingement MRI Study (FAIM)

2.1 Abstract

Introduction:

High level activity during adolescence is a recognised but poorly defined risk factor for cam morphology and varus leg alignment, and the effect of exercise on the developing acetabulum is unknown. Football players are an excellent population to investigate the pathogenesis of these conditions. Studies investigating the development of cam morphology, varus leg alignment, and acetabular retroversion and dysplasia require robust outcome measures with good validity and reproducibility. A large number of measures have been adopted in the literature, but there exists no agreed gold standard methodology or diagnostic threshold. The aim of this chapter is to define the methodology of the Femoroacetabular Impingement MRI Study (FAIM), and investigate imaging measures to be used in the study and determine their reproducibility.

Methods:

A longitudinal prospective observational cohort study was performed over three years on individuals from football club academies and an age-matched control population (9-18 years at baseline). Assessments consisted of questionnaires, clinical examination, and MRI of both hips. Measures that performed best were selected as outcome measures in this thesis; alpha angle to quantify cam morphology, epiphyseal extension ratios to characterise epiphyseal morphology, centre edge angle and acetabular anteversion to

characterise acetabular morphology, hip knee angle and the medial proximal tibial physis angle to characterise leg alignment, and T2 mapping to evaluate cartilage composition. Quantitative imaging readings were performed by two independent observers (clinical orthopaedic research fellows with a specialist interest in hip imaging) and repeated one month later. Reproducibility was assessed using intra- and inter-class correlations and Bland-Altman plots. The smallest detectable difference in measurements was calculated as the standard deviation of the mean difference between intra-observer readings from the same image multiplied by 1.96 (95% CI).

Results:

The cohort consisted of male academy footballers (121 at baseline and 69 at follow-up) and male and female controls (52 male and 54 female controls at baseline, and 35 male and 36 female controls at follow-up). Intra-class and inter-class correlations were greater than 0.90 for all primary outcome measurements in this thesis.

Conclusions:

A cohort of elite athletes and controls has been established, allowing the investigation of changes in hip morphology and leg alignment over three years. All the outcome measures discussed have demonstrated validity in published studies and have demonstrated excellent intra-observer and inter-observer reproducibility with little evidence of systematic bias or observer drift in this thesis. Insight into the strengths and weaknesses of each measurement facilitates the appropriate interpretation of results of future studies.

2.2 Introduction

High level activity during adolescence is a recognised but poorly defined risk factor for cam morphology and varus leg alignment[20,21], and the effect of exercise on the developing acetabulum is unknown. This is largely due to a lack of prospective research in adolescent cohorts using imaging modalities capable of visualizing the developing physis.

Football players are an excellent population to investigate the pathogenesis of cam morphology, abnormal acetabular morphology, and varus leg alignment for several reasons. First, football is the most widely played sport in the world, hence findings are likely to be applicable to the general population. Second, members of elite football academies follow an intense training programme from eight years of age. This standardised exercise programme, during which players have limited opportunity to participate in other sports, provides a well-controlled population for study. Third, football clubs continue to increase the duration and intensity of training, and this trend is now being replicated in other sports. It is not known whether this intense physical activity during growth is to the detriment of player health.

This chapter will discuss the development of a cohort of adolescent elite level footballers and age matched controls followed up over three years, and the imaging measures used to investigate changes in their hip and knee morphology. Robust methods for the quantification of cam morphology, acetabular morphology, leg alignment and cartilage composition are required to study disease pathogenesis. Measurements must demonstrate validity and reproducibility. Validity refers to the degree with which a

measurement reflects the concept under investigation (accuracy). Reproducibility describes variation in repeat measurements and hence the stability and consistency of readings (precision) (Appendix A1). A range of alternative measurements has been adopted in the literature to date. These are considered in detail in order to select optimal outcome measures for subsequent studies.

2.3 Aims

1) Define the methodology of the Femoroacetabular Impingement MRI Study (FAIM)
2) Investigate imaging measures to be used in this thesis and determine their reproducibility
3) Present baseline and follow-up characteristics of the FAIM cohort

2.4 Ethical Approval

Oxford University Medical Sciences Inter-Divisional Research Ethics Committee (MSDIDREC- C2-2013-11)

2.5 Study Design

This study is a longitudinal prospective observational cohort study to allow the assessment of hip morphology and leg alignment development within an individual. Hip morphology and leg alignment development in footballers (athletes) was compared with an age-matched general population control group. This thesis reports the study design and results from three year follow-up of this cohort.

2.5.1 Sample Age and Sex

The chronological age of proximal femoral physis closure is variable and estimated to be an average of 13 years for females and 15 years for males[214,219]. However, given the decreasing age of SUFE presentation[69], proximal femoral physeal closure may take place earlier than suggested by historical studies[219]. This observation is consistent with the decreasing age of sexual maturity[220]. In a cohort that included both sexes, Kienle et al reported an average age of proximal femoral physeal closure to be 13.4 ± 1.5 years (range 11-16)[31]. The criteria used to define physeal closure is also a source of variability.

The absence of cam morphology when the physis is open[31,32], and high prevalence of cam morphology when hips are skeletally mature led to the proposal that cam morphology develops around the time of physeal closure[29-32,51]. However, other studies

have reported cam morphology as early as ten years of age[30,56]. Therefore, the youngest age group in this study was selected as nine years at baseline. Football players sign with a club and commence standardised training aged eight years and clinical experience has shown that patients below this age are less tolerant of MRI. The upper age was selected as 18 years as at this age all participants would be expected to have reached lower limb skeletal maturity[219].

In order to compare hip development in females and males, the general population cohort includes both sexes. The well-documented differences in the prevalence of cam morphology between males and females may reveal valuable insights into the pathogenesis. Although participation in female football is growing rapidly worldwide, there is not yet equality with respect to player development. The footballer (athlete) cohort therefore includes only males, however, the Premiership Football Club where this study was carried out had their first intake of female academy players during follow-up period, allowing possible subsequent extension of this study to include female footballers. The high injury rates reported in adolescent female footballers is a particular concern and an area of current research[221].

2.5.2 Sample Size

The primary outcome measure of this study was change in average alpha angle at the anterosuperior femoral head-neck junction measured on MRI radial slices. Sample size calculations were based on existing literature at 80% power and 5% significance using a two-sided t-test, where only one hip was considered for each participant. The desired detectable difference and standard deviation are based on comparable cohorts.

In order to investigate the age of cam morphology development, the study sought to detect differences in alpha angle pre and post physeal closure in an athlete cohort and a general population control cohort. The smallest change in alpha angle is reported in control populations and Carsen et al found a mean change of 4.85 degrees and a maximum standard deviation of 7.05 degrees[32]. Calculations revealed 35 participants were required either side of physeal closure for each study population at baseline, and 35 participants were required to be followed-up until after physeal closure.

This study also aimed to investigate differences in the alpha angle between the athlete cohort and general population controls. When the physis is open, Siebenrock et al. found a mean difference of 6.2 degrees between athletes and controls and a maximum standard deviation of 7.4 degrees. Once the physis had closed there was a mean difference of 16.9 degrees and a maximum standard deviation of 7.6 degrees[84]. This is comparable to the reported 15 degree expected difference in alpha angle between patients with cam morphology and normal morphology[222]. Calculations revealed 24 participants were required pre-physeal closure in each cohort, and 5 patients post-physeal closure in each cohort at baseline. Siebenrock et al excluded symptomatic individuals from their control cohort which is not the case in this study, hence a greater number of participants may be required.

2.5.3 Study Population

The study design offers three cohorts to investigate cam lesion pathogenesis with the intention of extending the study to female footballers in the future. These groups are male footballers (athletes), male controls, and female controls. Participants were

recruited from the age of 9 to 18. Taking into account the sample size calculations, expected age of physeal closure, and available resource, adequate power was anticipated with a male athlete cohort of 100 and a general population cohort of 50 males and 50 females at baseline (Table 2-1). Cohorts were loaded for younger age groups to: i) Ensure an adequate number of individuals have an open physis to satisfy the power calculations. ii) Enhance the longitudinal component of the study as drop-out rates can be as high as 30% in athletic cohorts due to national and international relocation to continue their careers[51]. This is more common in players over the age of 16 on completion of their education.

Table 2-1 - FAIM recruitment target at baseline

Age at Baseline	Number of Participants		
	Football Academy	Controls	
	Male	Male	Female
9	20	10	10
10	20	10	10
11	10	5	5
12	10	5	5
13	10	5	5
14	10	5	5
15	10	5	5
16 - 18	10	5	5
Total	100	50	50

2.5.4 Inclusion and Exclusion Criteria

Inclusion criteria were solely whether or not a participant was a member of a target population. Since a control group was sought that represented an accurate cross-section of the general population, it was accepted that this group might also contain some high-level athletes.

To ensure a representative cohort of athletes and general population controls, the only exclusion criteria were previous hip surgery, because prior procedures are likely to influence hip development, contraindications to MRI, and an inability to provide informed consent.

2.5.5 Baseline Recruitment

2.5.5.1 Controls

Permission was sought from local schools to recruit a control population. A variety of forums were used to advertise the study, from delivering assemblies at schools, setting up stalls at parent-teacher meetings, and placing study information in newsletters. Emphasis was placed on explaining that individuals of all activity levels were sought, and that the primary aim was to understand how hips develop. A concern was that the collaboration with a football club might bias control groups towards more active individuals. At engagement events, interested parents were handed an invitation pack. The invitation pack included an invitation letter, participant information sheet, MRI safety form, consent form (with example of completed form), and a stamped addressed envelope for return. Queries were addressed through email or telephone

communication. The newsletter text contained a phone number and email address that interested parties could use to request an invitation pack. Individuals under 16 years of age required written consent from parents in order to participate.

2.5.5.2 Athletes

The study was performed in collaboration with Southampton Football Club (SFC). Academy players at SFC train in an age group defined by whether their birthday falls before or after 31st August. An Under 10 player at baseline was born before 31st August 2004. Participants were recruited in relation to their team rather than chronological age to facilitate the scheduling of assessments and to minimise disruption to their football training and education. The football club allocated every academy player a study ID and provided the research team these IDs and the team to which each player belonged. This ensured no personal details were shared prior to a player consenting to participate in the study. Study IDs by team were entered into STATA 14.1 (College Station, TX, USA) in ascending order. Each ID was assigned a random number based on a uniform distribution with range 0-1 and a seed on 17051982. These random numbers were then placed in ascending order within each team and the first 10 or 20 IDs were invited to participate. These IDs were passed onto the football club, who provided invitation packs to the selected players to take home to their parents. Since SFC academy football players often reside large distances from the club, living with host families for training days, it was not always possible to arrange face-to face meetings with parents. Participants were also able to hand completed packs to staff at the football club. When a player declined participation, the next ID from that age group was selected.

Participants were also recruited from Oxford United Football Club (OUFC). OUFC is an elite level football academy, but of smaller scale than SFC. Permission was sought from OUFC to attend training sessions and parent management meetings to advertise the meeting. All interested players and parents were handed an invitation pack. Study IDs for OUFC and control cohorts were replicated in a similar fashion to the SFC cohort such that assessors were blinded to participant characteristics such as cohort and age when interpreting data such as MRI scans.

2.5.6 Patient and Public Involvement

An essential issue to address with this research design was the potential impact of the results on player careers. If a football club is informed of previously undiagnosed pathology, the earning potential of a player may be adversely affected. Conversely, awareness of pathology might allow the football club to modify training or provide tailored strength and conditioning exercises to the benefit of a player. Therefore, the opinion of players and their parents was sought on how the data should be managed at parent engagement events organised by the football club. In total, the project outline was presented to 50 parents, and their ideas and concerns were sought. There was unanimous agreement from parents that the future health of their children outweighed future earning potential. As a result, very few had an objection to sharing all player data with the football club. The research team held reservations given the significance of many potential MRI findings, such as mild dysplasia, is not known in the context of footballer performance during their playing years. The approach was therefore to only pass on information relating to the presence and magnitude of cam lesion morphology to the club medical team. The consent form included a statement asking whether or not

participants were agreeable for details of their hip shape to be passed onto the football club. This required a 'yes' or 'no' response, and participants who declined the release of this information remained welcome to participate in the study. The justification for passing on information relating to cam morphology was that the prevalence amongst footballers is expected to be very high, and should a player develop symptomatic femoroacetabular impingement, physiotherapy is an effective management strategy[223]. Team coaches and club management who oversee player transfers did not have access to study data.

2.5.7 Follow-up Recruitment

2.5.7.1 Controls

Participants were invited for repeat assessment three years after initial baseline visit via post, email, and telephone. Participants were initially sent an invitation pack by post. The invitation pack included an invitation letter, participant information sheet, MRI safety form, consent form (with example of completed form), and a stamped addressed envelope for return. The invitation letter included a return slip with the option of not wishing to attend follow-up and also being fully withdrawn from the study for any future assessments. Some individuals had changed address following baseline assessment so emails were sent up to 1 month after letter invitation was sent. Emails included electronic copies of the invitation pack. Individuals who responded to invitation for follow-up assessment were contacted via email and telephone to arrange attendance for assessment.

2.5.7.2 Athletes

SFC participants who were still within the academy set-up were handed invitation packs by the football club. Completed packs could be sent directly back to the study team or football club. OUFC and SFC participants who had left the academy with a known forwarding address were contacted in the same way as controls.

2.6 Questionnaire

Participants completed a questionnaire on the day of assessment at both baseline and follow-up. Younger participants received assistance from parents and guardians, and if they were not present for the assessment, arrangements were made to complete the questionnaire during the preceding week.

2.6.1 Patient Demographics and Past Medical History

The following information was collected:

Demographics:

i) Date of Birth
ii) Sex
iii) Dominant Hand
iv) Dominant Leg
v) Weight
vi) Height
vii) Ethnicity

Past Medical History:

i) Medical Conditions
ii) Menstrual history (if female)
iii) Medications
iv) Supplements
v) Musculoskeletal History

a. Legg-Calve-Perthes, SUFE, Avascular Necrosis, or Dysplasia
b. Surgery
c. Fractures
d. Acute injuries in past year (unable to play sport for more than 2 weeks)
e. Chronic injuries in past year (modified activity for more than 4 weeks)

2.6.2 Activity Levels

Activity was evaluated using two methods:

i) SFC and OUFC Academy (elite footballer) versus general population controls
ii) Physical Activity Questionnaire (PAQ) for older children (aged 9–13 years) and adolescents (aged 14–18 years)[224]. (See Appendix A.1)

Academy football players commence intensive training at eight or nine years of age and follow a standardised age-specific training programme. Their principal playing position was documented. The control population was expected to include a wide range of activity levels. Accurate quantification of sports and exercise is challenging and this study used the validated Physical Activity Questionnaire for Older Children (PAQ-C) and for Adolescents (PAQ A)[224]. This collects data on sport and exercise undertaken during a seven-day period to provide an estimate of physical activity levels. It collects information on sport and exercise undertaken during an average week and provides a summary score of physical activity levels (a score of 1 indicates low physical activity, whereas a score of 5 indicates high physical activity)[225]. However, the score does not provide a measurement of duration or intensity of exercise. Participants were asked to complete this to reflect an average week during the current or most recent school term.

2.7 Imaging Measures

2.7.1 Assessment of Femoral Head Morphology

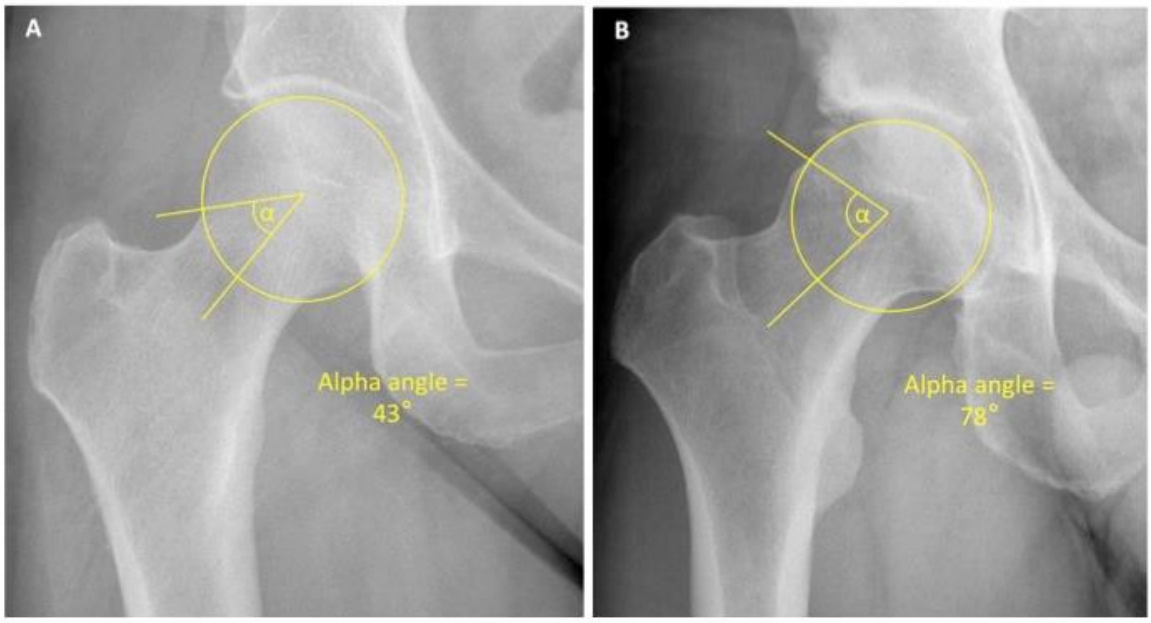
2.7.1.1 Magnitude of Cam Morphology

A large number of measurements have been proposed for the quantification of cam morphology and applied to a range of imaging modalities. Cam morphology is most frequently measured on anteroposterior pelvic radiographs due to the availability of this projection in large cohort studies. This projection will therefore be used to illustrate each measurement, however, three-dimensional imaging strategies are more sensitive for the diagnosis of cam morphology[213], as will be discussed.

2.7.1.1.1 Alpha Angle

The alpha angle was first described by Notzli et al[212] when the measurement was applied to axial oblique MR images. A line is drawn from the centre of a best-fit circle surrounding the femoral head to the midpoint of a line transecting the narrowest portion of the femoral neck. Another line is then drawn from the centre of the best-fit circle to where the contour of the femoral head first exits the best-fit circle. The angle between these two lines is denoted the alpha angle and increases with loss of concavity at the head-neck junction[212](Figure 2-1).

Figure 2-1: Anteroposterior radiographs with alpha angle measurement of a hip with normal morphology (A) and cam morphology (B)



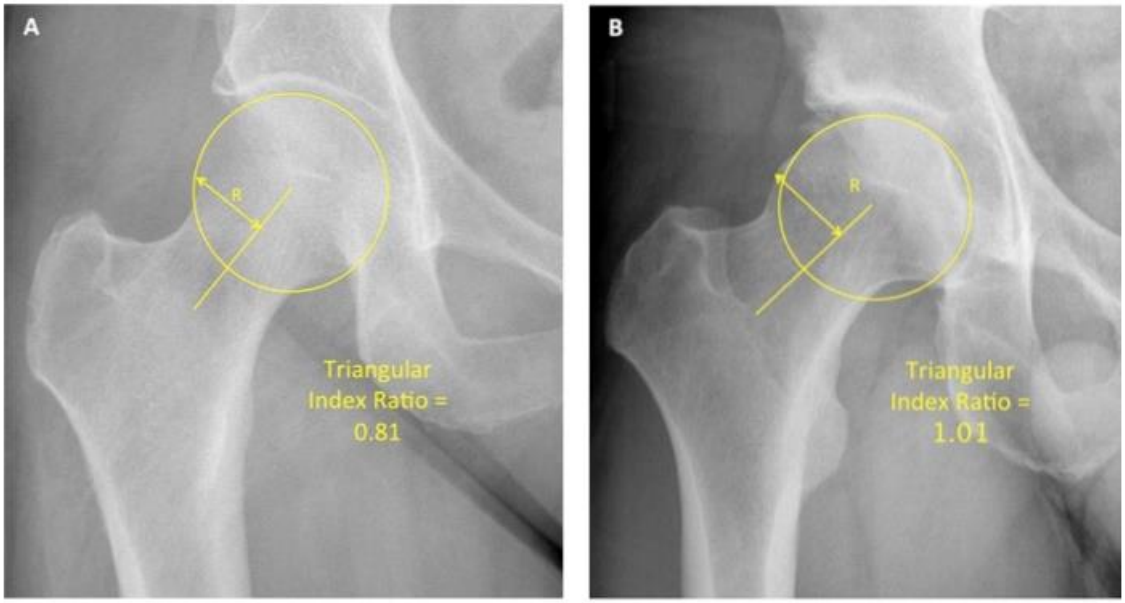
Notzli reported a mean alpha angle of 42 degrees for an asymptomatic control group compared with 74 degrees in patients with clinical femoroacetabular impingement, and suggested that angles greater than 50 degrees were abnormal[212]. The threshold for defining cam morphology has since been extensively investigated and there is no agreed value. Defining a threshold is further complicated by the application of this

measurement to different imaging protocols and different cohorts. The alpha angle has shown variable, albeit satisfactory reproducibility[22]. Alpha angle validity is demonstrated by its ability to predict chondropathy[226] and future osteoarthritis[15]. It is the most widely used measure of cam morphology in the current literature[227].

2.7.1.1.2 Triangular Index

Gosvig proposed an alternative measure of cam morphology denoted as the triangular index[228]. To determine this value, a best-fit circle around the femoral head and a line along the femoral neck axis are plotted, as with the calculation of the alpha angle. A point is then marked along the femoral neck axis at one-half radius lateral to the centre of the best-fit circle. From here, a line is drawn perpendicularly to the outer border of the femoral head-neck junction. The length from this point to the centre of the best-fit circle is recorded (R). (Figure 2-2)

Figure 2-2: Anteroposterior radiographs with triangular index ratio measurement of a hip with normal morphology (A) and cam morphology (B)

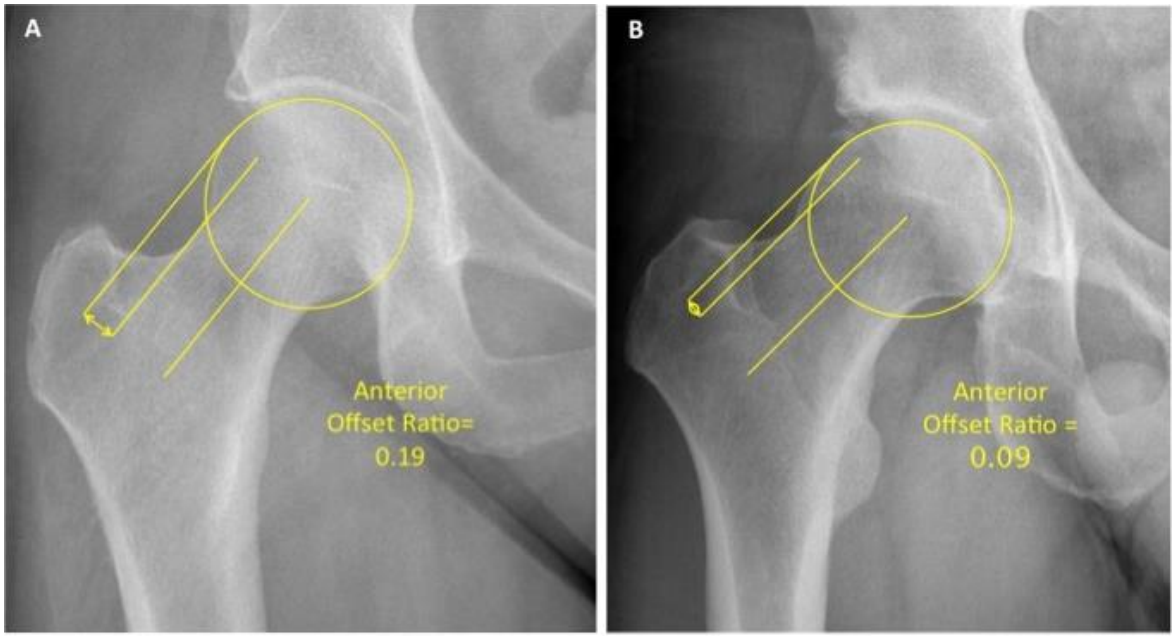


Gosvig stated that cam morphology is diagnosed when the length of line R exceeds the radius of the best-fit circle by >2mm on a radiograph with 1.2 magnification. It is also suggested that the triangular index is more reproducible than the alpha angle and less susceptible to inaccuracies resulting from variations in hip rotation on both anteroposterior and lateral radiographs[228]. The binary outcome that does not account for the size of the femoral head is a significant limitation of this measurement. However, triangular index has also been adopted as a continuous variable by expressing R as a ratio of the best-fit circle radius[91] (Figure 2-2). Triangular index has not been widely adopted in large longitudinal cohort studies and lacks the validity of alpha angle.

2.7.1.1.3 Offset

A number of alternative measurements focus on the offset between the femoral head and neck. A reduced head-neck offset is associated with symptomatic femoroacetabular impingement[229]. There are many different measurements of femoral head-neck offset[107,230]. The 'anterior offset ratio' (AOR) is frequently adopted[231]. A line is drawn along the central axis of the femoral neck (that does not necessarily pass through the centre of the femoral head) and parallel lines are then drawn along the anterior cortex of the femoral neck and along the most distant portion of the femoral head. The anterior offset is the perpendicular distance between these two parallel lines, and the AOR is calculated by dividing this value by the diameter of the femoral head (Figure 2-3).

Figure 2-3: Anteroposterior radiographs with anterior offset ratio measurement of a hip with normal morphology (A) and cam morphology (B)



Cam morphology is diagnosed if the AOR is less than 0.17[231]. As with most offset measurements, a limitation of this value is the subjective placement of the line along the

central neck axis, offering less reproducible readings than the Gosvig ratio and alpha angle[232]. As with the triangular index, offset measurements have not been widely adopted in large longitudinal cohort studies and lack the validity of alpha angle.

2.7.1.2 Alpha Angle as a Measure of Cam Morphology

Alpha angle is adopted as the primary measure of cam morphology in this thesis given the measurement has demonstrated good validity and reproducibility, and its widespread adoption in the current literature allows comparisons between studies. However, there is significant variation in how alpha angle is measured, which must be considered during study design and data analysis.

2.7.1.2.1 Imaging Strategy

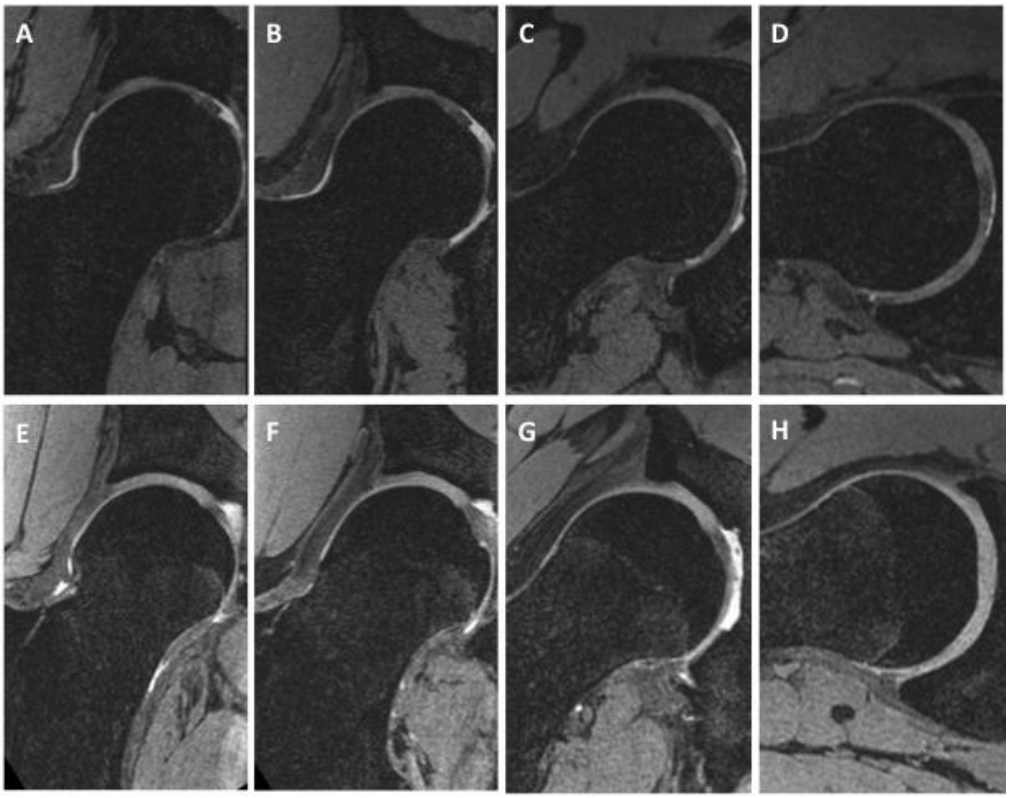
Measurements to quantify cam morphology are sensitive to the imaging strategy employed[232,233]. Radiography is the most widely adopted modality given it is rapid to acquire images, relatively inexpensive, and readily available. Anteroposterior pelvis radiographs are available for a number of large longitudinal cohort studies[15,91,92,234] and as a result cam morphology has been most extensively researched with alpha angle measurements on this projection. In a clinical setting, femoral head-neck asphericity is frequently assessed on an anteroposterior radiograph given this is the first-line investigation in most instances of hip pain. However, asphericity may be missed on this view and lateral projections are recommended[233]. Frequently adopted lateral views for imaging the proximal femur include cross-table lateral, Dunn view, and frog-leg lateral. Although the Dunn view in 45 degrees of hip flexion may be slightly more sensitive for the detection of cam morphology[235], the cross-table lateral view with internal rotation is

comparable and positioning is more straight-forward[233]. Intra- and inter-observer reliability is higher for cross-table lateral views, although a higher radiation dose may be required[236]. Studies report very conflicting conclusions as to the value of frog leg lateral views for the quantitative measurement of cam morphology[237,238]. A combination of anteroposterior pelvis and cross-table lateral hip with internal rotation views are the recommended radiographic protocol for clinical investigation of cam morphology[233]. This protocol also allows evaluation of acetabular morphology that is critical for the complete evaluation of femoroacetabular impingement[231].

Alpha angles may be maximal at the anterior or superior head-neck junction, however, they are most frequently maximal at an anterosuperior location[95,222,229,239,240]. As a result, cam morphology may not be fully visualised when imaging planes are limited to anteroposterior and lateral views[213]. CT and MRI have been utilised to allow three-dimensional assessment of morphology[241]. MRI may be preferred given it does not require ionising radiation and allows simultaneous assessment of the soft tissues such as cartilage and labrum. A disadvantage is that unlike CT, fully automated segmentation of bone morphology is not currently possible. Radial slices around the femoral neck axis allow direct assessment of head-neck morphology at any location. These are described in terms of a clockface with 12 o'clock superior, 3 o'clock anterior, 6 o'clock inferior, and 9 o'clock posterior for both the left and right hip. Radial slices are now considered the optimal method of quantifying cam morphology (Figure 2-4). Relying on only anteroposterior and lateral radiographs may fail to detect asphericity in over a third of cases[213]. Notzli measured the alpha angle on only an axial oblique MRI and this failed to identify 54% of cases where the alpha angle is raised when considering all radial planes[240]. In conclusion, to optimally evaluate cam morphology, a radiographic protocol

should include an anteroposterior and cross-table lateral view, and three-dimensional CT or MRI protocols should include imaging in radial planes. An issue that has not been well addressed to date is whether the MRI sequence employed influences cam morphology measurements. Measurements of cam morphology conventionally refer to bone rather than cartilage, although it may be important to also consider overlying cartilage morphology. A 3D gradient-echo water selective (Philips WATSf) pulse sequence was selected to measure cam morphology for the studies described in this thesis, as this provides excellent contrast between bone and cartilage, and good visualisation of cartilage morphology (Figure 2-4).

Figure 2-4: Superoanterior radial MRI planes in a participant with normal hip morphology (A-D) and cam morphology (E-F): 12 o'clock (A&E), 1 o'clock (B&F), 2 o'clock (C&G), and 3 o'clock (D&H).



2.7.1.2.2 Thresholds to Define Cam Morphology

There are no agreed diagnostic criteria to define cam morphology and this has resulted in a wide range of reported prevalence. Proposed alpha angle diagnostic thresholds range from 50 degrees to 83 degrees[212,228,232]. These thresholds are frequently based on statistical analysis, for example, 95% confidence intervals or standard deviations away from the mean within a cohort. Other authors have noted a bimodal distribution of alpha angle measurements. In a combined dataset of two general population cohorts consisting of 2005 participants, a normal distribution was noted up to an alpha angle of 60 degrees on anteroposterior radiographs. It was proposed that this bimodal distribution represented two discrete populations, and that alpha angles above 60 degrees define the presence of cam morphology in both males and females[22]. Interestingly, a bimodal distribution is not seen with other measures of cam morphology such as the Gosvig ratio, and this distribution may reflect the measurement tool rather than the pathology.

Alpha angle thresholds derived from statistical analysis may not offer values of clinical relevance, whereas general population longitudinal cohort studies provide insight into values that may represent pathological morphology. The CHECK cohort consists of individuals aged 45 to 65 years at baseline with early symptomatic osteoarthritis of the hip or knee. At baseline, no participant demonstrated radiographic hip osteoarthritis (Kellgren-Lawrence <2). Within 5 years of follow-up, 2.76% had developed hip osteoarthritis (Kellgren-Lawrence >2) (n=723)[15]. The Chingford cohort consists of a general population cohort of females aged 44 to 67 years at baseline recruited from a General Practice in London. Within 19 years of follow-up, 11% had developed incidental radiographic hip osteoarthritis (Kellgren-Lawrence > 2) (n=487)[91]. When these two

cohorts were combined, an alpha angle threshold of 78 degrees (95% CI 62 – 87 degrees) on an anteroposterior pelvis radiograph gave rise to the greatest area under the ROC curve at 0.69 (95% CI 0.62 – 0.75) and this was proposed as the threshold for pathological cam morphology in males and females[22]. It is likely that this threshold is different for each imaging strategy employed, and radiographs are less sensitive than radial plane MRI for the diagnosis of cam morphology[213]. Furthermore, the development of hip osteoarthritis secondary to cam morphology is likely to be influenced by a number of factors including activity levels, acetabular morphology, and inherent joint susceptibility[7]. The positive predictive value of cam morphology measured using the alpha angle for the development of osteoarthritis is thought to be as low as 6-25%[15]. There appears to be dose-response to the magnitude of cam morphology and it may be more valuable to study this relationship than to apply artificial diagnostic thresholds. Prospective study of the Chingford cohort gave an odds ratio 1.05 (95% CI 1.02-1.09) for every degree increase in alpha angle above 65 degrees on baseline anteroposterior radiographs for predicting the development of radiographic osteoarthritis at 19 years.

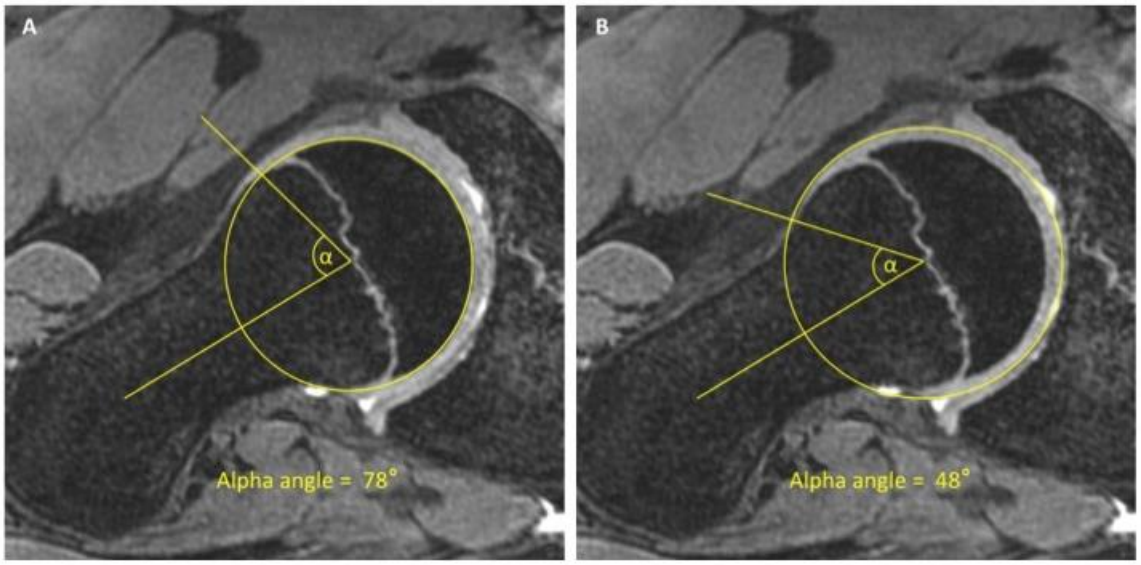
2.7.1.2.3 Measuring Cam Morphology in the Adolescent Hip

There are specific challenges to measuring alpha angles in skeletally immature hips. It may not be clear whether changes in hip morphology with age are pathological or represent normal development, and this may only be established by following hips to skeletal maturity. Also, whereas alpha angle is conventionally measured on bone morphology, in developmentally immature hips the secondary ossification centre does not provide an accurate representation of overall hip morphology, which is primarily determined by the epiphyseal cartilage and articular cartilage[242]. Alpha angle

measurements on articular cartilage rather than bone may be more clinically relevant at all stages of hip development given it is overlying cartilage that abuts the chondrolabral junction in femoroacetabular impingement. In early hip development, bone alpha angles are elevated because the femoral head ossification centre is small relative to the metaphysis (Figure 2-5). Cartilage alpha angles therefore appear to have greater validity over bone alpha angles as a measure of hip shape during development and are selected as the primary outcome measure for subsequent studies in this thesis.

Figure 2-5: Bone (A) and cartilage (B) alpha angle measurements at 3 o'clock in a ten year old male.

Note the artificially raised alpha angle in the bone measurement due to the relatively small epiphysis compared to the metaphysis.

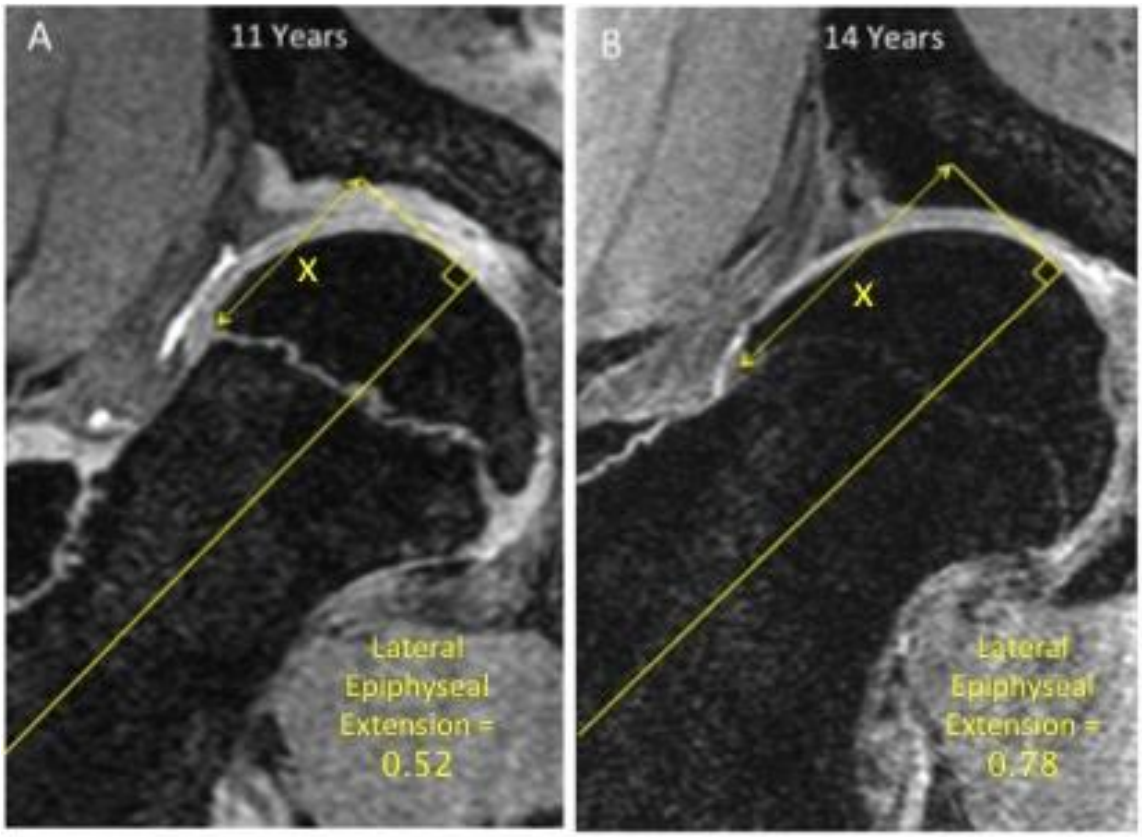


2.7.1.3 Assessment of Physeal Morphology

Epiphyseal extension is proposed as a mechanism of cam morphology development[102], and robust measures of physeal morphology are therefore required. Studies to date quantify epiphyseal extension as the distance from the medial femoral head to the most distal extent of the epiphysis along a line parallel to the axis of the femoral neck (created by a line extending from the centre of a best-fit circle surrounding the femoral head to the midpoint of a line transecting the narrowest portion of the femoral neck) and divided by the diameter of the femoral head[166]. This quantitative measurement is termed 'epiphyseal extension' in this thesis. Epiphyseal extension can be measured at each clockface on radial MRI planes (Figure 2-6).

Figure 2-6: Lateral epiphyseal extension measurements at 1 o'clock position.

Elite level football player at baseline age 11 years with normal morphology (A) and at follow-up age 14 years where the individual has developed cam morphology secondary to increased lateral epiphyseal extension (B). Lateral epiphyseal extension = x/femoral head diameter



SUFE is also postulated as a potential mechanism of cam morphology development[72,98-101]. The ratio between epiphyseal extension at opposing sides of the femoral head is termed 'physeal ratio' and is used to quantify physeal tilt. Physeal tilt measurements give rise to opposing trends in epiphyseal extension and SUFE.

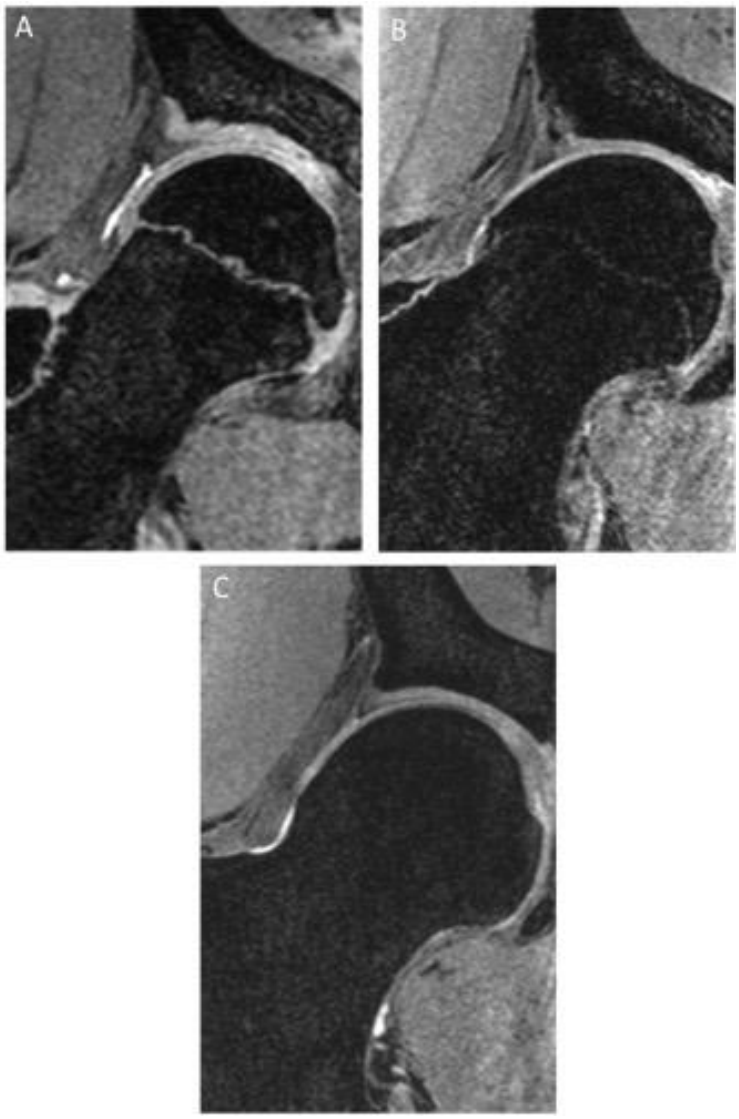
Once a physis is closed it is difficult to define the physeal scar on the gradient-echo water selective (WATSf) sequence, therefore, a 3D proton density fat saturation (PDFS) MRI sequence was included for the FAIM cohort that explored physeal development.

2.7.1.3.1 Physeal Maturity

Skeletal maturity can be qualitatively assessed by determining the stage of physeal maturity. The most commonly used methodology is to grade whether the physis of each hip is open, partially closed, or closed[52]. A physis is deemed partially closed when there is contact between the epiphysis and metaphysis but the physis remains visible. When considering physeal closure as a binary variable, a partially closed physis is considered closed. (Figure 2-7).

Figure 2-7: Appearances of an Open, Partially Closed, and Closed Physis on WATSf MRI Sequence

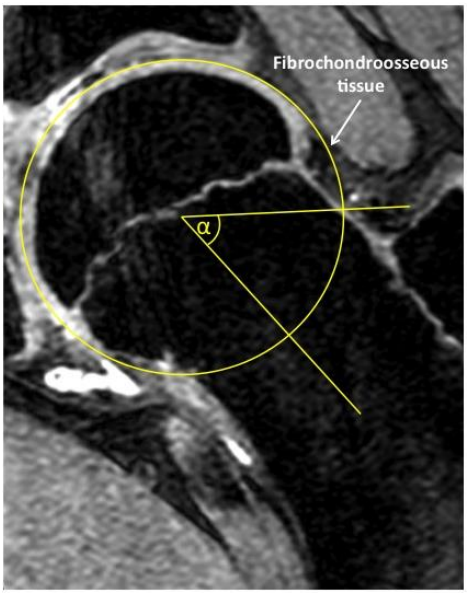
A: Open Physis B: Partially Closed Physis C: Closed Physis.



2.7.1.4 Assessment of Fibrochondroosseous Tissue

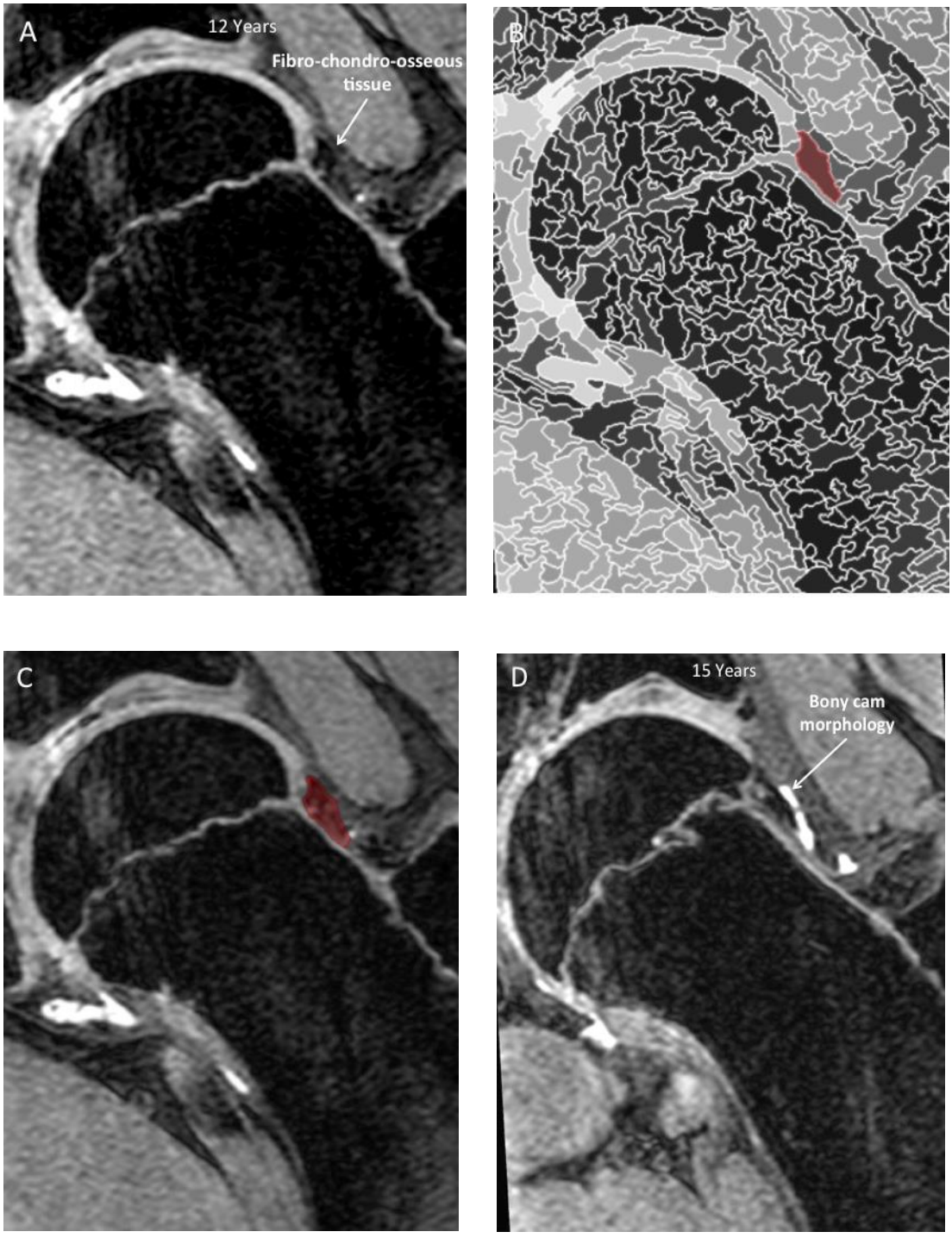
In the immature hip there is a discrete circumferential fibrochondroosseous structure at the femoral head-neck junction site that consists of the ossification groove of Ranvier and the perichondrial fibrous ring of La Croix. This structure is thought to be responsible for lateral expansion and structural support of the physis[54] (Chapter 1). Research to date has only qualitatively assessed this structure. Palmer et al[52] observed that the development of cam morphology was often preceded by soft tissue hypertrophy in the area around the perichondrial fibrous ring of La Croix. Although usually most pronounced at 1 o'clock, this hypertrophy and extension was concurrently observed at adjacent positions. This would suggest that the size of the fibrochondrooseous tissue at the femoral head-neck junction represents an important factor in the mechanism of cam morphology development. However, there exists no validated measure to quantify the size or location of this fibrochondroosseous tissue. Existing validated measures for femoral head-neck morphology, such as the alpha angle, were often found to be unable to account for the presence of this soft tissue hypertrophy (Figure 2-8).

Figure 2-8: MRI radial slice in 12 year old male with significant fibrochondrooseous tissue hypertrophy at the femoral head-neck junction. Measurement of the alpha angle fails to account for the tissue mass.



Due to a lack of validated measures in the existing literature custom designed software was used in this thesis to measure the Fibrochondroosseous Tissue Area (FTA) via a semi-automated segmentation methodology[243]. The software allows fully automated partitioning of radial slices into a terrain map, in which the intensity of each voxel represents its altitude in the terrain. The lowest layer of the hierarchy consists of the voxels in the source image. At each stage of the recursion a coarser layer of regions is generated such that each region contains sub-regions present in the layer below. Since different kinds of tissue have different scan intensity signatures, the gradients between areas of interest will be emphasised by this process. The boundaries between regions mould themselves around relevant boundaries between tissues. As the FTA is composed of different tissue than the surrounding epiphysis, metaphysis, physis, cartilage, labrum, and soft tissue it is identified as a separate tissue area in this process. Once the partition hierarchy is in place, user selection of the anatomical structure of interest proceeds. In this case the area of the terrain map that corresponds to the circumferential ossification groove of Ranvier and perichondrial fibrous ring of La Croix is selected from radial images to provide an average tissue area. (Figure 2-9)

Figure 2-9: Area of fibro-chondro-osseous tissue shown in an elite level football player at baseline age 12 years (A), with hierarchical partitioned terrain map overlaying the radial image (B) and user selection of the Fibrochondroosseous Tissue Area (C), and new bony cam morphology at follow-up age 15 years (D)



Text modified from:

- Fernquest et al. Segmentation of hip cartilage in compositional magnetic resonance imaging: A fast, accurate, reproducible, and clinically viable semi-automated methodology. J Orthop Res. 2018. PMID 2946917

2.7.2 Assessment of Acetabular Morphology

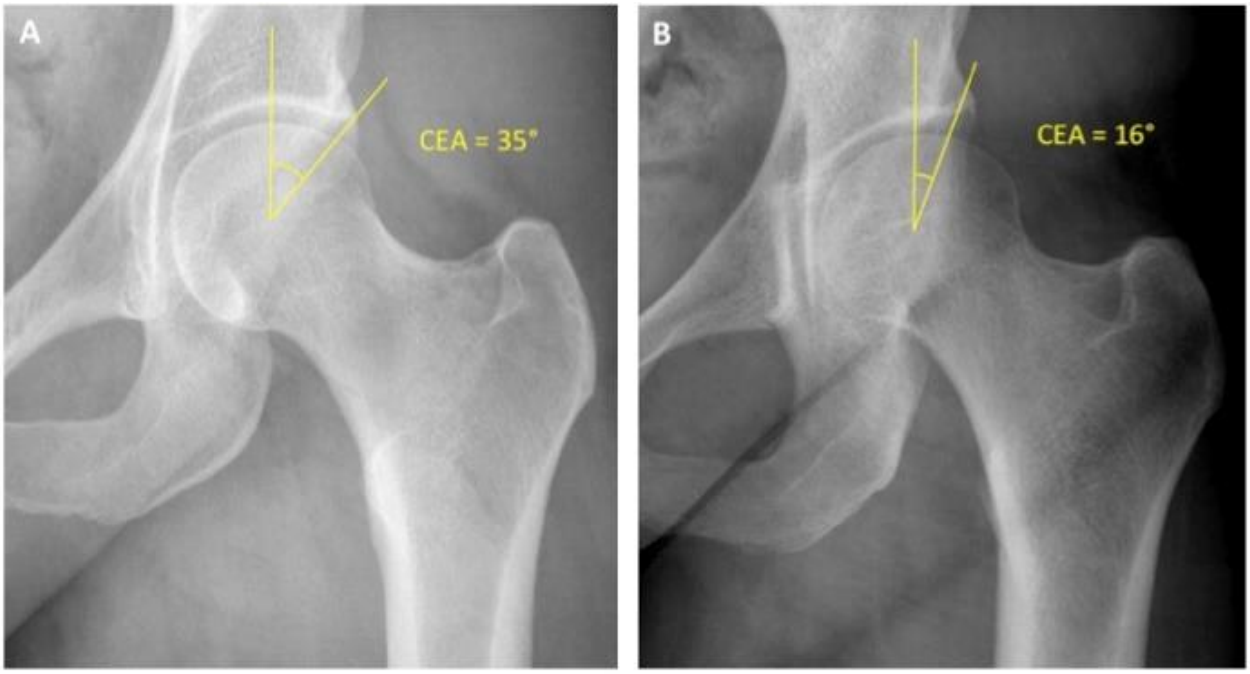
2.7.2.1 Assessment of Acetabular Shape

A number of measurements have been proposed for the quantification of acetabular shape and applied to a range of imaging modalities. Acetabular morphology is most commonly measured on anteroposterior radiographs, however three-dimensional imaging strategies such as CT and MRI are becoming more frequently used due to their increased sensitivity.

2.7.2.1.1 Lateral Centre Edge Angle (CEA)

The Centre-Edge Angle (CEA) was first described by Wiberg in 1939[112] as a measurement of femoral head coverage on AP radiographs of the pelvis. The lateral CEA is formed by the angle between a line from the centre of the femoral head to the lateral edge of the sourcil and a vertical line from the centre of the head (Figure 2-10). Wiberg reported values 25 degrees and above as normal, values between 20 degrees and 25 degrees to be borderline, and values less than 20 degrees to be diagnostic of acetabular dysplasia.

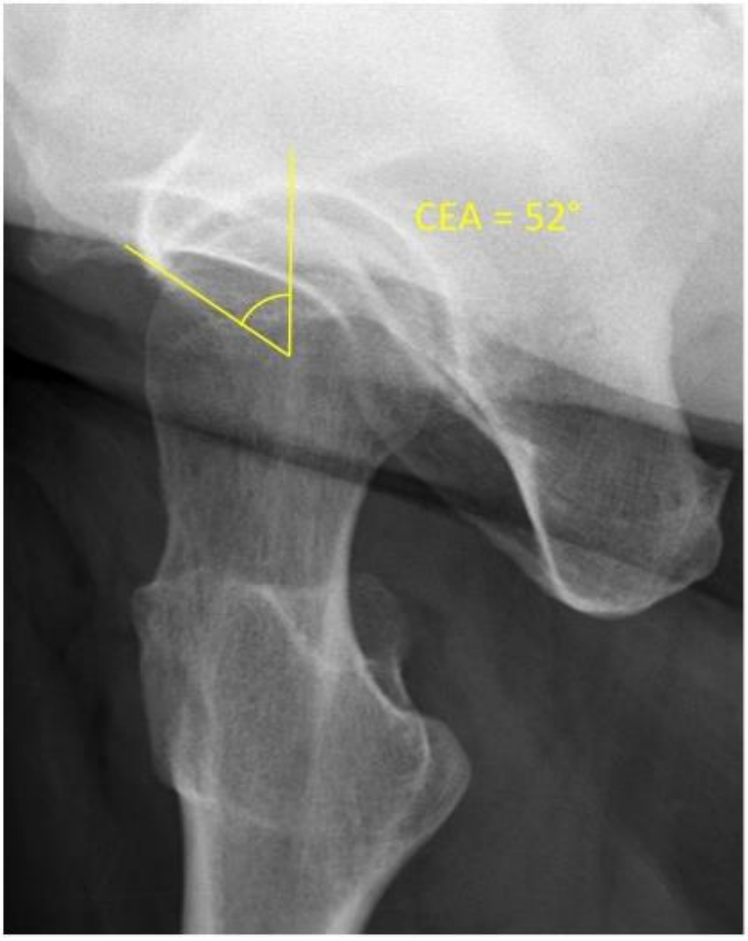
Figure 2-10: Anteroposterior radiographs with lateral centre edge angle measurement of a hip with normal morphology (A) and dysplasia (B)



2.7.2.1.2 Anterior CEA

The CEA measurement can also be applied to the anterior acetabulum through obtaining a lateral imaging view of the hip to determine anterior coverage of the femoral head[244]. The anterior CEA is formed by the angle between a line from the centre of the femoral head to the anterior edge of the acetabulum and a vertical line from the centre of the head (Figure 2-11). Lequesne and de Seze[244] stated that a value of 25 degrees and higher is normal, and a value of 20 degrees or less is seen with acetabular dysplasia.

Figure 2-11: Lateral radiographs with anterior Centre Edge Angle (CEA) measurement of a hip with normal morphology

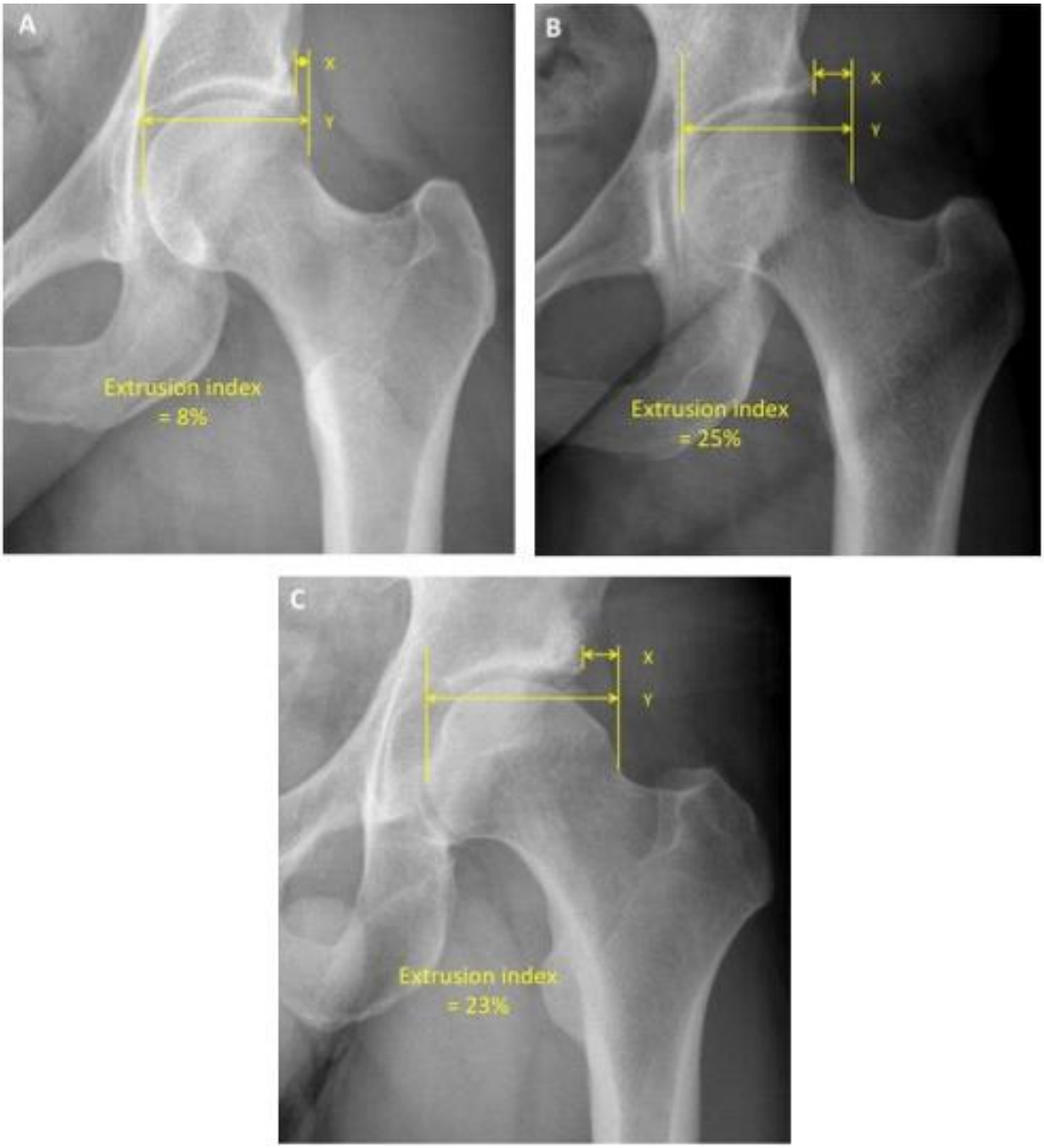


2.7.2.1.3 Femoral Head Extrusion Index

In 1950 Heyman[245] proposed an alternative measure of femoral head coverage, called the femoral head extrusion index. The femoral head extrusion index is the percentage of the femoral head that is not covered by the acetabulum (Figure 2-12). Heyman proposed that in normal hips, less than 25% of the femoral head is uncovered but values greater than 25% often are found in patients with acetabular dysplasia and can be much higher in patients with femoral head subluxation or dislocation. Murphy et al[13] suggested an uncovering of the femoral head of greater than 31% significantly predisposed to future OA. This measure has not been as extensively validated as the CEA and as such is less frequently used. Moreover, the measure may be confounded by the presence of abnormally shaped femoral heads, for example the abnormally shaped femoral head-neck junction seen in cam morphology may produce an artificially positive reading (Figure 2-12).

Figure 2-12: Anteroposterior radiographs with femoral head extrusion index measurement of a hip with normal morphology (A) and dysplasia (B).

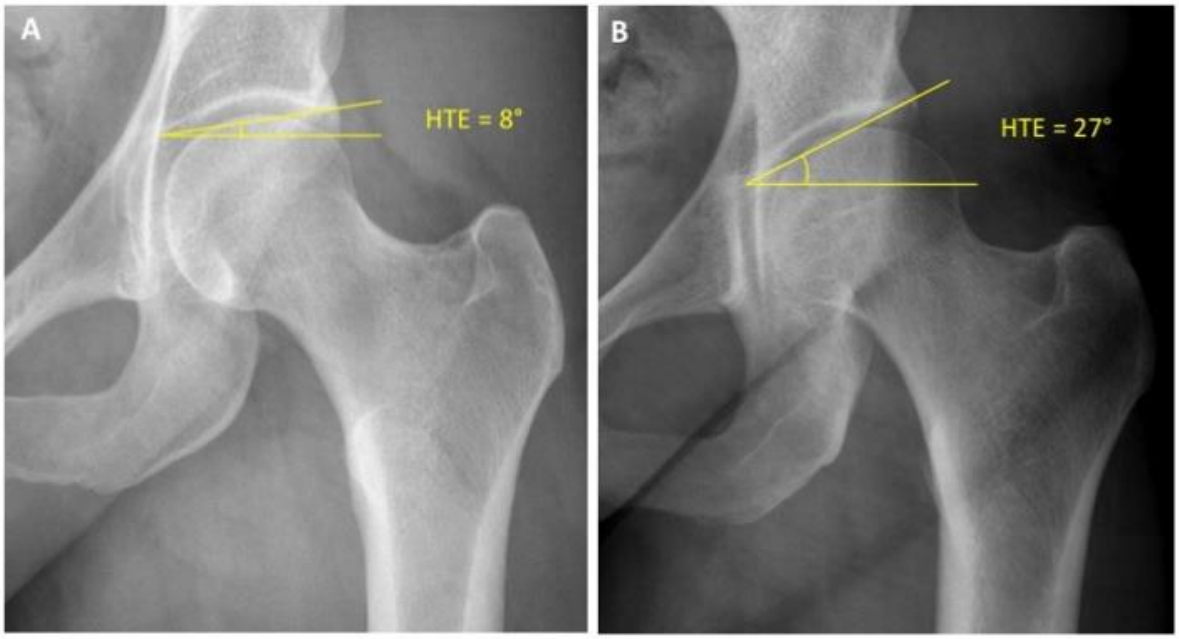
The femoral head extrusion index is the percentage of the femoral head that is not covered by the acetabulum (X/Y x 100). The presence of an abnormally shaped femoral head-neck junction, as is seen in cam morphology, may produce measurements of a similar magnitude to true dysplasia (C).



2.7.2.1.4 Acetabular Index of the Weight Bearing Surface

Rather than quantify the femoral head coverage, a number of alternative measures have attempted to define the shape of the acetabulum. The acetabular index of the weight bearing surface, also known as the Horizontal Toit Externe (HTE) or Tonnis angle, was first described by Lequesne in 1963[246]. The HTE attempts to quantify the angle of the weight bearing proportion of the acetabular roof, based on the assumption that in the dysplastic acetabulum the roof has a greater inclination. The HTE is the angle formed between a line parallel to the weight-bearing surface of the acetabulum and a horizontal line (Figure 2-13). Lequesne stated that values less than 10 degrees are normal and values greater than 10 degrees are common in patients with acetabular dysplasia. Murphy et al[13] suggested a HTE of greater than 15 degrees significantly predisposed to future OA. This measure has not been well validated and fails to accurately diagnose individuals with dysplasia who do not have increased inclination of the acetabular roof.

Figure 2-13: Anteroposterior radiographs with Horizontal Toit Externe angle measurement of a hip with normal morphology (A) and dysplasia (B)

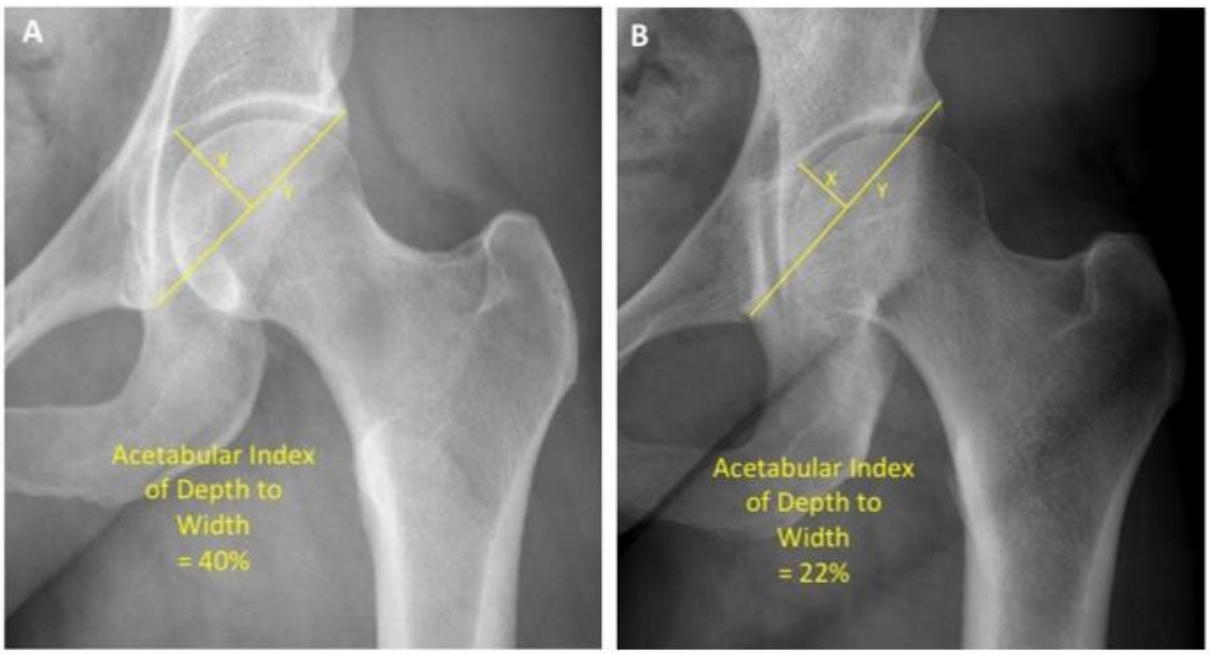


2.7.2.1.5 Acetabular Index of Depth to Width

Another measure of acetabular shape was proposed by Heyman[245] called the acetabular index of depth to width which gives an indication of the depth of the acetabulum. A line joining the lateral edge of acetabulum to the pelvic teardrop measures the acetabular width. A perpendicular line at the point of the greatest acetabular depth measures the acetabular depth (Figure 2-14). Murphy et al[13] found that the acetabular index of depth to width in patients with hips that did not develop severe arthritis by the age of 65 had a mean value of 48% whereas dysplastic acetabula in which secondary osteoarthritis was more likely to develop had an average depth to width ratio of 31%.

Figure 2-14: Anteroposterior radiographs with acetabular index of depth to width measurement of a hip with normal morphology (A) and dysplasia (B).

The acetabular index of depth to width = X/Y x 100.



2.7.2.2 Centre Edge Angle as a Measure of Femoral Head Coverage

The lateral CEA has been used to define hip dysplasia in the majority of studies to date. Given the measurement has demonstrated good validity and reproducibility, and its widespread adoption allows comparisons between studies, it has been adopted as the primary measure of femoral head coverage in this thesis. Two recent large cohort studies[247,248] using total hip arthroplasty as an end point validated that a decreased CEA is a primary risk factor for hip OA. However, there is significant variation in how the CEA is measured, which must be considered during study design and data analysis

2.7.2.2.1 Imaging Strategy

Measurement of the CEA was developed for adults using AP radiographs[112]. The majority of validation studies have also been performed using radiographs[13,218,249]. The CEA has also been used for three-dimensional imaging modalities such as CT. Indeed, the CEA on CT images has been used to map the development of the acetabulum in the immature skeleton[128-130]. However, the use of radiography in the skeletally immature fails to elicit the true dimensions of the acetabulum because the cartilaginous portions of the acetabular wall are underrepresented[63]. Measurement of the CEA using MRI in a skeletally immature cohort has been validated by Albers et al[132] and likely represents the best way to accurately assess femoral head coverage in an adolescent population. It is worth noting however that measurements taken from MRI may result in greater CEA values than those taken with CT due to the addition of cartilage increasing the distance of the lateral acetabulum from the femoral head centre. Though this may be a more accurate representation of true femoral head coverage than bone measurements from CT, results should be interpreted with care when comparing the magnitude of

measurements to thresholds defined by ionising radiation studies.

2.7.2.2.2 Thresholds to Define Acetabular Dysplasia

Wiberg[112] suggested that lateral CEA values below 20 degrees on an AP radiograph represented a dysplastic acetabulum. This value is often used in clinical settings to diagnose acetabular dysplasia. However, Wiberg also suggested that a lateral CEA below 25 degrees may represent a mild dysplasia, and this value has also been adopted. These values were validated by Cooperman et al[249] who followed thirty-two hips with a lateral CEA of less than 20 degrees for twenty-two years; almost all patients had osteoarthritis at the time of the final follow-up when they were a mean of 65 years old. However, the work by Murphy et al[13] suggested that the threshold should perhaps be lower. Murphy et al[13] followed the contralateral hip in 286 patients who had had total hip arthroplasty for OA secondary to dysplasia and observed that no patient in whom the hip survived into the seventh decade of life had a lateral center-edge angle of less than 16 degrees.

Hip instability has been reported despite a normal lateral CEA[250]. Even with subclinical or mild hip dysplasia, the poor coverage of the femoral head and relative lateralization of the hip center of rotation can produce an asymmetric concentration of force across the hip joint resulting in articular cartilage and labral damage[251-253]. As such, the diagnostic threshold of the lateral CEA for dysplasia remains uncertain. A systematic review of 18 studies on hip arthroscopy in the setting of hip dysplasia showed significant heterogeneity in lateral CEA values used to define hip dysplasia, ranging from 16 to 27 degrees[218]. Chegini et al[217] demonstrated through a finite element analysis that as lateral

CEA decreased cartilage stresses increased linearly during simulated walking. They found a significant increase in acetabular rim stress with a lateral CEA less than 25 degrees, which further validated Wiberg's[112] original suggestion of borderline dysplasia. The term borderline dysplasia further developed from natural history studies in asymptomatic hips performed to determine risk of progression to total hip arthroplasty[13,91]. Borderline dysplasia has been defined as a lateral CEA anywhere between 18 and 28 degrees[218].

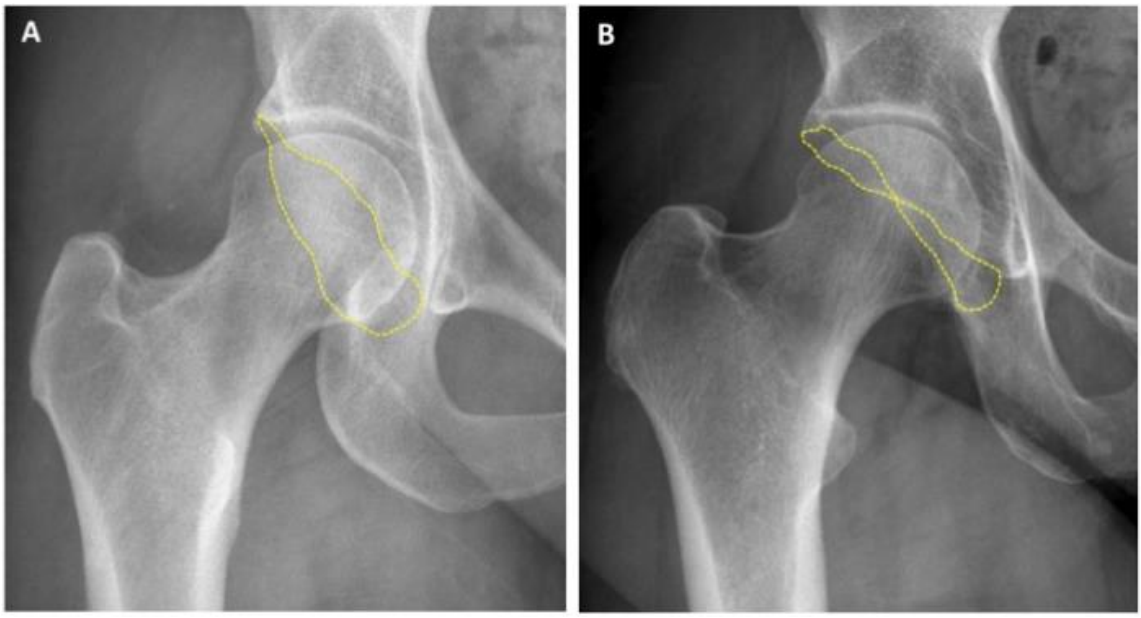
2.7.2.3 Assessment of Acetabular Version

Acetabular version refers to the orientation of the acetabulum with respect to the sagittal plane. If the acetabulum faces forward, anteversion is present but if it faces posteriorly, retroversion is present. A number of measures exist to assess acetabular version both qualitatively and quantitatively.

2.7.2.3.1 Cross-Over Sign

The cross-over sign was described by Meunier et al[254] as a means to qualitatively assess anteversion from AP radiographs. Cross-over sign is seen when the most proximal anterior acetabular rim appears lateral to the posterior rim, creating a figure eight, suggesting acetabular retroversion above this level. (Figure 2-15)

Figure 2-15: Anteroposterior radiographs with normal acetabulum in anteversion (A) and acetabulum displaying cross-over sign suggesting retroversion (B).

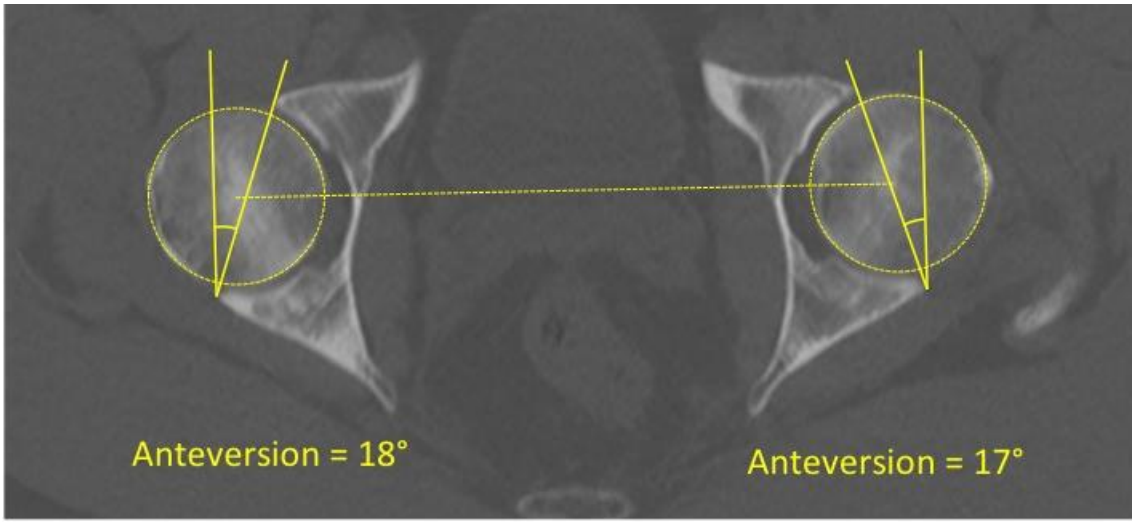


A positive cross-over-sign has been shown to be a reliable indicator of anteversion of less than 4 degrees[255]. However, interpreting radiographs and the reliability of the cross-over sign is diminished by superimposition of regular anatomical structures and also by the positioning of the pelvis. The relationship between the anterior and posterior acetabular rims is significantly affected by the amount of pelvic tilt[255-257]. As such, although the cross-over sign is widely used in the clinical setting to qualitatively diagnose acetabular retroversion it is unable to reliably provide a quantitative measure of the degree of version of the acetabulum

2.7.2.3.2 Anteversion Angle

Three-dimensional imaging has allowed quantitative assessment of the angle of anteversion of the acetabulum, with CT being most widely used[122,258-260]. Studies using CT scans have defined acetabular anteversion as a measurement in the axial plane at the level of the centre of the hip joint. Anteversion is described as the angle formed by a reference line perpendicular to a line connecting an anatomical reference point either side of the pelvis (such as the centre of the femoral head) and a line connecting the posterior and anterior margins of the acetabulum[129,261-264]. The angle of anteversion of the acetabulum has been widely used and validated in studies investigating the development of the acetabulum using CT in adolescents[30,127-131]. (Figure 2-16)

Figure 2-16: Axial slice through a CT scan of the pelvis at the centre of the hip joint showing measurement of acetabular anteversion. The reference line is formed between the femoral head centres.



2.7.2.4 Anteversion Angle as a Measure of Acetabular Orientation

The angle of anteversion in the axial plane is adopted as the primary measure of acetabular orientation in this thesis given the measurement has demonstrated good validity and reproducibility, and its widespread adoption in the current literature allows comparisons between studies. However, there is some variation in how the anteversion angle is measured, which must be considered during study design and data analysis.

3.7.2.4.1 Imaging Strategy

Controversy evolves from the fact that the acetabular opening gradually spirals from mild anteversion proximally to increasing anteversion distally. As such measurements of anteversion on CT scan slices in the axial plane may vary depending on the level of the CT scan slice, but there is no consensus at what level version can reproducibly be

measured. Moreover, pelvic tilt can significantly affect measurements if the readings are not referenced to a well defined and reliable osseous reference plane[257]. The majority of studies to date have measured acetabular version through the centre of the hip joint[129,261-264]. However, it should be kept in mind that measurements through the centre of the femoral head may fail to recognize a deficient acetabulum which is otherwise normally orientated if the deficiency is located in the superior part[265].

When investigating the skeletally immature acetabulum, CT is likely to fail to elicit the true dimensions of the acetabulum because the cartilaginous portions of the acetabular wall are underrepresented. As such MRI is likely to provide a superior means of imaging acetabular version in an adolescent cohort[132].

3.7.2.4.2 Thresholds to Define Acetabular Retroversion

There are no agreed diagnostic thresholds to define acetabular retroversion. However, Dandachli et al[266] took the mean acetabular version from CT scans of 36 normal hips in subjects aged 15 to 61 years and subtracted the 95% confidence interval. They determined 14.2 degrees as the limit below which true retroversion is defined. This threshold has not been extensively validated so care should be taken when interpreting results using this value to define acetabula retroversion.

2.7.3 Assessment of Leg Alignment Morphology

2.7.3.1 Assessment of Leg Alignment

A large number of measurements have been proposed for the assessment of leg alignment. Due to the involvement of hip, knee, and ankle anatomy there exists a plethora of required measurements and anatomical reference points. These were first proposed by Dugdale et al[267] for measurement on standing full leg length radiographs. These measures have been taken up in following studies of leg alignment using standing full leg length radiographs with little alteration to the methodology[133,134,171,268,269]. No study to date has investigated leg alignment in adolescents using MRI. MRI allows the measurement of physeal morphology in the skeletally immature, and the articulating morphology of non-ossified bones. In this chapter measures of leg alignment have been performed on weight bearing full leg length MRI images to display physeal measures not described in any previous literature.

2.7.3.1.1 Anatomical Reference Points

The centre of the femoral head is defined using concentric Mose circles[171]**.** The centre of the knee is defined as the mid-point of the tibial spines halfway between the intercondylar notches[171]**.** The centre of the ankle is defined as the mid-width of the talus. The proximal reference point of the femur is defined as the mid-point of the cortical width of the femur proximal to the knee by 2/3 of the femoral length. The distal reference point of the femur is defined as the mid-point of the cortical width of the femur proximal to the knee by 1/3 of the femoral length[171]. The proximal reference point of the tibia is defined as the mid-point of the cortical width of the tibia distal to the knee by 1/3 of the tibial length[171]. The distal reference point of the tibia is defined as the mid-point of

the cortical width of the tibia proximal to the ankle by 1/3 of the tibial length[171]. The physeal line of the distal femur is defined as the line connecting the medial and lateral edges of the distal femoral physis. The physeal line of the proximal tibia is defined as the line connecting the medial and lateral edges of the proximal tibial physis. The knee joint line of the femur is defined as the line connecting the most distal parts of the femoral condyles. The knee joint line of the tibia is defined as the line connecting the most proximal parts of the medial and lateral tibial plateau. The ankle joint line of the tibia is defined as the line of orientation of the articulating surface of the distal tibia.

2.7.3.1.2 Mechanical Femoral Axis

The mechanical femoral axis is defined as the line from the centre of the femoral head to the centre of the knee[171].

2.7.3.1.3 Mechanical Tibial Axis

The mechanical tibial axis is defined as the line from the centre of the knee to the centre of the ankle[171].

2.7.3.1.4 Anatomical Femoral Neck Axis

The anatomical axis of the femoral neck is defined as the line from the centre of the femoral head transecting the narrowest portion of the femoral neck.

2.7.3.1.5 Anatomical Femoral Axis

The anatomical axis of the femur is defined as the line bisecting the distal and proximal reference points of the femur.

2.7.3.1.6 Anatomical Tibial Axis

The anatomical axis of the tibia is defined as the line bisecting the distal and proximal reference points of the tibia.

2.7.3.1.7 Weight Bearing Line

The weight-bearing line (WBL) is defined as the line connecting the centre of the femoral head and the centre of the ankle.

2.7.3.2 Hip Knee Angle (HKA)

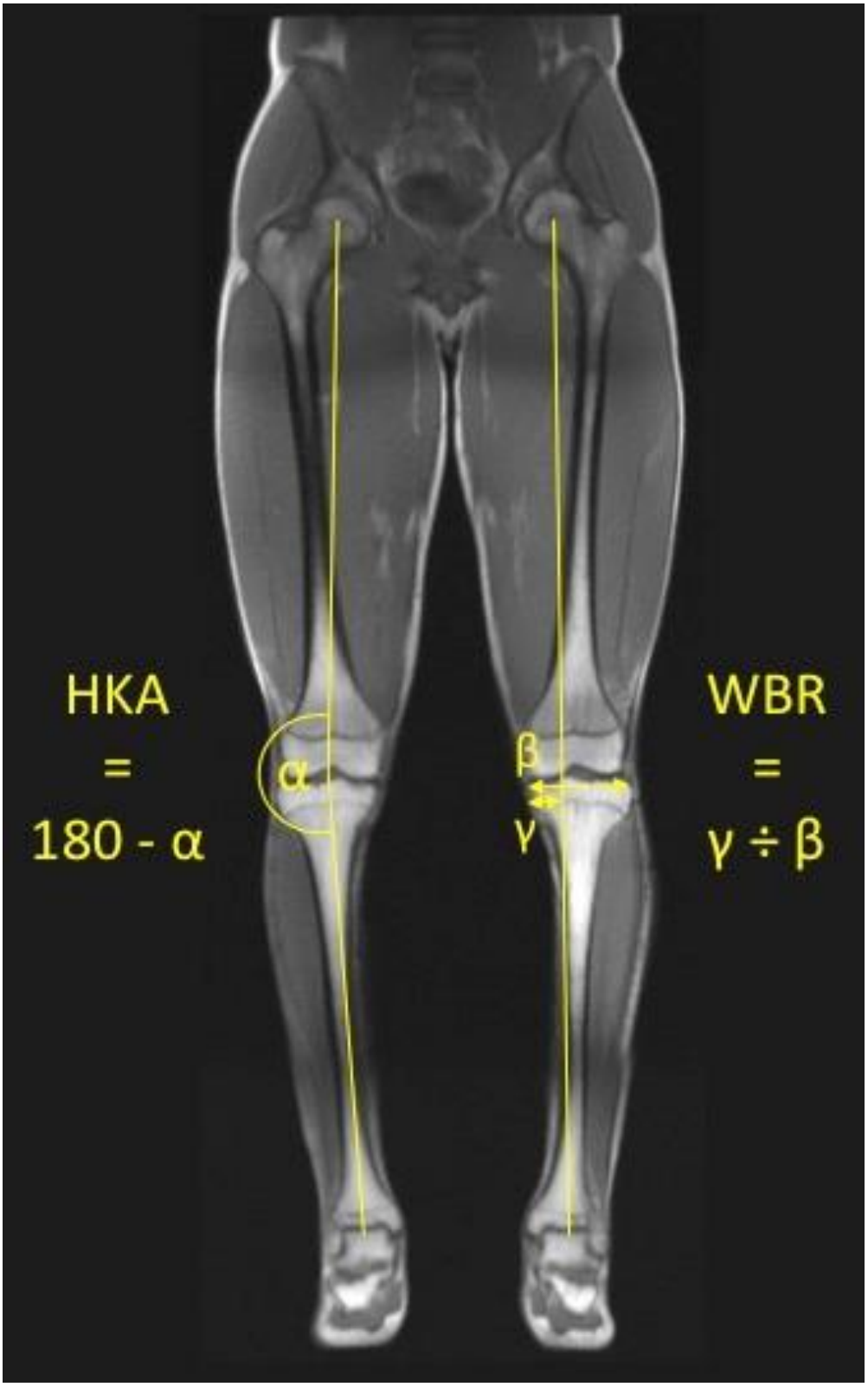
The Hip–Knee–Angle (HKA) is defined as the angle formed by the intercept of the femoral mechanical axis and the tibial mechanical axis[270-273]. The HKA is expressed as a deviation from 180° with a negative value for varus alignment and a positive value for valgus alignment[171]. (Figure 2-17)

2.7.3.3 Weight Bearing Ratio (WBR)

The Weight Bearing Ratio (WBR) is calculated by measuring the distance from the medial edge of the proximal tibia to the point where the load bearing axis intersects the

proximal tibia and dividing the measurement by the entire width of the tibia[268]. (Figure 2-17)

Figure 2-17: Full leg length weight bearing MRI of a 16 year old male showing Hip-Knee-Angle (HKA) and Weight-Bearing-Ratio (WBR) measures.



2.7.3.4 Mean Neck Shaft Angle (MNSA)

The Mean Neck Shaft Angle (MNSA) is defined as the intercept of the anatomical axis of the femur and the anatomical axis of the femoral neck[171]. (Figure 2-18)

2.7.3.5 Medial Proximal Femoral Angle (MPFA)

The Medial Proximal Femoral Angle (MPFA) is defined as the angle between the line connecting the tip of the greater trochanter with the centre of the femoral head and the anatomical femoral axis[171]. (Figure 2-18)

2.7.3.6 Lateral Proximal Femoral Angle (LPFA)

The lateral proximal femoral angle (LPFA) is defined as the angle between the line connecting the tip of the greater trochanter with the centre of the femoral head and the mechanical femoral axis[171]. (Figure 2-18)

2.7.3.7 Mechanical Lateral Distal Femoral Angle (mLDFA)

The Mechanical Lateral Distal Femoral Angle (mLDFA) is defined as the lateral intercept between mechanical axis of the femur and the knee joint line of the femur[171].(Figure 2-18)

2.7.3.8 Anatomical Lateral Distal Femoral Angle (aLDFA)

The Anatomical Lateral Distal Femoral Angle (aLDFA) is defined as the lateral intercept between the anatomical axis of the femur and the knee joint line of the femur. (Figure 2-18)

2.7.3.9 Joint Line Congruence Angle (JLCA)

The Joint Line Congruence Angle (JLCA) is defined as the lateral intercept between the knee joint line of the femur and the knee joint line of the tibia. (Figure 2-19)

2.7.3.10 Mechanical Medial Proximal Tibial Angle (mMPTA)

The mechanical medial proximal tibial angle (MPTA) is defined as the medial intercept between the mechanical tibial axis and the knee joint line of the tibia[171]. (Figure 2-18)

2.7.3.11 Anatomical Medial Proximal Tibial Angle (aMPTA)

The Anatomical Medial Proximal Tibial Angle (aMPTA) is defined as the medial intercept between the anatomical axis of tibia and the knee joint line of the tibia. (Figure 2-18)

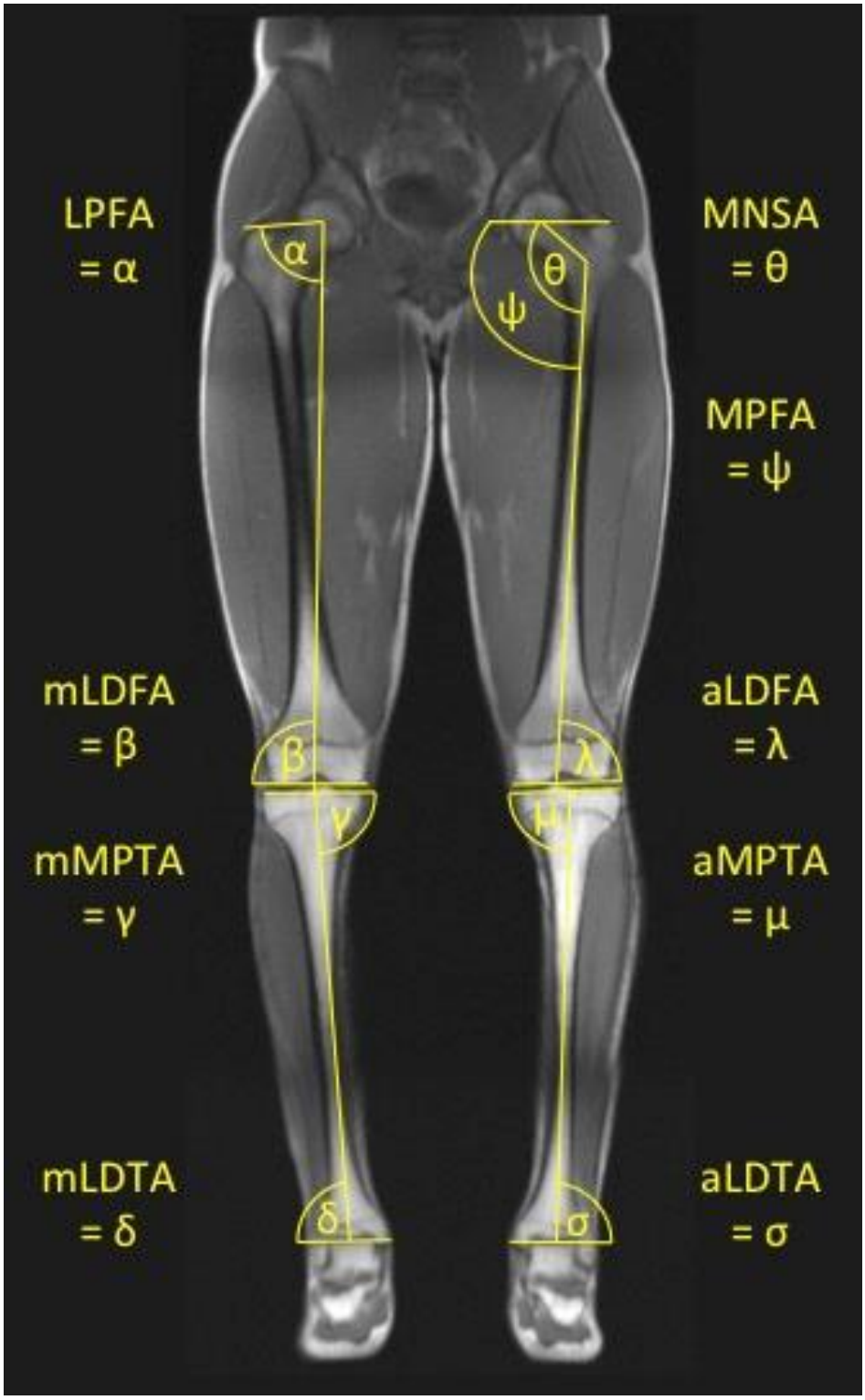
2.7.3.12 Mechanical Lateral Distal Tibial Angle (mLDTA)

The Mechanical Lateral Distal Tibial Angle (mLDTA) is defined as the lateral intercept between the mechanical axis of the tibia and the ankle joint line of the tibia. (Figure 2-18)

2.7.3.13 Anatomical Lateral Distal Tibial Angle (aLDTA)

The Anatomical Lateral Distal Tibial Angle (mLDTA) is defined as the lateral intercept between the anatomical axis of the tibia and the ankle joint line of the tibia. (Figure 2-18)

Figure 2-18: Full leg length weight bearing MRI of a 16 year old male showing Mean Neck Shaft Angle (MNSA), Medial Proximal Femoral Angle (MPFA), Lateral Proximal Femoral Angle (LPFA), Mechanical Lateral Distal Femoral Angle (mLDFA), Anatomical Lateral Distal Femoral Angle (aLDFA), Mechanical Medial Proximal Tibial Angle (mMPTA), Anatomical Medial Proximal Tibial Angle (aMPTA), Mechanical Lateral Distal Tibial Angle (mLDTA), and Anatomical Lateral Distal Tibial Angle (aLDTA) measures.



2.7.3.14 Leg Length Discrepancy

Leg length was defined as the length of the line connecting the centre of the femoral head to centre of ankle. Leg Length Discrepancy was defined as the difference in length between the left and right leg lengths.

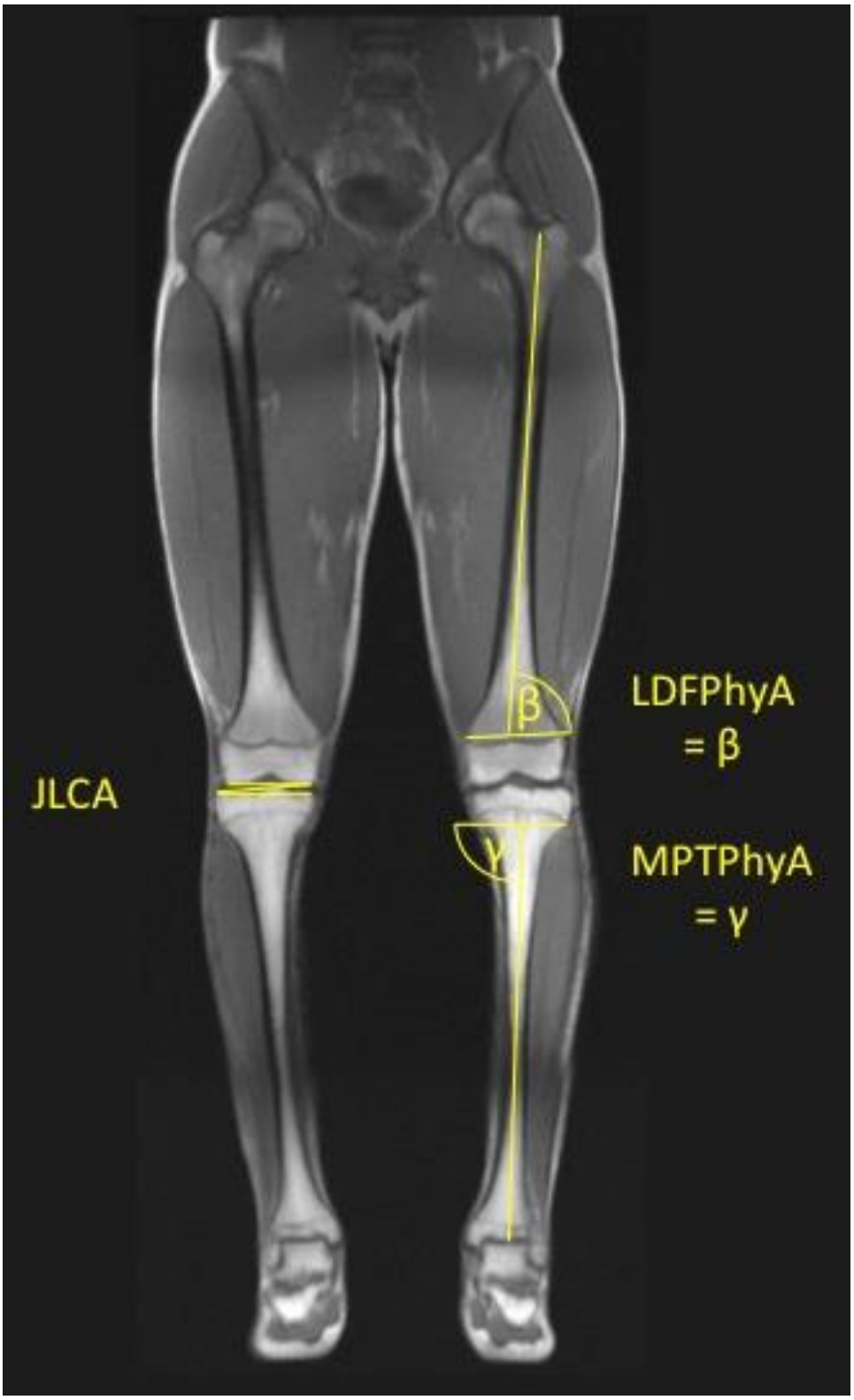
2.7.3.15 Medial Proximal Tibial Physis Angle (MPTPhyA)

Medial Proximal Tibial Physis Angle (MPTPhyA) is defined as the medial intercept between the anatomical axis of tibia and the physeal line of the proximal tibia. (Figure 2-19)

2.7.3.16 Lateral Distal Femoral Physis Angle (LDFPhyA)

The Lateral Distal Femoral Physis Angle (LDFPhyA) is defined as the lateral intercept between the anatomical axis of the femur and the physeal line of femur. (Figure 2-19)

Figure 2-19: Full leg length weight bearing MRI of a16 year old male showing Joint Line Congruence Angle (JLCA), Medial Proximal Tibial Physis Angle (MPTPhyA), and Lateral Distal Femoral Physis Angle (LDFPhyA) measures.



2.7.3.17 The Hip Knee Angle as a Measure of Leg Alignment

The HKA was chosen as the primary measure of leg alignment in this thesis given the measurement has demonstrated good validity and reproducibility, and its widespread adoption in the current literature allows comparisons between studies[133,134,143,171,267-269].

2.7.3.2.1 Thresholds to Define Varus Leg Alignment

There are no agreed diagnostic thresholds to define varus leg alignment. Leg alignment can be described as being varus if a negative HKA values is obtained[171], however it remains unknown at what magnitude varus alignment becomes pathological. Parratte et al[274] suggested that a HKA less than minus 3 degrees suggests constitutional varus alignment, and a HKA greater than 3 degrees suggests constitutional valgus alignment. These values were later used by Bellemans et al[143] in an observational cohort study of healthy individuals. However, these values are based on prior studies investigating leg alignment post total knee arthroplasty in an adult population[275]. As such, care should be when interpreting results from young healthy cohorts using these thresholds.

2.7.4 Assessment of Cartilage Composition

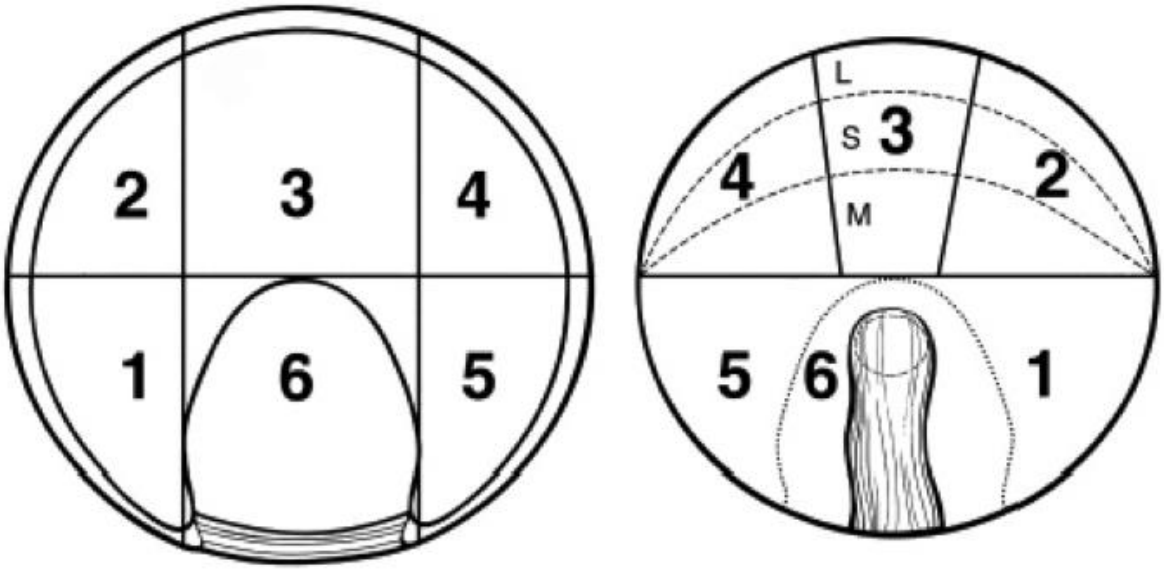
Compositional MRI is responsive to a large number of factors that must be controlled during studies. These may include physiological variables such as cartilage loading[276] or the delivery of contrast to the joint after intravenous administration[277]. Analytical factors include the mathematical algorithm used for image analysis. In addition, it may not be possible to compare results between studies due to the heterogeneity of pulse sequences.

A further challenge is that, unlike for knees[278], there is no agreed method of selecting regions of interest in hip cartilage. Osteoarthritis does not develop uniformly across the articular surfaces of a synovial joint[279]. Therefore, averaging relaxation times across the entire joint is insufficiently sensitive to detect early disease and regional evaluation is superior[280]. A systematic and reproducible method of defining regions of the acetabular and femoral cartilage is therefore required. Absolute values from individual regions can be assessed in isolation, or as a ratio to global cartilage values for an individual[96]. This latter approach is preferred since each hip then acts as an internal control for physiological variables. Several methods have been described for dividing the acetabular and femoral cartilage into regions. To ensure imaging studies are aligned with clinical findings, segmentation schemes are frequently based on maps developed to describe intra-articular pathology during hip arthroscopy. Two main approaches have been adopted in the orthopaedic literature: The 'geographic zone'[281] and 'clock-face'[282] approaches.

The geographic zones are superimposed as two vertical lines either side of the cotyloid fossa and a perpendicular horizontal line positioned at the superior margin of the

cotyloid fossa, producing six zones. Corresponding zones are superimposed upon the femoral head where the superior zones are divided into medial (M), superior (S) and lateral (L) regions[281] (Figure 2-20).

Figure 2-20: Geographic Zones of Right Hip. The clockface zones are orientated such that 12 o'clock is the most superior aspect of the acetabulum and the 6 o'clock position represents the middle of the transverse ligament. Modified from Ilizaliturri et al 2008[281]



The clockface zones are orientated such that 12 o'clock is the most superior aspect of the acetabulum and the 6 o'clock position represents the middle of the transverse ligament. The 3 o'clock position is always taken as the anterior position, hence the map is inverted for left and right hips[282]. The clockface system has also been adapted for the femoral head[283].

The geographic zone is proposed to be more reproducible than the clockface approach[281] by selecting intra-articular landmarks that are more easily visible during arthroscopy. However, the clockface system is more widely used in clinical practice and correlates well with the radial planes adopted for the evaluation of cam morphology (2.7.1.2.1). The studies in this thesis orientate the 12 o'clock position parallel to the axis of the proximal

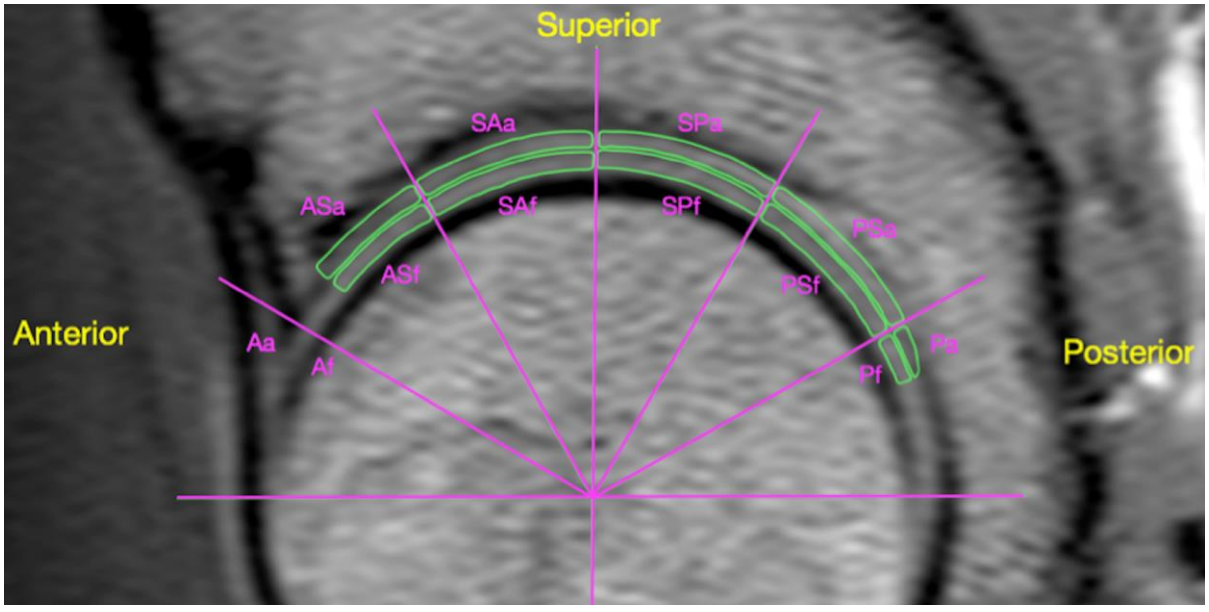
femoral diaphysis when the patient is supine, whether on the traction table for hip arthroscopy or for the acquisition of MR images.

2.7.4.1 Compositional MRI Acquisition

There is no standardised approach to compositional MRI acquisition. In order to facilitate correlation between compositional MRI, morphological MRI, and arthroscopic appearances, studies in this thesis acquire two-dimensional images in the true sagittal plane. Hips are positioned in 15 degrees of internal rotation and study participants lie supine. This protocol offers a compromise between the anteversion axis of the acetabulum and femoral neck. Femoral and acetabular cartilage is segmented using the clockface approach. (Figure 2-21)

Figure 2-21: Example Regions of Interest (ROI) for T2 Segmentation.

Anterior Acetabular Cartilage (Aa), AnteroSuperior Acetabular Cartilage (ASa), SuperoAnterior Acetabular Cartilage (SAa), SuperoPosterior Acetabular Cartilage (Spa), PosteroSuperior Acetabular Cartilage (PSa), Posterior Acetabular Cartilage (Pa), Anterior Femoral Cartilage (Af), AnteroSuperior Femoral Cartilage (ASf), SuperoAnterior Femoral Cartilage (SAf), SuperoPosterior Femoral Cartilage (SPf), PosteroSuperior Femoral Cartilage (PSf), Posterior Femoral Cartilage (Pf)



2.8 MRI Protocol

MRI scans were performed on a 3 Tesla Philips Achieva X-series platform (Philips Healthcare, Eindhoven, Netherlands) using a torso coil centred on the femoral heads. The right hip was imaged first in all participants. Four morphological sequences and one compositional sequence were used. Post acquisition processing and analysis details are given in each relevant chapter.

2.8.1 3D Water Selective Fluid (WATSf)

This sequence was used to image femoral head joint cartilage and bone and take alpha angle and epiphyseal extension measurements**.**

Sequence variant = 3D Gradient/Fast Field Echo with binomial pulse (1:3:3:1); Repetition time (TR) = 13.65ms; Echo time (TE) = 6.9ms; excitation Flip angle = 30 degrees; bandwidth = 145Hz/pixel; interpolated voxel size 0.29mm x 0.29mm x 0.4mm; averages= 2; acquired in true sagittal orientation.

2.8.2 3D Proton Density Fat Saturation (PDFS)

This sequence was used to image the physeal scar and labrum.

Sequence variant = 3D VISTA, Spin Echo; Repetition time (TR) = 1300ms; Echo time (TE) = 40ms; excitation Flip angle = 180 degrees; refocusing Flip angle =35 degrees; bandwidth 243Hz/pixel; interpolated voxel size 0.625mm x 0.625mm x 0.65mm; averages= 2; acquired in true sagittal orientation

2.8.3 Water Selective Volume Excitation (WAVE)

This sequence was used to image acetabular morphology and take Centre Edge-Angle and anteversion measurements.

Repetition time (TR) 10ms, echo time (TE) 4.9ms, flip angle 20 degrees, bandwidth 229Hz/pixel, FOV 380mm x 131mm x300mm, interpolated voxel size 0.69mm x 0.69mm x 1mm, no turbo factor.

2.8.4 Stacked T1 Weighted Turbo Spin Echo (TSE) Coronal Pelvis

This sequence was used to image whole leg length and take leg alignment measurements.

T1 Weighted Turbo Spin Echo (TSE) Coronal Pelvis: Turbo factor 5, Number of Sampling Excitations (NSA 2), FOV 490mm x 351 mm x 278mm, 10% overlap of FOV for stacking T1, 5 stacks along the coronal lower limb plane, voxel size 1.44 x 1.44 x 8mm reconstructed acquisition spatial resolution 1.8 x 2.6 x 8, no SENSE, reconstruction matrix 336mm x252mm, Repetition Time (TR) 1008ms, Echo Time (TE) 7.6ms, number of slices 31, slice gap 1mm, half scan 70%. Scans were acquired with knees in full extension in neutral position with patella perpendicular to the table, under simulated weight bearing titrated to match the participants weight.

2.8.5 T2 mapping

This sequence was used to image hip cartilage composition.

2D T2 mapping: Fast Spin Echo (FSE) pulse sequence, Repetition time (TR) 3500ms, 1st echo time (TE) 13.5ms, Echo Spacing (ES) 13.5ms, total number of echoes: 7 (13.5ms, 27ms, 30.5ms, 44ms, 57.5ms, 71ms, 94.5ms), Echo Train Length (ETL): 94.5ms, flip angle 180 degrees, Field Of View (FOV) 273mm x 150mm, bandwidth 191Hz/pixel, slice thickness 3mm, slice gap 0.8mm, acquisition matrix 292 x 278, reconstructed pixel size 0.51 x 0.52 x 3mm, NEX 1, SENSE factor: 2.0. Acquisition time 8 minutes. Acquired in true sagittal plane with the first slice referenced off the medial border of the femoral head with the remaining slices extending laterally.

2.9 Reproducibility Studies of Imaging Measures

Reproducibility was studied for each of the imaging outcome measures adopted in this thesis. Measurements were repeated by the principal investigator (SF) a minimum of 1 month after the initial measurements (intra-observer reproducibility), and also by a clinical research fellow with experience of musculoskeletal imaging research (inter-observer reproducibility). Images were selected at random from the FAIM cohort for morphological MRI readings ensuring these included ten hips with an open physis and ten with a closed physis. MRI scans were anonymised such that assessors were blinded to participant characteristics such as cohort and age. Alpha angle, lateral epiphyseal extension, and FTA measurements were performed on each hip in five planes, hence there were 100 readings for each measure. Each acetabular and leg alignment measure was performed once on each hip hence there were 20 readings per measure. Compositional MRI reproducibility was extensively validated in a separate study[284] on five MRI slices from ten randomly selected hips giving rise to 399 regions of interest. Reproducibility was assessed using intra-class and inter-class correlations (single measures and absolute agreement) and Bland Altman plots. The smallest detectable difference in measurements was calculated as the standard deviation of the mean difference between readings multiplied by 1.96. The Root Mean Square of the Coefficient of Variance (RMSCoV) was calculated as the root mean square of the change divided by the mean, multiplied by 100[285]. Statistical analysis was performed using STATA 14.1 (College Station, TX, USA).

Alpha Angle:

Intra observer ICC was 0.996 (95% CI:0.995 – 0.997), SDD was 3.388 degrees, and RMSCoV was 2.999%. Inter-observer ICC was 0.914 (95% CI:0.866 – 0.945), SDD was 4.219 degrees, and RMSCoV was 4.606%. Bland-Altman Plots in Appendix A-3 and Appendix A-4

Lateral Epiphyseal Extension:

Intra observer ICC was 0.998 (95% CI:0.997 – 0.0.999), SDD was 0.012, and RMSCoV was 0.864%. Inter-observer ICC was 0.988 (95% CI: 0.982 – 0.993), SDD was 0.014, and RMSCoV was 1.092%. Bland-Altman Plots in Appendix A-5 and Appendix A-6

Fibrochondroosseous Tissue Area (FTA):

Intra observer ICC was 0.957 (95% CI: 0.940 – 0.974), SDD was 10.027, and RMSCoV was 0.597%. Inter-observer ICC was 0.934 (95% CI: 0.908 – 0.960), SDD was 12.323, and RMSCoV was 0.739%. Bland-Altman Plots in Appendix A-7 and Appendix A-8

Lateral Centre Edge Angle (CEA):

Intra observer ICC was 0.9538 (95% CI: 0.922 – 0.995), SDD was 2.487, and RMSCoV was 4.648%. Inter-observer ICC was 0.916 (95% CI: 0.844 – 0.988), SDD was 2.676, and RMSCoV was 7.141%. Bland-Altman Plots in Appendix A-9 and Appendix A-10

Anterior Centre Edge Angle (CEA):

Intra observer ICC was 0.959 (95% CI: 0.924 – 0.995), SDD was 2.582, and RMSCoV was 2.841%. Inter-observer ICC was 0.943 (95% CI: 0.894 – 0.993), SDD was 3.579, and RMSCoV was 4.109%. Bland-Altman Plots in Appendix A-11 and Appendix A-12

Anteversion:

Intra observer ICC was 0.955 (95% CI: 0.915 – 0.994), SDD was 2.765, and RMSCoV was 4.659%. Inter-observer ICC was 0.917 (95% CI: 0.836 – 0.987), SDD was 2.886, and RMSCoV was 5.409%. Bland-Altman Plots in Appendix A-13 and Appendix A-14

Hip Knee Angle (HKA):

Intra observer ICC was 0.986 (95% CI: 0.973 – 0.998), SDD was 0.825, and RMSCoV was 30.224%. Inter-observer ICC was 0.949 (95% CI: 0.905 – 0.993), SDD was 1.604, and RMSCoV was 57.607%. Bland-Altman Plots in Appendix A-15 and Appendix A-16

Weight Bearing Ratio (WBR):

Intra observer ICC was 0.975 (95% CI: 0.954 – 0.997), SDD was 0.053, and RMSCoV was 7.677%. Inter-observer ICC was 0.962 (95% CI: 0.930 – 0.995), SDD was 0.068, and RMSCoV was 9.933%. Bland-Altman Plots in Appendix A-17 and Appendix A-18

Mean Neck Shaft Angle (MNSA):

Intra-observer ICC was 0.955 (95% CI: 0.916 – 0.994), SDD was 3.189, and RMSCoV was 1.219%. Inter observer ICC was 0.932 (95% CI: 0.874 – 0.991), SDD was 3.500, and RMSCoV was 1.411%. Bland-Altman Plots in Appendix A-19 and Appendix A-20

Medial Proximal Femoral Angle (MPFA):

Intra-observer ICC was 0.921 (95% CI: 0.853 – 0.989), SDD was 4.857, and RMSCoV was 2.829%. Inter observer ICC was 0.900 (95% CI: 0.807 – 0.984), SDD was 5.703, and RMSCoV was 3.316%. Bland-Altman Plots in Appendix A-21 and Appendix A-22

Lateral Proximal Femoral Angle (LPFA):

Intra observer ICC was 0.937 (95% CI: 0.881 – 0.992), SDD was 4.066, and RMSCoV was 2.309%. Inter-observer ICC was 0.901 (95% CI: 0.817 – 0.985), SDD was 5.230, and RMSCoV was 2.956%. Bland-Altman Plots in Appendix A-23 and Appendix A-24

Mechanical Lateral Distal Femoral Angle (mLDFA):

Intra observer ICC was 0.948 (95% CI: 0.904 – 0.993), SDD was 2.248, and RMSCoV was 1.277%. Inter-observer ICC was 0.916 (95% CI: 0.844 – 0.988), SDD was 2.683, and RMSCoV was 1.539%. Bland-Altman Plots in Appendix A-25 and Appendix A-26

Anatomical Lateral Distal Femoral Angle (aLDFA):

Intra observer ICC was 0.926 (95% CI: 0.863 – 0.990), SDD was 2.761, and RMSCoV was 1.683%. Inter-observer ICC was 0.916 (95% CI: 0.843 – 0.988), SDD was 2.958, and RMSCoV was 1.836%. Bland-Altman Plots in Appendix A-27 and Appendix A-28

Joint Line Congruence Angle (JLCA):

Intra observer ICC was 0.853 (95% CI: 0.731 – 0.975), SDD was 0.956, and RMSCoV was 12.243%. Inter-observer ICC was 0.759 (95% CI: 0.569 – 0.949), SDD was 1.276, and RMSCoV was 16.162%. Bland-Altman Plots in Appendix A-29 and Appendix A-30

Mechanical Medial Proximal Tibial Angle (mMPTA):

Intra observer ICC was 0.943 (95% CI: 0.894 – 0.993), SDD was 2.657, and RMSCoV was 1.530%. Inter-observer ICC was 0.929 (95% CI: 0.868 – 0.990), SDD was 3.061, and RMSCoV was 1.761%. Bland-Altman Plots in Appendix A-31 and Appendix A-32

Anatomical Medial Proximal Tibial Angle (mMPTA):

Intra observer ICC was 0.957 (95% CI: 0.920 – 0.995), SDD was 2.670, and RMSCoV was 1.588%. Inter-observer ICC was 0.941 (95% CI: 0.890 – 0.992), SDD was 3.111, and RMSCoV was 1.883%. Bland-Altman Plots in Appendix A-33 and Appendix A-34

Mechanical Lateral Distal Tibial Angle (mLDTA):

Intra observer ICC was 0.940 (95% CI: 0.888 – 0.992), SDD was 2.225, and RMSCoV was 1.245%. Inter-observer ICC was 0.894 (95% CI: 0.804 – 0.983), SDD was 2.728, and RMSCoV was 1.492%. Bland-Altman Plots in Appendix A-35 and Appendix A-36

Anatomical Lateral Distal Tibial Angle (aLDTA):

Intra observer ICC was 0.927 (95% CI: 0.865 – 0.990), SDD was 2.541, and RMSCoV was 1.458%. Inter-observer ICC was 0.926 (95% CI: 0.862 – 0.990), SDD was 2.895, and RMSCoV was 1.610%. Bland-Altman Plots in Appendix A-37 and Appendix A-38

Leg Length Discrepancy:

Intra observer ICC was 0.932 (95% CI: 0.874 – 0.991), SDD was 3.731, and RMSCoV was 2.349%. Inter-observer ICC was 0.899 (95% CI: 0.0.813 – 0.985), SDD was 4.638, and RMSCoV was 2.836%. Bland-Altman Plots in Appendix A-39 and Appendix A-40

Medial Proximal Tibial Physis Angle (MPTPhyA):

Intra observer ICC was 0.920 (95% CI: 0.851- 0.987), SDD was 1.987, and RMSCoV was 1.102%. Inter-observer ICC was 0.907 (95% CI: 0.828 – 0.986), SDD was 2.157, and RMSCoV was 1.206%. Bland-Altman Plots in Appendix A-41 and Appendix A-42

Lateral Distal Femoral Physis Angle (LDFPhyA):

Intra observer ICC was 0.932 (95% CI: 0.872 – 0.991), SDD was 2.435, and RMSCoV was 1.425%. Inter-observer ICC was 0.892 (95% CI: 0.801 – 0.983), SDD was 2.895, and RMSCoV was 1.698%. Bland-Altman Plots in Appendix A-43 and Appendix A-44

Compositional MRI – T2:

Intra-observer reproducibility combining all ROIs from T2 scans of the 10 hips in the sibkid cohort (n=399) was ICC 0.98 (95% CI: 0.97-0.98), RMSCoV 3.5% (95% CI: 2.6-6.1), and SDD 2.2ms (95% CI: 1.5-2.9). Inter-observer reproducibility combining all ROIs (n=283) was ICC 0.96 (95% CI: 0.95-0.96), RMSCoV 5.2% (95% CI: 4.0-6.3), and SDD 3.5 (95% CI: 2.8-4.2). Bland-Altman Plots in Appendix A-45 and Appendix A-46. Appendix A-47 - Intra and inter observer reproducibility of T2 image analysis for each region.

Text modified from:

- Fernquest S, Palmer A, Gammer B, et al. Compositional MRI of the Hip: Reproducibility, Effect of Joint Unloading, and Comparison of T2 Relaxometry with Delayed Gadolinium-Enhanced Magnetic Resonance Imaging of Cartilage. Cartilage. 2019:1947603519841670. PMID: 30971110

2.10 Cohort Characteristics

At baseline there were 228 individuals (449 hip MRIs) (mean age 151 months, SD 31). The baseline cohort comprised 103 male football players from Southampton Football Academy (SFC), 18 male football players from Oxford United Football Club Academy (OUFC), 52 male controls, and 55 female controls. Two football players declined the invitation to participate. The recruitment target was exceeded. MRI scans were incomplete due to claustrophobia or uninterpretable due to movement artifact in five hips (two male footballers and one female control). (Table 2-2)

140 individuals (280 hip MRIs) attended three-year follow-up (mean age 181 months, SD 32). Mean follow up was 36 months (SD 4). The follow-up cohort comprised 60 male football players from SFC, 9 male football players from OUFC, 35 male controls, and 36 female controls. All football players who remained a member of the football club, but no player who had been released from the club attended follow-up. Four individuals from the control cohort declined repeat assessment, two did not attend their arranged follow-up appointment, and thirty individuals did not respond to invitation. All follow-up MRI scans were interpretable. Loss to follow-up was 42% for SFC, 50% for OUFC, and 34% for Controls. (Table 2-2) (Figure 2-22)

Figure 2-22: Recruitment flowchart for study

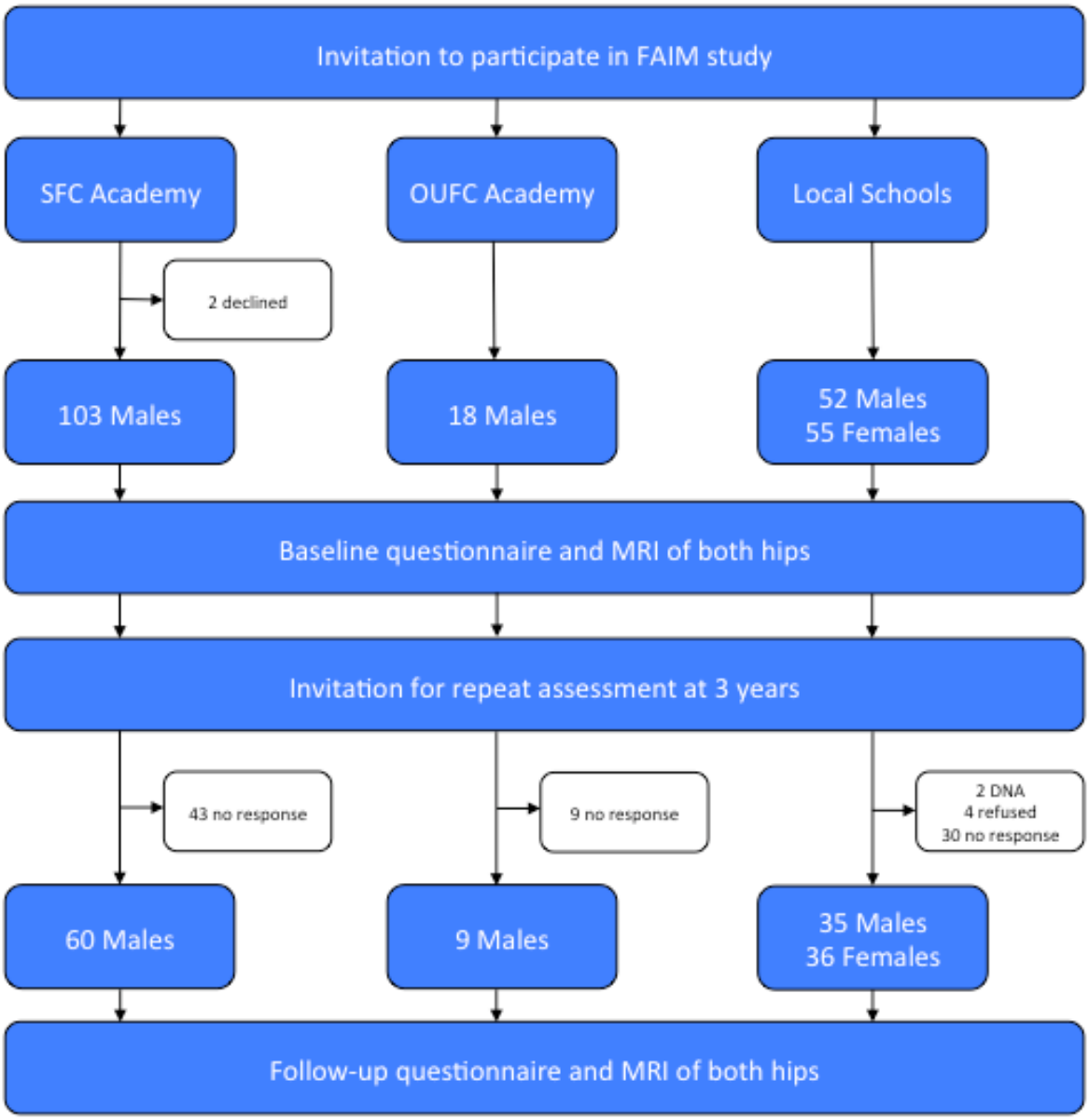


Table 2-2 - Cohort Demographics

		Male Footballers		Male controls		Female controls	
		Baseline Individuals (Hips)	**Follow-up Individuals (Hips)**	**Baseline Individuals (Hips)**	**Follow-up Individuals (Hips)**	**Baseline Individuals (Hips)**	**Follow-up Individuals (Hips)**
Age at baseline (years)	**9-10**	37 (73)	28 (56)	15 (30)	12 (24)	11 (22)	10 (20)
	11-12	32 (64)	22 (44)	14 (28)	10 (20)	6 (12)	5 (10)
	13-14	22 (44)	9 (18)	8 (16)	4 (8)	12 (24)	8 (16)
	15-16	20 (40)	7 (14)	13 (26)	8 (16)	19 (38)	9 (18)
	17-18	8 (16)	3 (6)	2 (4)	1 (2)	6 (12)	4 (8)
Total		119 (237)	69 (138)	52 (104)	35 (70)	54 (108)	36 (72)

2.10.1 Activity Levels

Within the study cohort, Physical Activity Questionnaire (PAQ) score decreased with increasing participant age, and this was the case for all cohorts (Table 2-3) (Figure 2-23). Elite male footballers had a significantly higher PAQ than male controls at baseline and follow-up. Adjusting for age, elite male footballers had a PAQ score 0.218 higher than male controls at baseline ($p=0.002$), and 0.405 higher than male controls at follow-up ($p<0.001$). Male controls had a significantly higher PAQ than female controls at baseline and follow-up. Adjusting for age, male controls had a PAQ score 0.282 higher than female controls at baseline ($p=0.001$), and 0.680 higher than female controls at follow-up ($p<0.001$). (Figure 2-24)

Table 2-3 - Mean and Standard Deviation of Physical Activity Questionnaire (PAQ)

		Male Footballers		Male controls		Female controls	
		Baseline Mean (±SD)	Follow-up Mean (±SD)	Baseline Mean (±SD)	Follow-up Mean (±SD)	Baseline Mean (±SD)	Follow-up Mean (±SD)
Age at baseline (years)	**9-10**	3.42 (±0.43)	3.43 (±0.86)	3.10 (±0.46)	3.19 (±0.77)	2.96 (±0.51)	2.49 (±0.80)
	11-12	3.36 (±0.65)	3.39 (±0.77)	3.28 (±0.55)	2.90 (±0.81)	2.72 (±0.76)	2.00 (±0.51)
	13-14	2.98 (±0.73)	3.05 (±0.32)	2.87 (±0.59)	2.12 (±0.67)	2.30 (±0.56)	1.52 (±0.38)
	15-16	2.51 (±0.65)	2.93 (±0.61)	2.22 (±0.64)	2.41 (±0.87)	2.14 (±0.65)	1.77 (±0.41)
	17-18	2.17 (±0.40)	2.71 (±0.23)	2.14 (±0.44)	3.17 (±0)	2.21 (±0.58)	2.85 (±0.96)
Average		3.11 (±0.71)	3.29 (±0.76)	2.86 (±0.69)	2.80 (±0.86)	2.42 (±0.69)	2.07 (±0.76)

Figure 2-23: Box and Whisker Plot of Physical Activity Questionnaire Score Versus Age at Baseline and Follow-up

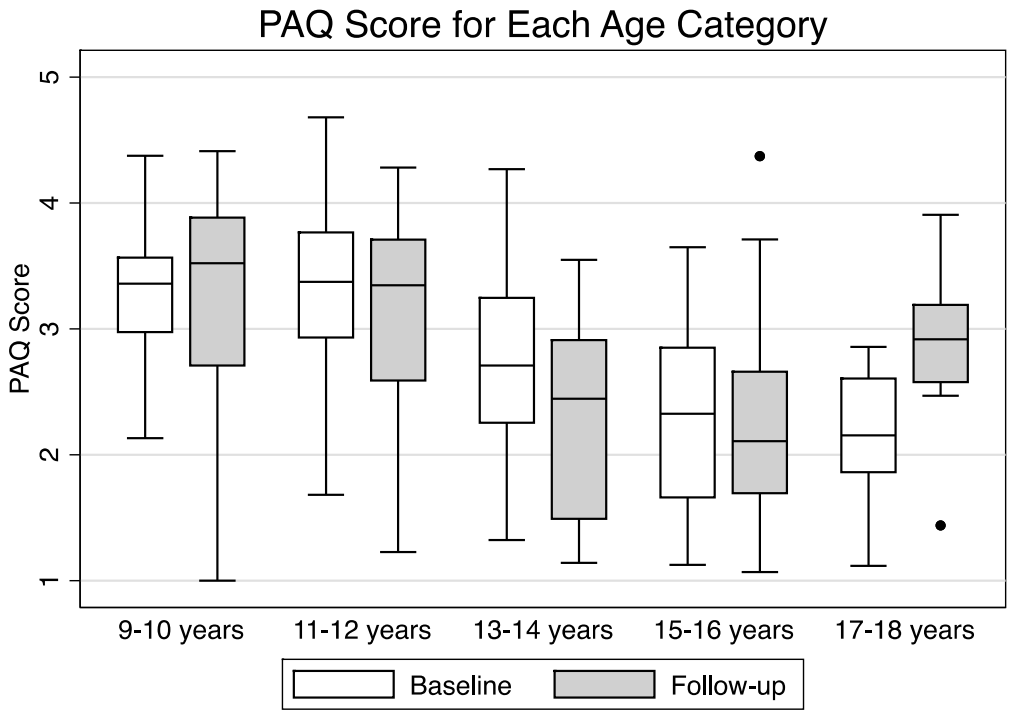
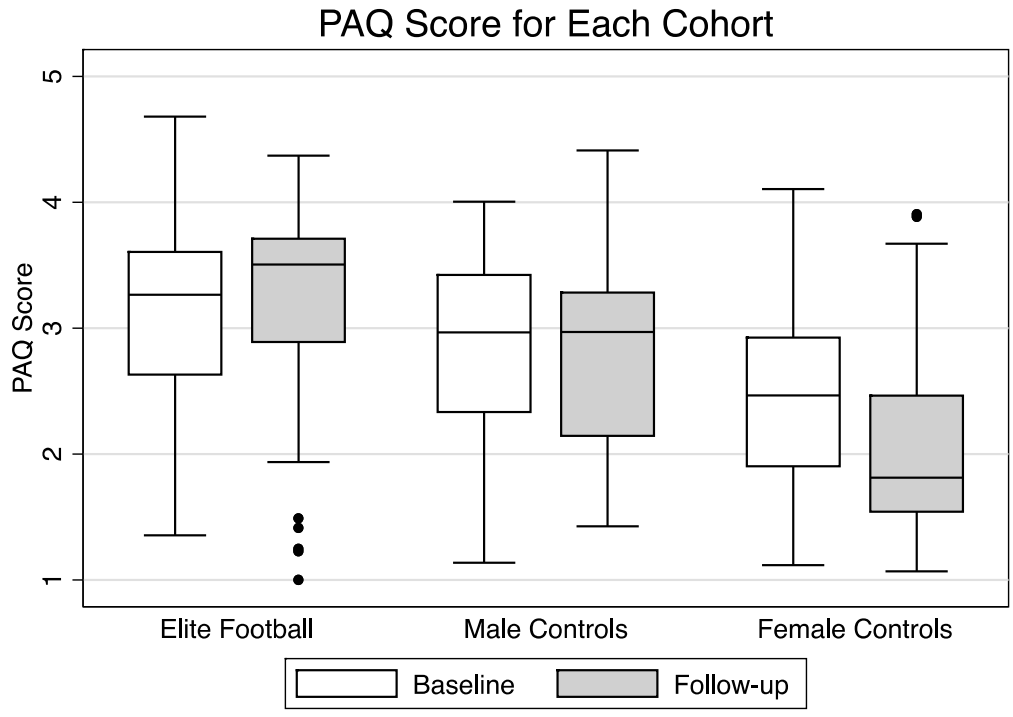


Figure 2-24: Box and Whisker Plot of Physical Activity Questionnaire Score Versus Cohort at Baseline and Follow-up



2.10.2 BMI

Mean BMI increased with age, and between baseline and follow-up, in all cohorts (Table 2-4) (Figure 2-25). Comparisons were therefore made using regression analysis with months of age as a covariate. At baseline there was no statistically significant difference in BMI between male controls and female controls (p=0.838), whereas male footballers had a statistically significant lower BMI than control males (coefficient -0.83, p=0.005). At follow-up there was no statistically significant difference in BMI between male footballers and male controls (p=0.378), whereas male controls had a statistically significant lower BMI than female controls (coefficient -1.403, p=0.029). Regression analysis with months of age as a covariate identified a statistically significant relationship between BMI and the Physical Activity Questionnaire at baseline (coefficient -0.086, p<0.001) and at follow-up (coefficient -0.626, p<0.001). (Figure 2-26) (Table 2-4)

Table 2-4 - Mean and Standard Deviation of Body Mass Index (BMI)

		Male Footballers		Male controls		Female controls	
		Baseline **Mean (±SD)**	**Follow-up** **Mean (±SD)**	**Baseline** **Mean (±SD)**	**Follow-up** **Mean (±SD)**	**Baseline** **Mean (±SD)**	**Follow-up** **Mean (±SD)**
Age at baseline (years)	**9-10**	16.91 (±1.83)	18.54 (±2.21)	17.97 (±2.49)	19.19 (±2.01)	17.05 (±1.98)	19.71 (±3.11)
	11-12	17.42 (±1.42)	19.17 (±1.85)	18.37 (±1.86)	20.03 (±2.63)	20.22 (±3.07)	24.90 (±4.10)
	13-14	19.16 (±1.71)	21.85 (±1.32)	20.51 (±4.94)	20.14 (±4.12)	22.31 (±4..31)	23.04 (±4.55)
	15-16	21.56 (±1.21)	22.88 (±0.69)	21.37 (±2.68)	23.65 (±2.43)	20.91 (±3.56)	23.08 (±4.55)
	17-18	22.42 (±1.93)	24.40 (±2.95)	22.76 (±0.56)	17.99 (±0.00)	20.87 (±1.89)	21.30 (±2.82)
Average		18.54 (±2.51)	19.83 (±2.55)	19.50 (±3.23)	20.43 (±3.04)	20.35 (±3.70)	22.26 (±4.05)

Figure 2-25: Box and Whisker Plot of Body Mass Index Versus Age at Baseline and Follow-up

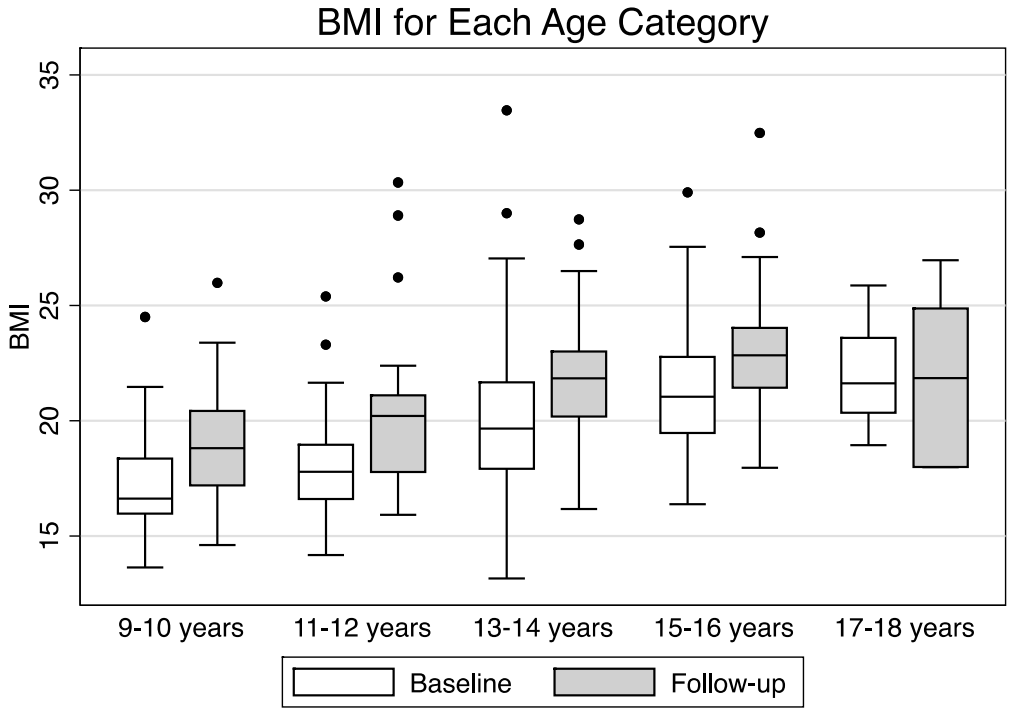
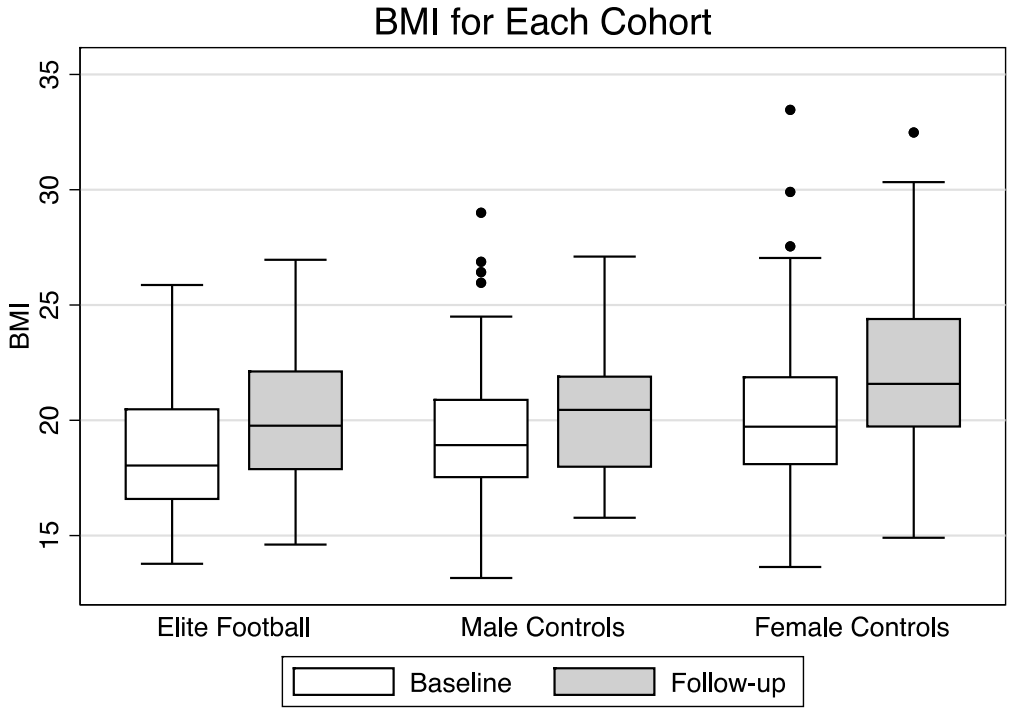


Figure 2-26: Box and Whisker Plot of Body Mass Index Versus Cohort at Baseline and Follow-up



2.10.3 Physeal Development

In the football academy cohort the physis of 161 hips were open, 30 hips were partially open, and 46 hips were closed at baseline, and the physis of 96 hips were open, 2 hips were partially open, and 40 hips were closed at follow-up. In the male control cohort the physis of 80 hips were open, 4 hips were partially open, and 20 hips were closed at baseline, and the physis of 38 hips were open, 6 hips were partially open, and 26 hips were closed at follow-up. In the female control cohort the physis of 32 hips were open, 2 hips were partially open, and 74 hips were closed at baseline, and the physis of 10 hips were open, 2 hips were partially open, and 60 hips were closed at follow-up. (Table 2-5) (Table 2-6)

Table 2-5 - Stage of Physeal Development by Age Group at Baseline.

		Male Footballers			Male Controls			Female Controls		
		Open	**Partially Open**	**Closed**	**Open**	**Partially Open**	**Closed**	**Open**	**Partially Open**	**Closed**
Age at baseline (years)	**9-10**	73	0	0	30	0	0	22	0	0
	11-12	64	0	0	28	0	0	10	2	0
	13-14	22	18	4	12	2	2	0	0	24
	15-16	2	10	28	10	2	14	0	0	38
	17-18	0	2	14	0	0	4	0	0	12
Total		161	30	46	80	4	20	32	2	74

Table 2-6 - Stage of Physeal Development by Age Group at Follow-up.

		Male Footballers			Male Controls			Female Controls		
		Open	**Partially Open**	**Closed**	**Open**	**Partially Open**	**Closed**	**Open**	**Partially Open**	**Closed**
Age at baseline (years)	**11-12**	26	0	0	12	0	0	8	0	4
	13-14	58	0	0	18	4	0	2	2	10
	15-16	12	2	14	8	2	6	0	0	10
	17-18	0	0	12	0	0	14	0	0	18
	Over 18	0	0	12	0	0	6	0	0	18
Total		96	2	40	38	6	26	10	2	60

Physeal closure was later in males than females. In males, the physis remained open in all participants at baseline and follow-up up to 13 years of age, and closed between the ages of 13 and 16 years (Figure 2-27, Figure 2-28, Figure 2-29, Figure 2-30). In females, the physis remained open in all participants at baseline and follow-up up to 11 years of age, and closed between the ages of 11 and 14 years (Figure 2-31, Figure 2-32).

Figure 2-27: Stage of Physeal Development at Baseline in Each Age group for Male Footballers

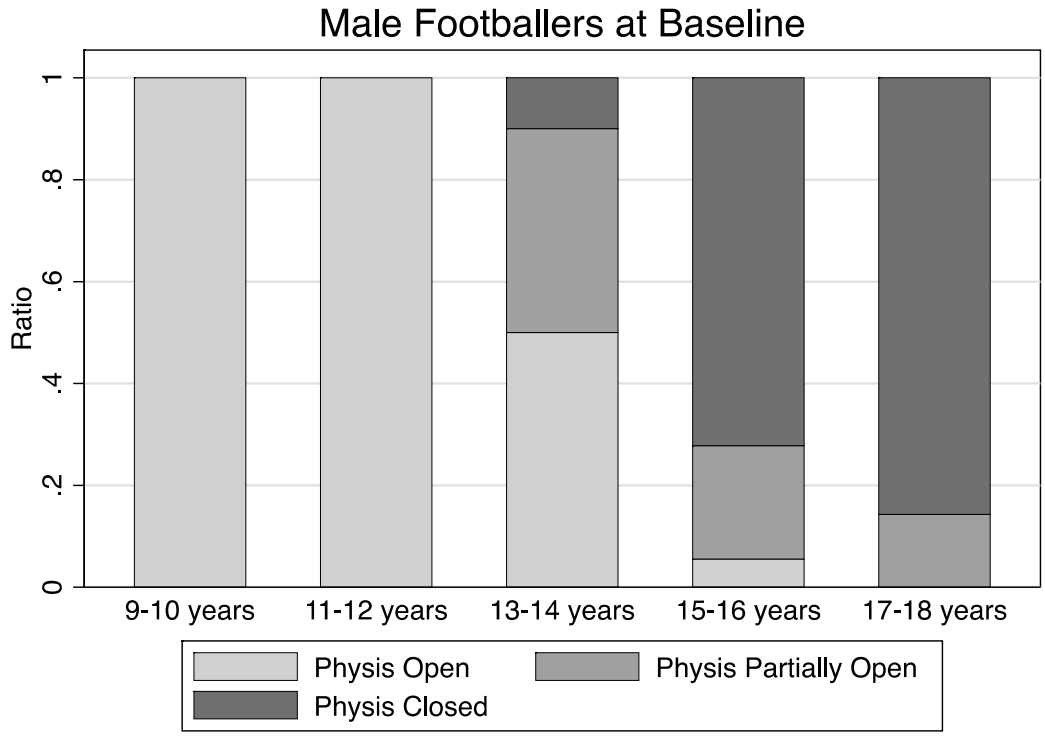


Figure 2-28: Stage of Physeal Development at Follow-up in Each Age group for Male Footballers

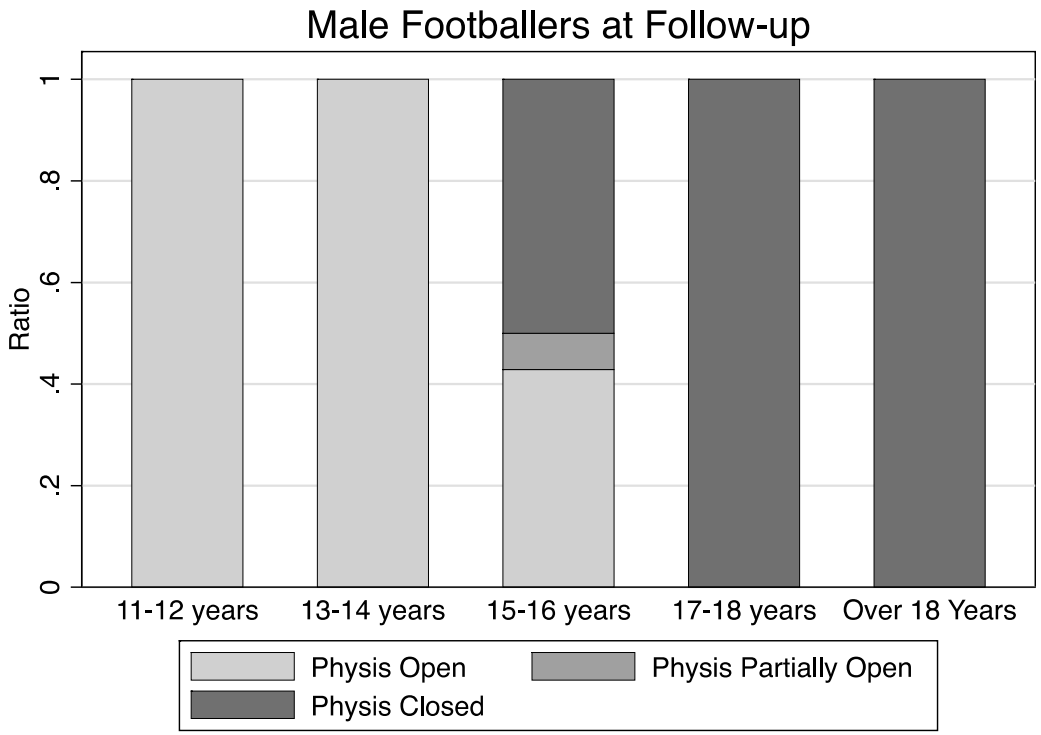


Figure 2-29: Stage of Physeal Development at Baseline in Each Age group for Male Controls

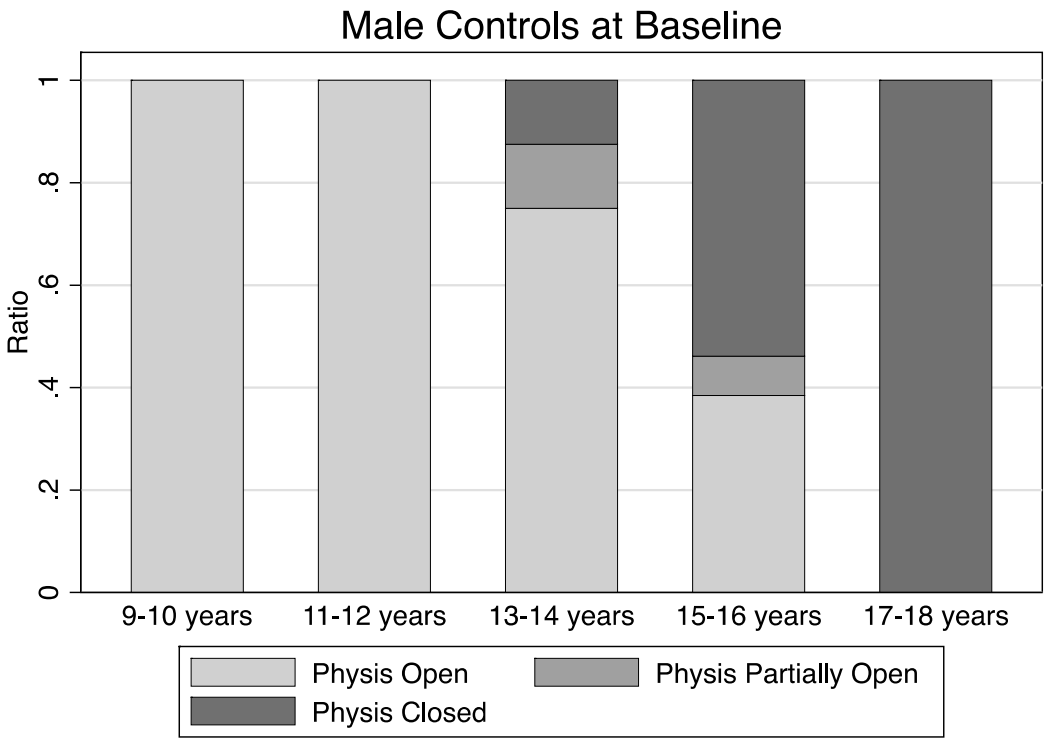


Figure 2-30: Stage of Physeal Development at Follow-up in Each Age group for Male Controls

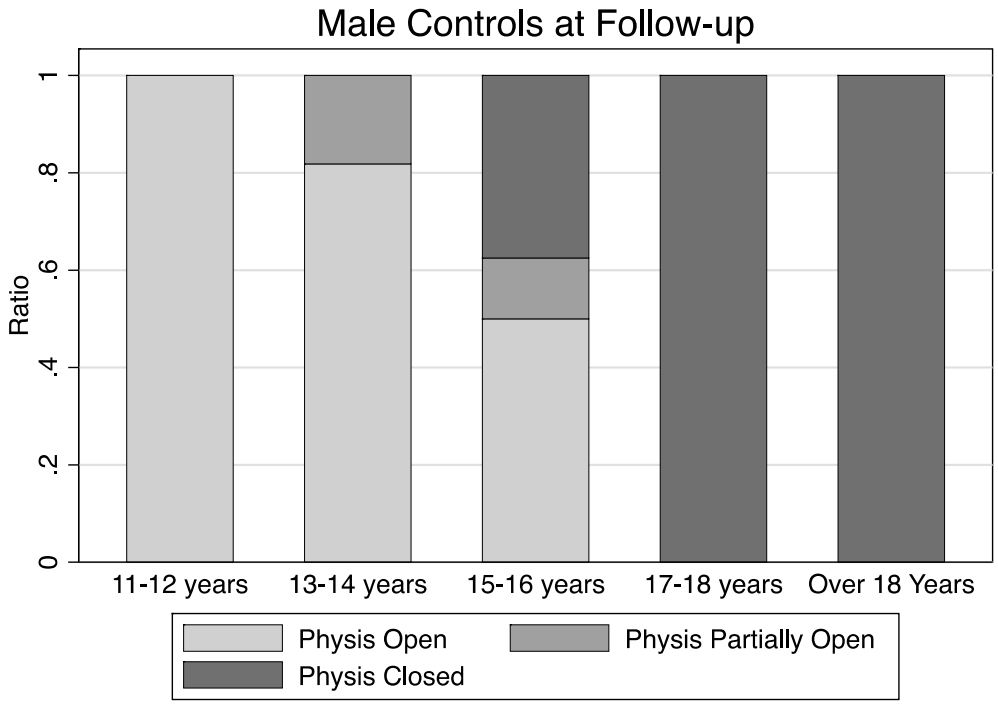


Figure 2-31: Stage of Physeal Development at Baseline in Each Age group for Female Controls

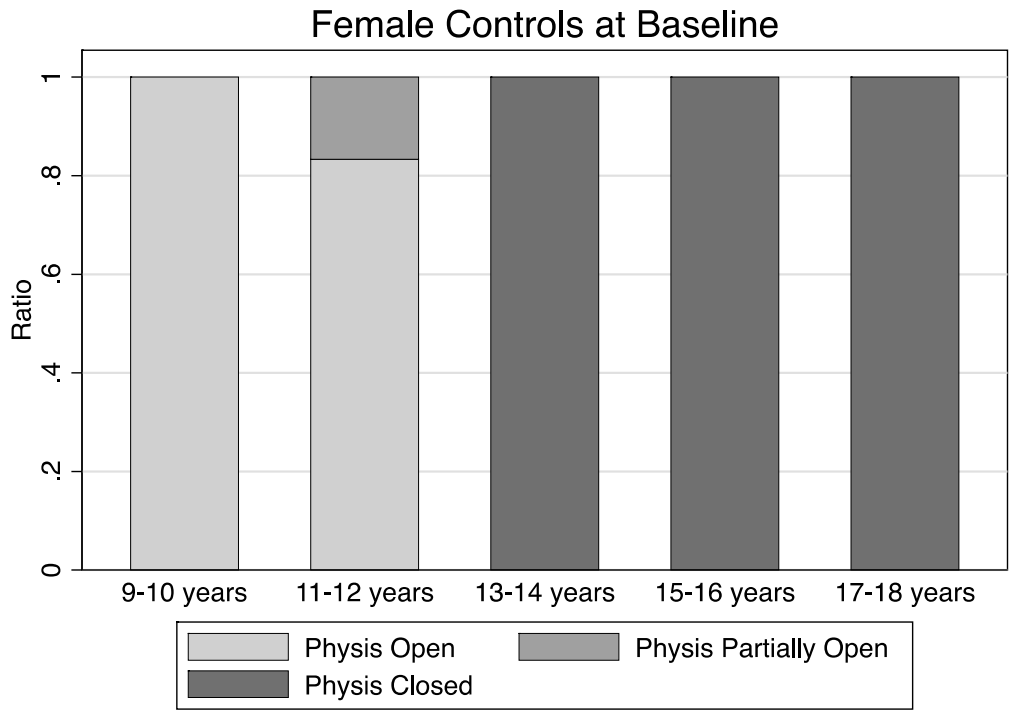
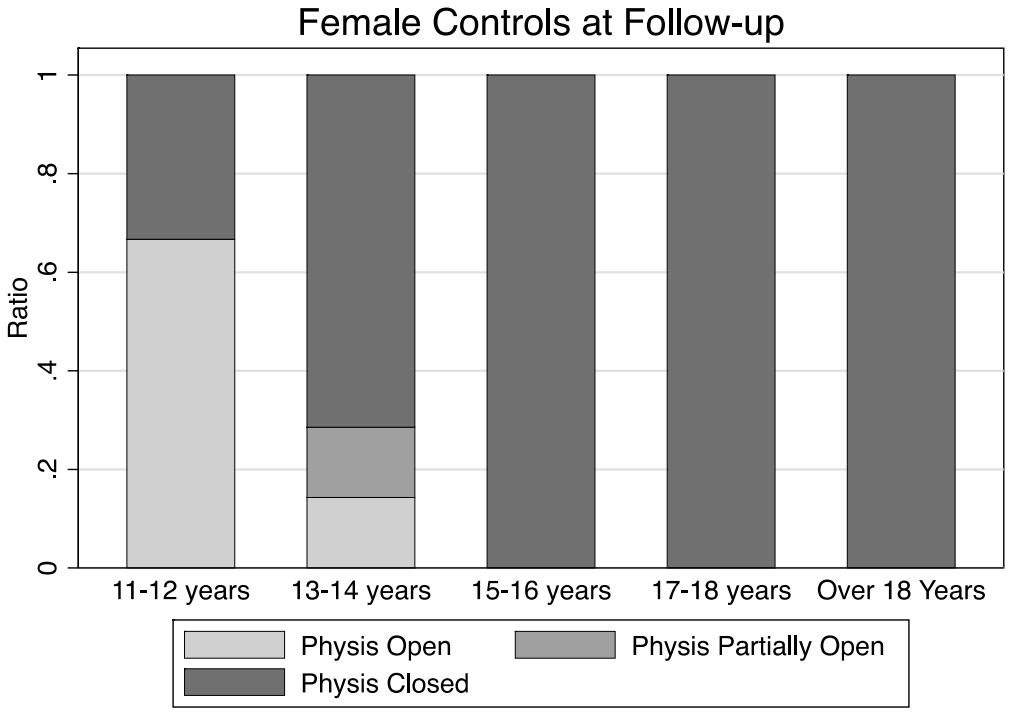


Figure 2-32: Stage of Physeal Development at Follow-up in Each Age group for Female Controls



2.11 Statistical Analysis and Data Diagnostics

Statistical calculations were performed using STATA V.14.1 (College Station, Texas, USA). Distribution of values was examined using histograms and kernel density plots (Appendix A-48 to A-57). Comparison of means was undertaken using an independent two-tailed Student's t-test for parametric data and Wilcoxon rank sum test for non-parametric data. To account for selection bias introduced by loss to follow-up and the sports nature of the study, inverse probability weighting with regression adjustment modelling[286] was adopted to assess variables that predict outcome variables. Multivariate linear regression modeling was used to evaluate the relationship between variables. Variables included in multivariate analysis were cohort, age, gender and activity level. Residual plots of the regression models demonstrated normal distributions but with evidence of heteroscedasticity (Appendix A-46 to A-55). Therefore, the Huber White Sandwich estimator was adopted with clustering for laterality to account for the inclusion of left and right hips that are not independent measurements in multivariate regression models. Clustering was not performed in inverse probability weighting. Interactions were evaluated with linear regression of each combination of variables that predict the outcome variable. None reached statistical significance; hence no interaction terms were included in the multivariate models. Receiver operating characteristic (ROC) analysis was performed on individual variables with a binary outcome at follow-up to determine predictive values of baseline variables. ROC analysis was performed for individual variables but also combined varibales where individual variables were rescaled to have a SD of 1, hence the aggregate biomarker weight gives an estimate of importance[287]. There were missing data for MRI outcomes in five hips at baseline due to incomplete scans and the remaining dataset was complete. No imputation was performed. Statistical significance was set at $p<0.05$.

2.12 Discussion

Football players are an excellent population to investigate the pathogenesis of cam morphology, abnormal acetabular morphology, and varus leg alignment.

In this chapter the development and characterization of a cohort of 121 elite level football players and 107 male and female age matched controls followed up over three years has been described. Significant loss to follow-up was observed; 42% loss in male footballers and 34% in age matched controls. This is a well recognized issue in elite sporting cohorts due to national and international relocation and low player retention[51] and forms a significant limitation of this thesis. However, our study remains adequately powered at the follow-up point with similar cohort demographics to baseline. Additionally, the use of Inverse Probability Weighting (IPW) as a statistical tool attempts to account for selection bias introduced by loss to follow-up[286].

Robust methods for the quantification of cam morphology, acetabular morphology, leg alignment and cartilage composition are required to study disease pathogenesis. Outcome measures in this thesis were selected based on performance in the existing literature as:

- Cam Morphology
    - Alpha Angle
- Physis Morphology
    - Lateral Epiphyseal Extension
- Acetabular Morphology

    - Lateral and Anterior Centre Edge Angle
    - Angle of Anteversion
- Leg Alignment
    - Hip-Knee-Angle
    - Medial Proximal Tibial Physis Angle
- Cartilage Composition
    - T2 Mapping

Reproducibility studies were performed for each of the variables using two readers with favorable results. The reported reproducibility for alpha angle was excellent and our results are similar to those reported in large cohort studies[228,232]. Retrospective clinical studies that do not report the use of specialist methods for measuring the alpha angle describe poor reproducibility[230]. The custom-designed software used in these studies is likely to have facilitated our strong reproducibility results. A key factor ensuring good intra-observer reproducibility is likely to be reader experience. Strong inter-observer reproducibility is enhanced with training and at least one hundred readings were made under supervision prior to performing independent measurements. This approach may not be feasible when applying measures to the routine clinical setting. The alpha angle threshold for defining cam morphology remains undetermined, particularly for the cartilage alpha angle that has been less widely reported in literature to date. It is also likely that the normal range for alpha angles will be different on each radial plane given the femoral neck is not perfectly cylindrical. It may be more appropriate to treat alpha angle as a continuous variable rather than defining thresholds.

Epiphyseal extension reproducibility compares favorably with similar reported physeal measurements[288]. Measurements of the physeal scar in hips with a closed physis are technically more challenging, however, using co-registered WATSf and PDFS sequences there is no statistically significant difference in the reproducibility of closed physis measurements compared with open physis measurements.

Acetabular measurements showed high reproducibility and were similar to those stated in similar studies[128]. The difficulty in measuring the acetabulum stems from the need to orientate the pelvis correctly rather than defining the appropriate anatomy. Determining correct acetabular orientation is made significantly easier by using three-dimensional CT or isotropic MRI imaging sequences, such as WAVE, where post acquisition adjustments can be made prior to taking measurements.

Leg alignment measures also showed high reproducibility and compared favorably with previous studies[134]. All measures of leg alignment had intraobserver ICCs above 0.9 apart from the JLCA. This is likely due to the small magnitude of the angles recorded for the JLCA, such that even a mild observer discrepancy represents a large change in the final measurement.

Only a few reproducibility studies for T2 mapping of the hip have been carried out to date[289,290]. In this study reproducibility of T2 analysis using regions of interest (ROI) methodology was high, consistent with previous reproducibility trials in the knee[291-293] and hip[290]. The reproducibility of individual ROIs varied significantly, with the greatest

variability seen at the chondrolabral junction and the posterior acetabulum. This is likely due to difficulties in identifying the cartilage boundaries in these regions. However, reproducibility still remained high in these areas.

In summary, a cohort of elite athletes and controls has been established, allowing the investigation of changes in hip and knee morphology over three years. All the outcome measures discussed have demonstrated validity in published studies and have demonstrated excellent intra-observer and inter-observer reproducibility with little evidence of systematic bias or observer drift. Insight into the strengths and weaknesses of each measurement facilitates the appropriate interpretation of results of future studies.

2.13 Acknowledgement

A significant acknowledgement must be made of the work that formed the basis for this thesis. Mr Antony Palmer developed the study methodology and recruited the baseline cohort. His cross sectional work looking at femoral head morphology at baseline formed a significant portion of his thesis and provided the baseline femoral head morphology data used in chapter 3 of this thesis.

Chapter 3 Femoral Head Morphology in Adolescence and the Effects of Activity

3.1 Abstract

Introduction:

Cam morphology develops during adolescence and predisposes individuals to future hip osteoarthritis. An improved understanding of cam development is required to determine whether the process is predictable or modifiable. The aim of this study was to characterise the risk factors, timing, and pathogenesis of cam formation.

Methods:

Longitudinal observational cohort study over three years of individuals from football club academies and an age-matched control population, aged 9-18 years at baseline. Assessments included questionnaires, clinical examination, and MRI of both hips. Alpha angle, epiphyseal extension, and fibrochondroosseous tissue area were measured on radial images.

Results:

The cohort consisted of male academy footballers (121 at baseline and 78 at follow-up), male controls (52 at baseline and 35 at follow-up) and female controls (55 at baseline and 36 at follow-up). Mean change in cartilage alpha angle was 12.4° (SD 8.4) for footballers, 7.3° (SD 6.0) for male controls and 4.0° (SD 4.1) for female controls. A positive correlation

existed between Physical Activity Questionnaire Score and change in cartilage average alpha angle (coefficient 0.79, p=<0.001). The greatest change in cartilage average alpha angle occurred in individuals aged 11-12 years at baseline (9.27 degrees, p< 0.001), with no significant change after 14 years of age. A positive correlation between cartilage average alpha angle and lateral epiphyseal extension was seen (r^2 = 0.29, p=0.029). Average fibrochondroosseous tissue area at baseline showed the greatest capability of predicting the development of cam morphology at 3 years with an area under the curve of 0.83.

Conclusions:

Males undertaking intense sporting activity during adolescence are at greatest risk of developing cam morphology, but there is no significant change in hip morphology after 14 years of age. These results are consistent with physiological adaptation and epiphyseal extension in response to hip loading during skeletal immaturity. Increased soft tissue hypertrophy at the anterolateral head-neck junction may precede and predict the development of cam morphology

3.2 Introduction

Cam morphology of the hip is prevalent within the general population and is a strong risk factor for the development of hip pain, osteoarthritis, and future total hip arthroplasty[15,88]. An improved understanding of cam morphology development is required to determine whether cam formation is preventable or modifiable.

Preventing the development of cam morphology formation requires the identification of individuals at risk, which studies to date suggest are males participating in high intensity sport during adolescence[33,51]. However, it is not known how to define high intensity sports, and at what age hips are most susceptible to developing cam morphology[25,105,113]. These uncertainties limit the development of strategies to prevent cam formation.

Most of the literature in this field consists of small cross-sectional cohort studies[31,32]. The absence of cam morphology when the physis is open[31,32], and high prevalence of cam morphology when hips are skeletally mature led to the proposal that cam morphology develops around the time of physeal closure[29-32,51]. Baseline data from our cohort demonstrated morphological changes consistent with early cam development in individuals from 10 years of age[29,30,33,52]. Longitudinal data is required to understand the development of cam morphology within the individual[294]. Studies using radiography[30,33,51] cannot assess the cartilaginous structures of skeletally immature hips. Control populations are also necessary to determine what threshold of activity predisposes to cam development.

3.3 Aims

1) Investigate changes in femoral head morphology with age
2) Investigate the effects of activity on the development of femoral head morphology
3) Explore the pathogenesis of cam development
4) Determine whether baseline risk factors in skeletally immature individuals can predict the development of cam morphology at follow-up

3.4 Methods

The methods for this study and justifications for imaging measures are discussed in chapter 2.

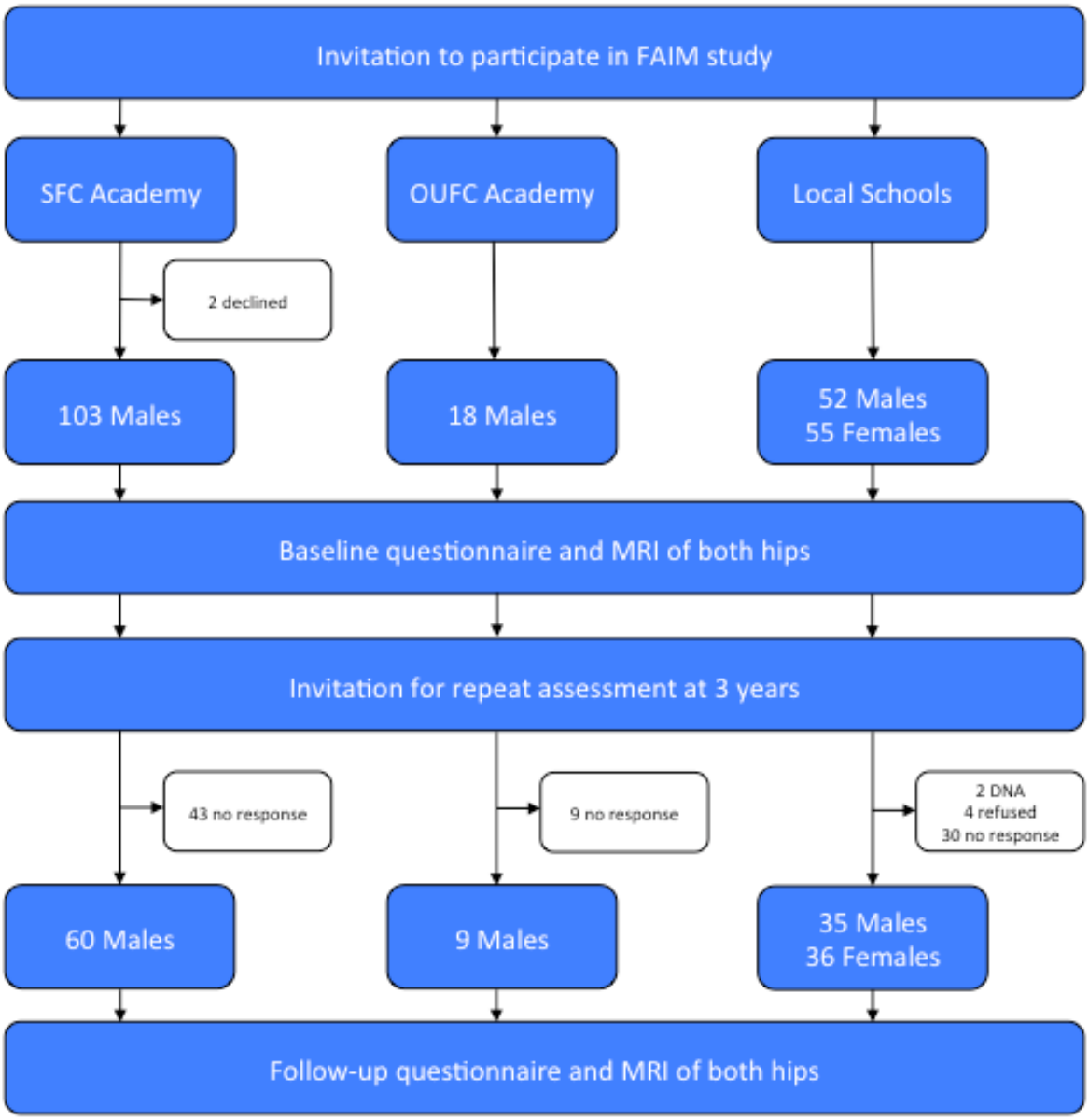
3.4.1 Study design

Longitudinal prospective observational cohort study.

3.4.2 Population

Individuals aged 9–18 years were recruited from Southampton Football Club (SFC) Academy, Oxford United Football Club (OUFC) Academy, and local schools (controls) at baseline. Participants were invited for repeat assessment three years after initial baseline visit via post, email, and telephone. Study IDs were generated for each participant such that assessors were blinded to participant characteristics such as cohort and age when interpreting data such as MRI scans (see chapter 2). Loss to follow-up was 42% for SFC, 50% for OUFC, and 34% for Controls. All football players who remained a member of the football club, but no player who had been released from the club attended follow-up. Four individuals from the control cohort declined repeat assessment, two did not attend their arranged follow-up appointment, and thirty individuals did not respond to invitation. (Figure 3-1)

Figure 3-1 – Recruitment flowchart for study.



3.4.3 Activity Levels

Activity was evaluated using two methods: i) SFC and OUFC Academy (elite footballer cohort) versus general population controls; ii) Physical Activity Questionnaire (PAQ) for older children (aged 9–13 years) and adolescents (aged 14–18 years)[224].

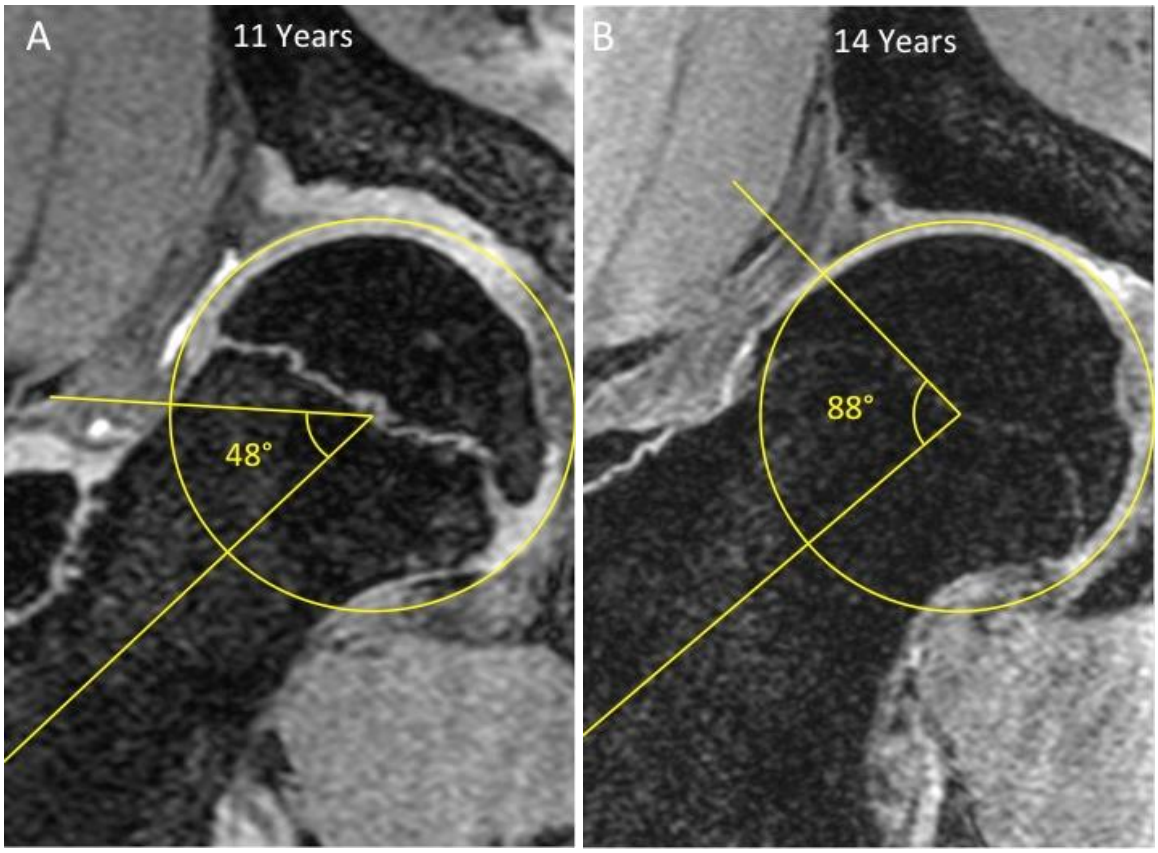
3.4.4 Imaging Protocol

Cam morphology was assessed with MRI of both hips using a 3 Tesla Philips Achieva platform and torso coil (Philips Healthcare). Three-dimensional (3D) water selective fluid (WATSf) sequence was used to image joint cartilage and bone, and 3D proton density fat saturation (PDFS) sequence was used to image the physeal scar. 3D multiplanar reconstructions were performed using OsiriX Software (V.6.0.2, Pixmeo). Radial images were acquired around the axis of the femoral neck at 30 degree intervals. The coronal axis (12 o'clock position) was positioned parallel to the axis of the proximal femur diaphysis[52]. MRI outcomes were incomplete due to claustrophobia or movement artifact in five hips at baseline (two participants in SFC cohort and one female control). The follow-up dataset was complete.

3.4.5 Imaging Measures

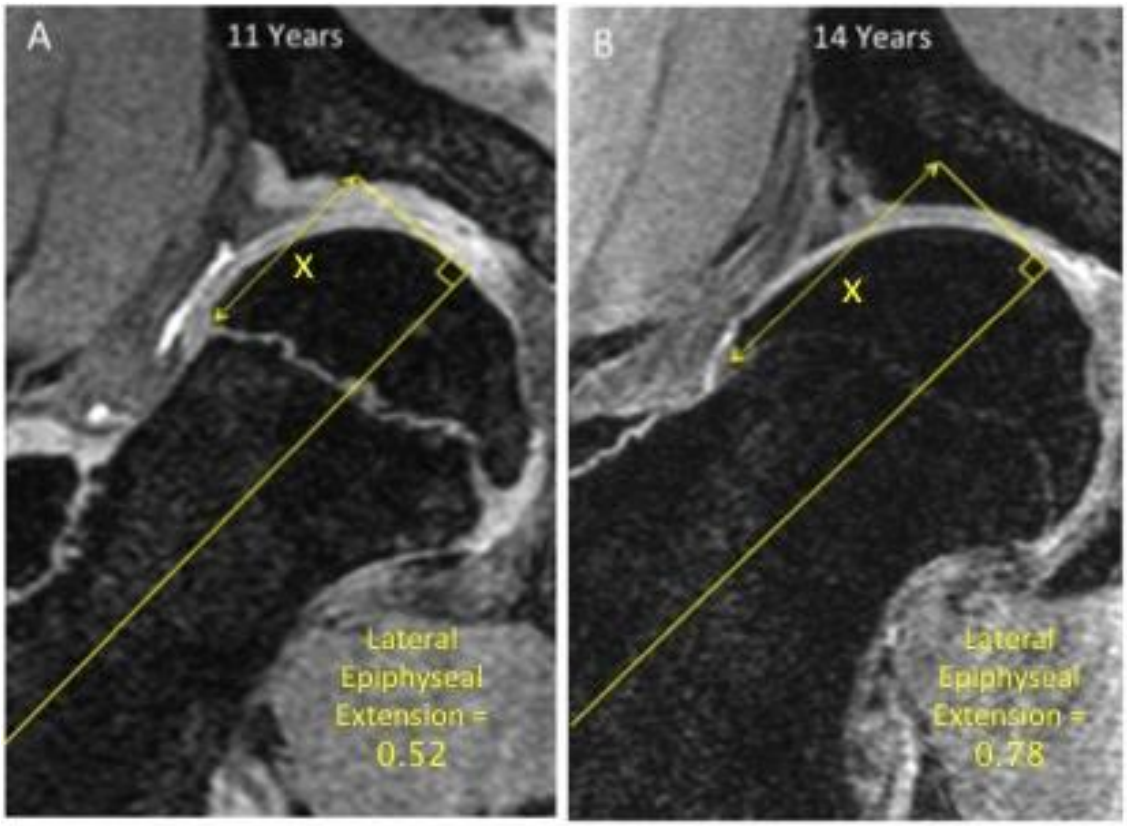
In this study cam morphology was quantified using the alpha angle for cartilage on radial slices from 11 o'clock, 12 o'clock, 1 o'clock, 2 o'clock, and 3 o'clock. Alpha angles above 60 degrees were taken to define the presence of cam morphology in skeletally mature individuals[22]. The primary outcome measure was change in mean cartilage alpha angle from 11 o'clock through to 3 o'clock. The magnitude of change in alpha angle between time points that represents a pathological value is unknown; therefore the change in average alpha angle between time points was treated as a continuous variable (Figure 3-2)

Figure 3-2 – Alpha angle in an elite level football player at baseline age 11 years (A) and at follow-up age 14 years (B). Change in alpha angle = 40 degrees.



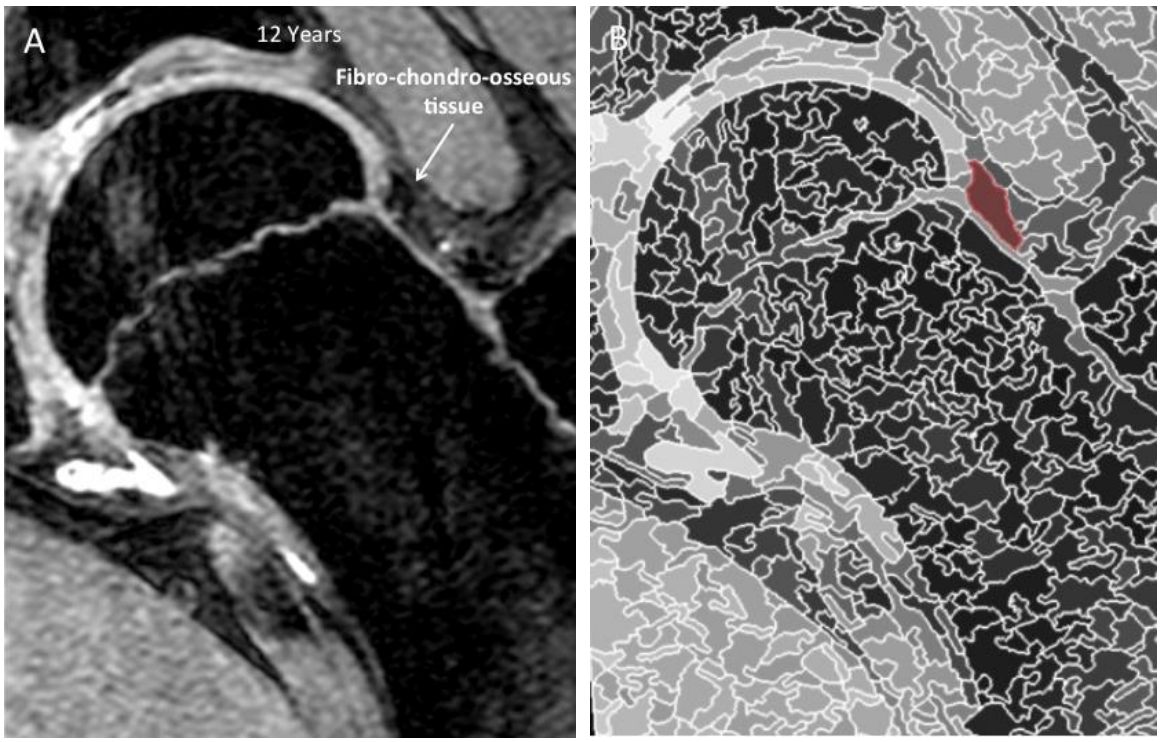
Epiphyseal morphology was quantified using epiphyseal extension[295] measured on radial slices at 11 o'clock, 12 o'clock, 1 o'clock, 2 o'clock and 3 o'clock (Figure 3-3). The mean epiphyseal extension was taken as the average measure from 11 o'clock through to 3 o'clock. The change in average epiphyseal extension was determined by subtracting the mean epiphyseal extension at baseline from follow-up (Figure 3-3). The physis of each hip was scored as either open, partially closed, or closed (see chapter 2).

Figure 3-3 – Lateral epiphyseal extension measurements at 1 o'clock position. Elite level football player at baseline aged 11 years with normal morphology (A) and at follow-up age 14 years (B). Change in lateral epiphyseal extension = 0.26



The ossification groove of Ranvier and the perichondrial fibrous ring of La Croix were quantified using a bespoke semi-automated methodology to segment the Fibrochondrooseous Tissue Area (FTA) at the femoral head-neck junction on radial slices at 11 o'clock, 12 o'clock, 1 o'clock, 2 o'clock and 3 o'clock (Figure 3-4). The mean FTA was taken as the average measure from 11 o'clock through to 3 o'clock. The FTA was measured at baseline only as it is believed to precede cam development[52].

Figure 3-4 – Area of Fibrochondroosseous Tissue shown in an elite level football player at baseline age 12 years (A), with hierarchical partitioned terrain map overlaying the radial image and user selection of the Fibrochondroosseous Tissue Area (B).



3.4.6 Statistical Analysis

See chapter 2 for details of statistical analysis. Inverse probability weighting with regression adjustment modelling[286] was adopted to assess variables that predict outcome variables. Multivariate linear regression modeling was used to evaluate the relationship between variables.

Receiver Operating Characteristic (ROC) analysis was performed on individual variables with a binary outcome of average alpha angle greater than 60 degrees at follow-up in individuals with an open physis and average alpha angle less than 60 degrees at baseline. An alpha angle of 60 degrees was taken to define cam morphology in this thesis based on epidemiological[22] and pathological[97] evidence, and the widespread adoption of this value within the literature. Baseline imaging measures chosen for investigation of capability of predicting cam development were lateral epiphyseal extension and FTA as these likely represent the mechanism of cam formation[52]. Baseline PAQ score was also chosen for investigation of capability of predicting cam development as high activity levels during youth are a recognised risk factor for cam development[33,51]. Baseline internal hip rotation on examination was also chosen for investigation of predictive capabilities. Loss of internal rotation range of motion (ROM) is often one of the first signs of FAI syndrome[78,97]. Loss of ROM is due to the femoral head-neck junction abutting the acetabulum, in adolescence this may occur due to soft tissue hypertrophy that may precede the development of the osseous cam lesion and so be predictive of future bony cam morphology.

In addition to individual variables, combined variables for baseline examination

measures (Internal rotation and PAQ score), baseline imaging measures (FTA and lateral epiphyseal extension), and combined baseline examination and imaging measures (internal rotation, PAQ score, FTA, and lateral epiphyseal extension) were produced. To create combined variables individual variables were rescaled to have a SD of one (denoted by bold text), hence the aggregate biomarker weight gives an estimate of importance[97,287].

Combined baseline examination measures = (0.26 x **PAQ score**) + (1.02 x **internal rotation range of motion**)

Combined baseline imaging measures = (1.00 x **FTA**) + (0.20 x **lateral epiphyseal extension**)

Combined baseline examination and imaging measures = (0.29 x **combined examination measures**) + (0.93 x **combined imaging measures**)

3.5 Results

3.5.1 Participant demographics

See chapter 2 for full participant demographics. At baseline there were 228 individuals (449 hip MRIs) (mean age 151 months, SD 31) and 140 individuals (280 hip MRIs) attended three-year follow-up (mean age 181 months, SD 32). Mean follow up was 36 months (SD 4). (Table 3-1 and 3-2)

Table 3-1 - Cohort demographics

		Male Footballers		Male controls		Female controls	
		Baseline Individuals (Hips)	**Follow-up Individuals (Hips)**	**Baseline Individuals (Hips)**	**Follow-up Individuals (Hips)**	**Baseline Individuals (Hips)**	**Follow-up Individuals (Hips)**
Age at baseline (years)	**9-10**	37 (73)	28 (56)	15 (30)	12 (24)	11 (22)	10 (20)
	11-12	32 (64)	22 (44)	14 (28)	10 (20)	6 (12)	5 (10)
	13-14	22 (44)	9 (18)	8 (16)	4 (8)	12 (24)	8 (16)
	15-16	20 (40)	7 (14)	13 (26)	8 (16)	19 (38)	9 (18)
	17-18	8 (16)	3 (6)	2 (4)	1 (2)	6 (12)	4 (8)
Total		119 (237)	69 (138)	52 (104)	35 (70)	54 (108)	36 (72)

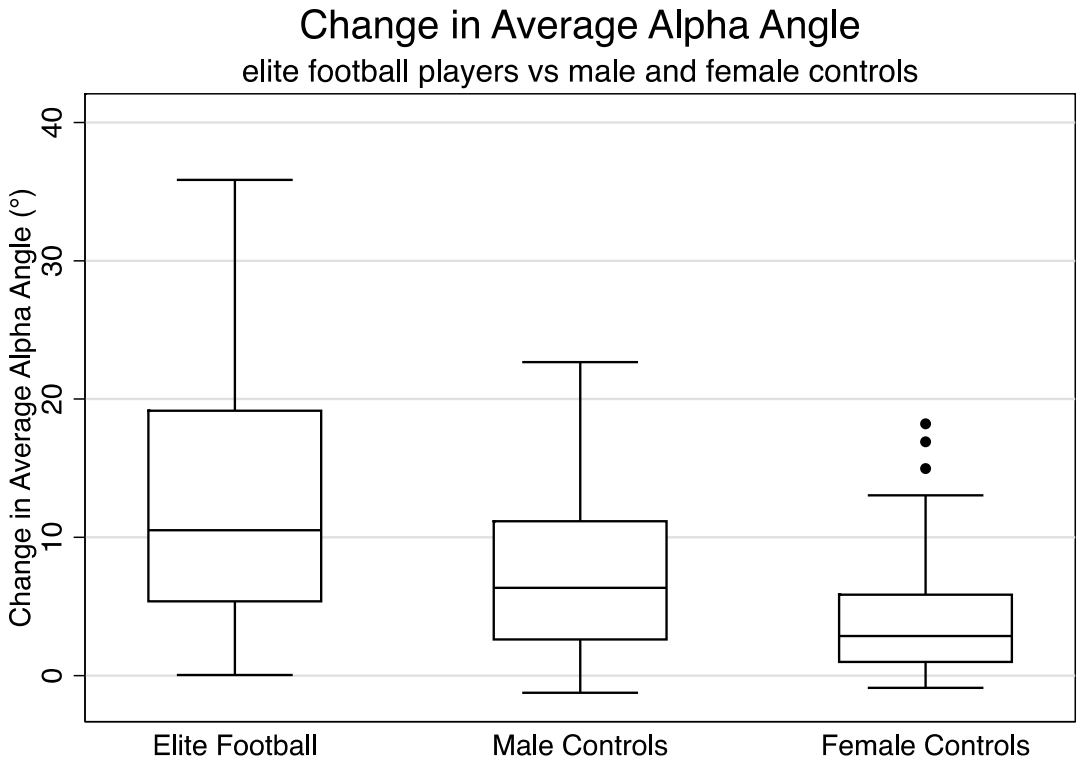
Table 3-2 - Mean Alpha Angle, Lateral Epiphyseal Extension, and Fibrochondroosseous Tissue Area at Baseline and Follow-up by Cohort and Age Group.

Age at Baseline (Years)	Male Footballers		Male Controls		Female Controls	
	Baseline Mean (±SD)	Follow-up Mean (±SD)	Baseline Mean (±SD)	Follow-up Mean (±SD)	Baseline Mean (±SD)	Follow-up Mean (±SD)
Average Alpha Angle (Degrees)						
9-10	48.31 (±4.04)	62.62 (±10.47)	47.76 (±3.00)	54.93 (±5.28)	47.86 (±3.83)	55.32 (±4.97)
11-12	50.37 (±4.95)	65.30 (±9.13)	50.43 (±4.82)	60.92 (±8.34)	52.08 (±5.42)	58.76 (±5.59)
13-14	61.41 (±8.81)	66.06 (±8.79)	56.75 (±5.11)	62.10 (±5.70)	50.43 (±4.76)	53.42 (±4.80)
15-16	65.88 (±12.55)	70.33 (±12.55)	60.29 (±9.26)	65.81 (±11.40)	50.73 (±7.01)	53.02 (±7.39)
17-18	66.43 (±15.57)	58.27 (±7.49)	58.13 (±2.80)	61.31 (±6.34)	54.34 (±7.33)	58.18 (±6.59)
Average	55.28 (±11.00)	64.52 (±10.19)	53.39 (±7.73)	60.13 (±8.84)	50.63 (±6.06)	55.12 (±6.13)
Lateral Epiphyseal Extension						
9-10	0.65 (±0.03)	0.68 (±0.03)	0.64 (±0.03)	0.68 (±0.05)	0.65 (±0.03)	0.72 (±0.03)
11-12	0.67 (±0.02)	0.74 (±0.05)	0.66 (±0.04)	0.71 (±0.04)	0.72 (±0.04)	0.76 (±0.04)
13-14	0.72 (±0.07)	0.76 (±0.04)	0.68 (±0.05)	0.77 (±0.04)	0.73 (±0.03)	0.77 (±0.02)
15-16	0.78 (±0.05)	0.78 (±0.05)	0.75 (±0.04)	0.77 (±0.04)	0.74 (±0.03)	0.78 (±0.03)
17-18	0.81 (±0.04)	0.78 (±0.06)	0.77 (±0.01)	0.77 (±0.03)	0.77 (±0.03)	0.78 (±0.03)
Average	0.70 (±0.07)	0.72 (±0.06)	0.68 (±0.06)	0.72 (±0.06)	0.72 (±0.05)	0.76 (±0.04)
Fibrochondroosseous Tissue Area (mm^2)						
9-10	96.00 (±47.74)	-	54.53 (±39.10)	-	61.12 (±41.52)	-
11-12	86.86 (±42.89)	-	70.66 (±30.24)	-	45.47 (±20.76)	-
13-14	81.17 (±36.30)	-	60.82 (±24.90)	-	48.42 (±0)	-
15-16	-	-	61.07 (±48.43)	-	-	-
17-18	-	-	-	-	-	-
Average	91.04 (±44.75)	-	62.27 (±34.06)	-	57.17 (±37.27)	-

3.5.2 Risk Factors for Cam Development

Elite football players had a significantly greater change in alpha angle than controls between baseline and follow-up. Adjusting for age elite football players had a change in average alpha angle 4.83 degrees greater than male controls ($p<0.001$) (Figure 3-5) (Table 3-3). Male controls had a significantly greater change in alpha angle than female controls between baseline and follow-up. Adjusting for age male controls had a change in average alpha angle 2.27 degrees greater than female controls ($p=0.016$). (Figure 3-5) (Table 3-3)

Figure 3-5 – Change in Average Cartilage Alpha Angle in Individuals from the Elite Footballer Cohort, Male Controls, and Female Controls. Box and whisker plot.



Individuals with high activity levels (PAQ score) had a significantly greater change in alpha angle than those with lower activity levels. Adjusting for age and gender individuals with a PAQ score between 3 and 4 and between 4 and 5 had a change in average alpha angle 0.58 degrees (p=0.008) and 3.20 degrees (p=0.025) greater than individuals with a PAQ less than 2 respectively (Figure 3-6). Controlling for age and gender there was a positive linear relationship between PAQ score and change in average cartilage alpha angle (coefficient = 0.79, p = <0.001) (Figure 3-7). (Table 3-3).

Figure 3-6 – Change in Average Cartilage Alpha Angle in Individuals with a PAQ Score below 2, 2-3, 3-4, and above 4 at baseline. Box and whisker plot

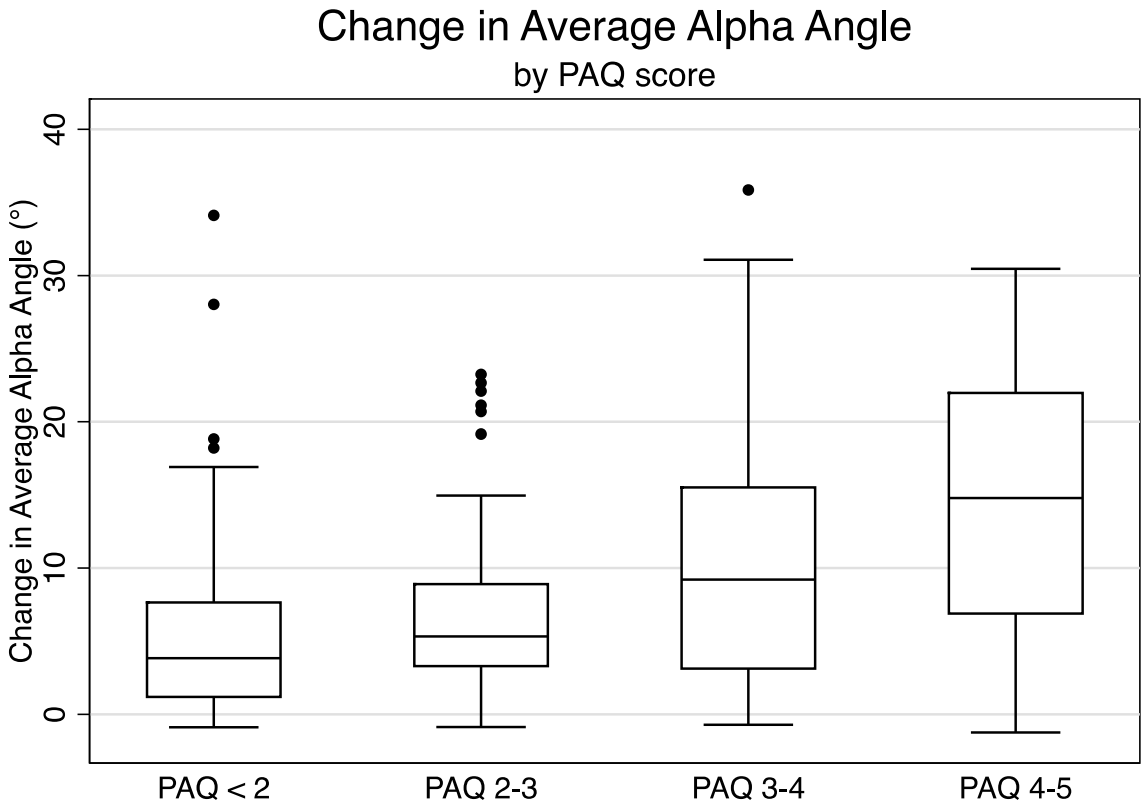
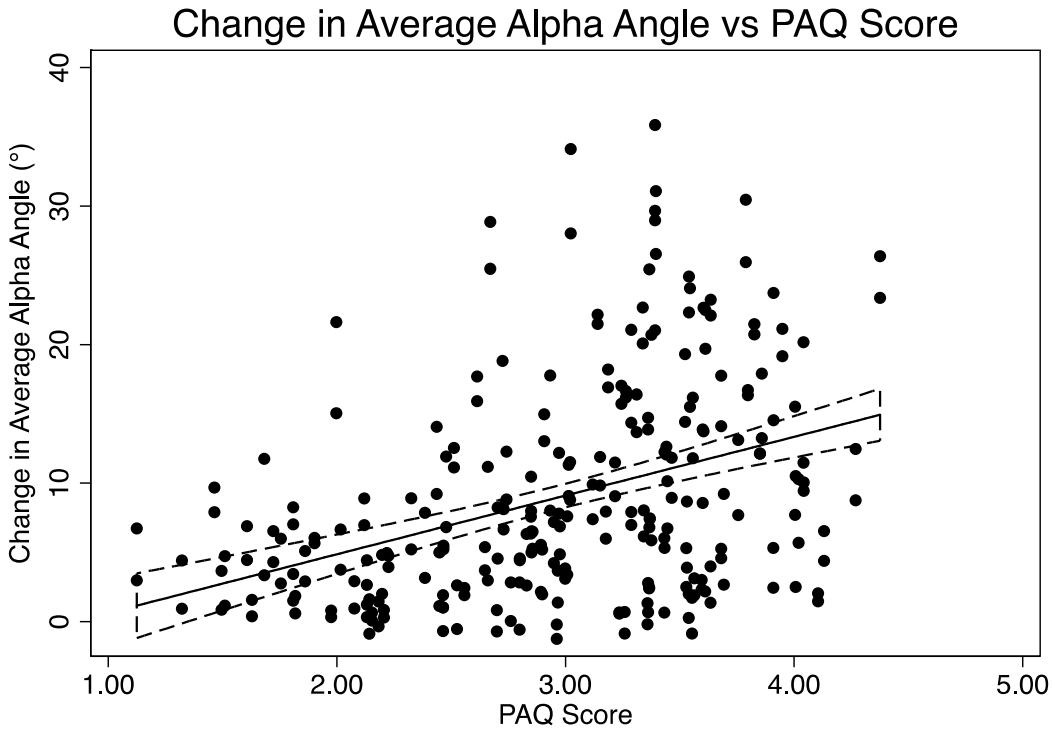


Figure 3-7 – Change in Average Alpha Angle versus PAQ Score. Scatter plot with 95% Confidence Intervals. Coefficient 0.79, $R^2 = 0.62$, p = <0.001



There was no significant association between leg dominance and change in average alpha angle. A significant association between BMI and alpha angle was observed in the univariate regression analysis, but this became insignificant when controlling for age, gender, and activity.

Table 3-3 - Predictors of change in average alpha angle. *Age and cohort as covariables. **Age, gender, and Physical Activity Questionnaire as covariables. ***Physeal maturity, gender, and Physical Activity Questionnaire as covariable

		Hips	Mean Change in Average Alpha Angle (±SD)	Univariate Regression			Multivariate Regression 1*			Multivariate Regression 2**			Multivariate Regression 3***		
				Coefficient	95% CI	P value	Coefficient	95% CI	P value	Coefficient	95% CI	P value	Coefficient	95% CI	P value
Age at Baseline	**Months of Age (Continuous)**	275	8.939 (±7.791)	-0.107	-0.123 to -0.09	0.007	-0.011	-0.022 to -0.001	0.037	0.004	-0.003 to 0.010	0.285			
	9-10 Years	97	11.371 (±8.741)	8.000	5.950 to 10.075	<0.001									
	11-12 Years	72	12.627 (±7.524)	9.268	7.210 to 11.327	<0.001									
	13-14 Years	42	5.393 (±4.465)	2.034	0.291 to 3.778	0.022									
	15-16 Years	48	3.455 (±2.742)	0.097	-1.263 to 1.456	0.889									
	17-18 Years	16	3.359 (±3.366)	-	-	-									
Physis	**Open**	151	12.591 (±8.256)	9.954	8.535 to 11.373	<0.001							9.291	7.499 to 11.083	<0.001
	Open-Closed	54	6.898 (±4.383)	5.693	3.943 to 7.444	<0.001							5.362	3.320 to 7.404	<0.001
	Closed	70	2.637 (±2.315)	-	-	-							-	-	-
Gender	**Male**	203	10.674 (±8.048)	6.627	5.172 to 8.023	<0.001				5.000	2.765 to 7.230	<0.001	2.099	1.255 to 2.943	<0.001
	Female	72	4.047 (±4.133)	-	-	-				-	-	-			
BMI		275	-	-0.768	-1.287 to -0.249	0.034									
Dominant Leg	**Dominant**	152	9.282 (±7.979)	0.766	1.070 to 2.602	0.413									
	Non Dominant	123	8.516 (±7.562)	-	-	-									
Cohort	**Footballers**	133	12.438 (± 8.449)	5.115	3.121 to 7.109	<0.001	4.832	2.844 to 6.821	<0.001						
	Male controls	70	7.323 (± 5.973)	-	-	-	-	-	-						
	Female controls	72	4.047 (±4.133)	-3.276	4.958 to -1.594	<0.001	-2.271	-4.124 to -0.430	0.016						
PAQ	**Continuous**			2.902	2.102 to 3.702	0.014				0.787	0.560 to 1.014	<0.001	0.995	0.550 to 1.440	<0.001
	< 2	68	5.740 (±6.610)	-	-	-									
	2-3	72	7.062 (±5.591)	1.322	-0.697 to 3.341	0.199									
	3-4	103	10.670 (±8.222)	4.930	2.710 to 7.150	<0.001									
	4-5	32	14.389 (±8.764)	8.649	5.277 to 12.020	<0.001									

3.5.3 Age of Cam Development

3.5.3.1 Chronological Age

The greatest change in alpha angle in all participants occurred in individuals aged 11-12 years at baseline, with no significant change occurring in individuals older than 14 years at baseline (Table 3-4) (Figure 3-8). The greatest change in alpha angle in footballers and male controls occurred in individuals aged 11-12 years at baseline. The greatest change in alpha angle in female controls occurred in individuals aged 9-10 years at baseline (Table 3-4). There was no significant change in alpha angle in male and female controls after 12 years of age at baseline, whereas alpha angle continued to increase until 14 years of age at baseline in footballers (Table 3-4) (Figures 3-9, 3-10, and 3-11).

Figure 3-8 – Change in average cartilage alpha angle with age for all participants. Age groups based on chronological age of participant at baseline. Box and whisker plot. Dashed line represents the alpha angle inter-observer SDD (4.22 degrees)

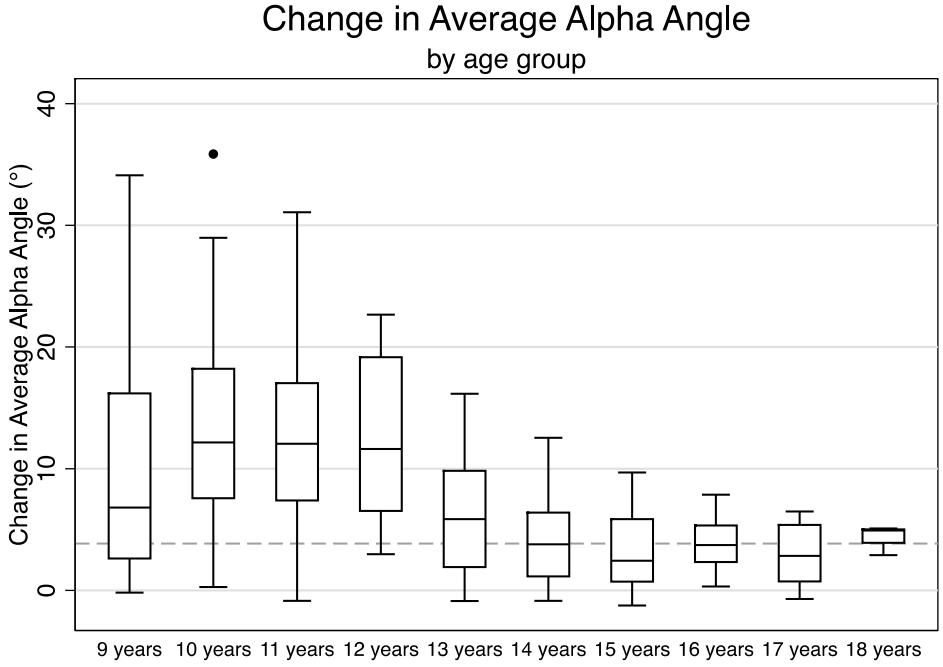


Table 3-4 - Change in average alpha angle with age by cohort

		Average Alpha Angle (±SD)			Univariate regression		
		Baseline	**Follow-up**	**Mean change**	**Coefficient**	**95% CI**	**P value**
Male Footballers							
Age at Baseline (Years)	**9-10**	48.312 (±4.041)	62.624 (±10.471)	14.659 (± 9.606)	9.726	7.029 to 12.424	<0.001
	11-12	50.372 (±4.953)	65.305 (±9.127)	15.026 (±7.355)	10.093	7.738 to 12.448	<0.001
	13-14	61.408 (±8.805)	66.064 (±8.790)	8.173 (±4.462)	3.240	1.066 to 5.414	0.003
	15-16	65.888 (±12.550)	70.327 (±12.554)	4.968 (±2.342)	0.035	-1.419 to 1.488	0.963
	17-18	66.429 (±15.570)	58.274 (±7.486)	4.933 (±1.157)	-	-	-
Average		55.279 (±11.005)	64.520 (±10.192)	12.438 (± 8.449)			
Male controls							
Age at Baseline (Years)	**9-10**	47.756 (±3.002)	54.930 (±5.284)	7.182 (±5.882)	2.810	-0.403 to 6.023	0.047
	11-12	50.434 (±4.818)	60.915 (±8.337)	11.210 (±6.842)	6.838	3.155 to 10.520	<0.001
	13-14	56.754 (±5.105)	62.10 (±5.699)	6.076 (±3.252)	1.704	-1.372 to 4.780	0.278
	15-16	60.289 (±9.260)	65.806 (±11.399)	3.667 (±3.175)	-0.705	-3.405 to 1.995	0.609
	17-18	58.128 (±2.801)	61.312 (±6.335)	4.372 (±2.286)	-	-	-
Average		53.395 (±7.728)	60.128 (±8.838)	7.323 (±5.973)			
Female controls							
Age at Baseline (Years)	**9-10**	47.856 (±3.825)	55.316 (±4.971)	7.684 (±4.999)	5.760	-1.590 to 1.922	<0.001
	11-12	52.076 (±5.421)	58.776 (±5.589)	5.387 (±3.424)	3.463	-1.835 to 1.834	0.007
	13-14	50.435 (±4.757)	53.417 (±4.804)	1.0924 (±2.155)	-0.000	0.938 to 5.987	1.000
	15-16	50.726 (±7.014)	53.022 (±7.394)	2.090 (±1.949)	0.166	3.137 to 8.383	0.853
	17-18	54.340 (±7.330)	58.182 (±6.595)	1.925 (±2.350)	-	-	-
Average		50.628 (±6.055)	55.119 (±6.128)	4.047 (±4.133)			

Figure 3-9 – Change in average cartilage alpha angle with age in male footballers. Age groups based on chronological age of participant at baseline. Box and whisker plot. Dashed line represents the alpha angle inter-observer SDD (4.22 degrees)

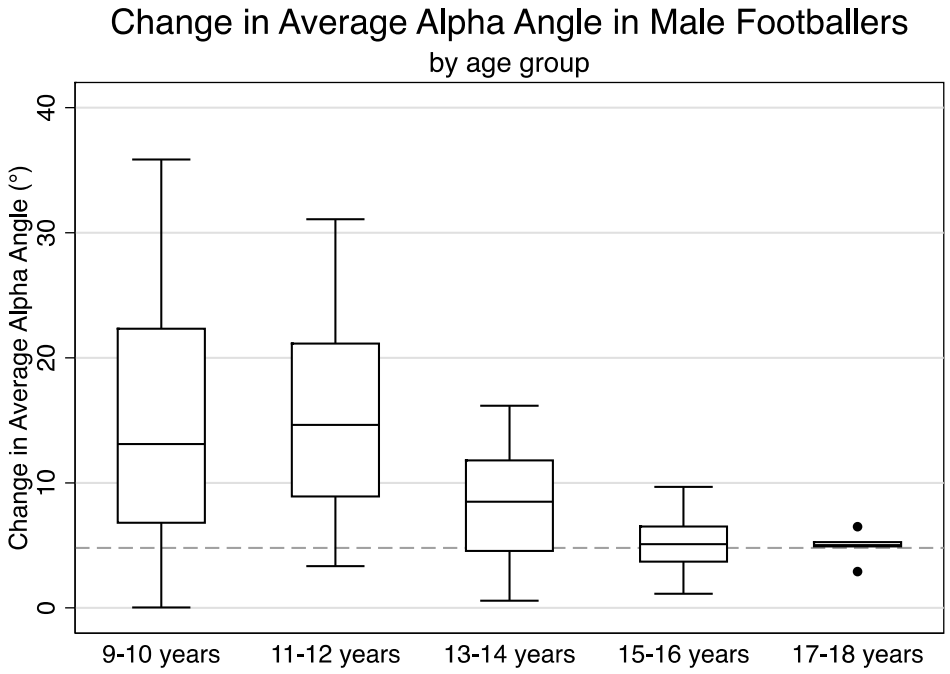


Figure 3-10 – Change in average cartilage alpha angle with age in male controls. Age groups based on chronological age of participant at baseline. Box and whisker plot. Dashed line represents the alpha angle inter-observer SDD (4.22 degrees)

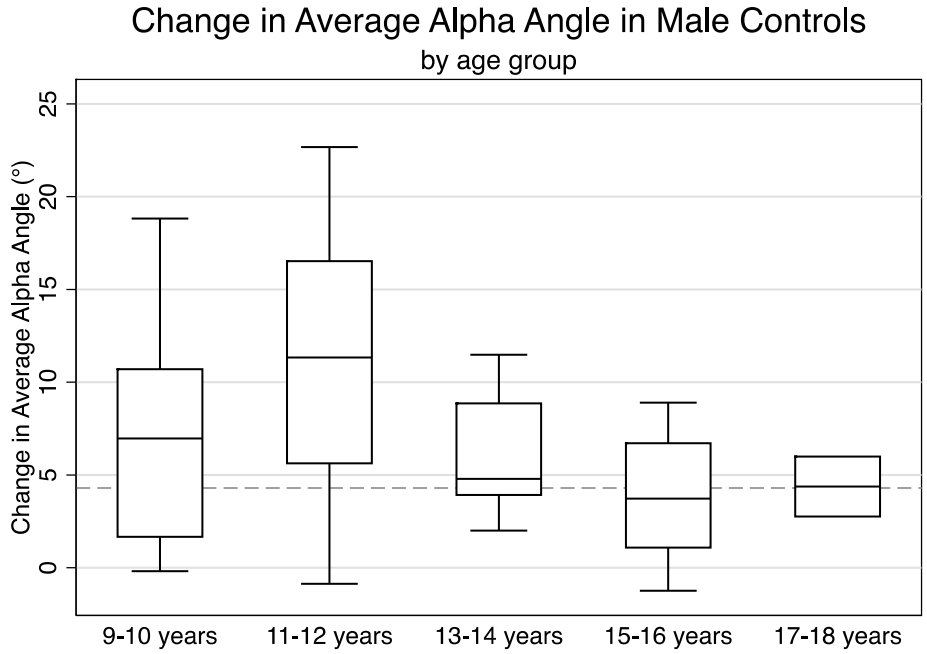
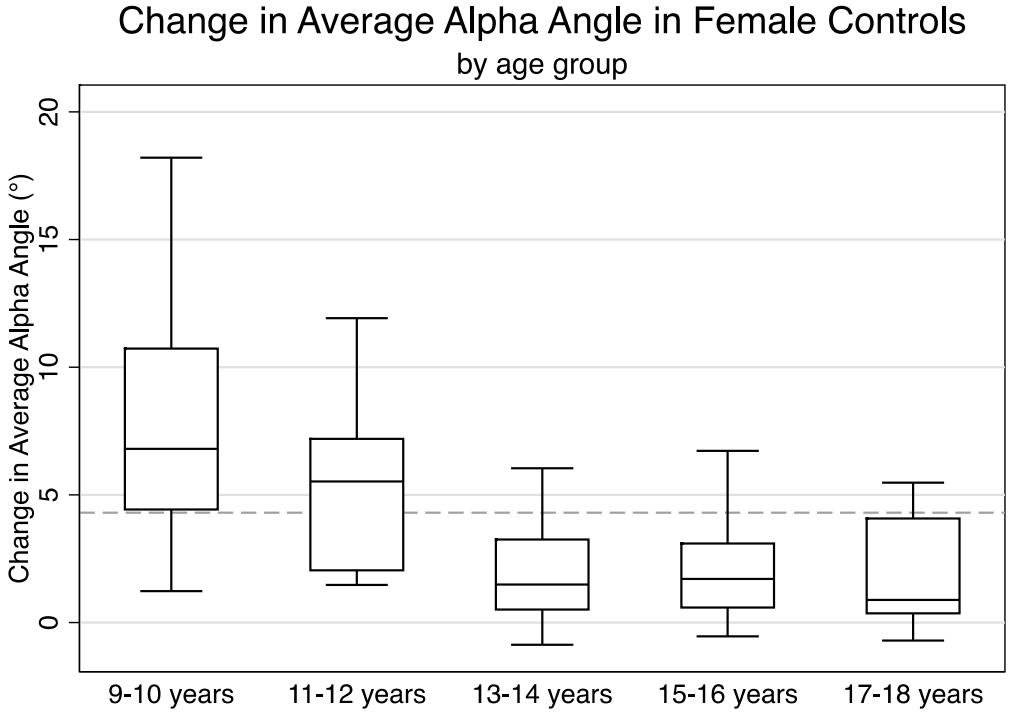


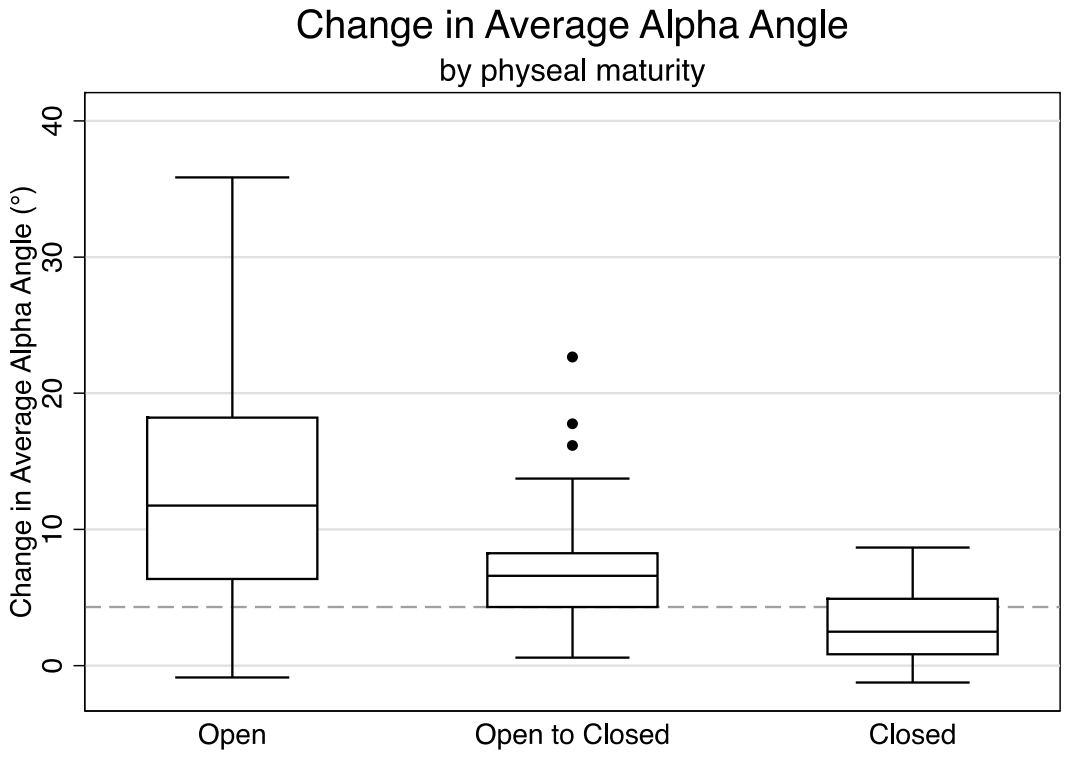
Figure 3-11 – Change in average cartilage alpha angle with age in female controls. Age groups based on chronological age of participant at baseline. Box and whisker plot. Dashed line represents the alpha angle inter-observer SDD (4.22 degrees)



3.5.3.2 Skeletal Maturity

Younger individuals with an open physis at both baseline and follow-up experienced the greatest change in alpha angle. Adjusting for activity level and gender individuals with an open physis at baseline and follow-up had a change in average alpha angle 9.29 degrees greater than individuals with a closed physis ($p<0.001$) (Figure 3-12). Individuals with a closed physis had a change in average alpha angle of 2.64 degrees between baseline and follow-up, which was not statistically significant and was less than the smallest detectable difference for intra- and inter-observer reproducibility measures for alpha angle (see chapter 2). (Table 3-3)

Figure 3-12 – Change in average cartilage alpha angle by physeal maturity. Box and whisker plot. Dashed line represents the alpha angle inter-observer SDD (4.22 degrees)



3.5.4 Location of Cam Development

The greatest change in average alpha angle occurred at the anterosuperior (1 o'clock) femoral head-neck junction. Elite footballers had significantly greater change in average alpha angle than male controls at the 12, 1, 2, and 3 o'clock positions, but not at the 11 o'clock position, with the greatest difference at the 1 o'clock position (Figure 3-13). Adjusting for age elite footballers had a change in average alpha angle 8.18 degrees greater at the 1'clock position than controls ($p<0.001$). (Table 3-5)

Figure 3-13 – Average Change in Alpha Angle by Position On Femoral Head-Neck Junction. Bar Chart.

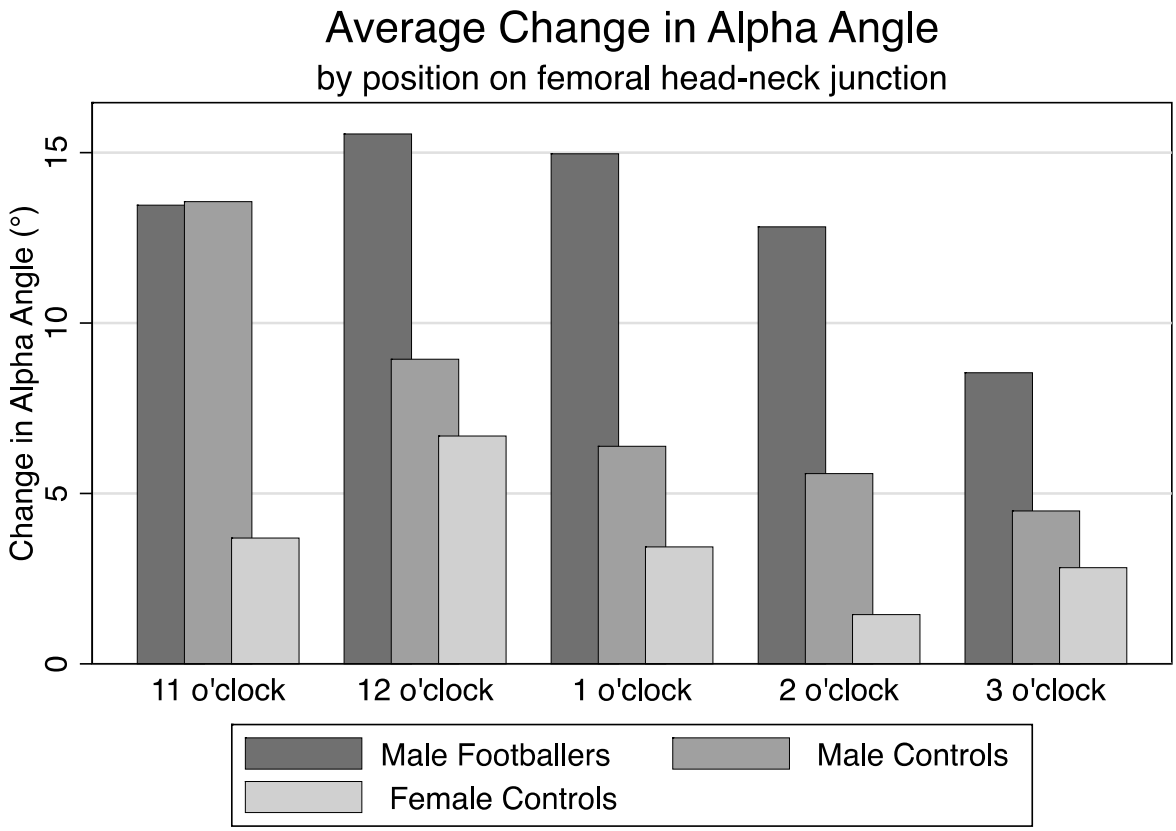


Table 3-5 - Change in alpha angle by position on femoral head-neck axis. *Age as a covariable

Position on Femoral Head-Neck Axis	Cohort	Change in average alpha angle (±SD)	Univariate Regression			Multivariate Regression*		
			Coefficient	95% CI	p Value	Coefficient	95% CI	p Value
11 o'clock	**Male Footballers**	13.459 (±15.311)	-0.098	-4.183 to 3.987	0.962	-0.666	-4.822 to 3.490	0.754
	Male Controls	13.557 (±13.575)	-	-	-	-	-	-
	Female Controls	3.694 (±7.941)	-9.863	-13.508 to -6.218	<0.001	-9.665	-13.764 to -5.565	<0.001
12 o'clock	**Male Footballers**	15.546 (±16.593)	6.610	2.673 to 10.546	0.001	6.194	2.122 to 10.267	0.003
	Male Controls	8.937 (±11.855)	-	-	-	-	-	-
	Female Controls	6.685 (±10.064)	-2.252	-5.848 to 1.344	0.220	-0.591	-4.878 to 3.696	0.787
1 o'clock	**Male Footballers**	14.961 (±15.572)	8.577	5.465 to 11.689	<0.001	8.184	5.068 to 11.300	<0.001
	Male Controls	6.384 (±7.108)	-	-	-	-	-	-
	Female Controls	3.433 (±6.715)	-2.951	-5.210 to -0.691	0.010	-1.865	-4.858 to 1.128	0.222
2 o'clock	**Male Footballers**	12.820 (±11.879)	7.405	4.795 to 10.015	<0.001	6.936	4.423 to 9.450	<0.001
	Male Controls	5.415 (±7.153)	-	-	-	-	-	-
	Female Controls	2.907 (±5.471)	-2.515	-4.591 to -0.424	0.018	-1.225	-3.618 to 1.169	0.316
3 o'clock	**Male Footballers**	8.542 (±8.329)	4.053	2.112 to 5.994	<0.001	3.697	1.761 to 5.634	<0.001
	Male Controls	4.489 (±5.734)	-	-	-	-	-	-
	Female Controls	2.825 (±4.189)	-1.663	-3.307 to -0.020	0.047	-0.781	-2.496 to 0.934	0.372

3.5.5 Location of Cam Development

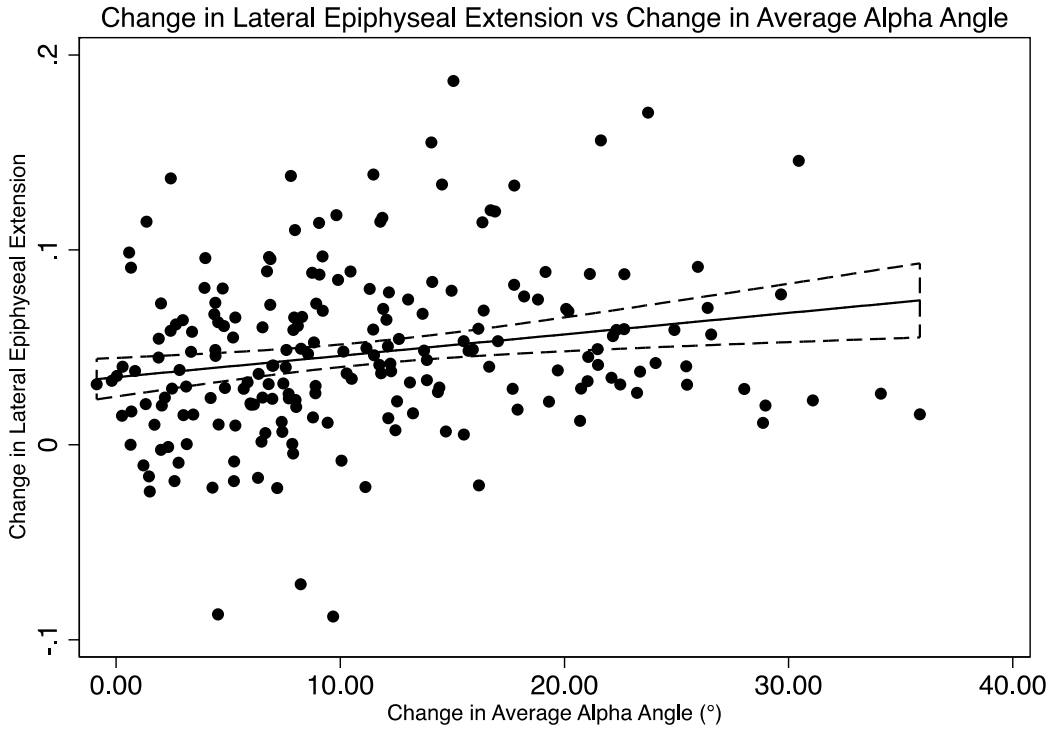
3.5.5.1 Lateral Epiphyseal Extension

A significant positive correlation was seen between change in average alpha angle and change in average lateral epiphyseal extension (coefficient=0.002, p=0.012). This correlation was significant at the 12, 1, and 2 o'clock positions, but not at 11 and 3 o'clock. A significant positive correlation was also seen between average follow-up alpha angle and average follow-up lateral epiphyseal extension (r^2 = 0.294, p=0.029) (Table 3-6). Adjusting for age elite footballers had a change in lateral epiphyseal extension 0.01 greater than male controls (p=0.019). There was no statistical difference in change in lateral epiphyseal extension between male and female controls.

Table 3-6 - Multivariate regression analysis of lateral epiphyseal extension with alpha angle by position on femoral head-neck axis. Age, gender, and activity level as covariables

Position on femoral head-neck axis	Regression of change in lateral epiphyseal extension with change in alpha angle			Regression of follow-up lateral epiphyseal extension with follow up alpha angle		
	Coefficient	95% CI	p Value	Coefficient	95% CI	p Value
Average	0.002	0.001 to 0.002	0.012	0.002	0.001 to 0.003	0.031
11 o'clock	0.000	-0.000 to 0.002	0.116	0.001	-0.001 to 0.002	0.084
12 o'clock	0.001	0.000 to 0.001	0.020	0.001	0.001 to 0.002	0.016
1 o'clock	0.002	0.001 to 0.003	0.034	0.002	0.002 to 0.002	0.004
2 o'clock	0.001	0.001 to 0.002	0.009	0.002	0.001 to 0.002	0.006
3 o'clock	0.000	-0.001 to 0.001	0.254	0.002	0.001 to 0.003	0.019

Figure 3-14 – Change in Lateral Epiphyseal Extension versus Change in Average Alpha Angle. Scatter plot with 95% Confidence Intervals. Coefficient=0.002, R^2 = 0.060, p=0.012



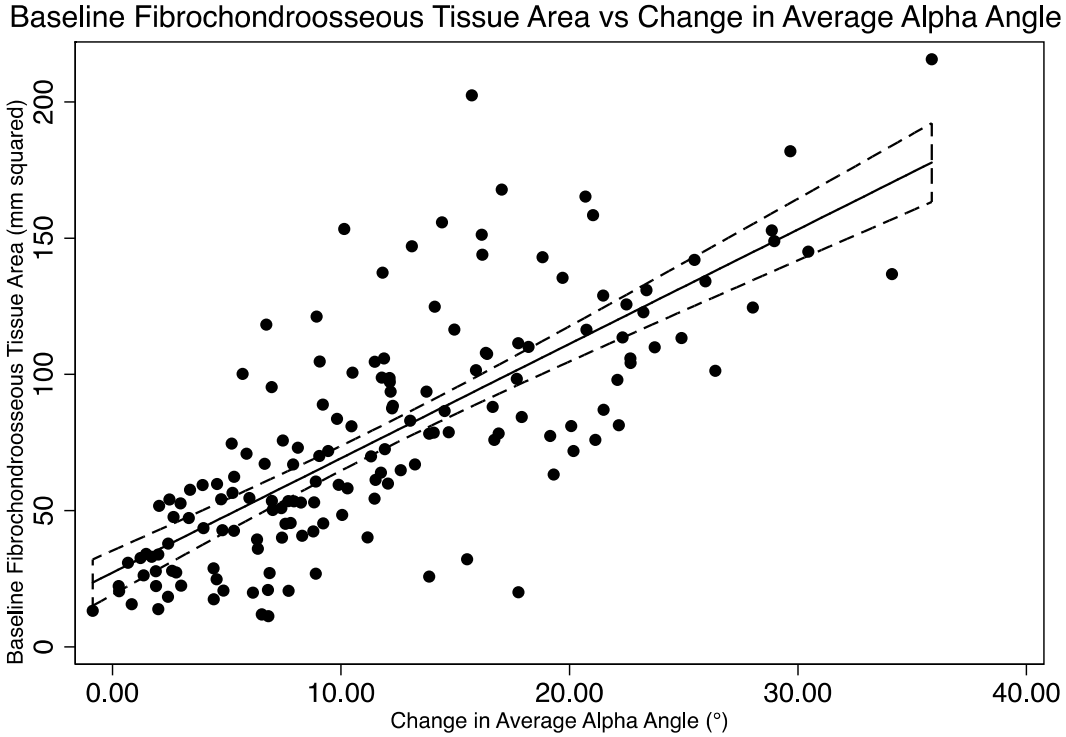
3.5.5.2 Fibrochondroosseous Tissue Area

A significant positive correlation was seen between baseline FTA and change in average alpha angle (coefficient 4.09, p = 0.003) (Figure 3-15). This correlation was significant at the 11, 12, 1, 2, and 3 o'clock positions (Table 3-7). Adjusting for age elite footballers had an FTA 28.92mm^2 greater than male controls at baseline (p<0.001). There was no statistical difference in FTA between male and female controls.

Table 3-7 - Multivariate regression analysis of Fibrochondroosseous Tissue Area with change in alpha angle by position on femoral head-neck axis. Age, gender, and activity level as covariables

Position on Femoral Head-Neck Axis	Regression of FTA with Change in Alpha Angle		
	Coefficient	95% CI	p Value
Average	4.09	3.86 to 4.33	0.003
11 o'clock	2.96	2.38 to 3.54	0.010
12 o'clock	3.21	1.45 to 4.98	0.027
1 o'clock	3.24	1.53 to 4.96	0.027
2 o'clock	2.85	0.24 to 5.47	0.046
3 o'clock	4.16	1.09 to 47.23	0.037

Figure 3-15 – Baseline Fibrochondroosseous Tissue Area versus Change in Average Alpha Angle. Scatter plot with 95% Confidence Intervals. Coefficient 4.09, $R^2 = 0.580$, p = 0.003



3.5.6 Predicting Cam Development

246 hips had an open physis and normal morphology (average alpha angle less than 60 degrees[22]) at baseline (mean age 134 months, SD 19). 180 of these hips were followed up at 3 years (mean age 167 months, SD 18). 87 of these hips showed evidence of cam morphology (average alpha angle greater than 60 degrees[22]) at follow-up.

Baseline variables selected as potential predictors of future cam morphology formation were internal rotation range of motion, PAQ score, lateral epiphyseal extension, and FTA.

No correlation existed between average alpha angle and FTA, average lateral epiphyseal extension, or PAQ score in individuals with an open physis and average alpha angle less than 60 degrees at baseline. A significant negative correlation was seen between internal rotation ROM and alpha angle in individuals with an open physis and average alpha angle less than 60 degrees at baseline (coefficient -0.26, $p = 0.011$)

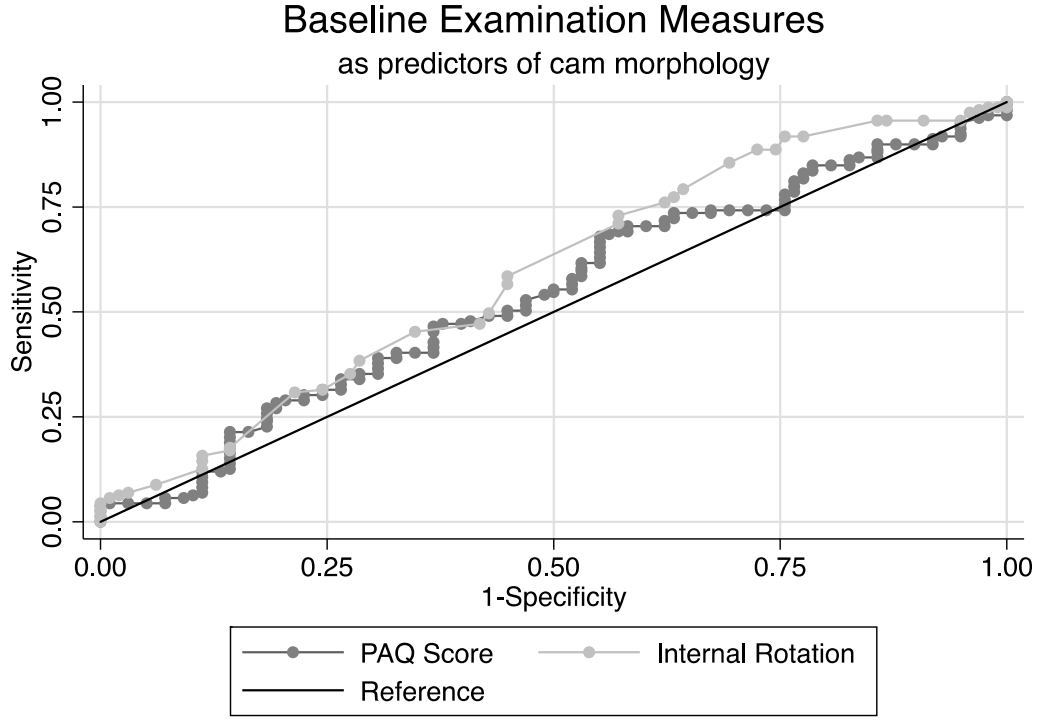
3.5.6.1 Examination Measures

PAQ score and internal rotation showed fair predictive capability for future cam morphology development. The ROC AUC for internal rotation range of motion was 0.61 (95% CI: 0.52 – 0.70), and for PAQ score was 0.62 (95% CI: 0.53 – 0.71). (Table 3-8) (Figure 3-16)

Table 3-8 - ROC Area and Cut Off Values for Cam Morphology Development; Internal Rotation, PAQ Score, Fibrochondroosseous Tussie Area, Latersal Epiphyseal Extension, and Combined Variables

	AUC	95% CI	Cut Off	Sensitivity	Specificity	Correctly classified
Baseline Examination Measures						
Internal Rotation	0.61	0.52 to 0.70	<35 degrees	54.90%	58.06%	56.10%
PAQ Score	0.62	0.53 to 0.71	2.98	72.55%	39.78%	60.16%
Baseline Imaging Measures						
Lateral Epiphyseal Extension	0.53	0.44 to 0.62	0.65	67.97%	41.94%	58.13%
Fibrochondroosseous Tissue Area	0.83	0.76 to 0.90	>75.94mm^2	76.00%	80.26%	78.15%
Combined Measures						
Combined Examination Measures	0.66	0.57 to 0.75	>-0.49	73.20%	51.61%	65.04%
Combined Imaging Measures	0.84	0.77 to 0.90	>-0.18	76.00%	82.89%	79.47%
Combined Imaging and Examination Measures	0.85	0.78 to 0.91	>-0.11	77.33%	82.89%	80.13%

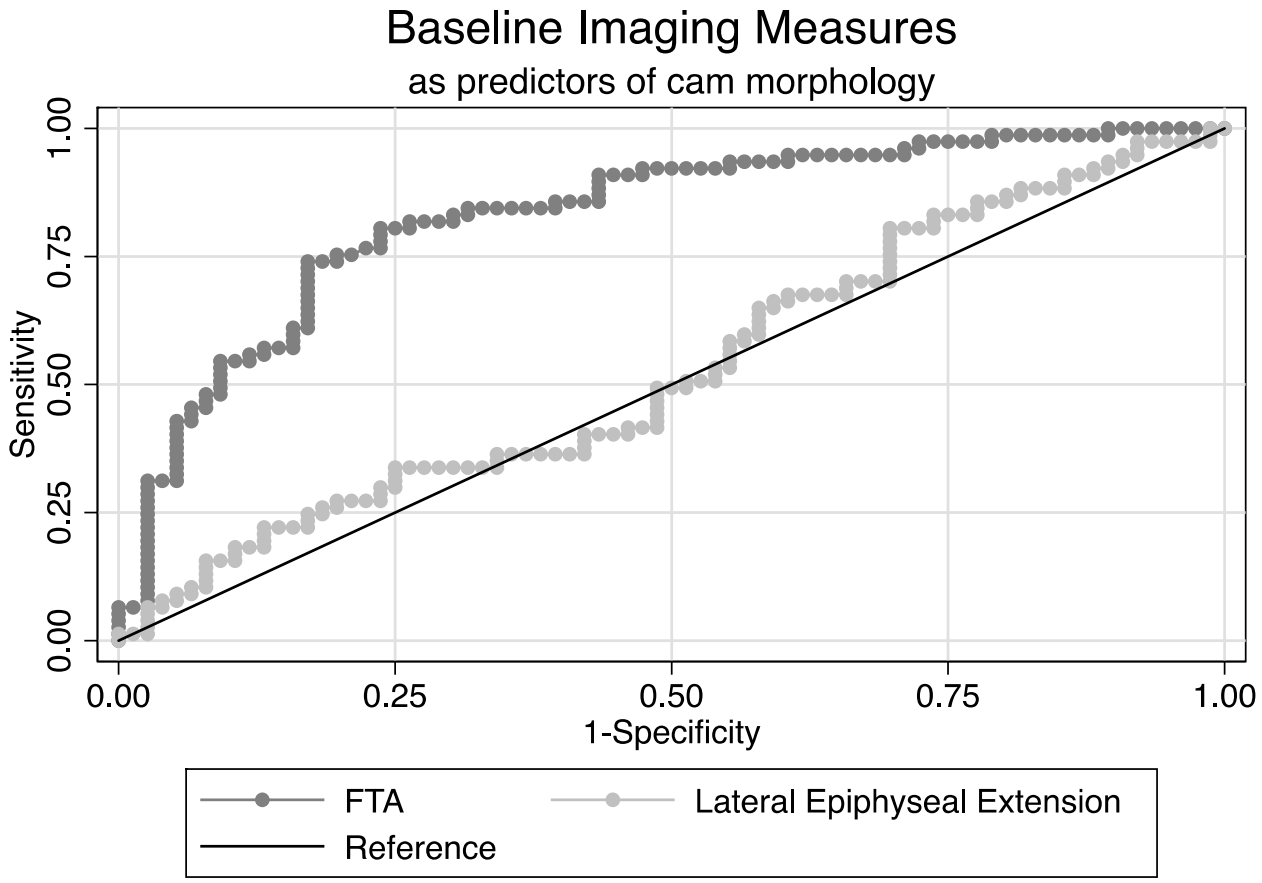
Figure 3-16 – ROC Curve for Examination Measures; Internal Rotation (AUC 0.61), and PAQ Score (AUC 0.62)



3.5.6.2 Imaging Measures

Average lateral epiphyseal extension showed poor predictive capability for future cam morphology development. The ROC AUC for average lateral epiphyseal extension was 0.53 (95% CI: 0.44 – 0.62). Average FTA showed excellent predictive capability for future cam morphology development. The ROC AUC for FTA was 0.83 (95% CI: 0.76 – 0.90). (Table 3-8) (Figure 3-17)

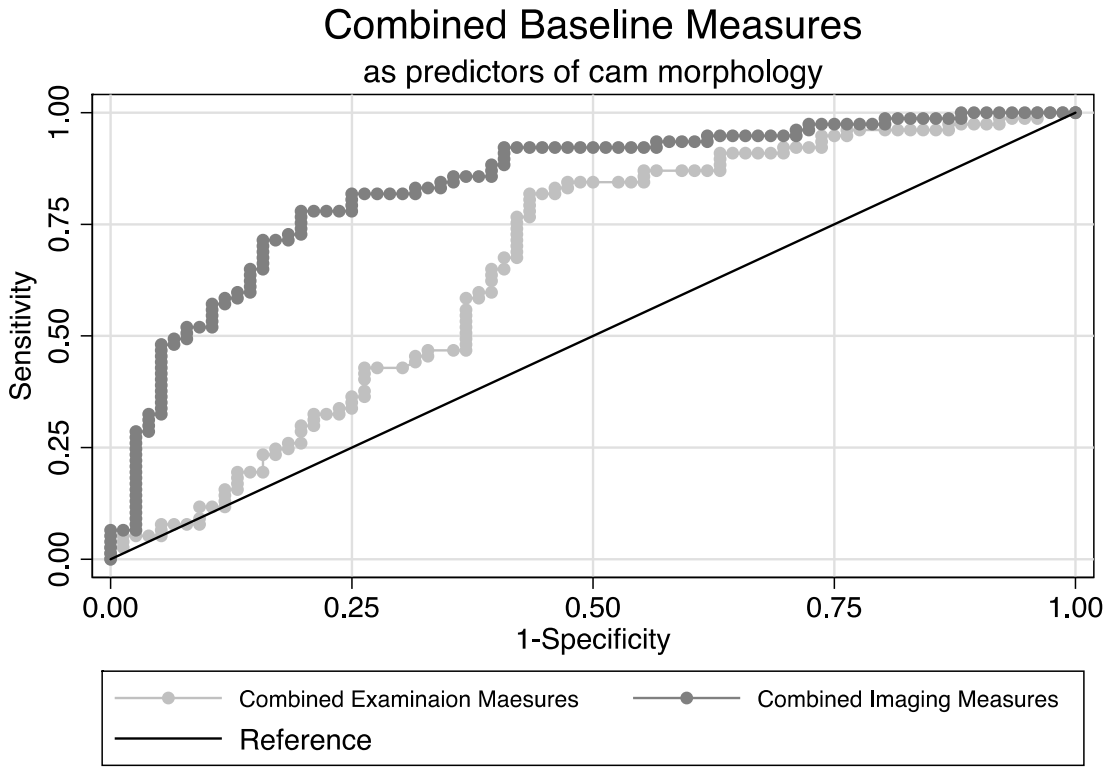
Figure 3-17 – ROC Curve for Imaging Measures; FTA (AUC 0.83), and average lateral epiphyseal extension (AUC 0.53)



3.5.6.3 Combined Variable Measures

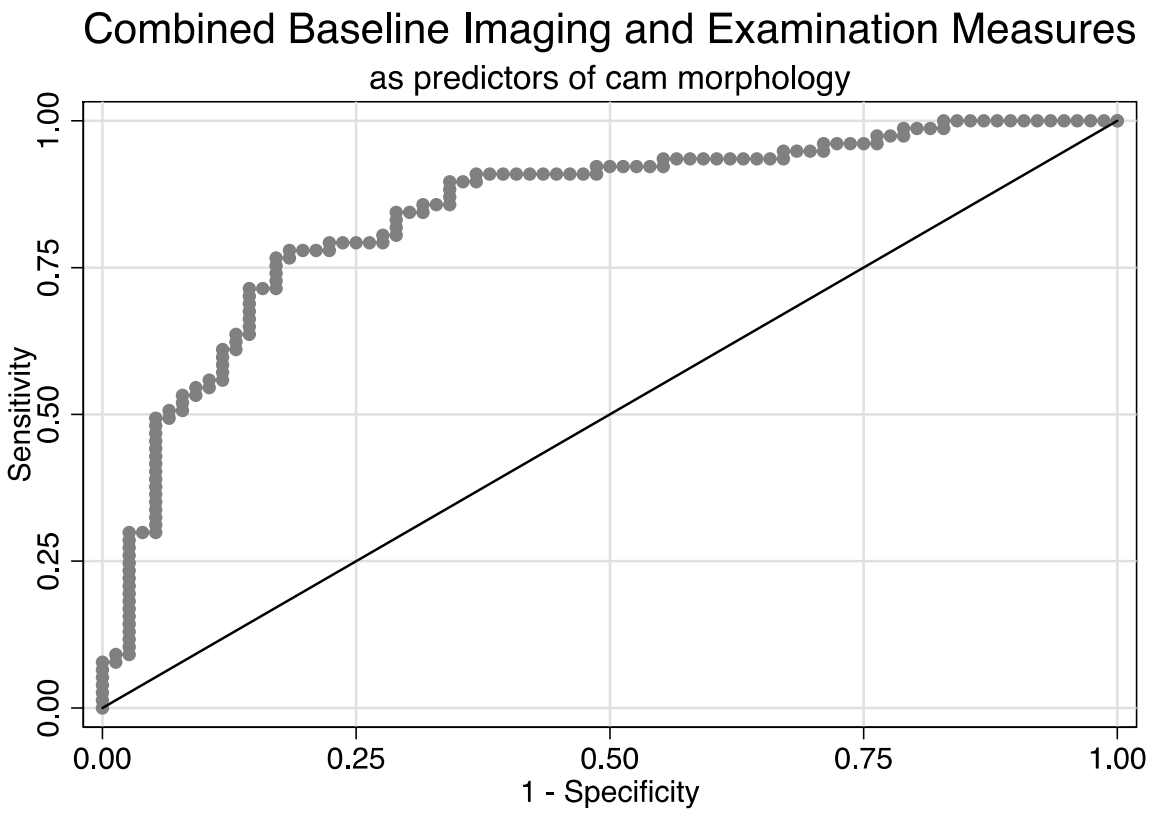
Combined baseline examination measures (internal rotation and PAQ score) showed fair predictive capability for future cam morphology development. The ROC AUC for combined baseline examination measures was 0.66 (95% CI: 0.57 – 0.75). It offers a sensitivity of 73.20% and specificity of 51.61%, where 65.04% of individuals are classified correctly. Combined baseline imaging measures (average epiphyseal extension and FTA) showed excellent predictive capability for future cam morphology development. The ROC AUC for combined baseline imaging measures was 0.84 (95% CI: 0.77 – 0.90). It offers a sensitivity 76.00% of and specificity of 82.89%, where 79.47% of individuals are classified correctly. (Table 3-8) (Figure 3-18)

Figure 3-18 – ROC Curve for Combined Measures; Baseline Examination Measures (AUC 0.66) and Baseline Imaging measures (AUC 0.84)



A combined variable consisting of baseline examination and imaging measures performed better than any individual measure with a statistically significant ROC AUC of 0.85 (95% CI: 0.78 – 0.91). It offers a sensitivity 77.33% of and specificity of 82.89%, where 80.13% of individuals are classified correctly. (Table 3-8) (Figure 3-19)

Figure 3-19 – ROC Curve for Combined Examination and Imaging Measures (AUC 0.85)



3.6 Discussion

The aim of this study was to characterise the risk factors, timing, and mechanism of cam development during adolescence. Identifying individuals at greatest risk of cam formation may allow the development of preventative strategies. This study demonstrates that males undertaking intense exercise between the ages of 11 and 14 years are at greater risk of developing cam morphology

3.6.1 Individuals at Risk of Cam Development

Our results demonstrate that activity level and gender play a significant role in the development of cam morphology[32,52,296]. The increase in alpha angle was 4.8 degrees greater in male footballers compared with male controls, and 6.8 degrees greater in male footballers compared with female controls, consistent with previously reported values[32,52,296]. Siebenrock et al. reported a mean difference in alpha angle between athletes and controls of 6.2 degrees in individuals with an open physis and 16.9 degrees with a closed physis[29]. The greatest difference in change in alpha angle was at the 1 o'clock position, as had been reported in previous studies[29].

Higher PAQ scores were also associated with a greater change in alpha angle. Activity levels have previously been reported to be higher in individuals with cam morphology[32]. A dose response relationship between training frequency and cam morphology in football players has been described previously[52,296]. However, the association with a physical activity questionnaire raises the possibility of a screening tool to identify

patients at risk of developing cam morphology, and individuals with a score above 3 are at significantly elevated risk. The PAQ score differentiates between active and inactive individuals[225], but focuses heavily on the number of sport or exercise sessions performed per week rather than the type, intensity, or duration. As with previous studies[33], there was no difference in alpha angle measurements between the dominant and non-dominant leg.

Change in average alpha angle was significantly greater in male controls than female controls. Although males on average had a higher PAQ score, this was controlled for in the regression models. This finding is consistent with reports from other cohorts where there is a lower prevalence of cam morphology in female than male populations[86,87]. These findings suggest cam morphology may have a gender-specific pathogenesis, though further research comparing male and female elite athlete cohorts is required to fully elucidate this relationship.

3.6.2 Age of Cam Development

Studies have demonstrated that cam morphology does not develop after skeletal maturity[294]. Similarly, in our study there was no statistically significant increase in alpha angle in individuals with a closed physis at baseline. Observed post physeal closure changes in alpha angle in other studies are likely due to positional artefact in radiography, which is overcome by using MRI.

In this study, the greatest change in alpha angle occurred between the ages of 9-10 years in females and 11-12 years in male controls and footballers. No significant change in average alpha angle occurred in individuals over 12 years in controls and over 14 years in footballers at baseline. This is consistent with our cross-sectional data from this cohort demonstrating no statistically significant increase in alpha angle beyond 14 years of age[52]. These findings support the proposal that cam morphology develops when hip development is responsive to load whilst the physis is open during active skeletal growth[52].

Mechanical loading is recognised as a key factor for normal bone development[66]. Increased levels of sex steroids, growth hormone peaks, insulin like growth factors and genetic factors at the start of adolescence may result in increased plasticity under loading[42]. This could provide a possible explanation for cam morphology development at this early age in active individuals. Finite element models of the hip show high mechanical stress on impact loading precisely where a cam deformity most frequently develops[103]. Excessive loading at the femoral head-neck junction at this key development time may trigger abnormal or excessive bone development, resulting in cam morphology formation.

3.6.3 Mechanism of Cam Development

Cam development was weakly associated with epiphyseal extension that was maximal at the 1 o'clock position. The relationship between epiphyseal extension and subsequent cam morphology is not well understood, but previous studies have also found weak

associations[51-53]. However, previous studies also report athletes show greater epiphyseal extension than controls[53]. Subtle morphological changes in physeal development have been reported in association with many sports[104], including the proximal humeral physis in baseball[297], and cam development is likely to represent a potentially modifiable physiological adaptation to load. A strong association was found between FTA and cam development. It may be that soft tissue hypertrophy and ossification at the femoral head neck junction represents a distinct and more likely mechanism for cam morphology formation than lateral epiphyseal extension.

3.6.4 Predicting Cam Development

This study suggests that in individuals with an open physis and a normal alpha angle the development of cam morphology can be predicted at three years follow up. Examination measures are able to predict future cam morphology poorly. Combining a high PAQ score with a low internal rotation can predict the development of cam morphology at 3 years with a sensitivity of 73.20%, and specificity of 51.61% where 64.04% of individuals are classified correctly. Lateral epiphyseal extension performed poorly at predicting future cam development, however average FTA measured on radial slices performed well. We found that an average FTA greater than 75.94mm^2 can predict the development of cam morphology at 3 years with a sensitivity of 76.00% and specificity of 80.26% where 78.15% of individuals are classified correctly. It should be noted that males are likely to have larger FTA values due to the greater size of their femoral head, and this may account for some of the predictive capabilities of the FTA. A Potential explanation for the discrepancy between imaging measures could be that an

increased FTA is a precursor to ossified cam development, whereas lateral epiphyseal extension is the mechanism by which the ossified cam lesion forms. As such, lateral epiphyseal extension will increase as the cam lesion grows, but not precede or predict it. However, the weak correlation between lateral epiphyseal extension and change in alpha angle should be kept in mind when interpreting these results.

An important observation is that the addition of other measures did not appear to offer a large improvement over FTA for predicting the development of cam morphology. A combination of baseline variables consisting of PAQ score, internal rotation ROM, lateral epiphyseal extension, and FTA provide an AUC of 0.85 with a sensitivity of 77.33% and specificity of 82.89%. FTA alone provides an AUC of 0.83. However, it should be noted that the FTA was developed for this study, and therefore is not a validated or widely used measure. It is also worth stressing that there is no agreed alpha angle threshold to define the presence of cam morphology. Accordingly, the results of this study should be interpreted with care.

3.6.5 Limitations

The main limitation of this study is the loss to follow-up. This is a well-recognised issue in elite sporting cohorts due to national and international relocation and low player retention[51]. However, our study remains adequately powered at the follow-up point with similar cohort demographics to baseline (Table 3-1). A further limitation is that the control group may not be representative of the general population due to participation

bias in sports and exercise projects. Additionally, activity levels may have varied on an individual basis between baseline and follow up. However, no significant difference was seen in PAQ scores between time points (Table 2-3). Further limitations apply to using the alpha angle as a morphological measure. There exists no universally agreed diagnostic threshold for cam morphology and a quantitative value for pathological change in alpha angle is unknown[295]. Moreover, hips may undergo further epiphyseal extension resulting in worsening asphericity without a rise in alpha angle. Follow up of this cohort beyond full skeletal maturity may determine what constitutes a pathological change in femoral morphology.

3.6.6 Conclusion

The development of cam morphology is greatest age 9-10 in females and 11-12 in males. There is no significant change in alpha angle beyond age 12 years for controls and 14 years for footballers. High physical activity in males during adolescence, such as elite level football, is strongly associated with cam development. A Physical Activity Questionnaire warrants further exploration as a potential screening tool for individuals at greatest risk of developing cam morphology.

Chapter 4 Acetabular Morphology in Adolescence and the Effects of Activity

4.1 Abstract

Introduction:

Abnormal acetabular morphology is associated with adverse clinical outcomes. An improved understanding is required to determine whether the development of acetabular pathology is predictable or modifiable. The aim of this study was to characterise the risk factors and timing of abnormal acetabular morphology formation during adolescence.

Methods:

Longitudinal observational cohort study over three years of individuals from football club academies and an age-matched control population aged 9-18 years at baseline. Assessments included questionnaires, clinical examination, and MRI of both hips. Alpha angle, lateral Centre Edge Angle (CEA), anterior CEA, and acetabular anteversion were measured from MRI images.

Results:

Cohort consisted of 25 male academy footballers, 33 male and 33 female controls. Individuals aged 11-12 years at baseline experienced the greatest change in lateral CEA

(3.69 degrees, p<0.001), and anterior CEA (5.39 degrees, p<0.001). The greatest change in anteversion (4.19 degrees, p=0.004) was seen in 13-14 year olds. Male footballers had significantly less change in lateral CEA (-1.80 degrees, p<0.001), anterior CEA (-3.42 degrees, p <0.001), and anteversion (-1.56 degrees, p=0.047) than male controls. A negative correlation existed between Physical Activity Questionnaire Score and change in lateral CEA (coefficient -0.62, p=0.043), change in anterior CEA (coefficient -3.21, p=0.039), and change in anteversion (coefficient -0.59, p=0.048). A negative correlation was seen between change in average alpha angle and change in lateral CEA (coefficient -0.08, p=0.018), and change in anterior CEA (coefficient –0.11, p=0.014).

Conclusions:

Males undertaking intense sporting activity during adolescence, and individuals that develop aspherical femoral heads (cam morphology), are at greatest risk of developing abnormal acetabular morphology during adolescence. Activity levels during adolescence may be used to predict the development of mild acetabular dysplasia.

4.2 Introduction

Abnormal acetabular morphology is associated with adverse clinical outcomes[298]. Developmental Dysplasia of the Hip (DDH) is a known risk factor for hip osteoarthritis (OA)[23-25]. As lateral coverage of the femoral head decreases the stress placed on intra-articular cartilage increases linearly[217], such that even subclinical and mild forms of DDH have been shown to lead to cartilage and labral damage[251-253]. Acetabular retroversion has also been implicated in several pathologic hip processes and future hip OA[41,120,122,128]. An improved understanding of acetabular development is required to determine whether abnormal morphology is preventable or modifiable.

Changes in acetabular morphology and version over the course of adolescent skeletal development have not been well characterised[127]. Accordingly, the aetiology and pathogenesis of abnormal acetabular anatomy remains largely unknown. The limited studies performed have only assessed the bony acetabulum during adolescence retrospectively using radiography[30,129,214-216]. Little is known about the development of the cartilaginous articular surface.

Skeletal development is dependent upon genetic and environment factors[40]. While a positive association has been shown between male gender and activity levels and the risk of cam morphology[32,33,51,52], the effect of these factors on acetabular morphology and version is unknown. Acetabular concavity is dependent upon its interaction and articulation with the spherical femoral head[59,60]. A high prevalence of retroverted acetabula has been reported in patients with Femoroacetabular Impingement (FAI)[30,121].

However, the effect of the aspherical femoral head seen in cam-type FAI on the developing acetabulum is unclear.

4.3 Aims

1) Investigate the changes in acetabular morphology with age
2) Investigate the effects of activity on the development of acetabular morphology and version
3) Determine the effects of femoral head asphericity on the development of acetabular morphology and version
4) Determine whether baseline risk factors in skeletally immature individuals can predict the development of acetabular dysplasia and retroversion at follow-up

4.4 Methods

The methods for this study and justifications for imaging measures are discussed in chapter 2.

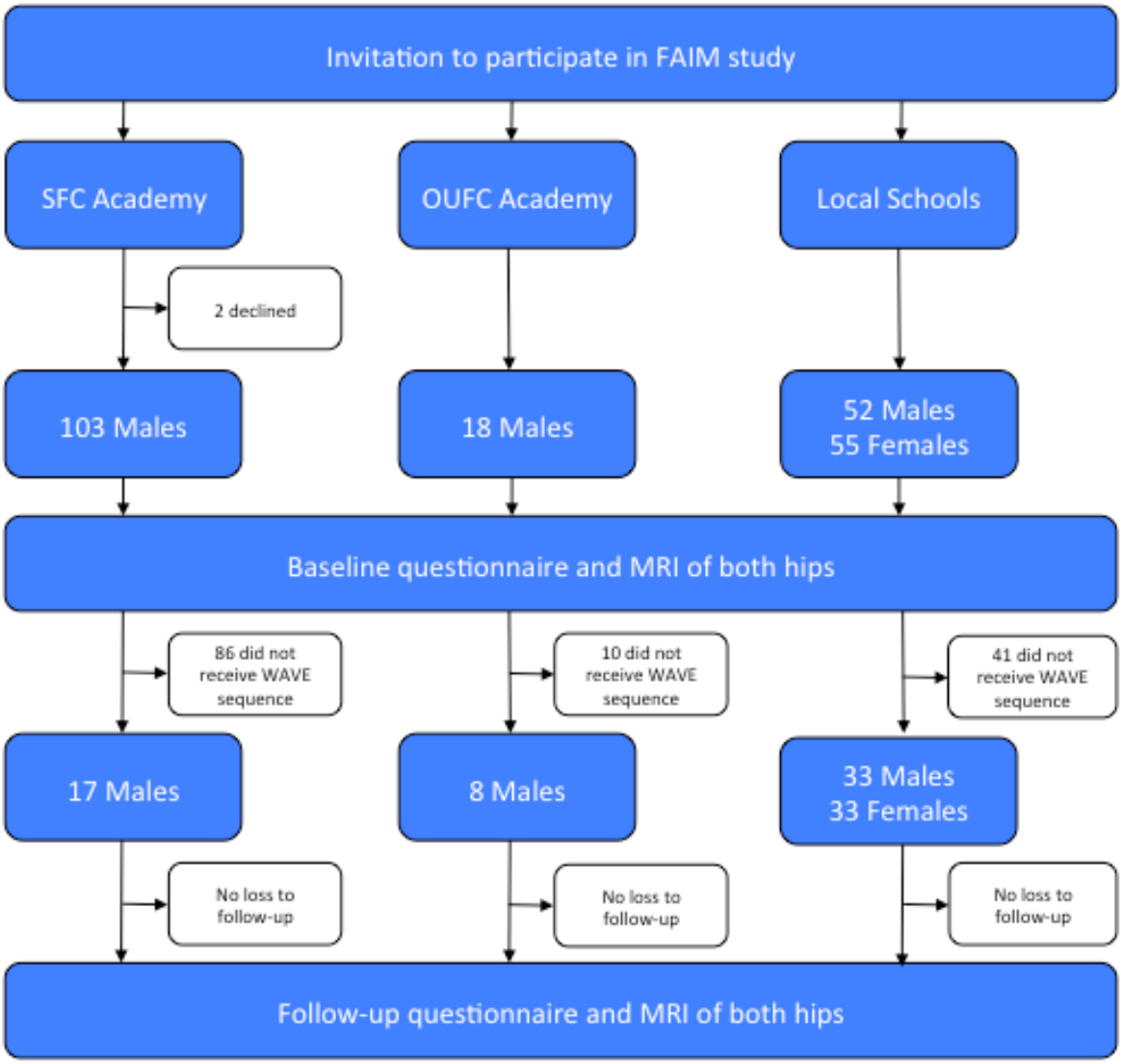
4.4.1 Study design

Longitudinal prospective observational cohort study.

4.4.2 Population

Individuals aged 9–18 years were recruited from Southampton Football Club (SFC) Academy, Oxford United Football Club (OUFC) Academy, and local schools (controls) at baseline. Participants were invited for repeat assessment three years after initial baseline visit via post, email, and telephone. Study IDs were generated for each participant such that assessors were blinded to participant characteristics such as cohort and age when interpreting data such as MRI scans (see chapter 2). Not all individuals at baseline received the acetabular morphology MRI sequence (WAVE), as this sequence was only available on the scanner in Oxford and not the mobile scanner used to image the majority of the SFC cohort. However, there was no loss to follow-up amongst individuals who did have the required sequence at baseline. (Figure 4-1)

Figure 4-1 - Recruitment flowchart for study.



4.4.3 Activity Levels

Activity was evaluated using two methods: i) SFC and OUFC Academy (elite footballer cohort) versus general population controls; ii) Physical Activity Questionnaire (PAQ) for older children (aged 9–13 years) and adolescents (aged 14–18 years)[224].

4.4.4 Imaging Protocol

Femoral and acetabular morphology was assessed with MRI of both hips using a 3 Tesla Philips Achieva platform and torso coil (Philips Healthcare). Three-dimensional (3D) water selective fluid (WATSf) sequence was used to image femoral cartilage and bone, and Water Selective Volume Excitation (WAVE) sequence was used to image pelvis cartilage and bone.

For both acetabular and femoral morphological measures 3D multiplanar reconstructions were performed using OsiriX Software (V.6.0.2, Pixmeo). To determine acetabular morphology pelvic orientation was standardized in three planes: i) To account for pelvic tilt the sagittal plane was orientated with a plane connecting the Anterior Superior Iliac Spine and the centre of the pubic symphysis. ii) To account for rotation, the coronal and axial planes were aligned with a line connecting the centre of both femoral heads. iii) To determine femoral head-neck junction morphology radial images were acquired around the axis of the femoral neck at 30 degree intervals. The coronal axis (12 o'clock position) was positioned parallel to the axis of the proximal femur diaphysis[52]. The MRI datasets at baseline and follow-up were complete.

4.4.5 Imaging Measures

Acetabular morphology was quantified using three measures: i) Lateral Centre Edge Angle (CEA); defined as the angle between a line drawn from the centre of the femoral head to the lateral border of the cartilaginous acetabulum, and a line from the centre of the femoral head perpendicular to the reference line connecting the centre of both femoral heads (Figure 4-2). ii) Anterior CEA; defined as the angle between a line from the centre of the femoral head to the anterior border of the cartilaginous acetabulum, and a line from the centre of the femoral head parallel to the line of sagittal orientation (Figure 4-3). iii) Anteversion; defined as the angle between a line drawn from the posterior border of the cartilaginous acetabulum to anterior border of cartilaginous acetabulum, and a line perpendicular to the line connecting the centre of both femoral heads (Figure 4-4).

Figure 4-2 - Coronal Image from WAVE Sequence Illustrating Measurement of Lateral Centre Edge Angle.

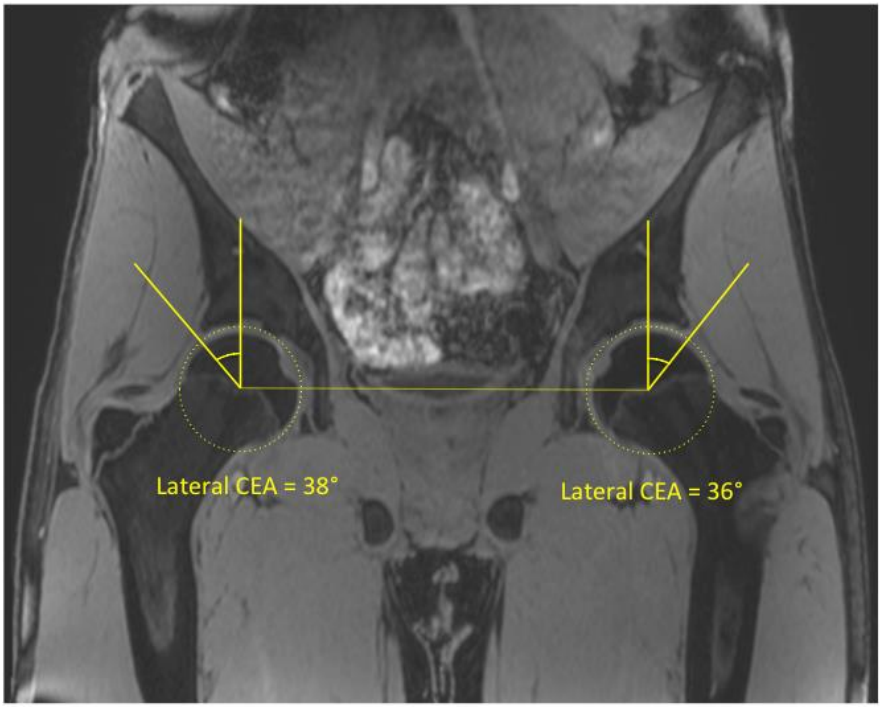


Figure 4-3 - Sagittal Image from WAVE Sequence Illustrating Measurement of Anterior Centre Edge Angle

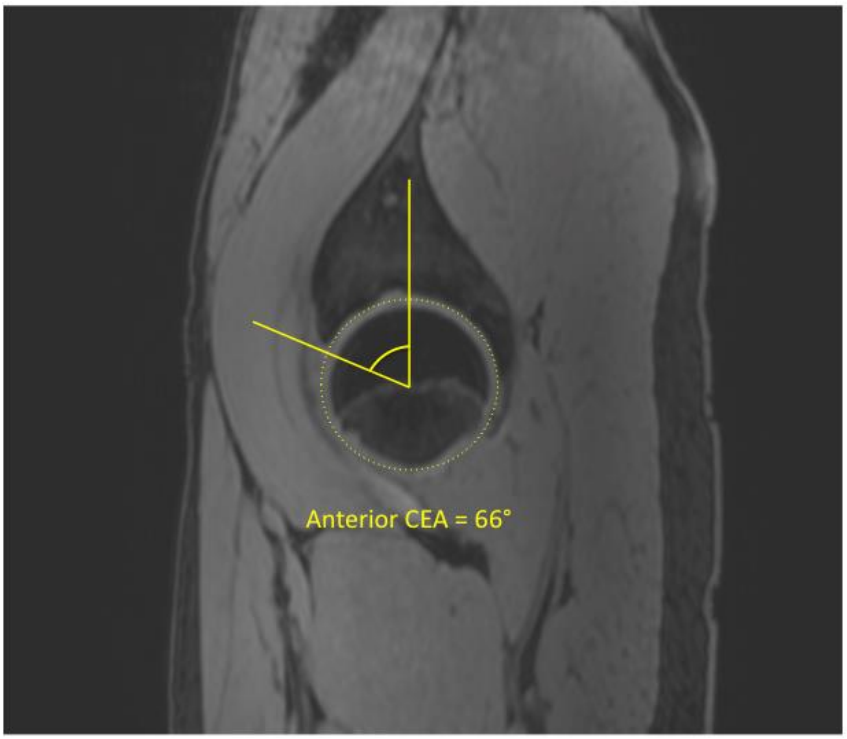
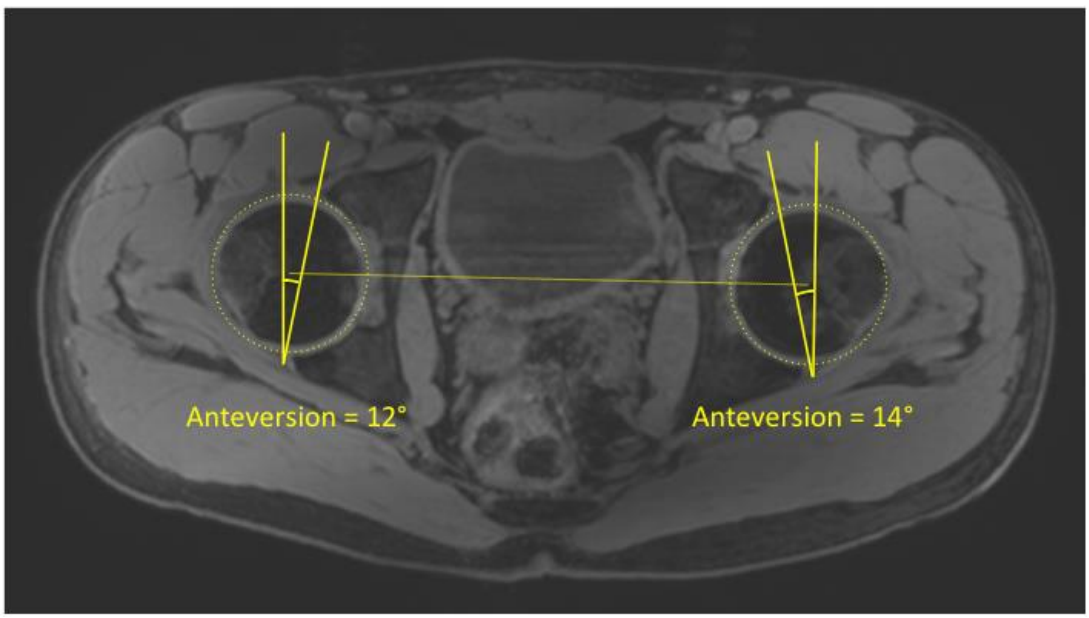


Figure 4-4 - Axial image from WAVE Sequence Illustrating Measurement of Angle of Anteversion



The triradiate cartilage was considered open if it corresponded to level 1 (open) or level 2 (partially ossified) and closed if it corresponded to level 3 of the modified Oxford system (closed)[299]. Lateral CEA values between 20 and 25 degrees were taken to define mild acetabular dysplasia, and less than 20 degrees to define acetabular dysplasia[112,217]. Angle of anteversion values less than 14.2 degrees were taken to define the presence of acetabular retroversion[266]. Acetabular measures were performed using OsiriX Software (V.6.0.2, Pixmeo).

Femoral head-neck junction morphology was quantified using the average alpha angle for cartilage on radial slices from 11 o'clock, 12 o'clock, 1 o'clock, 2 o'clock, and 3 o'clock (chapter 2). Alpha angle was measured using custom-developed software (OxMorf 2.1.0).

4.4.6 Statistical analysis

See chapter 2 for details of statistical analysis. Inverse probability weighting with regression adjustment modelling[286] was adopted to assess variables that predict outcome variables. Multivariate linear regression modeling was used to evaluate the relationship between variables.

To determine whether baseline characteristics can predict future mild acetabular dysplasia Receiver Operating Characteristic (ROC) analysis was performed on individual variables with a binary outcome of lateral CEA less than 25 degrees at follow-

up in individuals with an open physis and lateral CEA less than 25 degrees at baseline. To determine whether baseline characteristics can predict future acetabular retroversion ROC analysis was performed on individual variables with a binary outcome of angle of anteversion less than 14.2 degrees at follow-up in individuals with an open physis and angle of anteversion less than 14.2 degrees at baseline. Baseline measures chosen for investigation of predictive capability were PAQ score and average alpha angle. These measures were chosen as this study shows high activity levels and large increases in alpha angle are associated with a smaller increase in femoral head coverage with age.

4.5 Results

4.5.1 Participant demographics

91 individuals had both hips imaged with WAVE sequence at baseline and follow-up (182 hips). The cohort consisted of 25 elite male footballers (mean age at baseline 139 months (SD 32 months)), 33 male controls (mean age at baseline 151 months (SD 30 months)), and 33 female controls (mean age at baseline 159 months (SD 34 months)). Mean follow-up was 36 months (SD 4 months). (Table 4-1).

Table 4-1 - Cohort demographics

		Male Footballers (Hips)	**Male Controls (Hips)**	**Female Controls (Hips)**
Age at Baseline (Years)	**9-10**	15 (30)	10 (20)	10 (20)
	11-12	5 (10)	10 (20)	5 (10)
	13-14	2 (4)	4 (8)	7 (14)
	15-16	0	8 (16)	7 (14)
	17-18	3 (6)	1 (2)	4 (8)
Total		25 (50)	33 (66)	33 (66)

4.5.2 Change in Acetabular Morphology with Age

4.5.2.1 Chronological Age

This study found that lateral CEA, anterior CEA, and anteversion increase with age. (Table 4-2) (Figure 4-5, Figure 4-6, and Figure 4-7).

Table 4-2 - Mean Lateral and Anterior CEA, and Angle of Anteversion at Baseline and Follow-up by Cohort and Age Group.

Age at Baseline (Years)	All Individuals		Male Footballers		Male Controls		Female Controls	
	Baseline Mean (±SD)	Follow-up Mean (±SD)	Baseline Mean (±SD)	Follow-up Mean (±SD)	Baseline Mean (±SD)	Follow-up Mean (±SD)	Baseline Mean (±SD)	Follow-up Mean (±SD)
Lateral CEA								
9-10	31.108 (±4.610)	34.986 (±5.053)	31.730 (±3.848)	33.381 (±4.676)	29.632 (±3.185)	33.671 (±3.276)	31.653 (±4.745)	38.710 (±5.303)
11-12	33.132 (±4.286)	37.457 (±5.014)	32.981 (±4.138)	36.501 (±2.676)	31.248 (±3.248)	34.838 (±4.001)	37.050 (±3.904)	43.652 (±3.012)
13-14	35.044 (±6.403)	39.154 (±4.667)	37.471 (±3.664)	38.854 (±0.371)	31.065 (±5.391)	40.029 (±3.186)	36.625 (±6.772)	38.740 (±5.976)
15-16	39.435 (±7.704)	40.443 (±7.431)	-	-	39.361 (±7.698)	40.208 (±7.224)	39.519 (±8.000)	40.711 (±7.926)
17-18	38.225 (±4.610)	38.864 (±4.519)	37.764 (±2.951)	37.799 (±3.208)	38.117 (±3.869)	38.178 (±3.392)	38.598 (±6.069)	39.835 (±5.707)
Average	34.113 (±6.087)	37.365 (±5.755)	33.164 (±4.358)	34.973 (±4.422)	32.911 (±6.224)	36.516 (±5.426)	36.035 (±6.648)	40.026 (±5.976)
Anterior CEA								
9-10	50.542 (±6.183)	55.334 (±6.584)	52.547 (±6.409)	53.783 (±6.773)	48.617 (±4.871)	55.737 (±5.772)	59.461 (±6.340)	57.259 (±6.799)
11-12	54.577 (±5.851)	60.256 (±7.139)	54.662 (±5.684)	56.877 (±7.200)	54.326 (±6.615)	59.868 (±6.670)	54.993 (±4.828)	64.411 (±6.547)
13-14	54.841 (6.614±)	57.900 (±7.001)	51.331 (±3.336)	50.668 (±2.748)	50.774 (±3.172)	54.943 (±5.886)	58.167 (±7.088)	61.656 (±6.099)
15-16	58.238 (±10.019)	59.072 (±9.928)	-	-	57.064 (±10.063)	57.960 (±10.273)	59.581 (±10.170)	60.344 (±9.740)
17-18	60.500 (±5.600)	60.788 (±5.468)	60.258 (±9.383)	60.291 (±9.088)	60.372 (±0.016)	60.102 (±1.191)	60.692 (±2.052)	61.332 (±2.045)
Average	54.187 (±7.625)	57.878 (±7.569)	53.801 (±6.831)	54.933 (±7.221)	53.012 (±7.548)	57.563 (±7.389)	55.654 (±8.128)	60.423 (±7.230)
Anteversion								
9-10	12.180 (±4.410)	13.698 (±6.199)	10.215 (±3.789)	10.320 (±6.131)	12.204 (±3.195)	13.769 (±3.445)	15.106 (±4.837)	18.693 (±5.102)
11-12	12.371 (±5.195)	16.138 (±4.954)	8.693 (±5.122)	13.429 (±3.560)	11.228 (±3.108)	14.960 (±3.680)	18.337 (±3.585)	21.205 (±5.034)
13-14	16.027 (±7.293)	20.817 (±3.987)	13.235 (±4.223)	16.616 (±3.595)	15.767 (±7.080)	20.485 (±3.680)	16.974 (±8.233)	22.208 (±3.506)
15-16	17.505 (±5.465)	19.268 (±4.511)			15.405 (±6.230)	18.183 (±4.834)	19.905 (±3.196)	20.508 (±3.915)
17-18	18.189 (±3.734)	18.791 (±4.217)	15.692 (±4.170)	16.064 (±3.905)	20.085 (±1.496)	21.200 (±1.153)	19.587 (±2.921)	20.233 (±4.076)
Average	14.178 (±5.703)	16.617 (±5.859)	10.810 (±4.551)	12.135 (±5.278)	13.355 (±5.014)	16.239 (±4.546)	17.553 (±5.370)	20.233 (±4.488)

Figure 4-5 - Lateral CEA plotted against age for all participants from baseline and follow-up. Polynomial regression fit with 95% CI

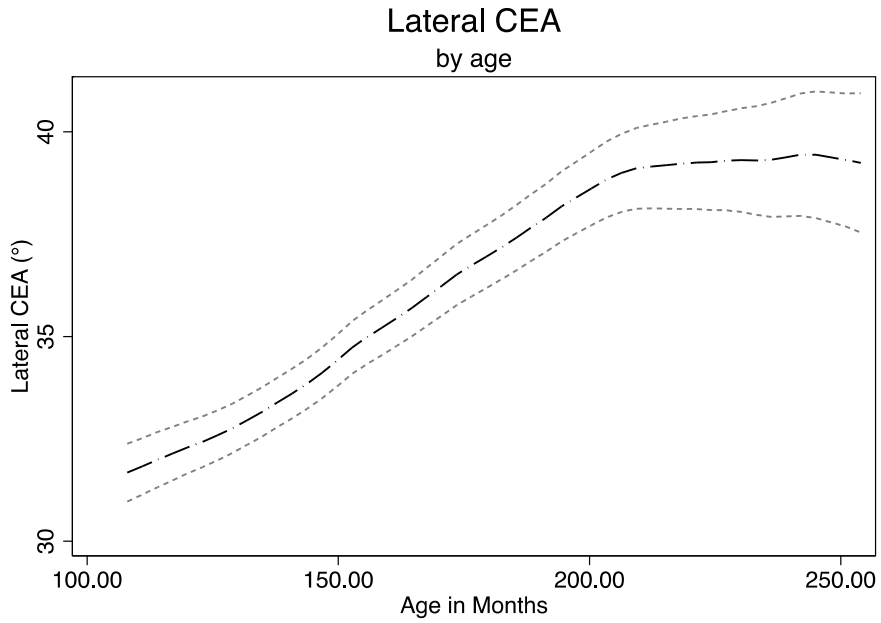


Figure 4-6 - Anterior CEA plotted against age for all participants from baseline and follow-up. Polynomial regression fit with 95% CI

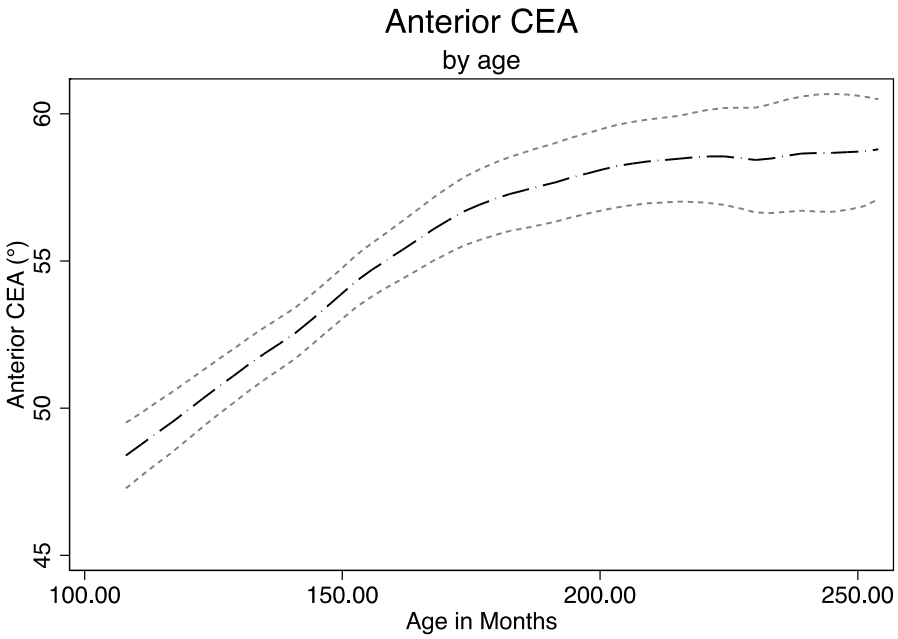
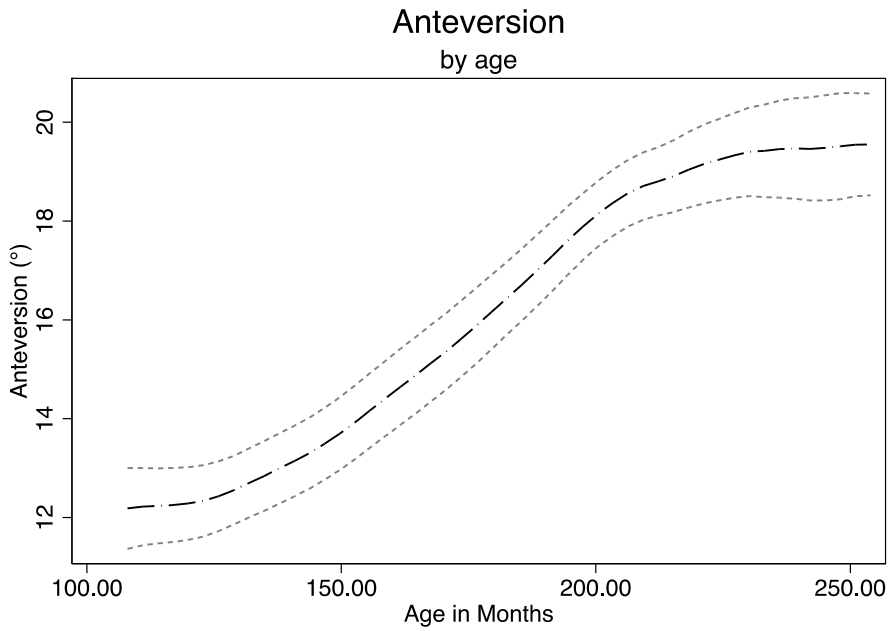


Figure 4-7 - Angle of anteversion plotted against age for all participants from baseline and follow-up. Polynomial regression fit with 95% CI



The greatest change in lateral CEA and anterior CEA in all participants occurred in individuals aged 11-12 years at baseline (Table 4-3 and Table 4-4) (Figure 4-8 and Figure 4-9). The greatest change in anteversion in all participants occurred in individuals aged 13-14 years at baseline. No significant change in lateral CEA or anteversion in all participants occurred in individuals older than 14 years at baseline. (Table 4-5) (Figure 4-10)

Table 4-3 - Predictors of Change in Lateral CEA. *Age and cohort as covariables. **Age, gender and activity level as covariables. ***Physeal maturity, gender, and activity levels as covariables

Lateral CEA															
		Hips	Mean Change Angle (±SD)	Univariate Regression			Multivariate Regression 1*			Multivariate Regression 2**			Multivariate Regression 3***		
				Coefficient	95% CI	P value	Coefficient	95% CI	P value	Coefficient	95% CI	P value	Coefficient	95% CI	P value
Age at Baseline	**Months (Continuous)**	182		-0.036	-0.039 to -0.033	0.004	-0.047	-0.052 to -0.042	0.046	-0.050	-0.055 to -0.045	<0.001			
	9-10 Years	70	3.878 (±3.833)	3.239	-0.258 to 0.995	<0.001									
	11-12 Years	40	4.325 (±3.650)	3.686	1.634 to 5.307	<0.001									
	13-14 Years	26	4.110 (±4.757)	3.471	2.501 to 4.872	<0.001									
	15-16 Years	30	1.008 (±1.373)	0.369	2.262 to 4.215	0.249									
	17-18 Years	16	0.639 (±0.840)	-	-	-									
Physis	**Open**	92	3.789 (±3.632)	2.467	1.641 to 3.293	<0.001							4.052	2.443 to 5.662	<0.001
	Open-Closed	36	4.867 (±4.968)	3.544	1.902 to 5.187	<0.001							3.716	2.171 to 5.261	<0.001
	Closed	52	1.322 (±1.379)	-	-	-							-	-	-
Gender	**Male**	116	2.831 (±3.667)	-1.159	-2.276 to -0.042	0.042				-0.348	-1.942 to -1.247	0.669	-2.048	-2.982 to -1.116	<0.001
	Female	66	3.991 (±3.750)	-	-	-				-	-	-	-	-	-
BMI		182	-	-0.115	-0.391 to 0.160	0.118									
Dominant Leg	**Dominant**	105	3.342 (±3.128)	-0.214	-1.298 to 0.870	0.699									
	Non Dominant	77	3.128 (±3.621)	-	-	-									
Cohort	**Footballers**	50	1.809 (±3.169)	-1.796	--3.063 to -0.529	0.005	-2.048	--3.260 to -0.836	0.001						
	Male Controls	66	3.605 (±3.849)	-	-	-	-	-	-						
	Female Controls	66	3.991 (±3.750)	0.385	-0.901 to 1.672	0.557	1.776	0.336 to 3.217	0.016						
PAQ	**Linear**	182	-	-0.674	-1.544 to 0.196	0.064				-0.746	-1.014 to -0.478	<0.001	-1.125	-1.732 to -0.517	<0.001
	< 2	54	4.220 (±4.372)	-	-	-									
	2-3	52	3.147 (±3.803)	-1.072	-1.437 to -0.707	<0.001									
	3-4	62	2.860 (±3.079)	-1.360	-1.474 to -1.246	<0.001									
	4-5	14	1.641 (±2.654)	-2.578	-2.647 to -2.509	<0.001									

Table 4-4 - Predictors of Change in Anterior CEA. *Age and cohort as covariables. **Age, gender and activity level as covariables. ***Physeal maturity, gender, and Physical Activity Questionnaire as covariables

Anterior CEA															
		Hips	Mean Change Angle (±SD)	Univariate Regression			Multivariate Regression 1*			Multivariate Regression 2**			Multivariate Regression 3***		
				Coefficient	95% CI	P value	Coefficient	95% CI	P value	Coefficient	95% CI	P value	Coefficient	95% CI	P value
Age at Baseline	**Months (Continuous)**	182		-0.058	-0.093 to -0.022	0.031	-0.073	-0.083 to -0.062	0.036	-0.070	-0.082 to -0.058	<0.001			
	9-10 Years	70	4.792 (±5.021)	4.504	3.282 to 5.725	<0.001									
	11-12 Years	40	5.679 (±6.067)	5.391	3.501 to 7.281	<0.001									
	13-14 Years	26	3.060 (±4.887)	2.772	0.896 to 4.648	0.004									
	15-16 Years	30	0.834 (±1.378)	0.546	-0.056 to 1.148	0.076									
	17-18 Years	16	0.288 (±0.753)	-	-	-									
Physis	**Open**	92	4.150 (±4.491)	2.886	1.631 to 4.141	<0.001							3.711	1.951 to 5.470	<0.001
	Open-Closed	36	6.042 (±6.835)	4.778	2.414 to 7.143	<0.001							5.132	3.000 to 7.263	<0.001
	Closed	52	1.264 (±3.202)	-	-	-							-	-	-
Gender	**Male**	116	3.077 (±4.086)	-1.692	-3.345 to -0.039	0.045				-1.700	-3.674 to 0.274	0.091	-2.048	-2.980 to -1.116	<0.001
	Female	66	4.769 (±6.175)	-	-	-							-	-	-
BMI		182		-0.241	-0.518 to 0.035	0.057									
Dominant Leg	**Dominant**	105	3.551 (±5.006)	0.332	-1.132 to 1.796	0.657									
	Non Dominant	77	3.882 (±5.010)	-	-	-									
Cohort	**Footballers**	50	1.132 (±2.344)	-3.419	-4.675 to -2.164	<0.001	-4.364	-5.749 to -2.979	<0.001						
	Male Controls	66	4.551 (±4.504)	-	-	-	-	-	-						
	Female Controls	66	4.769 (±6.175)	0.218	-1.612 to 2.048	0.815	1.261	-0.725 to 3.247	0.213						
PAQ	**Linear**	182		-0.571	-1.245 to 0.103	0.059				-0.746	-1.014 to -0.478	<0.001	-1.125	-1.732 to 0.517	<0.001
	< 2	54	3.944 (±4.983)	-	-	-									
	2-3	52	3.821 (±6.425)	-0.123	-0.955 to 0.708	0.771									
	3-4	62	3.512 (±4.046)	-0.433	-0.549 to -0.317	<0.001									
	4-5	14	3.027 (±2.591)	-0.918	-1.970 to 0.134	0.087									

Table 4-5 - Predictors of Change in Angle of Anteversion. *Age and cohort as covariables. **Age, gender and activity level as covariables. ***Physeal maturity, gender, and Physical Activity Questionnaire as covariables

Anteversion															
		Hips	Mean Change Angle (±SD)	Univariate Regression			Multivariate Regression 1*			Multivariate Regression 2**			Multivariate Regression 3***		
				Coefficient	95% CI	P value	Coefficient	95% CI	P value	Coefficient	95% CI	P value	Coefficient	95% CI	P value
Age at Baseline	**Months (Continuous)**	182		-0.003	-0.039 to 0.032	0.460	-0.015	-0.019 to -0.011	0.048	-0.015	-0.017 to -0.013	<0.001			
	9-10 Years	70	1.517 (±4.730)	0.915	-0.545 to 2.376	0.219									
	11-12 Years	40	3.767 (±3.919)	3.165	1.628 to 4.702	<0.001									
	13-14 Years	26	4.790 (±7.225)	4.188	1.300 to 7.076	0.004									
	15-16 Years	30	1.763 (±2.303)	1.161	-0.096 to 2.418	0.070									
	17-18 Years	16	0.602 (±2.025)	-	-	-									
Physis	**Open**	92	2.276 (±4.541)	0.382	-1.293 to 2.059	0.654							0.418	-1.345 to 2.181	0.642
	Open-Closed	36	3.926 (±4.036)	2.034	0.124 to 3.944	0.037							2.407	0.805 to 4.009	0.003
	Closed	52	1.892 (±5.199)	-	-	-							-	-	-
Gender	**Male**	116	2.212 (±4.080)	-0.625	-2.167 to 0.916	0.426				-0.474	-2.084 to 1.136	0.564	-2.084	-2.980 to -1.116	<0.001
	Female	66	2.838 (±5.648)	-	-	-									
BMI		182		0.091	-0.769 to 0.950	0.408									
Dominant Leg	**Dominant**	105	2.854 (±5.301)	-0.979	-2.280 to 0.321	0.140									
	Non Dominant	77	1.874 (±3.698)	-	-	-									
Cohort	**Footballers**	50	1.325 (±4.774)	-1.559	-3.095 to -0.233	0.047	-1.659	-1.895 to -1.422	0.040						
	Male Controls	66	2.884 (±3.349)	-	-	-	-	-	-						
	Female Controls	66	2.838 (±5.648)	-0.047	-1.619 to 1.525	0.954	-0.129	-1.745 to 1.487	0.875						
PAQ	**Linear**	182		-0.531	-1.627 to 0.565	0.102				-0.746	-1.014 to -0.478	<0.001	-1.125	- 1.732 to - 0.517	<0.001
	< 2	54	3.458 (±5.261)	-	-	-									
	2-3	52	2.159 (±4.511)	-1.298	-1.590 to -1.007	<0.001									
	3-4	62	1.614 (±4.382)	-1.844	-2.142 to -1.546	<0.001									
	4-5	14	3.209 (±4.094)	-0.249	-3.433 to 2.936	0.878									

Figure 4-8 - Change in Lateral CEA with Age in All Individuals. Age groups based on chronological age of participant at baseline. Box and Whisker Plot.

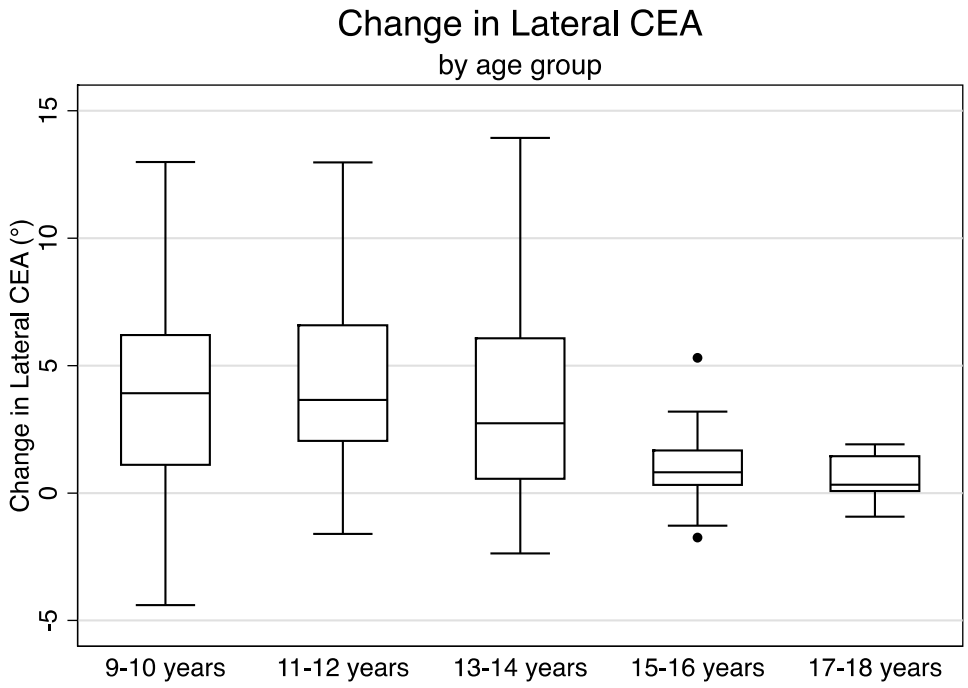


Figure 4-9 - Change in Anterior CEA with Age in All Individuals. Age groups based on chronological age of participant at baseline. Box and Whisker Plot.

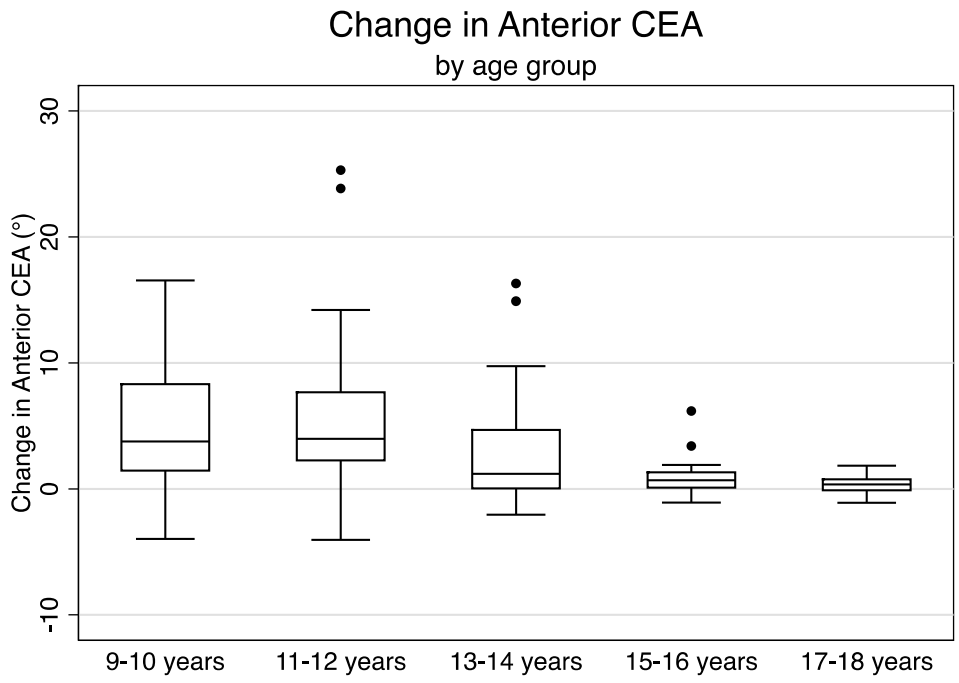
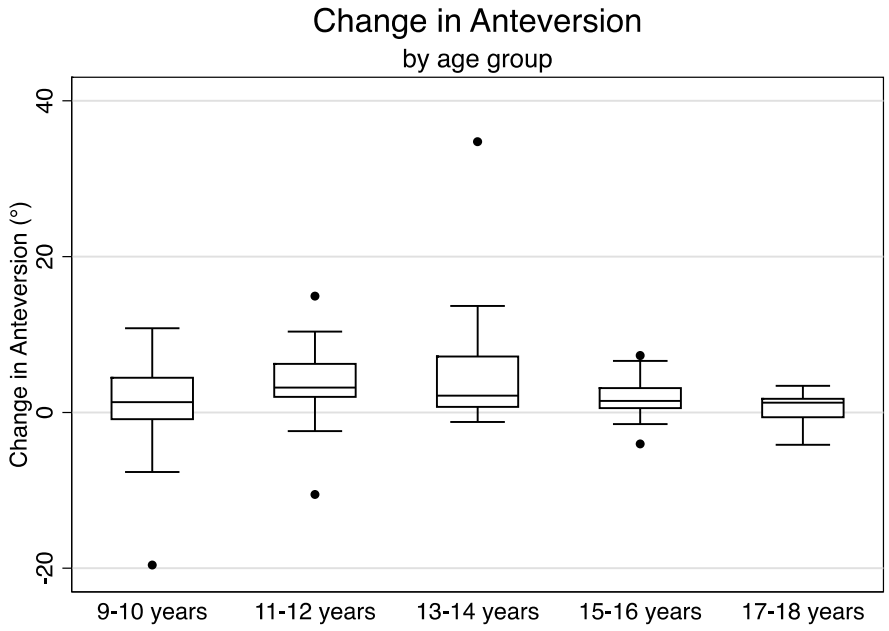


Figure 4-10 - Change in Anteversion with Age in All Individuals. Age groups based on chronological age of participant at baseline. Box and Whisker Plot.



The greatest change in lateral CEA, anterior CEA, and anteversion in male footballers occurred in individuals aged 11-12 years at baseline, with no significant change occurring in individuals older than 12 years at baseline. The greatest change in lateral CEA and anteversion in male controls occurred in individuals aged 13-14 years at baseline. The greatest change in anterior CEA in male controls occurred in individuals aged 9-10 years at baseline. The greatest change in lateral CEA, anterior CEA, and anteversion in female controls occurred in individuals aged 9-10 years, 11-12 years, and 13-14 years at baseline respectively. No significant change in acetabular morphology or version occurred in female controls older than 14 years at baseline. In male controls no significant change in lateral CEA or anterior CEA occurred after 14 years of age at baseline, but anteversion showed significant change up to 16 years at baseline. (Table 4-6)

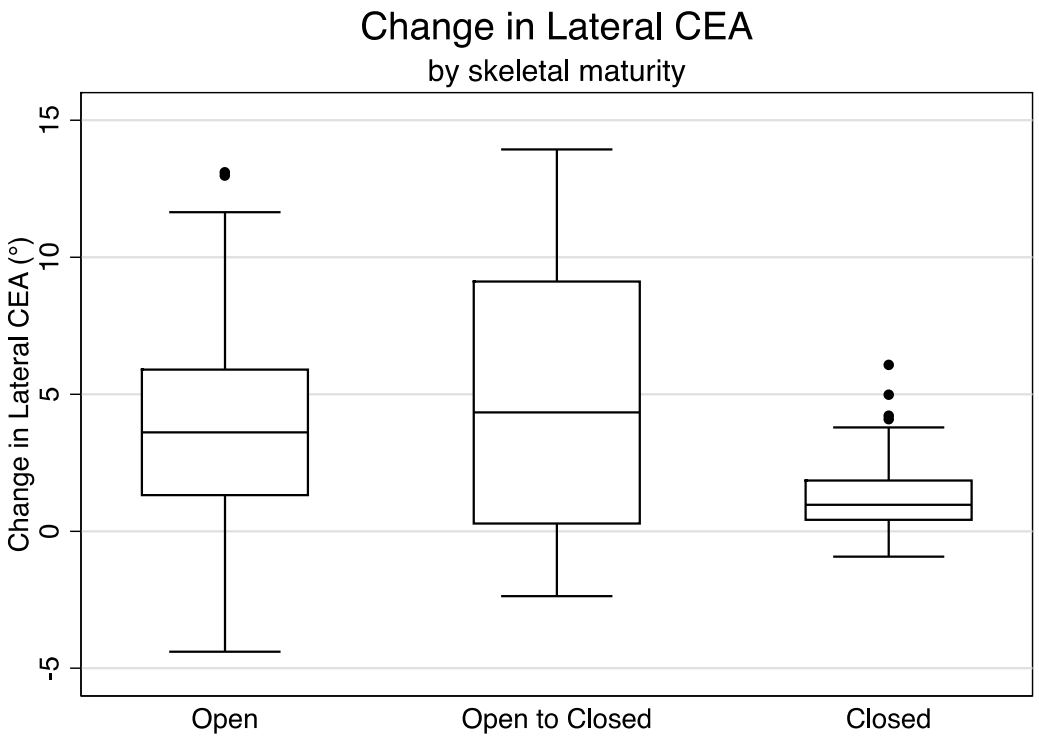
Table 4-6 - Change in acetabular morphology and version with age by cohort.

		Lateral CEA				Anterior CEA				Anteversion			
		Mean Change (±SD)	Change in Lateral CEA Univariate Regression			Mean Change (±SD)	Change in Anterior CEA Univariate Regression			Mean Change (±SD)	Change in Lateral CEA Univariate Regression		
			Coefficient	95% CI	P value		Coefficient	95% CI	P value		Coefficient	95% CI	P value
Male Footballers													
Age at Baseline (Years)	**9-10**	1.651 (±3.285)	1.616	0.395 to 2.837	0.009	1.236 (±2.614)	1.231	0.226 to 2.235	0.016	0.105 (±4.953)	-0.267	-2.307 to 1.773	0.798
	11-12	3.520 (±3.245)	3.485	1.536 to 5.433	<0.001	2.215 (±1.869)	2.210	1.040 to 3.381	<0.001	4.736 (±3.921)	4.364	1.826 to 6.902	0.001
	13-14	1.383 (±3.324)	1.348	-1.500 to 4.196	0.354	-0.664 (±1.358)	-0.669	-1.890 to 0.552	0.283	3.381 (±4.933)	3.009	-1.310 to 7.328	0.172
	15-16												
	17-18	0.035 (±0.539)	-	-	-	0.005 (±0.552)	-	-	-	0.372 (±1.453)	-	-	-
Male Controls													
Age at Baseline (Years)	**9-10**	4.039 (±2.363)	3.978	2.866 to 5.091	<0.001	7.120 (±4.960)	7.390	4.979 to 9.801	<0.001	1.565 (±3.498)	0.450	-1.082 to 1.981	0.565
	11-12	3.590 (±3.492)	3.529	1.966 to 5.093	<0.001	5.541 (±3.723)	5.811	3.848 to 7.775	<0.001	3.732 (±2.891)	2.617	1.337 to 3.897	<0.001
	13-14	8.964 (±5.366)	8.903	5.394 to 12.413	<0.001	4.169 (±4.231)	4.439	1.464 to 7.414	0.003	4.718 (±5.046)	3.603	0.315 to 6.891	0.032
	15-16	0.847 (±1.692)	0.786	-0.143 to 1.715	0.097	0.896 (±1.789)	1.166	-0.265 to 2.597	0.110	2.778 (±2.261)	1.662	0.538 to 2.786	0.004
	17-18	0.061(±0.477)	-	-	-	-0.270 (±1.175)	-	-	-	1.116 (±0.343)	-	-	-
Female Controls													
Age at Baseline (Years)	**9-10**	7.057 (±3.579)	5.820	4.230 to 7.410	<0.001	7.798 (±4.619)	7.159	5.133 to 9.185	<0.001	3.587 (±4.890)	2.941	0.227 to 5.655	0.034
	11-12	6.603 (±3.710)	5.366	3.141 to 7.590	<0.001	9.417 (±9.891)	8.778	2.944 to 14.612	0.003	2.868 (±5.622)	2.222	-1.510 to 5.954	0.043
	13-14	2.115 (±2.095)	0.878	-0.265 to 2.022	0.132	3.490 (±5.535)	2.850	0.019 to 5.682	0.049	5.233 (±8.957)	4.587	-0.254 to 9.429	0.063
	15-16	1.192 (±0.913)	-0.045	-0.680 to 0.590	0.890	0.763 (±0.730)	0.124	-0.465 to 0.712	0.681	0.603 (±1.793)	-0.043	-1.997 to 1.911	0.966
	17-18	1.237 (±0.673)	-	-	-	0.640 (±0.709)	-	-	-	0.646 (±2.672)	-	-	-

4.5.2.2 Skeletal Maturity

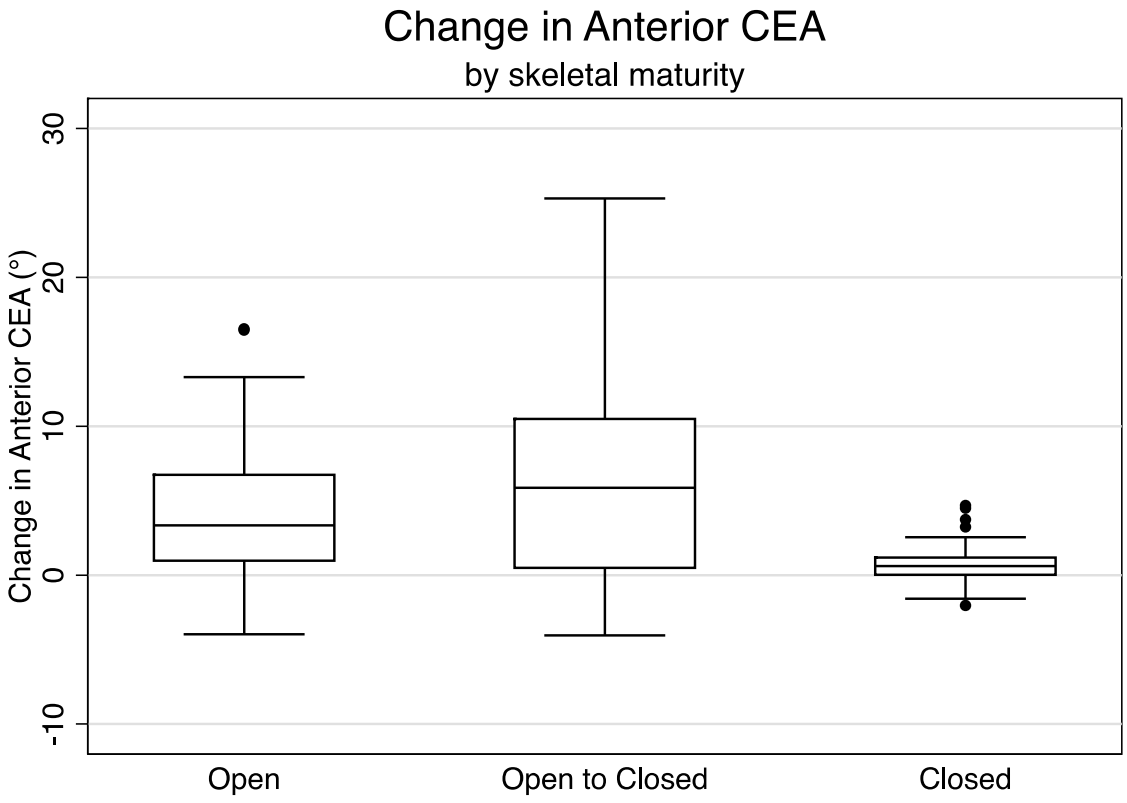
Individuals with an open physis at both baseline and follow-up experienced larger change in lateral CEA than individuals with a closed physis. Adjusting for activity level and gender, individuals with an open physis at baseline and follow-up had a change in lateral CEA 4.05 degrees greater than individuals with a closed physis ($p<0.001$). Individuals with a closed physis had a change in lateral CEA of 1.32 degrees between baseline and follow-up, which was not statistically significant. (Table 4-3) (Figure 4-11)

Figure 4-11 - Change in Lateral CEA by Skeletal Maturity. Box and whisker plot



Individuals with an open physis at baseline and closed physis at follow-up experienced greater change in anterior CEA than individuals with an open or closed physis. Adjusting for activity level and gender, individuals with an open physis at baseline and a closed physis at follow-up had a change in anterior CEA 5.13 degrees greater than individuals with a closed physis ($p<0.001$). Individuals with a closed physis had a change in anterior CEA of 1.26 degrees between baseline and follow-up, which was not statistically significant. (Table 4-4) (Figure 4-12)

Figure 4-12 - Change in Anterior CEA by Skeletal Maturity. Box and whisker plot.



Individuals with an open physis at baseline and closed physis at follow-up experienced greater change in anteversion than individuals with an open or closed physis. Adjusting for activity level and gender, individuals with an open physis at baseline and a closed physis at follow-up had a change in anteversion 2.41 degrees greater than individuals with a closed physis ($p<0.001$). Individuals with a closed physis had a change in anteversion of 1.89 degrees between baseline and follow-up, which was not statistically significant. (Table 4-5) (Figure 4-13)

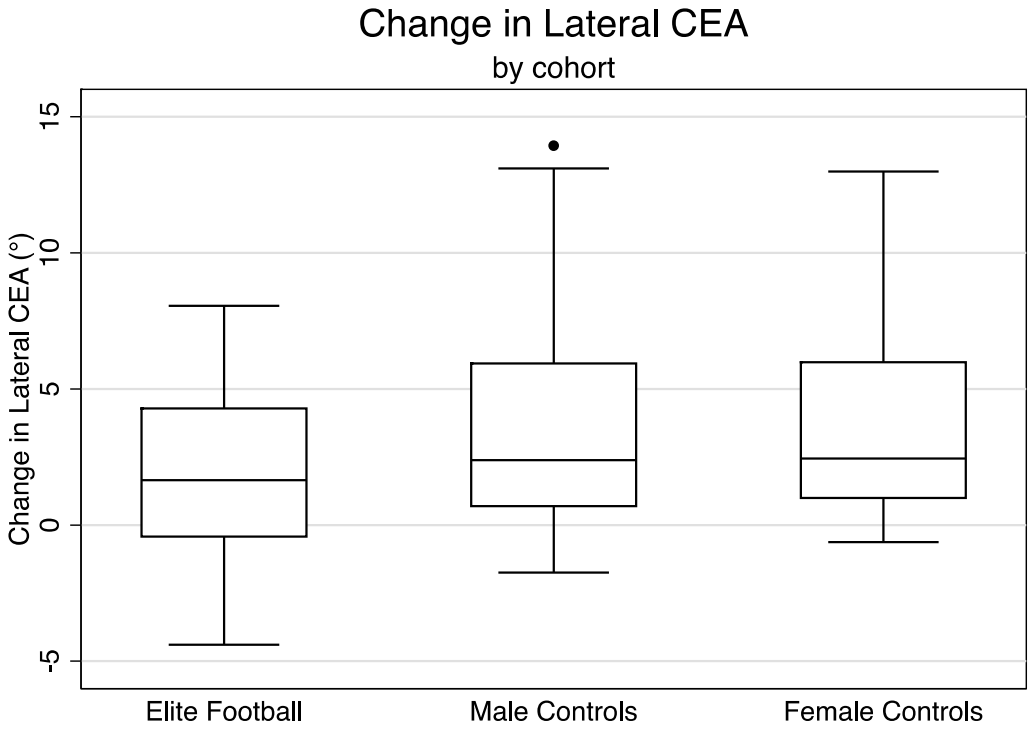
Figure 4-13 - Change in Anteversion by Skeletal Maturity. Box and whisker plot.



4.5.3 Risk Factors for Abnormal Acetabular Morphology Development

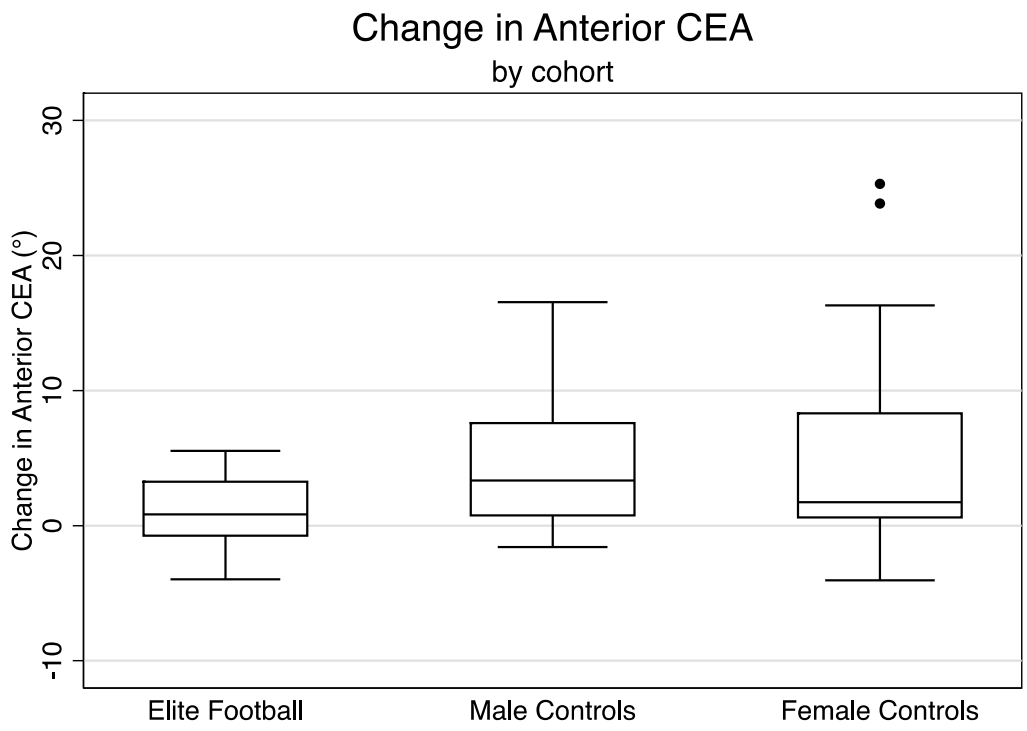
Elite level football players had significantly less change than controls in lateral CEA, anterior CEA, and anteversion between baseline and follow-up. Adjusting for age elite male footballers had a change in lateral CEA 2.05 degrees less than male controls (p=0.001). (Table 4-3) (Figure 4-14)

Figure 4-14 - Change in Lateral CEA by Cohort. Box and whisker plot.



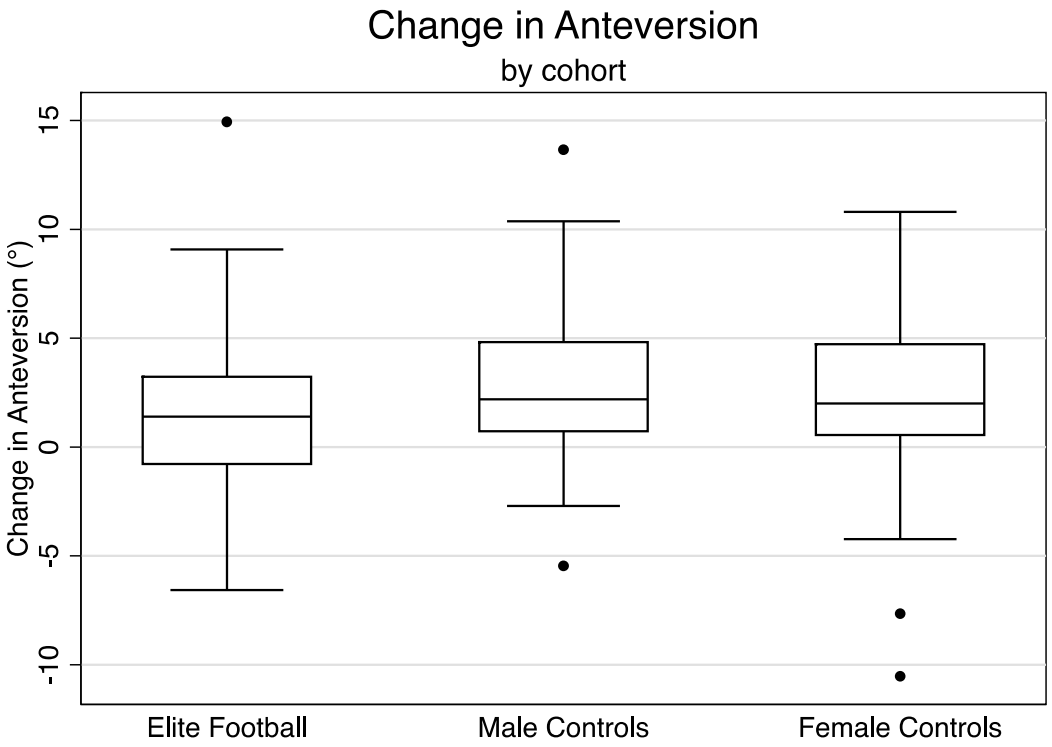
Adjusting for age elite male footballers had a change in anterior CEA 4.36 degrees less than male controls ($p<0.001$). (Table 4-4) (Figure 4-15)

Figure 4-15 - Change in Anterior CEA by cohort. Box and whisker plot.



Adjusting for age elite male footballers had a change in anteversion 1.66 degrees less than controls (p=0.040). (Table 4-5) (Figure 4-16)

Figure 4-16 - Change in Angle of Anteversion by Cohort. Box and whisker plot.



Males showed less change in lateral CEA and anterior CEA than females between baseline and follow-up. This difference was significant in univariate regression analysis, but was not significant in multivariate anlaysis when controlling for age and activity level. No significant difference was seen between males and females in change in angle of anteversion. (Table 4-4, Table 4-4, and Table 4-5).

Individuals with high activity levels (PAQ score) had significantly less change in lateral CEA, anterior CEA and anteversion than individuals with low activity levels. Adjusting

for age and gender in a multivariate linear regression model there was a significant negative linear relationship between PAQ score and change in lateral CEA (coefficient -0.62, p = 0.043), PAQ score and change in anterior CEA (coefficient -3.21, p = 0.039), and PAQ score and change in angle of anteversion (coefficient -0.59, p = 0.048).

Adjusting for age and gender, individuals with a PAQ score between 2 and 3, between 3 and 4, and between 4 and 5 had a change in lateral CEA 0.98 degrees ($p < 0.001$), 2.54 degrees ($p<0.001$), and 3.49 degrees ($P < 0.001$) less than individuals with a PAQ less than 2 respectively. Adjusting for age and gender, individuals with a PAQ score between 3 and 4, and between 4 and 5 had a change in anterior CEA 1.65 degrees ($p < 0.001$), and 1.57 degrees ($P < 0.001$) less than individuals with a PAQ less than 2 respectively. Adjusting for age and gender individuals with a PAQ score between 2 and 3, and between 3 and 4 had a change in angle of anteversion 1.20 degrees ($p < 0.001$), and 2.03 degrees ($p = 0.006$) less than individuals with a PAQ less than 2 respectively.

There was no significant association between leg dominance and change in lateral CEA, anterior CEA, or angle of anteversion. No significant association was seen between BMI and change in lateral CEA, anterior CEA, or angle of anteversion. (Table 4-3, Table 4-4, and Table 4-5)

4.5.4 Relationship Between Femoral and Acetabular Morphology

Mean average alpha angle at baseline was 51.80 degrees (SD 7.14 degrees), and at follow-up was 60.55 degrees (SD 9.39 degrees). Individuals with a larger increase in Alpha Angle had significantly less change in lateral and anterior CEA. Adjusting for age, gender, and activity level there was a significant negative linear relationship between change in average alpha angle and change in lateral CEA (coefficient -0.082, p = 0.018) (Figure 4-17), and change in average alpha angle and change in anterior CEA (coefficient –0.114, p = 0.014) (Figure 4-18). No significant linear relationship was seen between change in average alpha angle and change in angle of anteversion (coefficient 0.064, p = 0.316).

Figure 4-17 - Change in Lateral CEA versus Change in Average Alpha Angle. Scatter plot with 95% Confidence Intervals. Coefficient –0.114, R^2 = 0.090, p = 0.014

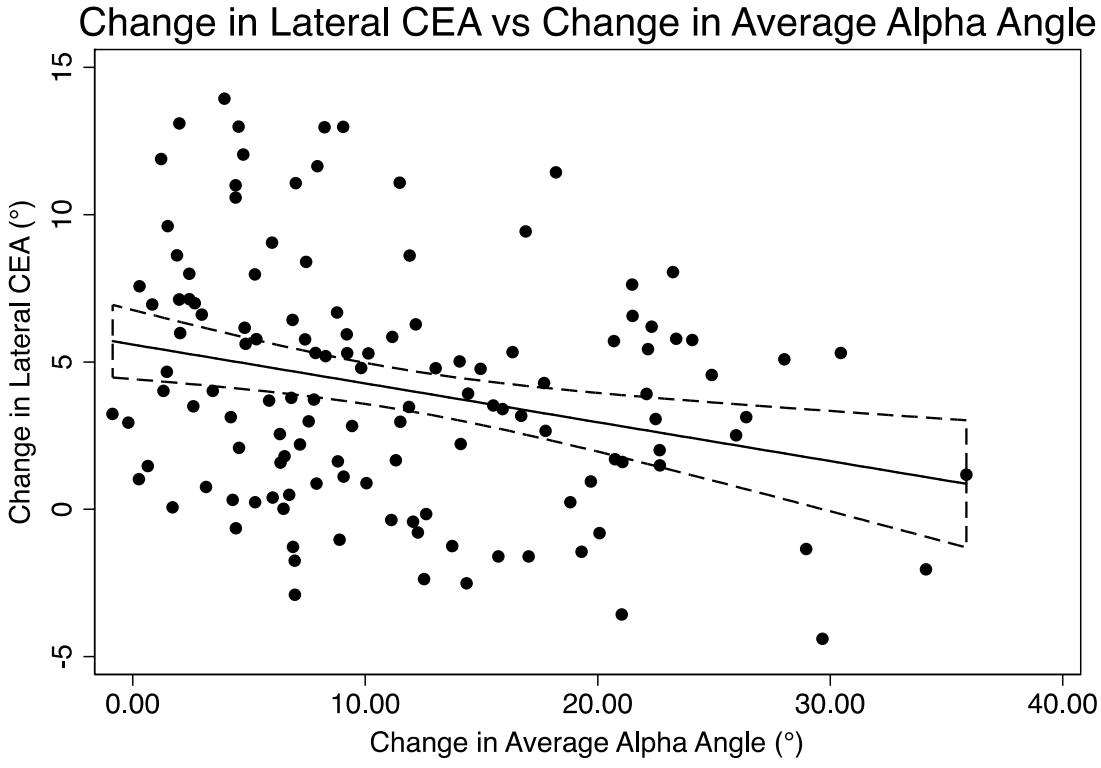
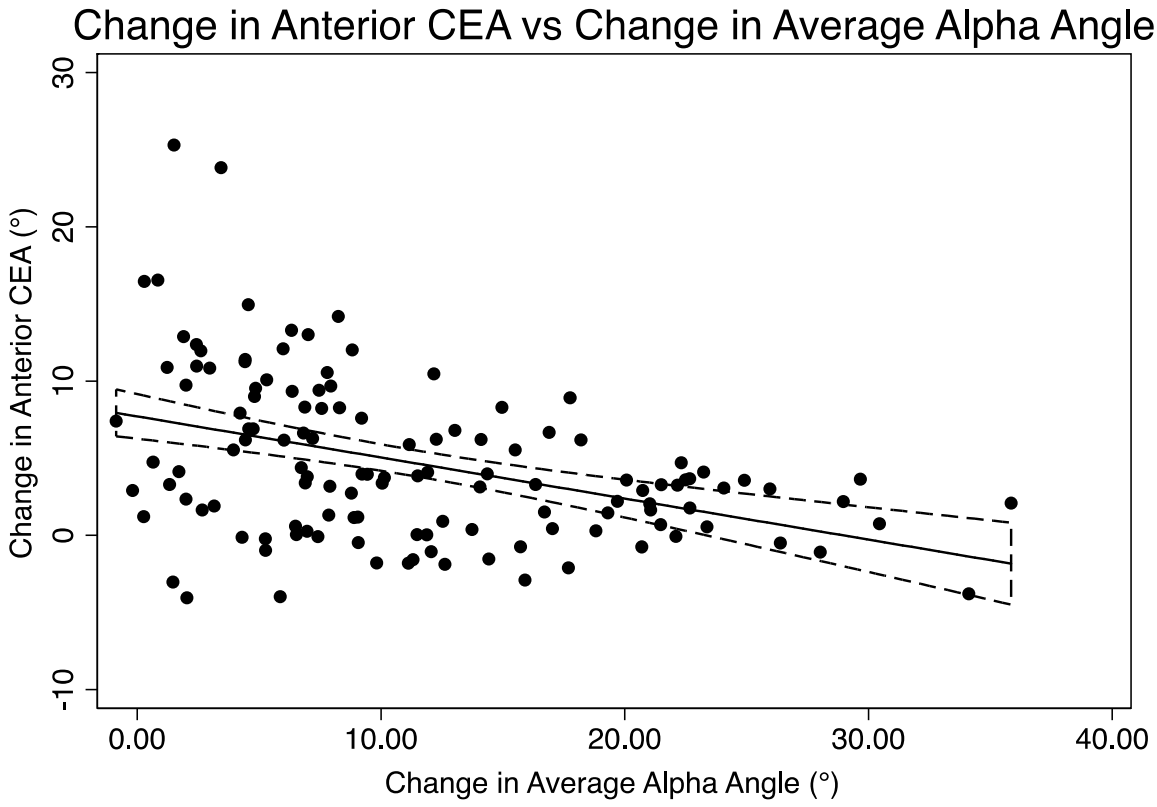


Figure 4-18 - Change in Anterior CEA versus Change in Average Alpha Angle. Scatter plot with 95% Confidence Intervals. Coefficient = - 0.064, R^2 = 0.020 , p = 0.316



4.5.5 Predicting Abnormal Acetabular Morphology

4.5.5.1 Acetabular Dysplasia

40 hips had an open physis and evidence of mild dysplasia (lateral CEA between 20 and 25 degrees[112,217]) at baseline (mean age 127 months, SD 18). All of these hips were followed up at 3 years (mean age 163 months, SD 20). 36 of these hips had a closed physis at follow-up. 9 of these hips showed evidence mild dysplasia at follow-up. No hips showed evidence of dysplasia at baseline or follow-up (lateral CEA less than 20 degrees[112]).

Baseline variables selected as potential predictors of future mild acetabular dysplasia were PAQ score and average alpha angle. No correlation existed between lateral CEA and PAQ score, and lateral CEA and average alpha angle, in individuals with an open physis and lateral CEA less than 25 degrees at baseline. Accordingly ROC analysis of baseline variables was not performed.

4.5.5.2 Acetabular Retroversion

87 hips had an open physis and evidence of acetabular retroversion (angle of anteversion less than 14.2 degrees[266]) at baseline (mean age 134 months, SD 22). All of these hips were followed up at 3 years (mean age 169 months, SD 22). 12 of these hips had a closed physis at follow-up. 53 of these hips showed evidence of acetabular retroversion at follow-up.

Baseline variables selected as potential predictors of future mild acetabular dysplasia were PAQ score and average alpha angle. No correlation existed between angle of anteversion and PAQ score, and angle on anteversion and average alpha angle, in individuals with an open physis and angle of anteversion less than 14.2 degrees at baseline. Accordingly ROC analysis of baseline variables was not performed.

4.6 Discussion

The aim of this study was to determine the change in acetabular morphology with age and to characterise the risk factors for abnormal development during adolescence. Identifying individuals at risk of abnormal acetabular morphology may allow the development of preventative strategies. This study demonstrates that males undertaking intense exercise between the ages of 11 and 14 years, and individuals that develop cam morphology, are at greatest risk of developing abnormal acetabular morphology.

4.6.1 Change in Acetabular Morphology with Age

Studies have demonstrated acetabular version and femoral head coverage increase with age[1,30] and are greater in individuals with a closed rather than open physis[128,132]. However, changes in acetabular morphology over the course of adolescent skeletal development have not been well characterized[127].

Our results demonstrate that lateral CEA, anterior CEA, and anteversion increase with age, with significant changes occurring from 9 years. In this study the greatest change in acetabular morphology occurred between the ages of 11 and 12 years at baseline in all individuals. No significant change occurred after 14 years of age in male and female controls. In male footballers no significant change in acetabular morphology was seen after 12 years of age.

These findings agree with previous reports that acetabular morphology causing abnormal femoral head coverage may be present from 12 years[30]. However, our results would suggest that significant changes in anteversion occur earlier than previously reported. Monazzam et al reported increases in anteversion only after 12 years of age[30]. Weiner et al reported no age-dependent differences of acetabular version in a population aged from 6 months to 17 years[129]. However, it should be noted that these studies were based on CT measurements, which fail to measure the true dimensions of the developing cartilaginous acetabular wall in skeletally immature individuals[63].

4.6.2 Risk Factors for Abnormal Acetabular Morphology

Our results demonstrate that activity level and gender play a significant role in the development of acetabular morphology. High activity levels were associated with reduced acetabular growth resulting in less femoral head coverage. The change in lateral CEA, anterior CEA, and anteversion was 2.0 degrees, 4.4 degrees, and 1.7 degrees less in male footballers than male controls respectively. Higher PAQ scores were also associated with significantly less change in acetabular morphology and anteversion. These associations with PAQ score remained significant when controlling for alpha angle also.

While a positive association has been shown between activity levels and the risk of cam morphology[32,33,51,52] the effect of activity levels on acetabular morphology and version remains unknown. A dose response relationship between training frequency and cam morphology in elite athletes has been described previously[52,296]. The stepwise decrease in

change in lateral CEA, anterior CEA, and anteversion with increasing PAQ scores seen in this study would suggest a similar relationship exists between training frequency and acetabular morphology. The PAQ score differentiates between active and inactive individuals[225], but focuses on the frequency rather than type, intensity, or duration of sport or exercise sessions performed per week. Accordingly further research is required to determine the effect of these aspects of activity on developing acetabular morphology.

A statistical association existed between male gender and reduced development of femoral head coverage when compared to females. It is worth noting that males on average had higher PAQ scores and although this was controlled for in the regression models it may account for the association seen with gender. However, this finding is in agreement with reports from other cohorts where males showed lower lateral CEA values[30]. No significant difference was found in change in anteversion between males and females. This is consistent with the findings of Hingsammer et al in adolescants[128], and in contrast to adult studies of normal hip morphology which show females to have increased anteversion compared to males[300-302]. Our findings offer some evidence to suggest that the development of reduced femoral head coverage in adolescence may have a gender-specific pathogenesis, though further research comparing male and female elite athlete cohorts is required to fully elucidate this relationship. As with cam morphology there was no significant association between leg dominance and change in acetabular morphology[52].

Our findings are consistent with acetabular morphology developing in response to load during active skeletal growth, similarly to cam morphology[52]. Mechanical loading is recognised as a key factor for normal bone development[66]. Increased levels of sex steroids, growth hormone peaks, insulin like growth factors and genetic factors at the start of adolescence may result in increased response to loading[42]. This could provide a possible explanation for changes in acetabular morphology development at this age in active individuals. Excessive loading at the anterolateral acetabular rim through activity at this key development time may trigger abnormal or inhibited bone development, resulting in dysplastic or retroverted acetabula.

4.6.3 Effect of Femoral Morphology on Acetabular Morphology

A larger increase in alpha angle was associated with less change in anterior and lateral CEA. This suggests the development of asphericity at the femoral head-neck junction (cam morphology) and reduced acetabular development resulting in less femoral head coverage may be associated. High levels of femoral head asphericity in acetabular dysplasia have previously been described[303]. It is believed that as the triradiate cartilage of the pelvis grows the concavity of the acetabulum develops in response to its interaction and articulation with the spherical femoral head[59,60]**.** Asphericity of the femoral head in adults has been shown to result in impingement against the anterolateral acetabular rim with movement[78]. The development of cam morphology and impingement during adolescence may result in retardation of growth of the anterior and lateral acetabular walls as a compensatory mechanism. However, it may also be that high activity simply results in growth abnormalities at both the proximal femoral physis

and acetabular triradiate cartilage, and cam morphology does not impact acetabular development. Further study and follow-up of this cohort to skeletal maturity is required to fully elucidate the extent of this relationship.

4.6.4 Predicting Abnormal Acetabular Morphology

In this study no correlation existed between baseline PAQ score and change in anterior or lateral CEA, or anteversion. Activity levels alone are therefore unlikely to offer predictive capabilities for determining the development of abnormal acetabular morphology. This may be due to the multifactorial nature of acetabular development, and the majority of acetabular development taking place in childhood as opposed to adolescence.

4.6.5 Limitations

The main limitation of this study is the relatively small sample size. A subset of our baseline cohort underwent the necessary MRI sequence to quantify acetabular morphology. Another limitation is that the control group may not be representative of the general population due to participation bias in sports and exercise projects. Further limitations apply to the measurement methodology for acetabular morphology. Measuring acetabular morphology through the centre of the femoral head may fail to recognize more superior deficiencies. However, there is no consensus as to what level in the acetabulum morphology should be measured[41]. It is also likely that there is inadequate adjustment of cofounders in this study, which may be responsible for some

significant associations. Moreover, there is no agreed diagnostic threshold for acetabular dysplasia or acetabular retroversion. The results in this study for the predictive capabilities of baseline variables should therefore be interpreted with care.

4.6.6 Conclusion

The greatest changes in acetabular morphology development take place between 11-12 years. There is no significant change in acetabular morphology beyond 14 years in male and female controls, and 12 years in male footballers. Physical activity during adolescence is strongly associated with reduced femoral head coverage and increased acetabular retroversion in males. The development of cam morphology is associated with reduced femoral head coverage development in adolescence.

Chapter 5 Leg Alignment in Adolescence and the Effects of Activity

5.1 Abstract

Introduction:

Leg alignment develops throughout childhood and during adolescence. Abnormal leg alignment, such as varus or valgus alignment, predisposes to soft tissue injury and future osteoarthritis. An improved understanding of abnormal leg alignment development is required to determine whether the process is predictable or modifiable. The aim of this study was to characterise the risk factors, timing, and pathogenesis of varus leg alignment.

Methods:

Cross sectional observational cohort study of individuals from football club academies and an age-matched control population, aged 11-21 years. Assessments included questionnaires, clinical examination, and full leg length MRI scans. Primary imaging outcome measures were Hip Knee Angle (HKA), Medial Proximal Tibial Physeal Angle (MPTPhyA), and Alpha Angle.

Results:

The cohort comprised 58 elite male footballers, 34 male controls, and 34 female controls. HKA decreased with age, with the greatest decrease occurring between 13 to 16 years

(HKA 1.11 degrees (SD 2.10)), with no significant change after 16 years. Skeletally immature elite male footballers had a HKA 0.87 degrees less than male controls and 2.22 degrees less than female controls. Skeletally mature elite male footballers had a HKA 2.28 degrees less than male controls and 3.73 degrees less than female controls. A negative correlation existed between HKA and Physical Activity Questionnaire Score (coefficient -0.24, p=0.029). A negative correlation existed between HKA and alpha angle (coefficient -0.75, p = 0.003). A positive correlation existed between HKA and MPTPhyA (coefficient 0.32, p = 0.008). Physical Activity Questionnaire Score at baseline showed the greatest capability of predicting the development of varus leg alignment at 3 years with an area under the curve of 0.69.

Conclusions:

The development of varus leg alignment is greatest age 13 to 16 years in male footballers and male controls. Females remained in valgus alignment throughout adolescence. There is no significant change in leg alignment after 16 years of age. Physical activity during adolescence is strongly associated with the development of varus leg alignment in males. A low MPTPhyA is likely to represent physiological adaptation to load and be the mechanism by which varus alignment develops.

5.2 Introduction

Varus leg alignment (genu varum) increases risk for the development of knee osteoarthritis[10,26-28] and is associated with higher tensions at the ACL[144,145], meniscal tears, patellofemoral pain syndrome[146-148], and shin splints[149]. An improved understanding of leg alignment development is required to determine whether abnormal morphology is preventable or modifiable.

Leg alignment is believed to continue to develop after childhood during adolescence as the distal femoral physis and proximal tibial physis mature[135]. The development of genu varum during late childhood is considered atypical[137,139] and may place adverse biomechanical stresses upon the cartilage[10]. The age at which this occurs is unclear with some studies stating genu varum appears at around 13-14 years of age[135,139,153], and others at 16 years of age[148]. However, these findings are based on clinical examination measures and the development of genu varum in relation to the stage of skeletal maturity has yet to be investigated using imaging in an adolescent cohort.

Leg alignment is determined by both modifiable and non-modifiable parameters, which include gender[143,151], obesity[152], and athletic activity[135,153]. A higher prevalence of varus leg alignment exists in retired soccer players than a general population of the same age[20], and studies have shown that athletic activity is associated with greater varus leg alignment in boys[135,153]. However, there exist no imaging studies investigating the effect of activity on leg alignment in an adolescent cohort. Evidence from skeletally mature

cohorts would suggest there is an association between cam morphology and varus leg alignment[133,134], but this is yet to be investigated in an adolescent cohort.

The development of abnormal varus leg alignment is likely secondary to biomechanical overload at the medial proximal tibial physis[156-158]. However, no studies have imaged the tibial physis in an adolescent cohort. Accordingly, the mechanism of genu varum development remains largely unknown.

5.3 Aims

1) Investigate the changes in leg alignment with age
2) Investigate the effect of activity on the development of leg alignment
3) Investigate which lower limb anatomical parameters contribute to varus leg alignment
4) Characterise the mechanism of varus leg alignment formation
5) Determine if baseline measures can predict varus leg alignment

5.4 Methods

The methods for this study and justifications for imaging measures are discussed in chapter 2.

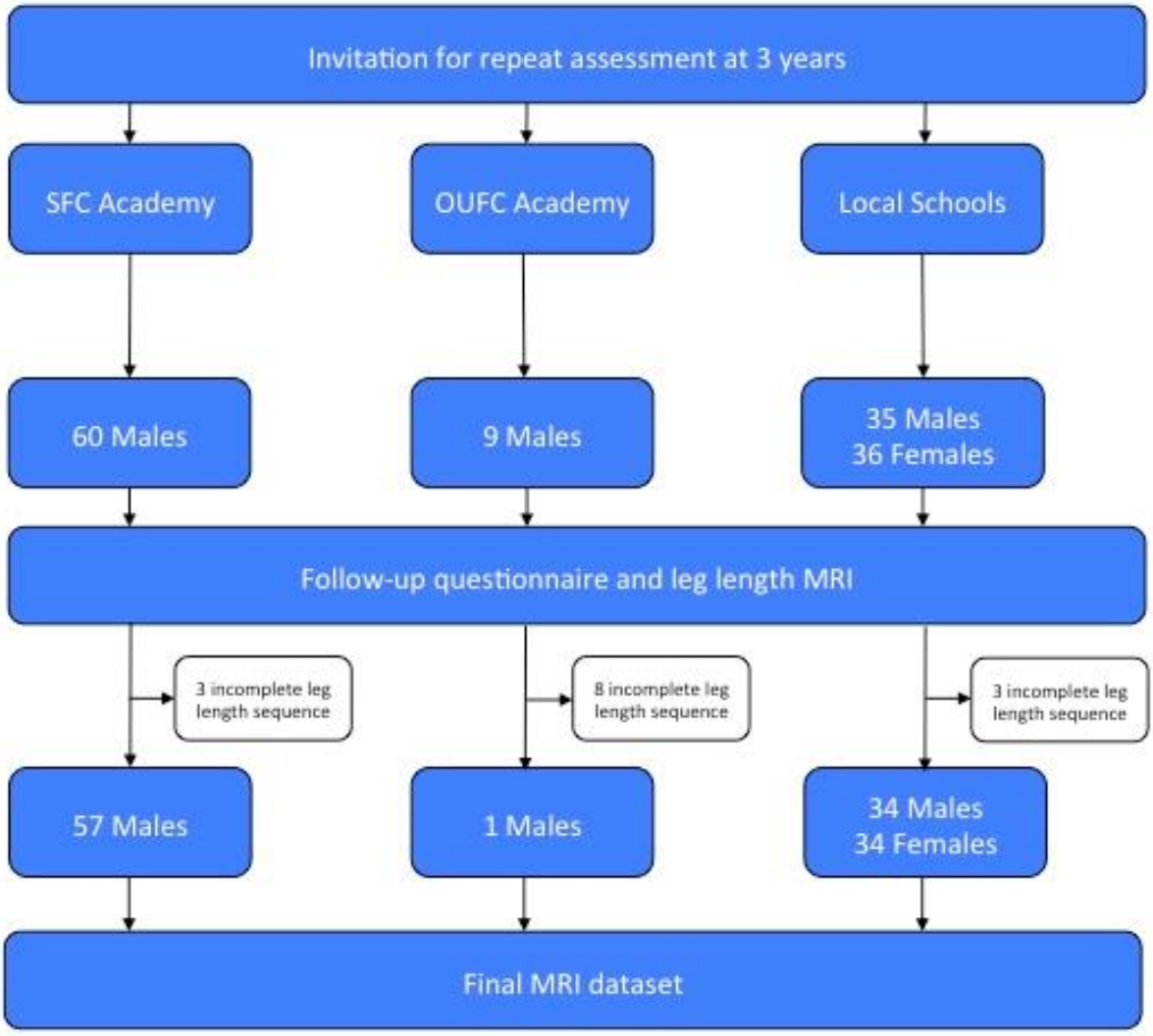
5.4.1 Study design

Cross sectional observational cohort study.

5.4.2 Population

Individuals aged 9–18 years were recruited from Southampton Football Club (SFC) Academy, Oxford United Football Club (OUFC) Academy, and local schools (controls) at baseline. Participants were invited for repeat assessment three years after initial baseline visit via post, email, and telephone. Study IDs were generated for each participant such that assessors were blinded to participant characteristics such as cohort and age when interpreting data such as MRI scans (see chapter 2). Four individuals from the control cohort declined repeat assessment, two did not attend their arranged follow-up appointment, and thirty individuals did not respond to invitation. All individuals who attended follow-up assessment and underwent MRI scanning were eligible for this study. Leg length MRI sequence outcomes were incomplete in 14 individuals (28 legs) due to movement artefact. (Figure 5-1)

Figure 5-1 - Recruitment flowchart for study.



5.4.3 Activity Levels

Activity was evaluated using two methods: i) SFC and OUFC Academy (elite footballer cohort) versus general population controls; ii) Physical Activity Questionnaire (PAQ) for older children (aged 9–13 years) and adolescents (aged 14–18 years)[224].

5.4.4 Imaging Protocol

Leg length and femoral morphology were assessed with MRI of both hips using a 3 Tesla Philips Achieva platform and torso coil (Philips Healthcare). Three-dimensional (3D) water selective fluid (WATSf) sequence was used to image femoral cartilage and bone, and stacked T1 weighted Turbo Spin Echo (TSE) coronal pelvis was used to image whole leg length. Leg length sequences were acquired with knees in full extension in neutral position with patella perpendicular to the table, feet shoulder width apart, under simulated weight bearing titrated to approximately match the participants' weight. Individual scans were taken in sequence of the pelvis, upper legs, lower legs, and feet and stitched together to produce a single image which includes both lower limbs.

3D multiplanar reconstructions were performed using OsiriX Software (V.6.0.2, Pixmeo). The centre of the hip, knee, and ankle joints were aligned to standardise orientation and ensure the entirety of the leg length was visible in the coronal view.

5.4.5 Imaging Measures

The methodologies for leg alignment imaging measures are discussed in Chapter 2 (2.7.3). The primary outcome measure in this study was the Hip Knee Angle (HKA). The HKA is defined as the angle formed by the intercept of the femoral mechanical axis and the tibial mechanical axis[270-273]. The HKA is expressed as a deviation from 180° with a negative value for varus alignment and a positive value for valgus alignment[171] (Figure 5-2). HKA values below -3 degrees were taken to define the presence of varus leg alignment[143,274]. Leg alignment was also quantified by the Weight Bearing Ratio (WBR). The WBR is calculated by measuring the distance from the medial edge of the proximal tibia to the point where the load bearing axis intersects the proximal tibia and dividing the measurement by the entire width of the tibia[268] (Figure 5-2). Varus leg alignment likely develops secondary to biomechanical overload at the medial tibial physis[156-158], as such medial tibial physeal morphology was quantified using the Medial Proximal Tibial Physis Angle (MPTPhyA) (Figure 5-3).

Further leg alignment measures investigated were; Mean Neck Shaft Angle (MNSA), Medial Proximal Femoral Angle (MPFA), Lateral Proximal Femoral Angle (LPFA), Mechanical Lateral Distal Femoral Angle (mLDFA), Anatomical Lateral Distal Femoral Angle (aLDFA), Joint Line Congruence Angle (JLCA), Mechanical Medial Proximal Tibial Angle (mMPTA), Anatomical Medial Proximal Tibial Angle (aMPTA), Mechanical Lateral Distal Tibial Angle (mLDTA), Anatomical Lateral Distal Tibial Angle (aLDTA), Leg Length Discrepancy, and Lateral Distal Femoral Physis Angle (LDFPhyA). (Figure 5-4)

Figure 5-2 - Full leg length weight bearing MRI of a 16 year old male showing Hip-Knee-Angle (HKA) and Weight-Bearing-Ratio (WBR) measures.

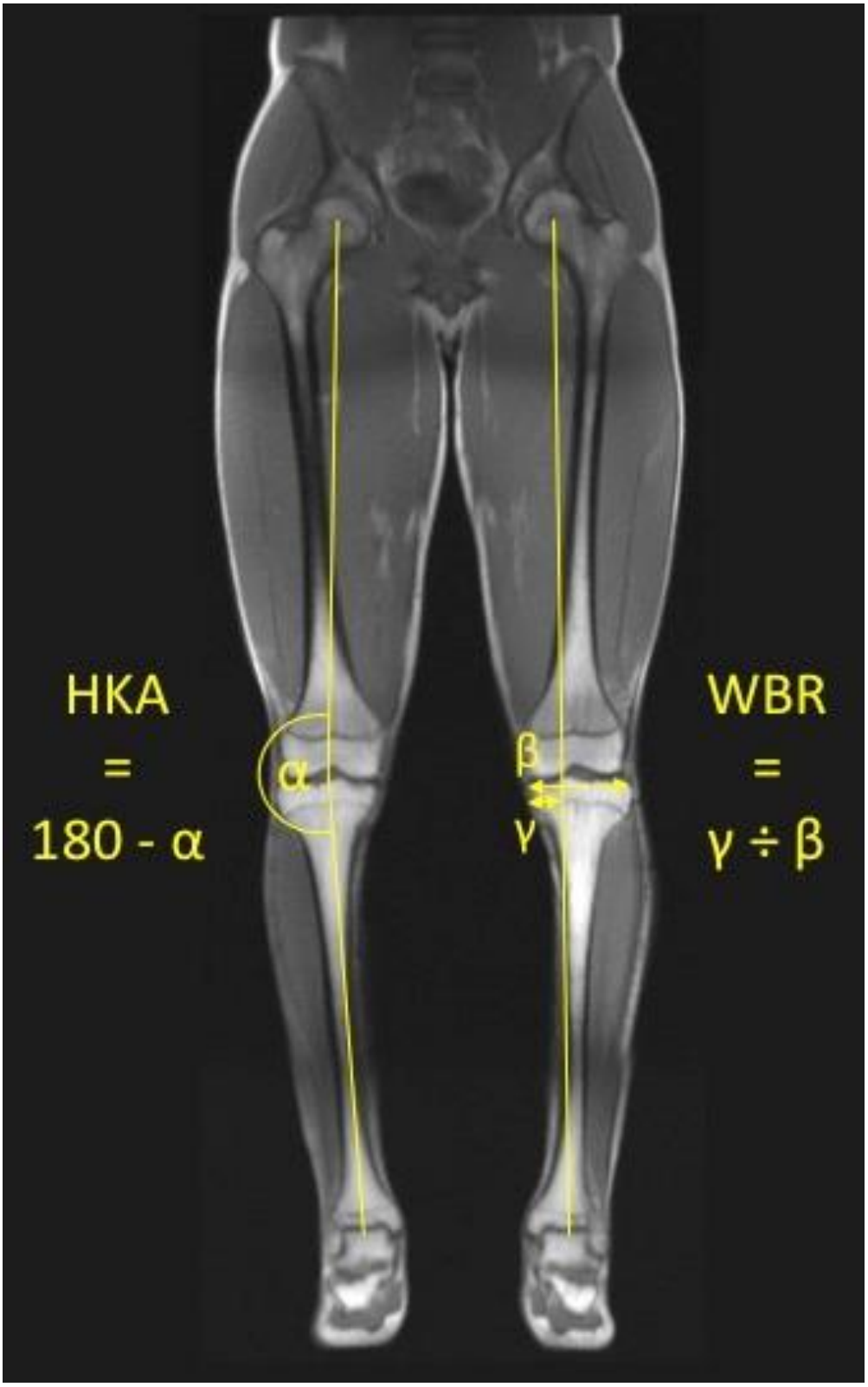


Figure 5-3 - Full leg length weight bearing MRI of a 16 year old male showing Joint Line Congruence Angle (JLCA), Medial Proximal Tibial Physis Angle (MPTPhyA), and Lateral Distal Femoral Physis Angle (LDFPhyA) measures.

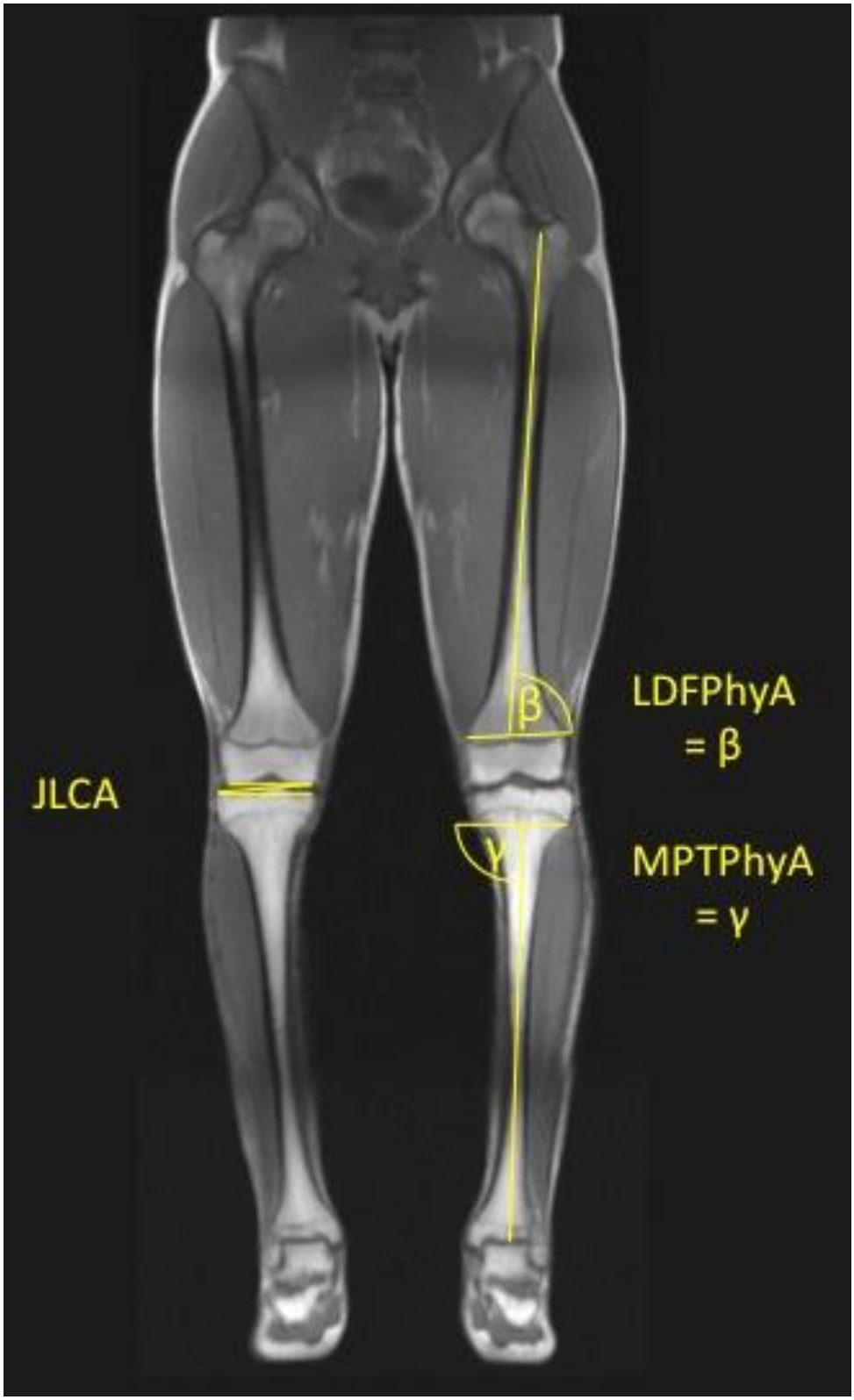
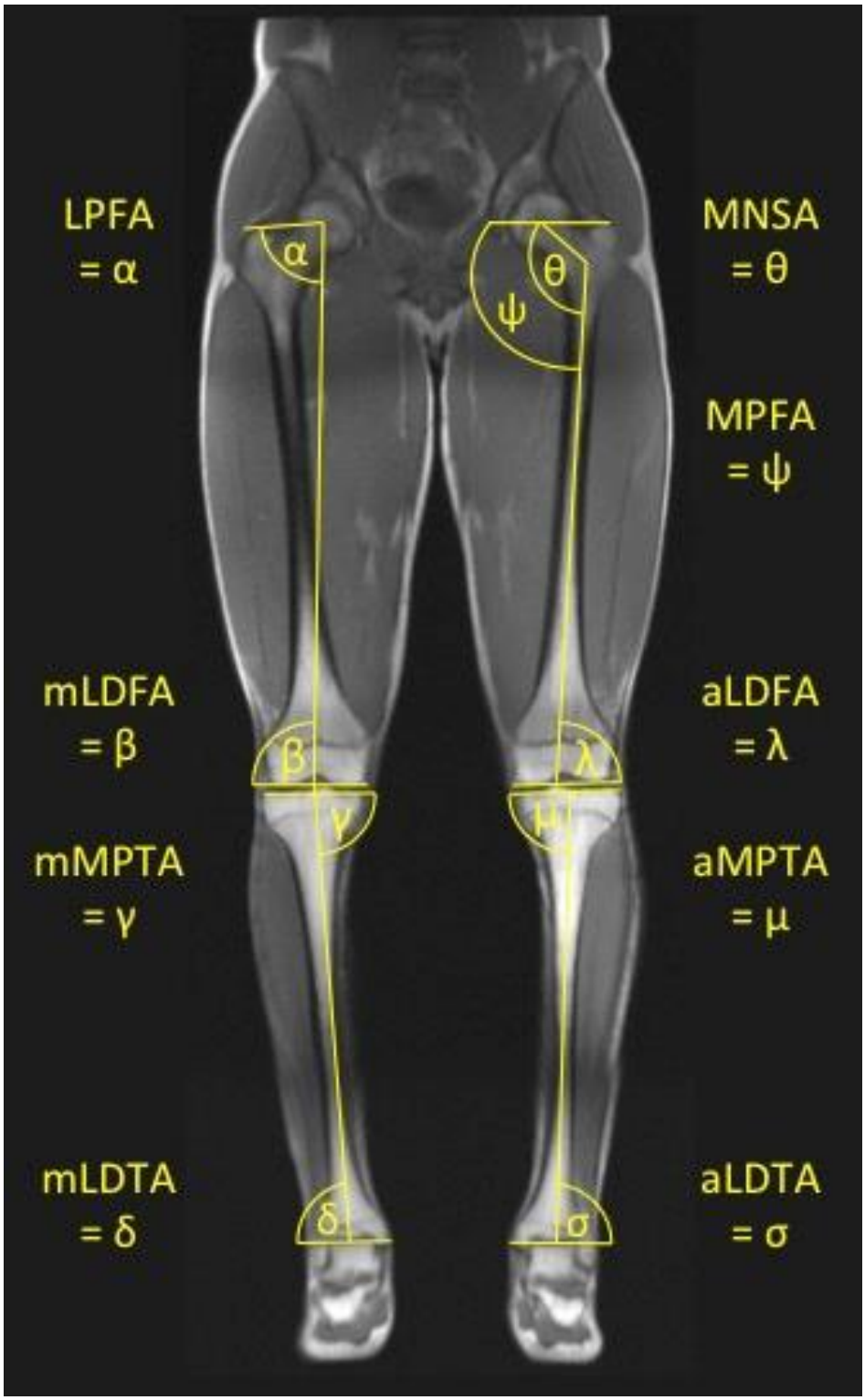


Figure 5-4 - Full leg length weight bearing MRI of a 16 year old male showing Mean Neck Shaft Angle (MNSA), Medial Proximal Femoral Angle (MPFA), Lateral Proximal Femoral Angle (LPFA), Mechanical Lateral Distal Femoral Angle (mLDFA), Anatomical Lateral Distal Femoral Angle (aLDFA), Mechanical Medial Proximal Tibial Angle (mMPTA), Anatomical Medial Proximal Tibial Angle (aMPTA), Mechanical Lateral Distal Tibial Angle (mLDTA), and Anatomical Lateral Distal Tibial Angle (aLDTA) measures.



5.4.6 Statistical Analysis

See chapter 2 for in depth details of statistical analysis. Inverse probability weighting with regression adjustment modelling[286] was adopted to assess variables that predict outcome variables. Multivariate linear regression modeling was used to evaluate the relationship between variables.

Receiver Operating Characteristic (ROC) analysis was performed on individual variables with a binary outcome of Hip Knee Angle less than -3 degrees[143,274] at follow-up in individuals with an open physis at baseline. Baseline measures chosen for investigation of capability of predicting varus leg alignment were PAQ score. PAQ score was chosen for investigation as high activity levels during youth are a recognised risk factor for varus leg alignment[135,139,143,148,153,171]. No clinically relevant imaging measures were available at baseline for predication of leg alignment.

5.5 Results

5.5.1 Participant demographics

126 individuals (252 legs) (mean age 185 months, SD 32 months) completed leg length MRI scans. The cohort comprised 58 elite male footballers (mean age 178 months (SD 29 months)), 34 male controls (mean age 185 months (SD 32 months)), and 34 female controls (mean age 197 months (SD 35 months)). (Table 5-1)

Table 5-1 - Cohort demographics

		Male Footballers (Hips)	Male Controls (Hips)	Female Controls (Hips)
Age (Years)	**11-12**	12 (24)	6 (12)	6 (12)
	13-14	23 (46)	11 (22)	7 (14)
	15-16	12 (24)	7 (14)	5 (10)
	17-18	5 (10)	7 (14)	8 (16)
	Over 18	6 (12)	3 (6)	8 (16)
Total		58 (116)	34 (68)	34 (68)

5.5.2 Change in Leg Alignment with Age

5.5.2.1 Chronological Age

This study found that leg alignment becomes more varus with age (Table 5-2) (Figure 5-5). A significant decrease in HKA was present in all individuals from 11 years of age, with no significant change in HKA after 16 years of age. Mean leg alignment values for each age group were valgus up to 14 years of age and became varus from 15 years. (Table 5-3)

Male footballers showed a clear decrease in HKA with age, with the greatest change occurring between 13 and 16 years, and no significant change in leg alignment after 16 years of age. Mean leg alignment values for male footballers were valgus up to 14 years of age, becoming varus from 15 years. (Table 5-4) (Figure 5-6 and Figure

Table 5-2 - Hip Knee Angle, Weight Bearing Ratio, and Medial Proximal Tibial Physeal Angle by Cohort and Age Group.

	All Individuals Mean (±SD)	Male Footballers Mean (±SD)	Male Controls Mean (±SD)	Female Controls Mean (±SD)
Hip Knee Angle				
11-12	1.185 (±1.745)	0.857 (±1.538)	0.429 (±1.775)	2.599 (±1.369)
13-14	1.107 (±2.096)	0.968 (±2.400)	1.533 (±1.436)	0.892 (±1.917)
15-16	-0.298 (±2.627)	-1.543 (±2.704)	-0.104 (±1.456)	2.418 (±1.378)
17-18	-0.292 (±2.016)	-2.485 (±1.392)	-0.559 (±1.291)	1.312 (±1.394)
Over 18	-0.541 (±2.014)	-2.768 (±0.584)	0.199 (±0.763)	0.852 (±1.489)
Average	0.383 (±2.254)	-0.306 (±2.590)	0.453 (±1.616)	1.507 (±1.654)
Weight Bearing Ratio				
11-12	0.482 (±0.081)	0.467 (±0.070)	0.446 (±0.075)	0.549 (±0.072)
13-14	0.483 (±0.118)	0.476 (±0.136)	0.507 (±0.074)	0.470 (±0.110)
15-16	0.419 (±0.120)	0.369 (±0.123)	0.428 (±0.073)	0.528 (±0.095)
17-18	0.423 (±0.130)	0.296 (±0.074)	0.431 (±0.139)	0.495 (±0.086)
Over 18	0.418 (±0.091)	0.378 (±0.103)	0.430 (±0.086)	0.444 (±0.077)
Average	0.451 (±0.115)	0.424 (±0.128)	0.458 (±0.096)	0.492 (±0.094)
Medial Proximal Tibial Physeal Angle				
11-12	92.564 (±2.867)	90.919 (±2.128)	92.851 (±1.936)	95.567 (±2.465)
13-14	93.188 (±2.902)	92.907 (±2.734)	92.720 (±2.252)	94.845 (±3.846)
15-16	92.006 (±3.491)	90.414 (±2.584)	93.065 (±2.801)	95.899 (±3.846)
17-18	91.729 (±3.793)	89.193 (±3.373)	92.281 (±3.272)	93.713 (±3.522)
Over 18	90.743 (±3.146)	88.573 (±2.841)	92.927 (±1.816)	91.639 (±2.859)
Average	92.173(±3.319)	91.111 (±3.146)	97.771 (±2.412)	94.201 (±3.603)

Figure 5-5 - Hip Knee Angle (HKA) with Age for All Individuals. Age groups based on chronological age of participants at time of MRI scan. Box and whisker plot

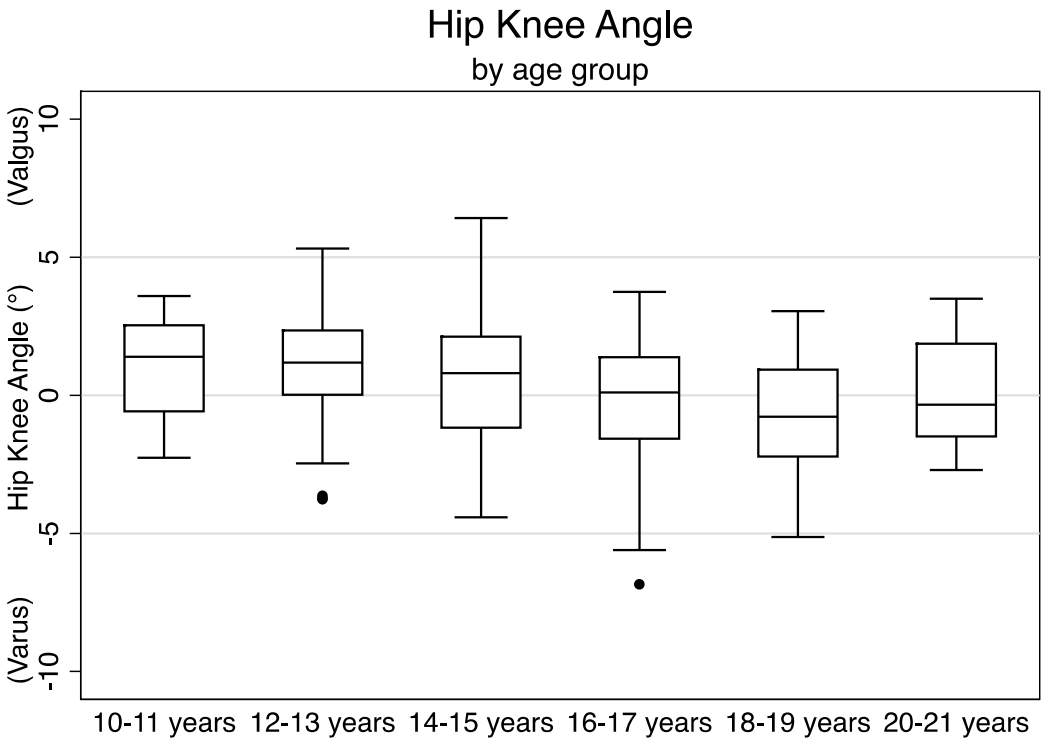


Table 5-3 - Predictors of change in Hip Knee Angle. *Age and cohort as covariables. **Age, gender and activity level as covariables. ***Physeal maturity, gender, and activity levels as covariables

		Hips	Mean HKA (±SD)	Univariate regression			Multivariate regression 1*			Multivariate regression 2**			Multivariate regression 3***		
				Coefficient	95% CI	P value	Coefficient	95% CI	P value	Coefficient	95% CI	P value	Coefficient	95% CI	P value
Age at baseline	**Months (continuous)**	252					-0.031	-0.036 to -0.026	<0.001	-0.032	-1.938 to -1.229	<0.001			
	11-12 years	48	1.185 (± 1.745)	1.726	0.900 to 2.553	<0.001									
	13-14 years	82	1.107 (±2.096)	1.648	0.843 to 2.452	<0.001									
	15-16 years	48	-0.298 (±2.627)	0.243	-0.749 to 1.236	0.631									
	17-18 years	40	-0.292 (±2.016)	0.249	-0.660 to 1.157	0.592									
	Over 18 years	34	-0.541 (±2.014)	-	-	-									
Physis	**Open**	136	0.816 (±2.090)	-0.884	-1.431 to -0.336	0.002							-	-	-
	Closed	116	-0.067 (±2.322)	-	-	-							-1.365	-1.949 to -0.781	<0.001
Gender	**Male**	186	-0.029 (±2.307)	-2.047 to 1.024	-1.906 to -1.166	<0.001				-1.475	-2.054 to -0.896	<0.001	-1.676	-2.439 to -0.914	<0.001
	Female	68	1.507 (±1.654)	-	-	-				-	-	-	-	-	-
BMI		252	-	-0.041	-0.071 to -0.011	0.036									
Dominant leg	**Dominant**	139	0.580 (±2.100)	0.436	-0.996 to 0.124	0.127									
	Non Dominant	115	0.144 (±2.415)	-	-	-									
Cohort	**Footballers**	118	-0.306 (±2.590)	-0.759	-1.360 to -0.157	0.013	-0.867	-1.436 to -0.300	0.003						
	Male controls	68	0.453 (±1.616)	-	-	-	-	-	-						
	Female controls	68	1.507 (±1.654)	1.054	0.509 to 1.600	<0.001	1.155	0.568 to 1.743	<0.001						
PAQ	**Linear**	252								-0.744	-0.973 to -0.515	<0.001	-0.762	-1.122 to -0.401	<0.001
	< 2	62	1.076 (±1.621)	-	-	-									
	2-3	68	-0.323 (±2.325)	-1.399	-2.112 to -0.687	<0.001									
	3-4	92	0.611 (±2.413)	-0.465	-0.530 to -0.400	<0.001									
	4-5	30	0.075 (±2.160)	-1.001	-1.026 to -0.976	<0.001									

Table 5-4 - Hip Knee Angle with Age by Cohort. Univariate Regression.

		Mean (±SD)	Univariate Regression		
			Coefficient	95% CI	P value
Male Footballers					
Age (Years)	**11-12 years**	0.857 (±1.538)	3.265	2.944 to 4.305	<0.001
	13-14 years	0.968 (±2.400)	3.736	2.980 to 4.491	<0.001
	15-16 years	-1.543 (±2.704)	1.226	0.120 to 2.331	0.030
	17-18 years	-2.485 (±1.392)	0.283	-0.595 to 1.161	0.527
	Over 18 years	-2.786 (±0.584)	-	-	-
Male Controls					
Age (Years)	**11-12 years**	0.429 (±1.775)	0.231	-0.880 to 1.342	0.687
	13-14 years	1.533 (±1.436)	1.335	0.526 to 2.144	0.001
	15-16 years	-0.104 (±1.456)	-0.330	-1.225 to 0.619	0.520
	17-18 years	-0.559 (±1.291)	-0.758	-1.615 to 0.099	0.083
	Over 18 years	0.199 (±0.763)	-	-	-
Female Controls					
Age (Years)	**11-12 years**	2.599 (±1.369)	1.747	0.723 to 2.771	0.001
	13-14 years	0.892 (±1.917)	0.040	-1.158 to 1.238	0.947
	15-16 years	2.418 (±1.378)	1.566	0.491 to 2.641	0.004
	17-18 years	1.312 (±1.394)	0.460	-0.508 to 1.428	0.352
	Over 18 years	0.852 (±1.489)	-	-	-

Figure 5-6 - Hip Knee Angle (HKA) with age for elite footballers, male controls, and female controls. Polynomial regression fit with 95% CI.

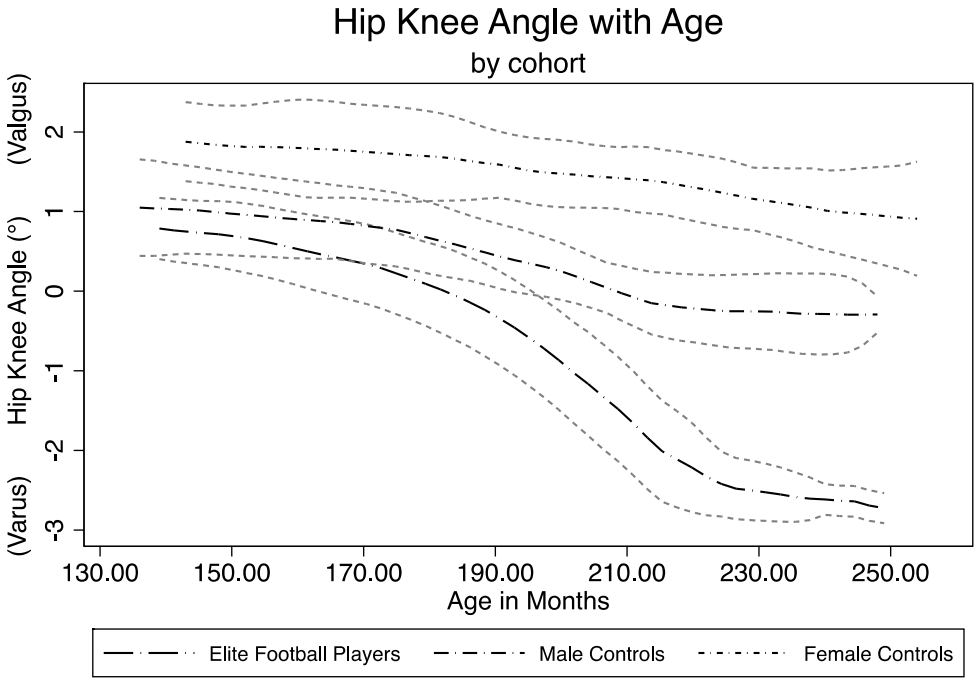
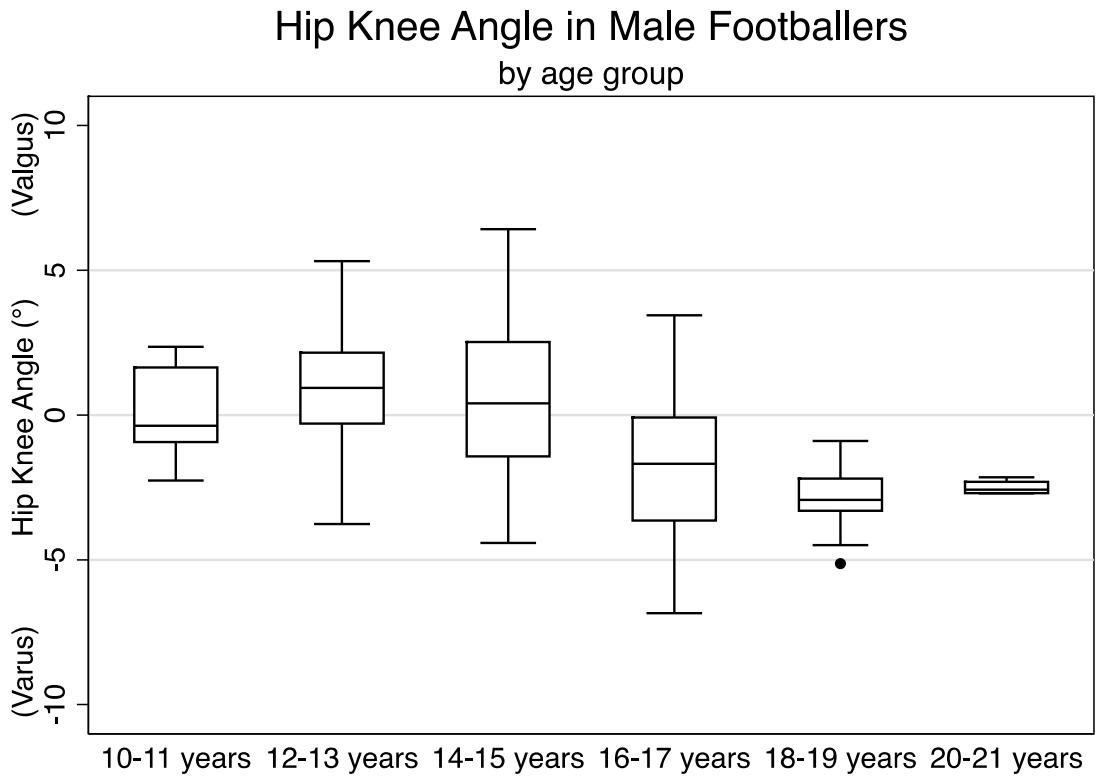


Figure 5-7 - Hip Knee Angle (HKA) with Age for Male Footballers. Age groups based on chronological age of participants at time of MRI scan. Box and whisker plot

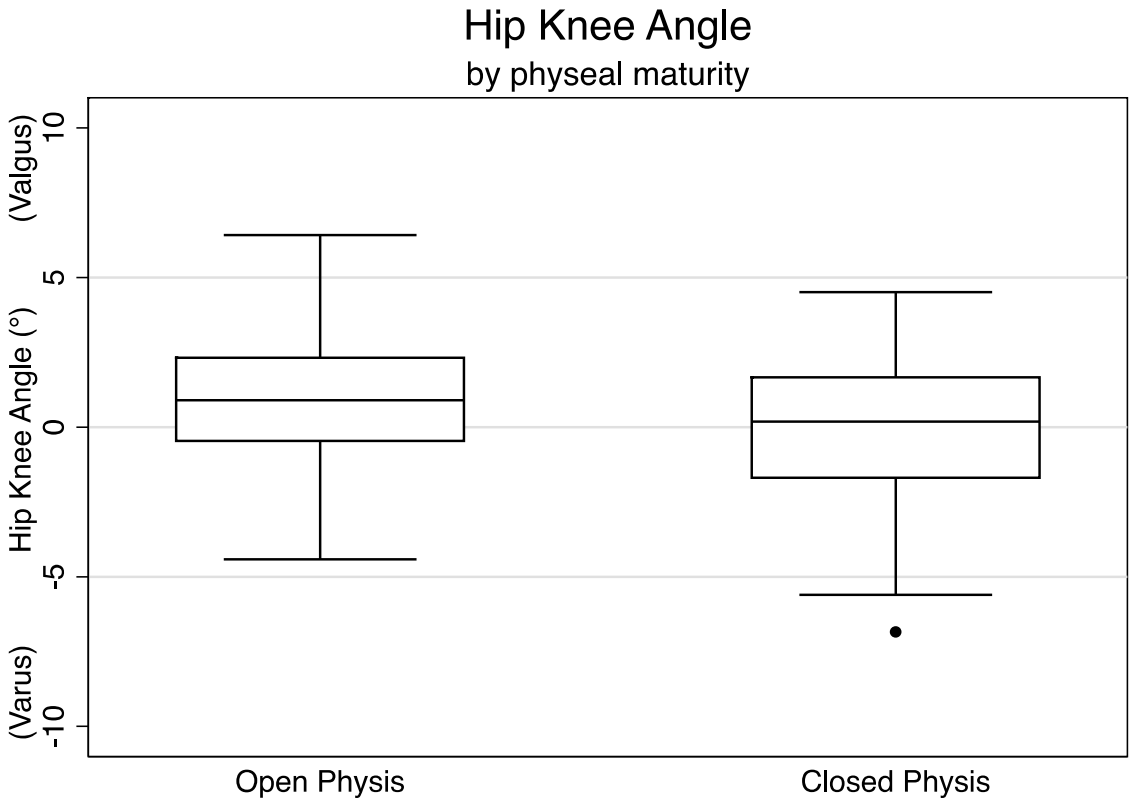


Male controls had a decrease in HKA with age, changing from valgus to varus alignment after 14 years of age. Female controls also showed a general decrease in HKA with age, however the pattern was less clear. Female controls remained in valgus alignment throughout all age groups. (Table 5-4)

5.5.2.2 Skeletal Maturity

Individuals with an open physis had valgus leg alignment and individuals with a closed physis had varus leg alignment. Adjusting for activity level and gender, individuals with a closed physis had a HKA 1.37 degrees less than individuals with an open physis ($p<0.001$). (Table 5-3) (Figure 5-8)

Figure 5-8 - Hip Knee Angle by Physeal Maturity. Box and whisker plot



5.5.3 Risk Factors for Varus Leg Alignment

Elite level football players had significantly more varus leg alignment than controls. Adjusting for age, elite male footballers had a HKA 0.87 degrees less than male controls ($p<0.001$) and 2.22 degrees less than female controls ($p<0.001$) (Table 5-3) (Figure 5-9). In skeletally mature individuals mean HKA for elite male footballers was -2.38 degrees (SD 2.01, range -6.85 to 3.44), for male controls was -0.97 degrees (SD 1.23, range -2.59 to 1.96), and for female controls was 1.35 degrees (SD 1.68, range -2.66 to 4.51). Elite male footballers had a HKA 2.28 degrees less than male controls ($p<0.001$) and 3.73 degrees less than female controls ($p<0.001$). (Figure 5-10).

Figure 5-9 - Hip Knee Angle by Cohort. Box and whisker plot.

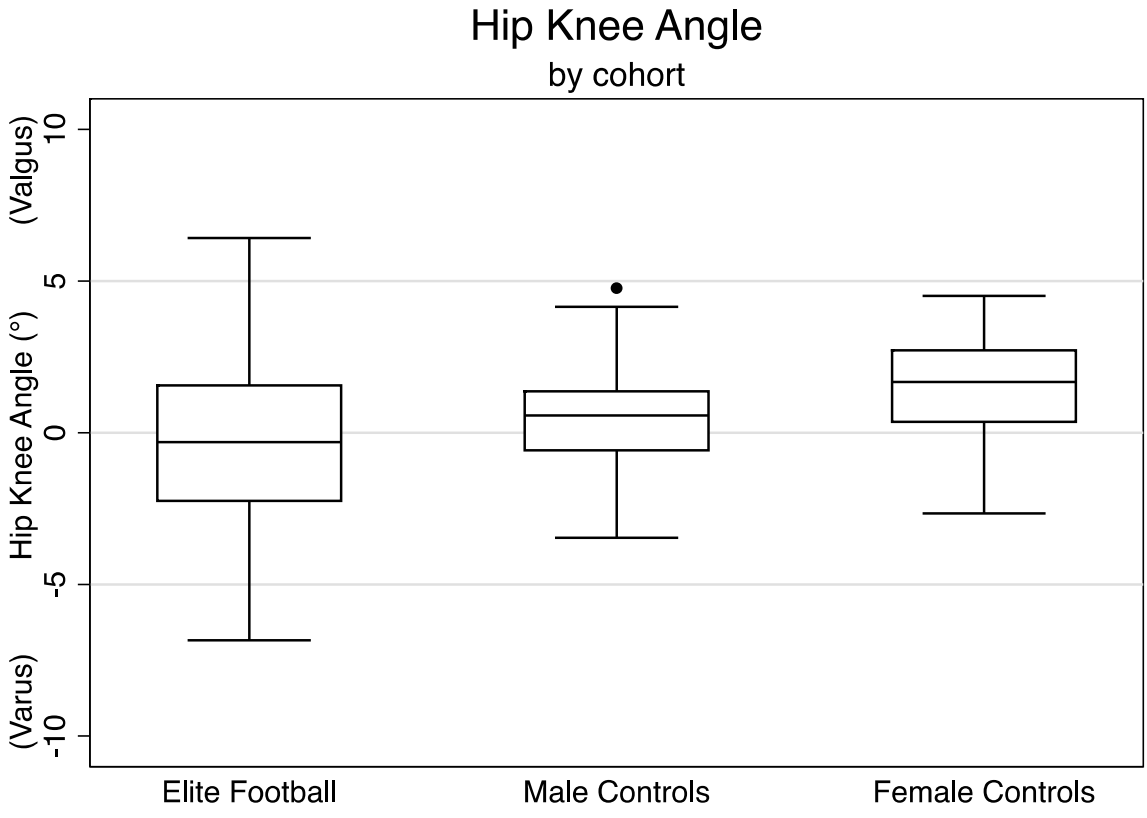
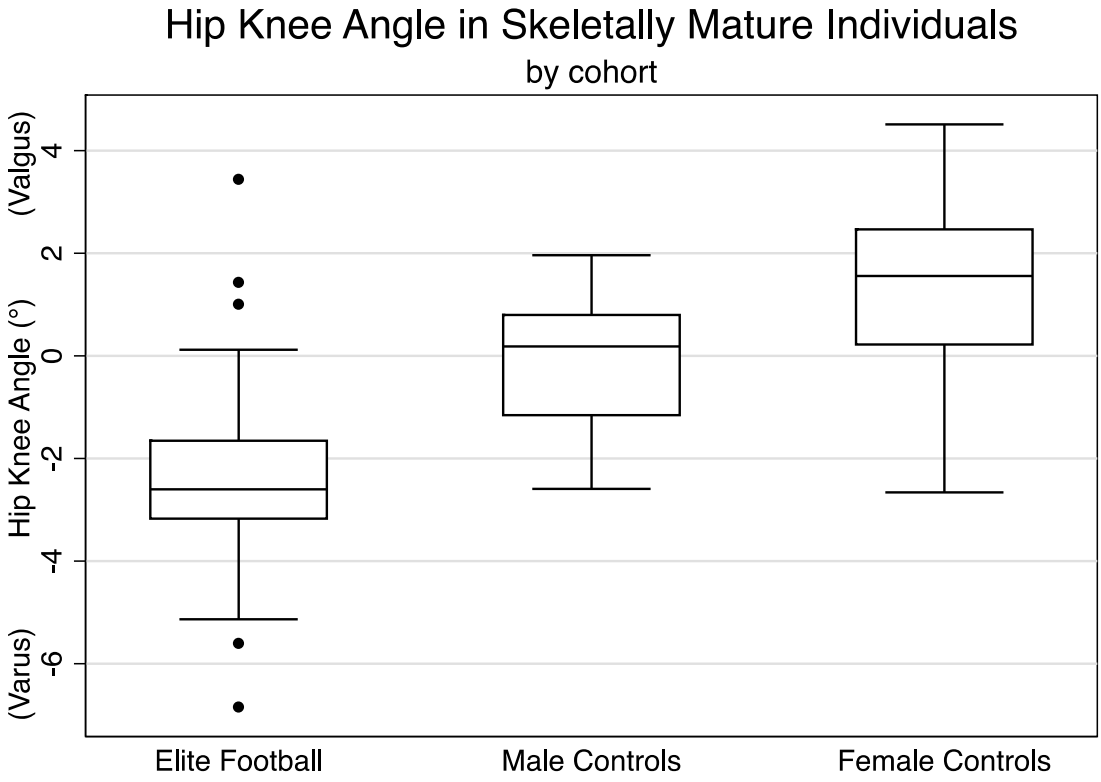


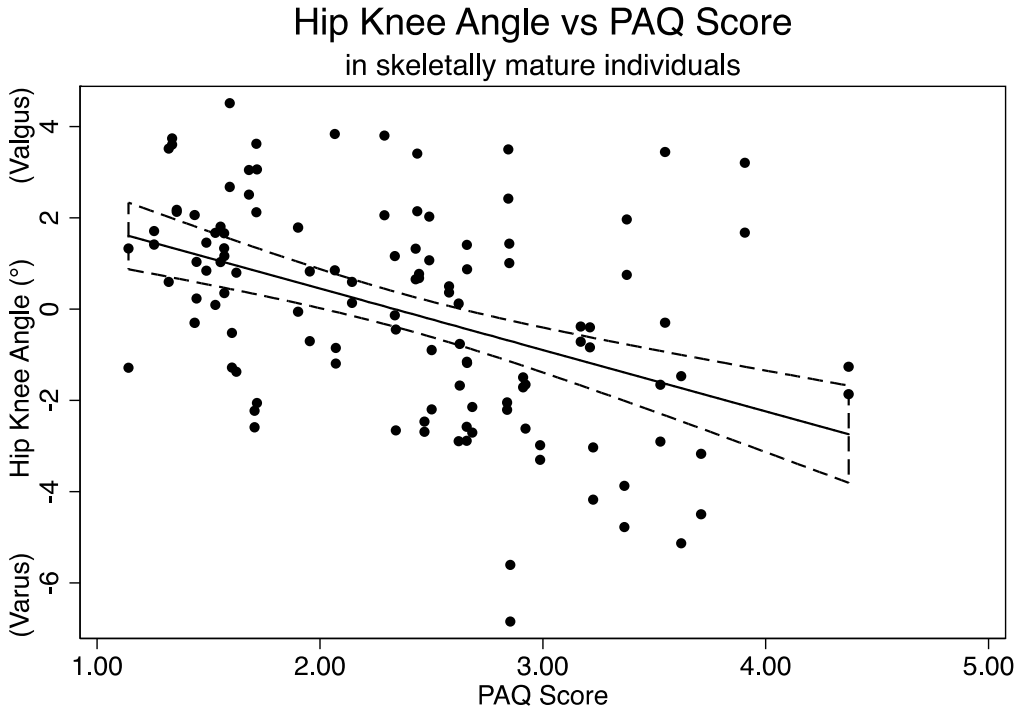
Figure 5-10 - Hip Knee Angle in Skeletally Mature Individuals by Cohort. Box and whisker plot.



Males had significantly more varus leg alignment than females. Adjusting for age and activity level, males had a HKA 1.48 degrees less than females ($p<0.001$) (Table 5-3). Adjusting for age and activity levels, skeletally mature males had a HKA 2.05 degrees less than females ($p<0.001$).

Individuals with high activity levels (PAQ score) had significantly more varus leg alignment than individuals with low activity levels. Adjusting for age and gender in a multivariate linear regression model there was a significant negative linear relationship between PAQ score and HKA (coefficient -0.24, $p=0.029$). Adjusting for gender in skeletally mature individuals there was a significant negative linear relationship between PAQ score and HKA (coefficient -0.54, $p=0.028$).

Figure 5-11 - Hip Knee Angle Versus PAQ score in Skeletaly Mature Individuals. Linear regression fit with 95% CI



Adjusting for age and gender individuals with a PAQ score between 2 and 3, between 3 and 4, and between 4 and 5 had HKA 1.40 degrees ($p < 0.001$), 0.47 degrees ($p<0.001$), and 1.03 degrees ($P < 0.001$) less than individuals with a PAQ less than 2 respectively.

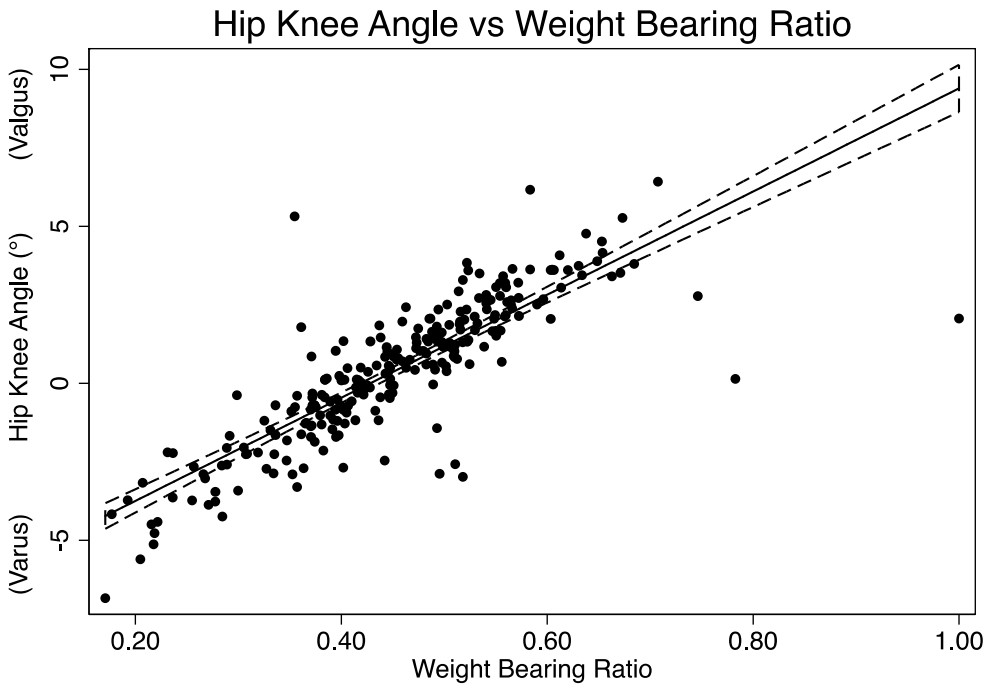
Significant association was seen between BMI and HKA in univariate but not multivariate regression analysis. There was no significant association between leg dominance and HKA. (Table 5-3)

5.5.4 Anatomical Associations with Varus Leg Alignment

In this study individuals with a high alpha angle had more varus leg alignment. A negative linear relationship existed between average alpha angle and HKA (coefficient -0.75, p = 0.003). (Table 5-5)

Individuals with more varus leg alignment had a lower Weight Bearing Ratio. A positive linear relationship existed between Weight Bearing Ratio and HKA (coefficient 0.04, p=0.015) (Figure 5-12) (Table 5-5). Elite level football players had significantly lower WBR than controls. Adjusting for age elite male footballers had a WBR 0.042 lower than male controls (p=0.010) and 0.083 lower than female controls (p<0.001). There was no significant association between Weight Bearing Ratio and PAQ score.

Figure 5-12 - Hip Knee Angle versus Weight Bearing Ratio. Linear regression fit with 95% CI



A positive linear relationship existed between between Anatomical Medial Proximal Tibial Angle (aMPTA) and HKA (coefficient 0.31, p=0.017), Anatomical Lateral Distal Tibial Angle (aLDTA) and HKA (coefficient 0.07, p=0.018), and Mechanical Lateral Distal Femoral Angle (mLDFA) and HKA (coefficient 0.21, p=0.020). There was no significant association between HKA and Mean Neck Shaft Angle (MNSA), Lateral Proximal Femoral Angle (LPFA), Medial Proximal Femoral Angle (MPFA), Anatomical Lateral Distal Femoral Angle (aLDFA), Joint Line Congruence Angle (JLCA), Medial Mechanical Proximal Tibial Angle (mMPTA), Mechanical Lateral Distal Tibial Angle (mLDTA), or Leg length discrepancy. (Table 5-5)

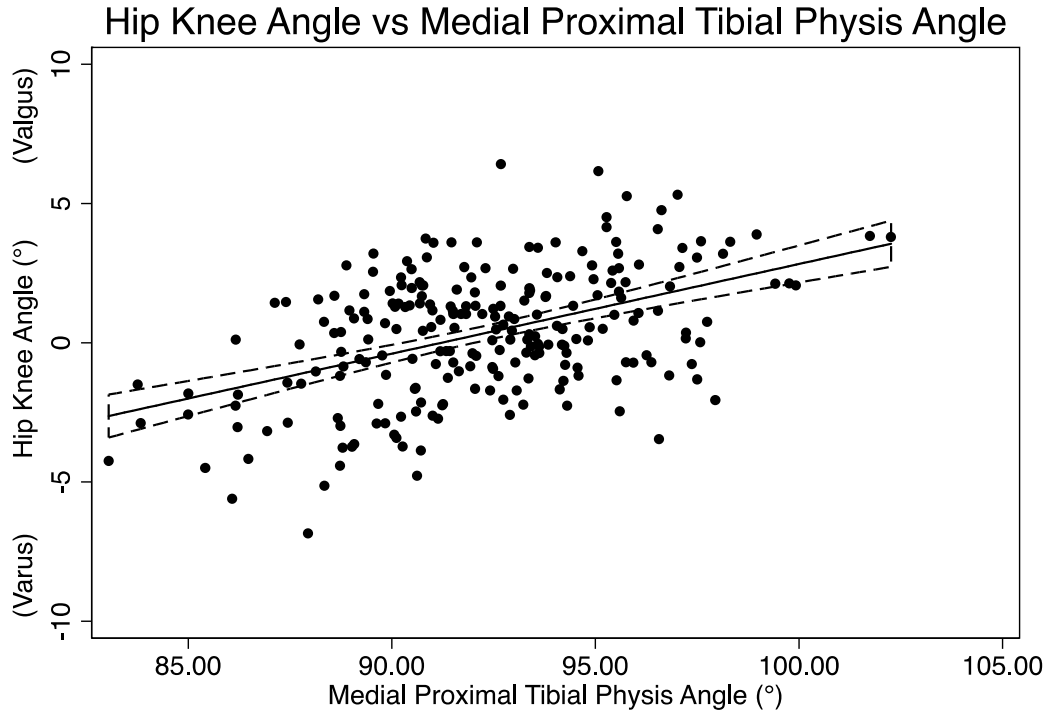
Table 5-5 - Hip Knee Angle Regression Analysis with Measures of Leg Alignment. Multivariate regression adjusting for age, gender and activity level.

Measure	Mean (±SD)	Linear regression		
		Coefficient	95% CI	P value
Average Alpha Angle	60.597 (±9.620)	-0.750	-0.80 to -0.70	0.003
Weight-Bearing-Ratio (WBR)	0.451 (±0.115)	0.042	0.030 to 0.055	0.015
Medial Proximal Tibial Physis Angle (MPTPhyA)	92.273 (±3.319)	0.322	0.270 to 0.375	0.008
Anatomical Medial Proximal Tibial Angle (aMPTA)	88.135 (±3.852)	0.312	0.205 to 0.419	0.017
Anatomical Lateral Distal Tibial Angle (aLDTA)	90.248 (±3.844)	0.066	0.042 to 0.090	0.018
Mechanical Lateral Distal Femoral Angle (mLDFA))	88.330 (±2.730)	0.210	0.127 to 0.293	0.020
Lateral Distal Femoral Physis Angle (LDFPhyA)	84.953 (±3.871)	-0.060	-0.947 to 0.827	0.550
Joint Line Congruence Angle (JLCA)	3.632 (±1.133)	-0.058	-0.582 to 0.467	0.396
Mean Neck Shaft Angle (MNSA)	131.413 (±9.141)	-0.008	-0.017 to 0.001	0.055
Medial Proximal Femoral Angle (MPFA)	85.311 (±4.763)	-0.025	-0.643 to 0.594	0.703
Lateral Proximal Femoral Angle (LPFA)	88.650 (±4.545)	-0.067	-0.525 to 0.390	0.312
Anatomical Lateral Distal Femoral Angle (aLDFA)	82.478 (±3.277)	-0.087	-0.517 to 0.344	0.238
Mechanical Medial Proximal Tibial Angle (mMPTA)	88.063 (±2.933)	0.216	-0.145 to 0.578	0.083
Mechanical Lateral Distal Tibial Angle (mLDTA)	90.235 (±3.669)	-0.134	-0.435 to 0.166	0.111
Leg Length Discrepancy	2.10×10^{-17} (0.728)	-0.352	-7.264 to 6.559	0.634

5.5.5 Mechanism of Varus Knee Morphology Formation

Mean average Medial Proximal Tibial Physis Angle (MPTPhyA) was 92.27 degrees (SD 3.32 degrees). In this study individuals with a lower MPTPhyA had more varus leg alignment. A positive linear relationship existed between MPTPhyA and HKA (coefficient 0.32, p = 0.008) (Table 5-5) (Figure 5-13). Elite level football players had significantly lower MPTPhyA values than controls. Adjusting for age, elite male footballers had MPTPhyA 1.85 degrees lower than male controls (p<0.001) and 3.51 degrees lower than female controls (p<0.001). Individuals with high activity levels (PAQ score) had a significantly lower MPTPhyA than individuals with low activity levels. There was a negative linear relationship between PAQ score and MPTPhyA (coefficient -0.05, p=0.025).

Figure 5-13 - Hip Knee Angle versus Medial Proximal Tibial Physis Angle. Linear regression fit with 95% CI



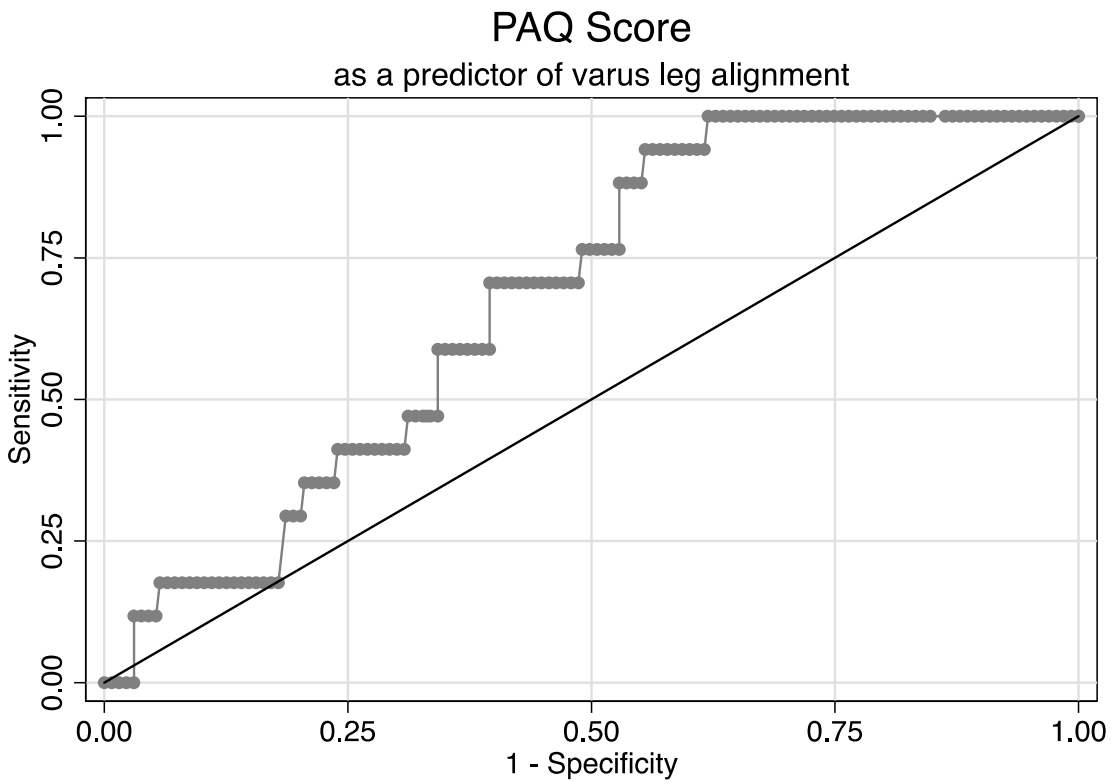
5.5.6 Predicting Varus Leg Alignment

18 hips showed evidence of varus leg alignment (HKA less than -3 degrees[143,274]) at follow-up. Baseline PAQ score showed some capability for predicting varus leg alignment at 3 years. The ROC AUC for PAQ score was 0.69 (95% CI: 0.590 to 0.783). (Table 5-6) (Figure 5-14)

Table 5-6 - ROC Area and Cut Off Values for Varus Leg Alignment Development; PAQ Score

	AUC	95% CI	Cut Off	Sensitivity	Specificity	Correctly classified
Baseline PAQ Score	0.687	0.590 to 0.783	>3.62	41.18%	76.05%	73.93%

Figure 5-14 - ROC Curve for PAQ Score as a Predictor of Varus Leg Alignment (AUC 0.69)



5.6 Discussion

The aim of this study was to investigate the development of leg alignment with age and to characterise the risk factors for varus leg alignment. Identifying individuals at risk of varus alignment may allow the development of preventative strategies. This study demonstrates that males undertaking intense exercise between the ages of 11 and 16 years are at greatest risk of developing varus leg alignment, which may be secondary to changes at the medial proximal tibial physis.

5.6.1 Change in Leg Alignment with Age

Studies have demonstrated that leg alignment progresses from varus alignment in the infant to valgus alignment in early childhood then back towards varus alignment in adolescence[136-138]. However, changes in leg alignment during adolescence have not been well characterised due to limited imaging studies.

Our results demonstrate that leg alignment moves from valgus towards varus during adolescence. In this study a decrease in HKA was present in all individuals from 11 years of age. The greatest move towards varus alignment occurred between the ages of 14 and 15 years, with no significant decrease in HKA occurring after 16 years in male footballers and female controls, and 14 years in male controls.

These findings agree with previous reports, and the change from valgus to varus alignment in males at 14-15 years corresponds to clinical examination findings from previous studies[135,148]. However, our results would suggest that leg alignment stops evolving after 16 years of age. This disagrees with the clinical findings of Thijs et al[135] who suggested the intermalleolar distance increased up until 18 years of age. However, the cohort used by Thijs et al consisted of entirely caucasian males, none of whom practiced football. The comparative diversity in ethnicity, gender, and sports practice in the cohort used in this study may account for some of the differences in our findings compared to those by Thijs et al.

Leg alignment is believed to develop during adolescence as the distal femoral physis and proximal tibial physis mature[135]. In this study individuals with an open physis had valgus leg alignment and individuals with a closed physis had varus leg alignment. This furthers the argument that leg alignment changes take place in the immature skeleton, and agrees with previous reports that moving from valgus to varus alignment occurs towards the end of skeletal growth[136].

5.6.2 Risk Factors for Varus Leg Alignment

Our results demonstrate that activity level and gender play a significant role in the development of varus leg alignment. In skeletally mature individuals elite male footballers had a HKA 2.28 degrees less than male controls and 3.73 degrees less than

female controls. Higher PAQ scores were also significantly associated with more varus leg alignment.

While athletes have been shown to have more varus HKA values in adult cohorts[143,171], the effects of high activity on the HKA in adolescents was previously unknown. The degree of varus alignment in skeletally mature elite level footballers in this study compares favourably with elite football players from previous adult cohorts where HKA was -2.7 to -3.2 degrees[171]. Skeletaly mature control males in this study also had a very similar mean HKA compared to controls from previous cohorts where HKA was -0.9 degrees[171].

It is worth noting that although the differences in HKA between cohorts and age groups appear small they remain greater than the intra-observer and inter-observer smallest detectable difference, which were 0.83 degrees and 1.60 degrees respectively (Chapter 2). Moreover, these small values are likely to be clinically significant, as a leg alignment deviation of only 3 degrees from neutral is considered abnormal[143,274].

Males had significantly more varus leg alignment than females. Although males on average had higher PAQ scores, this was controlled for in the regression models. This finding is in agreement with reports from other cohorts where males showed greater clinical and imaging measures of varus alignment[143,151,171]. However, female controls in this study showed a mean valgus leg alignment, whereas a mean varus alignment has

previously been reported in female control cohorts[171]. Further research comparing male and female elite athlete cohorts is required to fully elucidate the role of gender in the development of leg alignment.

It has been previously suggested that the kicking movement might be partly responsible for the difference in HKA between elite football players and controls[139,148,153]. However, in our study there was no significant difference between the dominant and non-dominant legs of elite footballers or controls, which is in agreement with the findings of Colyn et al[171].

5.6.3 Effect of Femoral Morphology on Leg Alignment

In this study individuals with a high alpha angle had more varus leg alignment. Cam morphology is thought to develop around 11-14 years of age[52], which precedes the development of varus leg alignment as found in this study. This would suggest that the development of cam morphology might impact leg alignment development and predispose to varus morphology. This association between cam morphology and abnormal leg alignment has previously been identified in adult cohorts, where individuals with tibia vara were more likely to have cam morphology[133,134]**.** However, it is perhaps more likely that high activity levels affect both the proximal and distal femoral physis but at different stages of development, and the presence of cam morphology does not play an active role in the development of leg alignment. Further

study is required to elucidate the extent of the relationship between cam morphology and varus leg alignment to determine if the association is causal or not.

5.6.4 Mechanism of Varus Leg Alignment Development

Varus leg alignment was associated with lower MPTPhyA values in this study. The mechanism of development of varus leg alignment is not well understood, however a low medial proximal tibial angle has been associated with varus leg alignment in previous adult imaging studies[171]. The aetiology of genu varum is likely multifactorial but biomechanical overloading of the proximal medial tibial physis is likely to represent a key pathomechanism[156-158]. Besier et al[304] measured external loading of the knee joint during running and cutting manoeuvres. They reported that varus and valgus loads placed on the joint increased dramatically during cutting tasks compared with normal running. Cook et al[157] showed that mechanical overload of the physis leads to a progressive deformity. Varus alignment is likely to represent a potentially modifiable physiological adaptation to load. Indeed, it has been suggested that developmental genu varum may be beneficial for balance and stability during youth[170] and may therefore offer an advantage in adolescent elite footballers.

5.6.5 Predicting Varus Leg Alignment

This study suggests that in individuals with an open physis the PAQ score may be able to predict the development of varus leg alignment at three years follow-up. PAQ score can predict the development of varus leg alignment with a sensitivity of 41.18%, and

specificity of 76.05% where 73.93% of individuals are classified correctly. However, as the HKA was not measured at baseline this finding should be interpreted with care as the nature of the preceding leg alignment is unknown.

5.6.6 Limitations

The main limitation of this study is the relatively small sample size and cross-sectional design. However, the full leg length MRI sequence was only available at the follow-up time point. Further limitations apply to the measurement methodology of full leg length MRI scans, the use of which has not previously been validated. However, our measurement methodology showed high reproducibility (see chapter 2). Moreover, there is no agreed diagnostic threshold for varus leg alignment. The results in this study for the predictive capabilities of baseline variables should therefore be interpreted with care.

5.6.7 Conclusion

The development of varus leg alignment is greatest age 13 to 16 years. There is no significant change in leg alignment after 16 years of age. Physical activity during adolescence is strongly associated with the development of varus leg alignment in males. A lower MPTPhyA value is likely to represent physiological adaptation to load and be the mechanism by which varus leg alignment develops.

Chapter 6 Cartilage Composition in Adolescence and the Effects of Activity

6.1 Abstract

Introduction:

The development of cartilage composition during adolescence and the effect of exercise on cartilage composition remain largely unknown. Although cam morphology may be evident from early adolescence it is unknown when associated cartilage damage first occurs. The aim of this study was to investigate the development of cartilage composition with age, and determine the effects of activity and cam morphology on cartilage composition during adolescence.

Methods:

Cross sectional observational cohort study of individuals from football club academies and an age-matched control population, aged 9-18 years. Assessments included questionnaires, clinical examination, and T2 mapping of hips. Primary imaging outcome measures were T2 relaxation time of acetabular and femoral cartilage, and average alpha angle.

Results:

The cohort consisted of 109 elite male footballers, 49 male controls, and 51 female controls. Acetabular cartilage T2 values decreased with age in elite footballers. No clear pattern of change in acetabular cartilage T2 values was evident in male or female controls. No pattern of change in femoral cartilage T2 values with age was evident in any cohort. Individuals with a closed physis had an acetabular cartilage T2 value 7.86ms less than individuals with an open physis. No difference existed in femoral cartilage T2 values between individuals with an open and closed physis. Elite male footballers had an acetabular cartilage T2 value 4.85ms greater than male controls ($p<0.001$). No difference in femoral cartilage T2 value existed between elite footballers and male controls. A significant positive correlation existed between Physical Activity Questionnaire Score and acetabular cartilage T2 value (coefficient 1.072, $p<0.001$) and femoral cartilage T2 value (coefficient 0.660, $p=0.032$). Males had femoral cartilage T2 values 6.19ms greater than females ($p<0.001$). No difference in acetabular cartilage T2 values existed between males and females. No correlation existed between alpha angle and anterosuperior acetabular cartilage T2 value and no difference in T2 value existed between individuals with and without cam morphology.

Conclusions:

Acetabular cartilage T2 values decrease with age and are greater in high physical activity individuals during adolescence, suggesting significant changes to cartilage composition and architecture. Cam morphology is not associated with anterosuperior acetabular

cartilage damage during adolescence. Further longitudinal research is required to validate these findings.

6.2 Introduction

The effect of exercise on cartilage in weight bearing joints is poorly understood. Healthy cartilage requires compressive loading from physical activity to develop normally and maintain form and function[193]. However, excessive loading resulting from high-intensity or long-duration exercise can lead to cartilage damage[194]. Morphological MRI studies in adults have found no difference in cartilage thickness between athletes and controls[206,207]. However, the nature and extent of changes to cartilage composition induced by exercise, and whether these are protective or predispose to OA, remains unclear.

Hyaline articular cartilage consists of chondrocytes embedded in an extracellular matrix that is comprised mainly of collagen in the form of a rigid meshwork of triple-helical fibrils, proteoglycans with chains of glycosaminoglycans (GAGs), cations, and water molecules[172,173]. Animal studies have suggested that physical exercise increases the GAG content in weight-bearing cartilage[195-198]. In vitro, cyclic compression of cartilage simulating walking markedly stimulates GAG synthesis[202]. It has been shown that enzymatic GAG depletion of cartilage decreases its indentation stiffness[203], suggesting increased GAG levels are a functional means to withstand higher mechanical demands.

Compositional Magnetic Resonance imaging (MRI) techniques are increasingly used as non-invasive surrogate markers of cartilage composition clinically in identifying early OA[178] and in professional sport to identify athletes at risk of injury and in post-injury scenarios[190,191]. T2 mapping is one of the most widely used compositional sequences and is thought to be sensitive to the water and GAG content of cartilage and the integrity of

the collagen network[185-187]. Some compositional studies in adults have suggested that increases in activity levels result in increased GAG levels[209,211]. However, other studies in older healthy adults have suggested that raised activity levels result in disorientation of collagen fibres and low GAG levels[210].

The effect of exercise on developing cartilage composition in skeletally immature individuals is unknown. During growth chondrocytes are believed to develop different phenotypes by adapting to local functional requirements within the joint to produce GAG rich areas[204,205]. This would suggest that exercise during skeletal maturation might determine the cartilage composition of weight bearing joints.

Cam morphology results in reduced GAG in the acetabular cartilage of asymptomatic patients who go on to develop radiographic osteoarthritis[97]. It is unknown when these changes first occur. Cam morphology may be evident from 14 years of age[52], but cartilage volume loss visible on radiographs may not be present for a number of decades[91]. The length of time prior to radiographic changes that cam morphology starts to cause compositional change remains uncertain.

6.3 Aims

1) Investigate the changes in cartilage composition with age
2) Investigate the effect of activity on cartilage composition during adolescence
3) Investigate the effect of cam morphology on cartilage composition in adolescence

6.4 Methods

The methods for this study and justifications for imaging measures are discussed in chapter 2.

6.4.1 Study design

Cross sectional observational cohort study.

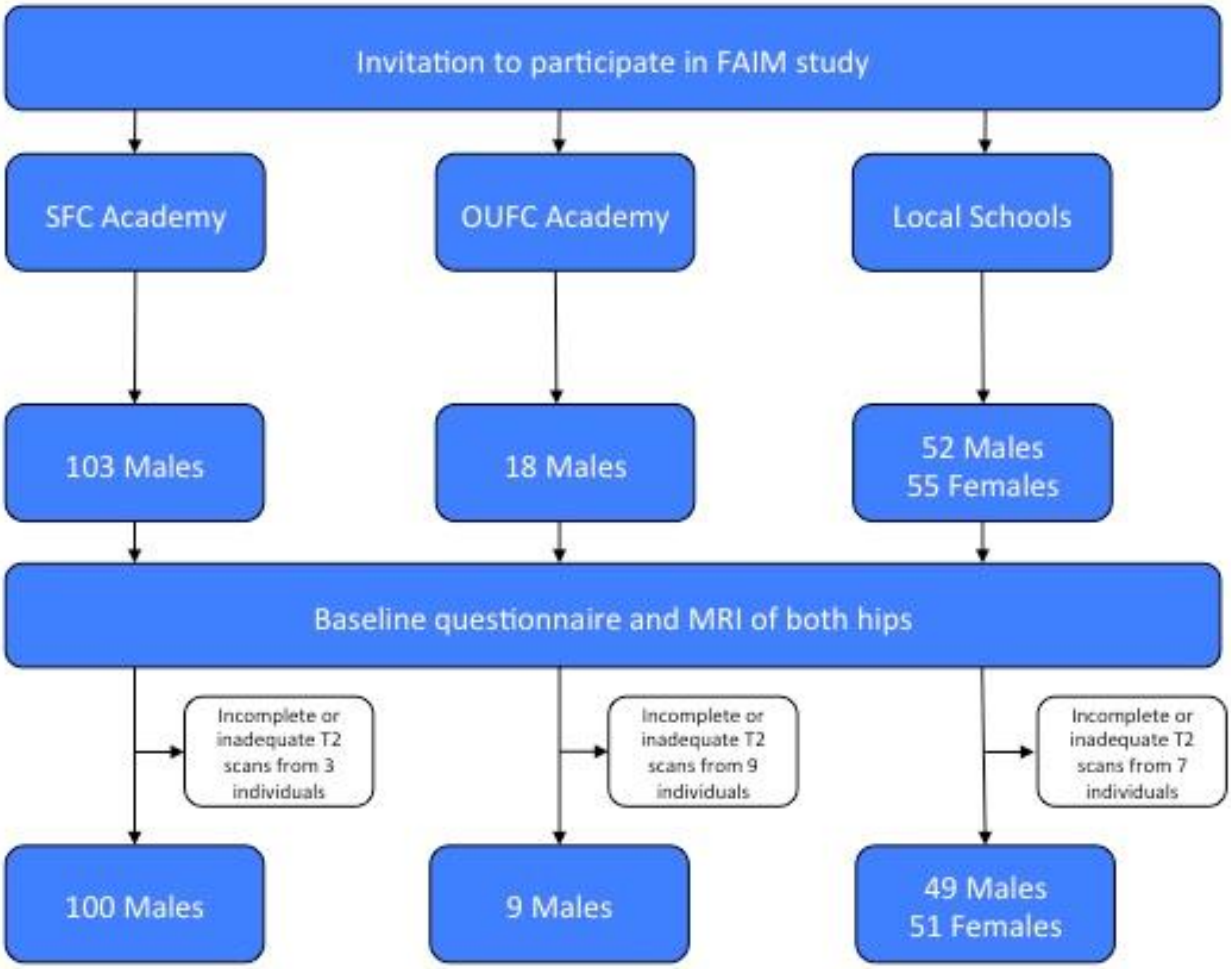
6.4.2 Population

Individuals aged 9–18 years were recruited from Southampton Football Club (SFC) Academy, Oxford United Football Club (OUFC) Academy, and local schools (controls) at baseline. Study IDs were generated for each participant such that assessors were blinded to participant characteristics such as cohort and age when interpreting data such as MRI scans (see chapter 2). All individuals underwent T2 scanning at baseline. T2 MRI sequence outcomes were inadequate or incomplete in 19 individuals due to movement artefact. (Figure 6-1)

6.4.3 Activity Levels

Activity was evaluated using two methods: i) SFC and OUFC Academy (elite footballer cohort) versus general population controls; ii) Physical Activity Questionnaire (PAQ) for older children (aged 9–13 years) and adolescents (aged 14–18 years)[224].

Figure 6-1 - Recruitment flowchart for study.



6.4.4 Imaging Protocol

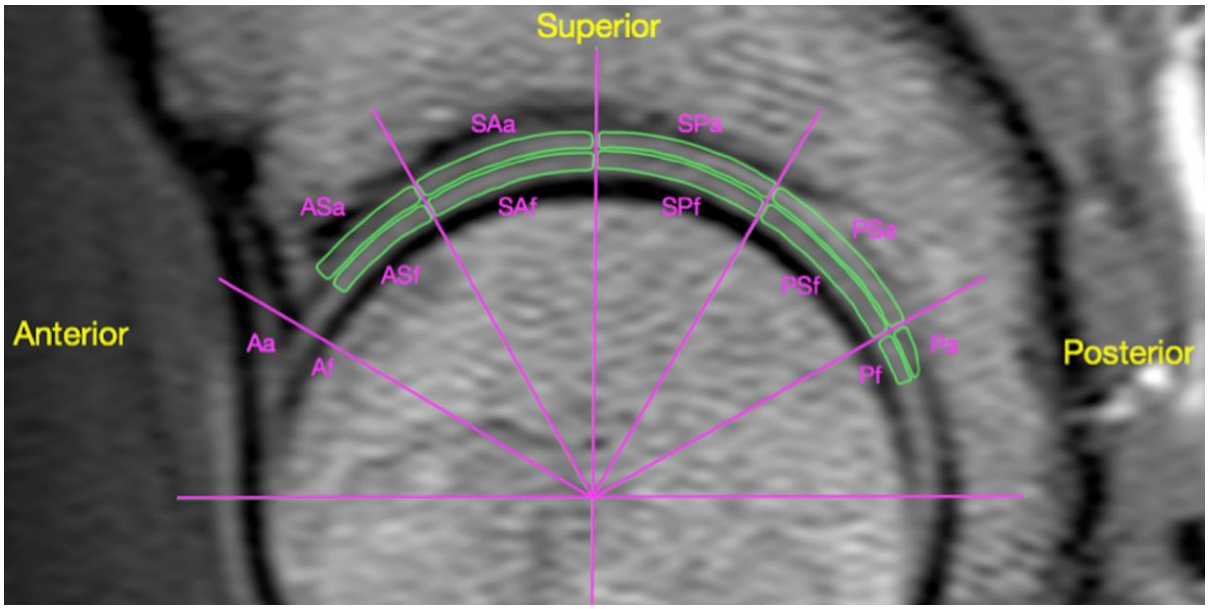
Cartilage composition and hip morphology were assessed with MRI of both hips using a 3 Tesla Philips Achieva platform and torso coil (Philips Healthcare). T2 mapping was used to image hip cartilage composition. T2 mapping sequences were acquired in true sagittal plane, with the first slice referenced off the medial border of the femoral head with the remaining slices extending laterally, at the end of scanning protocols to avoid the effects of cartilage loading[284]. Three-dimensional (3D) water selective fluid (WATSf) sequence was used to image femoral head morphology. Radial images were acquired around the axis of the femoral neck at 30 degree intervals. The coronal axis (12 o'clock position) was positioned parallel to the axis of the proximal femur diaphysis[52]

6.4.5 Imaging Measures

T2 mapping values were quantified using manual segmentation performed with OsiriX Software (V.6.0.2, Pixmeo). MRI datasets were incomplete in 19 individuals due to movement artifact. Regions of Interest (ROI) were developed based on a clockface around the centre of the femoral head at 30 degree intervals. Regions were referenced from the 12 o'clock position that passes through the centre of the femoral head parallel to the axis of the proximal femur diaphysis. The 3 o'clock boundary was positioned perpendicular to this line and represented an anterior position for both hips. Femoral and acetabular cartilage were segmented separately and ROIs were not extended beyond where there was adjacent femoral and acetabular cartilage, hence did not include the chondrolabral junction (Figure 6-2).

Figure 6-2 - Regions of Interest (ROI) for T2 Segmentation.

Anterior Acetabular Cartilage (Aa), AnteroSuperior Acetabular Cartilage (ASa), SuperoAnterior Acetabular Cartilage (SAa), SuperoPosterior Acetabular Cartilage (Spa), PosteroSuperior Acetabular Cartilage (PSa), Posterior Acetabular Cartilage (Pa), Anterior Femoral Cartilage (Af), AnteroSuperior Femoral Cartilage (ASf), SuperoAnterior Femoral Cartilage (SAf), SuperoPosterior Femoral Cartilage (SPf), PosteroSuperior Femoral Cartilage (PSf), Posterior Femoral Cartilage (Pf)



Each scan gave approximately 15 sagittal slices through the hip. The number of slices per hip from which articular cartilage was segmented varied between patients depending on hip size and image quality but was consistently between 4 and 6. Quantitative T2 (T2 Mapping) maps were generated using custom code (MATLAB R2015a, MathWorks, Natick, MA, USA). Quantitative T2 maps were generated using a sum of squares algorithm on co-registered echo time images and fitting a mono-exponential T2 recovery curve using a non-linear algorithm. The time to complete imaging analysis and subsequent processing for each individual ranged from 90 to 120 minutes.

To investigate differences in cartilage composition with age and effect of activity cartilage was analysed as acetabular and femoral cartilage separately. To investigate the effect of cam morphology on cartilage composition the anterosuperior acetabular cartilage was used as this is the area of cartilage where GAG loss is first observed[97]. Anterosuperior acetabular cartilage comprised Anterior Acetabular Cartilage (Aa), AnteroSuperior Acetabular Cartilage (ASa), and SuperoAnterior Acetabular Cartilage (SAa) from slices throughout the whole joint.

Cam morphology was quantified using the alpha angle for cartilage on radial slices from 11 o'clock, 12 o'clock, 1 o'clock, 2 o'clock, and 3 o'clock. Alpha angles above 60 degrees were taken to define the presence of cam morphology in skeletally mature individuals[22].

6.4.6 Statistical Analysis

See chapter 2 for details of statistical analysis. Inverse probability weighting with regression adjustment modelling[286] was adopted to assess variables that predict outcome variables. Multivariate linear regression modeling was used to evaluate the relationship between variables.

6.5 Results

6.5.1 Participant Demographics

209 individuals (409 hips) (mean age 155 months, SD 32 months) had completed T2 scans of sufficient quality to manually segment. The cohort comprised 109 elite male footballers (mean age 150 months (SD 31 months), 49 male controls (mean age 153 months (SD 30 months), and 51 female controls (mean age 168 months (SD 33 months). (Table 6-1)

Table 6-1 – Cohort Demographics

		Male Footballers (Hips)	Male Controls (Hips)	Female Controls (Hips)
Age (Years)	**9-10**	36 (72)	14 (27)	11(21)
	11-12	28 (55)	14 (27)	6 (12)
	13-14	20 (39)	6 (12)	11 (22)
	15-16	18 (35)	13 (25)	17 (34)
	17-18	7 (13)	2 (4)	6 (11)
Total		109 (214)	49 (95)	51 (100)

6.5.2 Change in Cartilage Compositional with Age

6.5.2.1 Chronological Age

This study found no clear pattern of change in hip cartilage T2 values with age (Table 6-2). Acetabular cartilage T2 values decreased with age but there was no significant difference in acetabular cartilage T2 values after 11 years in all individuals (Table 6-3) (Figure 6-3). There was no consistent pattern of change in femoral cartilage T2 values with age in all individuals. (Table 6-2 and Table 6-4) (Figure 6–4)

Table 6-2 – Acetabular Cartilage, Femoral Cartilage, and Anterosuperior Acetabular cartilage T2 Values by Cohort and Age Group.

Age (Years)	All Individuals Mean (±SD)	Male Footballers Mean (±SD)	Male Controls Mean (±SD)	Female Controls Mean (±SD)
Acetabular Cartilage T2 Value				
9-10	57.602 (±7.857)	60.401 (±7.784)	51.783 (±5.693)	55.487 (±5.611)
11-12	56.111(±7.537)	57.444 (±5.909)	51.459 (±6.138)	60.462 (±11.712)
13-14	52.181 (±8.827)	55.391(±6.526)	49.351 (±4.878)	48.035 (±11.657)
15-16	50.451 (±9.330)	51.849 (±4.662)	53.890 (±15.558)	46.482 (±4.431)
17-18	50.801 (±14.812)	47.656 (±7.419)	46.319 (±1.250)	56.147 (±21.761)
Average	54.183 (±9.385)	56.555 (±7.559)	51.708 (±9.341)	51.455 (±11.473)
Femoral Cartilage T2 Value				
9-10	51.179 (±7.743)	50.892 (±8.439)	52.925 (±6.087)	49.916 (±7.051)
11-12	51.802 (±7.362)	50.534 (±6.878)	53.790 (±6.704)	53.141 (±9.660)
13-14	55.616 (±10.348)	60.415 (±8.629)	52.959 (±5.744)	48.556 (±10.775)
15-16	53.759 (±9.376)	58.695 (±6.669)	57.248 (±10.674)	46.112 (±4.870)
17-18	50.094 (±4.519)	52.371 (±5.215)	49.812 (±2.873)	47.506 (±2.424)
Average	52.633 (±8.558)	53.902 (±8.699)	54.182 (±7.739)	48.445 (±7.658)
Anterosuperior Acetabular Cartilage T2 Value				
9-10	57.909 (±12.408)	61.303 (±13.182)	51.872 (±10.549)	54.033 (±6.930)
11-12	55.739 (±10.851)	56.688 (±6.898)	50.147 (±6.458)	63.968 (±22.542)
13-14	51.652 (±10.478)	56.169 (±7.703)	49.114 (±6.542)	45.031 (±5.544)
15-16	49.586 (±12.855)	52.746 (±5.905)	53.690 (±21.469)	43.316 (±5.544)
17-18	48.576 (±11.555)	47.790 (±8.378)	43.634 (±0.568)	51.302 (±16.045)
Average	53.742 (±12.257)	56.961 (±10.230)	51.165 (±13.041)	49.301 (±13.558)

Figure 6-3 – Acetabular Cartilage T2 Values with Age for All Individuals. Age groups based on chronological age of participants at time of MRI scan. Box and whisker plot

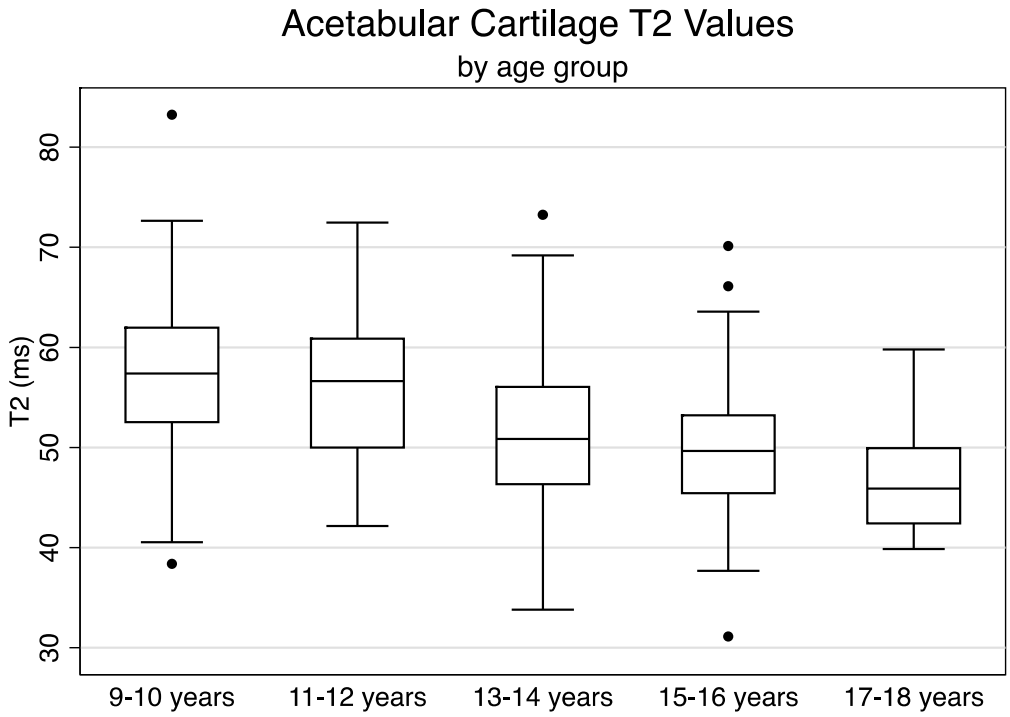


Figure 6-4 – Femoral Cartilage T2 Values with Age for All Individuals. Age groups based on chronological age of participants at time of MRI scan. Box and whisker plot

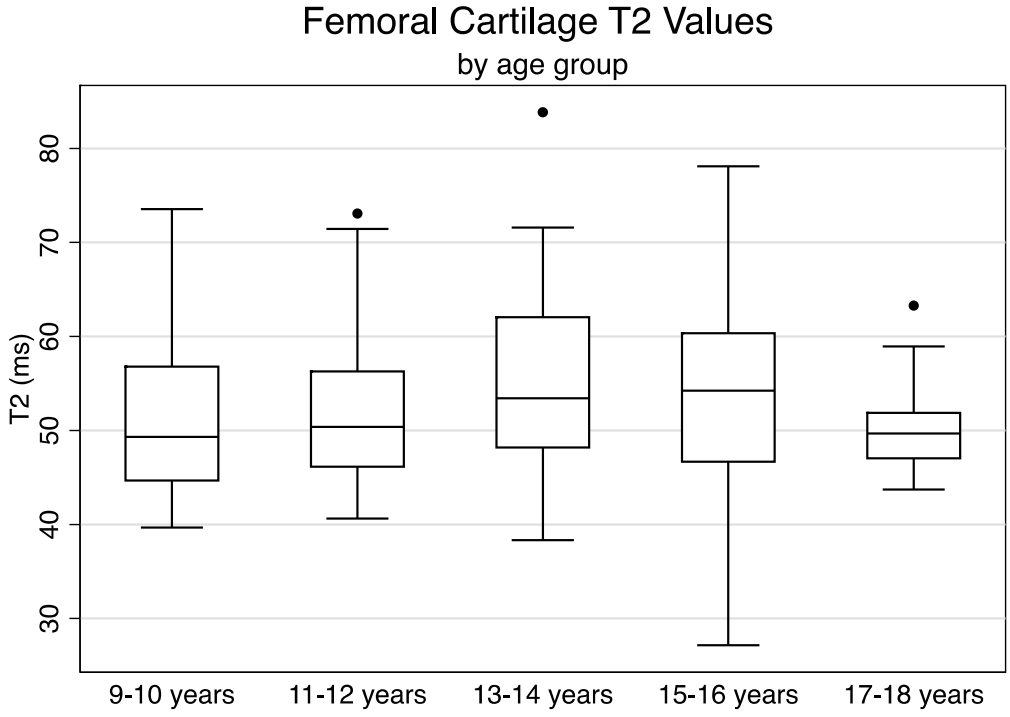


Table 6-3 – Predictors of Acetabular Cartilage Values. *Age and cohort as covariables. **Age, gender and activity level as covariables. ***Physeal maturity, gender, and activity levels as covariables

		Hips	Mean Acetabular Cartilage T2 Value (±SD)	Univariate Regression			Multivariate Regression 1*			Multivariate Regression 2**			Multivariate Regression 3***		
				Coefficient	95% CI	P value	Coefficient	95% CI	P value	Coefficient	95% CI	P value	Coefficient	95% CI	P value
Age	**Months (continuous)**			-0.097	-0.198 to 0.004	0.052	0.010	0.004 to 0.017	0.002	0.003	-0.007 to 0.012	0.573			
	9-10 Years	120	57.602 (±7.857)	6.802	1.235 to 12.368	0.017									
	11-12 Years	94	56.111(±7.537)	5.310	-0.287 to 10.907	0.063									
	13-14 Years	73	52.181 (±8.827)	1.380	-4.370 to 7.131	0.638									
	15-16 Years	94	50.451 (±9.330)	-0.035	-6.055 to 5.355	0.904									
	17-18 Years	28	50.801 (±14.812)	-	-	-									
Physis	**Open**	250	56.797 (±8.428)	-	-	-							-	-	-
	Closed	159	50.122 (±9.402)	-6.675	-8.474 to -4.876	<0.001							-7.863	-11.305 to -4.420	<0.001
Gender	**Male**	309	55.065 (±8.436)	3.610	1.183 to 6.036	0.004				1.867	0.692 to -4.425	0.153	1.182	0.648 to 1.716	<0.001
	Female	100	51.455 (±11.472)	-	-	-				-	-	-	-	-	-
BMI		409	-	-0.510	-1.798 to 0.778	0.125									
Dominant Leg	**Dominant**	226	54.259 (±9.773)	0.170	-1.639 to 1.979	0854									
	Non Dominant	183	54.089 (±8.907)	-	-	-									
Cohort	**Footballers**	214	56.555 (±7.559)	4.847	2.723 to 6.971	<0.001	4.848	2.818 to 6.878	<0.001						
	Male controls	95	51.708 (±9.341)	-	-	-	-	-	-						
	Female controls	100	51.455 (±11.473)	-0.253	-3.168 to 2.662	0.865	1.907	-0.811 to 4.624	0.169						
PAQ	**Linear**			2.939	1.647 to 4.231	0.022				1.072	0.673 to 1.472	<0.001	1.412	1.042 to 1.781	<0.001
	< 2	70	49.873 (±8.978)	-	-	-									
	2-3	149	54.065 (±11.233)	4.192	1.436 to 6.947	0.003									
	3-4	168	55.538 (±7.297)	5.665	3.304 to 8.025	<0.001									
	4-5	22	58.337 (±6.221)	8.464	5.176 to 11.752	<0.001									

Table 6-4 – Predictors of Femoral Cartilage Values. *Age and cohort as covariables. **Age, gender and activity level as covariables. ***Physeal maturity, gender, and activity levels as covariables

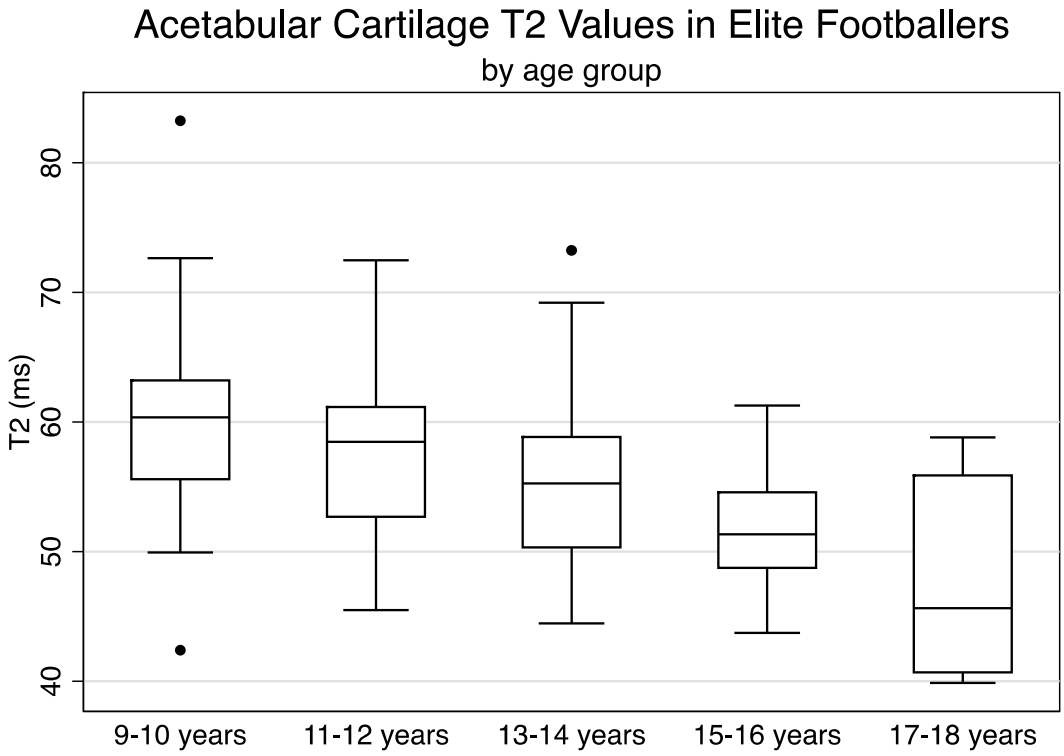
		Hips	Mean Femoral Cartilage T2 Value (±SD)	Univariate Regression			Multivariate Regression 1*			Multivariate Regression 2**			Multivariate Regression 3***		
				Coefficient	95% CI	P value	Coefficient	95% CI	P value	Coefficient	95% CI	P value	Coefficient	95% CI	P value
Age	**Months (continuous)**			0.022	-0.848 to 0.130	0.229	0.014	0.005 to 0.023	0.002	0.003	-0.007 to 0.012	0.573			
	9-10 Years	120	51.179 (±7.743)	1.084	-1.062 to 3.230	0.322									
	11-12 Years	94	51.802 (±7.362)	1.708	-0.504 to 3.920	0.130									
	13-14 Years	73	55.616 (±10.348)	5.522	2.648 to 8.395	<0.001									
	15-16 Years	94	53.759 (±9.376)	3.665	1.164 to 6.166	0.004									
	17-18 Years	28	50.094 (±4.519)	-	-	-									
Physis	**Open**	250	52.259 (±7.956)	-	-	-							-	-	-
	Closed	159	53.257 (±9.471)	0.998	0.776 to 2.773	0.270							1.156	-1.037 to 3.348	0.302
Gender	**Male**	309	53.988 (±8.404)	5.542	3.780 to 7.305	<0.001				6.192	4.067 to 8.316	<0.001	1.182	0.648 to 1.716	,0.001
	Female	100	48.455 (±7.658)	-	-	-				-	-	-	-	-	-
BMI		409		0.310	-0.175 to 0.796	0.078									
Dominant Leg	**Dominant**	226	52.992 (±8.736)	0.803	-0.852 to 2.459	0.342									
	Non Dominant	183	52.189 (±8.335)	-	-	-									
Cohort	**Footballers**	214	51.902 (±8.699)	-0.280	-2.216 to 1.656	0.777	-0.208	-2.076 to 1.661	0.827						
	Male controls	95	54.182 (±7.739)	-	-	-	-	-	-						
	Female controls	100	48.445 (±7.658)	-5.736	-7.887 to -3.585	<0.001	-4.722	-7.113 to -2.330	<0.001						
PAQ	**Linear**			0.733	0.172 to 1.295	0.038				0.660	0.238 to 1.082	0.032	0.513	-0.304 to 1.330	0.079
	< 2	70	50.061 (±9.102)	-	-	-									
	2-3	149	53.597 (±8.507)	3.537	1.020 to 6.054	0.006									
	3-4	168	52.794 (±8.163)	2.734	0.285 to 5.182	0.029									
	4-5	22	53.049 (±9.034)	2.988	-1.264 to 7.241	0.168									

Table 6-5 – T2 cartilage value with Age by Cohort. Univariate Regression.

		Acetabular T2 Values				Femoral T2 Values				Anterosuperior Acetabular T2 Values			
		Mean (±SD)	Univariate Regression			Mean (±SD)	Univariate Regression			Mean (±SD)	Univariate Regression		
			Coefficient	95% CI	P value		Coefficient	95% CI	P value		Coefficient	95% CI	P value
Male Footballers													
Age (Years)	**9-10**	60.401 (±7.784)	12.745	8.479 to 17.012	<0.001	50.892 (±8.439)	-1.479	-4.821 to 1.862	0.386	61.303 (±13.182)	13.514	8.195 to 18.832	<0.001
	11-12	57.444 (±5.909)	9.789	5.616 to 13.961	<0.001	50.534 (±6.878)	-1.838	-5.117 to 1.442	0.272	56.688 (±6.898)	8.898	4.164 to 13.632	<0.001
	13-14	55.391(±6.526)	7.745	3.364 to 12.106	0.001	60.415 (±8.629)	8.044	4.228 to 11.860	<0.001	56.169 (±7.703)	8.379	3.395 to 13.363	0.001
	15-16	51.849 (±4.662)	4.193	0.030 to 8.357	0.048	58.695 (±6.669)	6.324	2.837 to 9.811	<0.001	52.746 (±5.905)	4.956	0.174 to 9.738	0.042
	17-18	47.656 (±7.419)	-	-	-	52.371 (±5.215)	-	-	-	47.790 (±8.378)	-	-	-
Average		56.555 (±7.559)				53.902 (±8.699)				56.961 (±10.230)			
Male Controls													
Age (Years)	**9-10**	51.783 (±5.693)	5.464	3.105 to 7.823	<0.001	52.925 (±6.087)	3.113	-0.208 to 6.433	0.066	51.872 (±10.549)	8.238	4.304 to 12.173	<0.001
	11-12	51.459 (±6.138)	5.140	2.633 to 7.647	<0.001	53.790 (±6.704)	3.979	0.499 to 7.458	0.025	50.147 (±6.458)	6.513	4.075 to 8.952	<0.001
	13-14	49.351 (±4.878)	3.032	0.184 to 5.879	0.037	52.959 (±5.744)	3.147	-0.806 to 7.101	0.119	49.114 (±6.542)	5.480	1.913 to 9.047	0.003
	15-16	53.890 (±15.558)	7.571	1.502 to 13.639	0.014	57.248 (±10.674)	7.436	2.666 to 12.206	0.002	53.690 (±21.469)	10.057	1.797 to 18.317	0.017
	17-18	46.319 (±1.250)	-	-	-	49.812 (±2.873)	-	-	-	43.634 (±0.568)	-	-	-
Average		51.708 (±9.341)				54.182 (±7.739)				51.165 (±13.041)			
Female Controls													
Age (Years)	**9-10**	55.487 (±5.611)	-0.659	-13.142 to 11.823	0.918	49.916 (±7.051)	2.410	-0834 to 5.655	0.145	54.033 (±6.930)	2.731	-6.762 to 12.223	0.573
	11-12	60.462 (±11.712)	4.315	-9.490 to 18.120	0.540	53.141 (±9.660)	5.636	0.227 to 11.044	0.041	63.968 (±22.542)	12.666	-2.527 to 27.859	0.102
	13-14	48.035 (±11.657)	-8.112	-21.264 to 5.040	0.227	48.556 (±10.775)	1.051	-3.555 to 5.657	0.655	45.031 (±5.544)	-6.271	-16.677 to 4.135	0.238
	15-16	46.482 (±4.431)	-9.665	-22.014 to 2.683	0.125	46.112 (±4.870)	-1.394	-3.507 to 0.719	0.196	43.316 (±5.544)	-7.986	-17.211 to 1.239	0.090
	17-18	56.147 (±21.761)	-	-	-	47.506 (±2.424)	-	-	-	51.302 (±16.045)	-	-	-
Average		51.455 (±11.473)				48.445 (±7.658)				49.301 (±13.558)			

Male footballers showed a clear decrease in acetabular cartilage T2 values with age, with significant difference between age groups occurring up to 18 years of age (Table 6-5) (Figure 6-5). No consistent pattern of change in acetabular cartilage T2 values with age was observed in male or female controls. No consistent pattern of change in femoral cartilage T2 values with age was observed in any cohort. (Table 6-5)

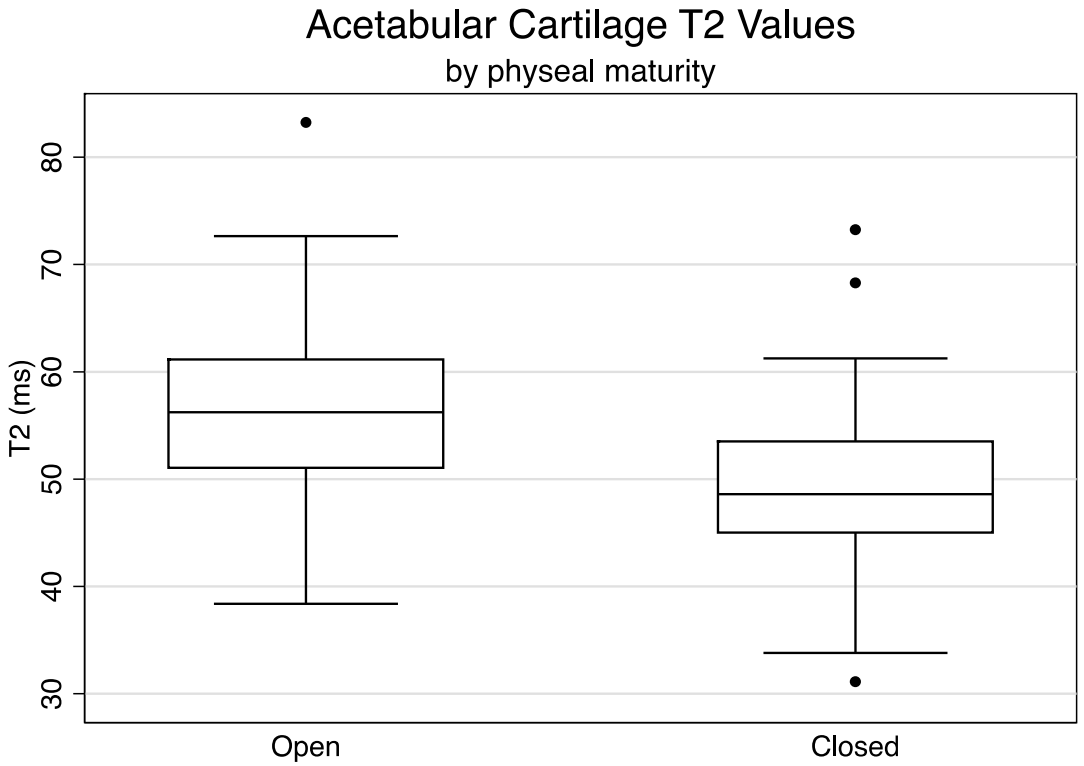
Figure 6-5 – Acetabular Cartilage T2 Values with Age for Elite Male Footballers. Age groups based on chronological age of participants at time of MRI scan. Box and whisker plot



6.5.2.2 Skeletal maturity

Individuals with a closed physis had significantly lower acetabular cartilage T2 values than individuals with an open physis. Adjusting for activity level and gender, individuals with a closed physis had an acetabular cartilage T2 value 7.86ms less than individuals with an open physis ($p<0.001$) (Table 6-3) (Figure 6-6). There was no significant difference in femoral cartilage T2 values between individuals with an open and closed physis. (Table 6-4)

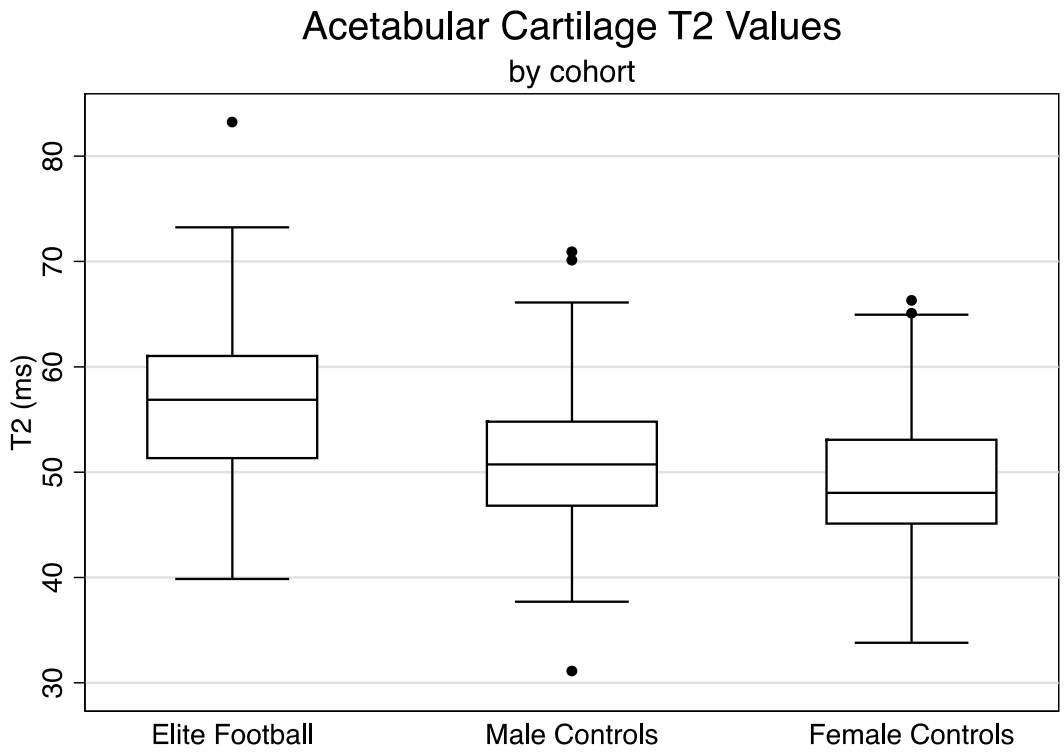
Figure 6-6 – Acetabular Cartilage T2 Values by Physeal Maturity in All Individuals. Box and whisker plot



6.5.3 Factors Affecting Cartilage Composition

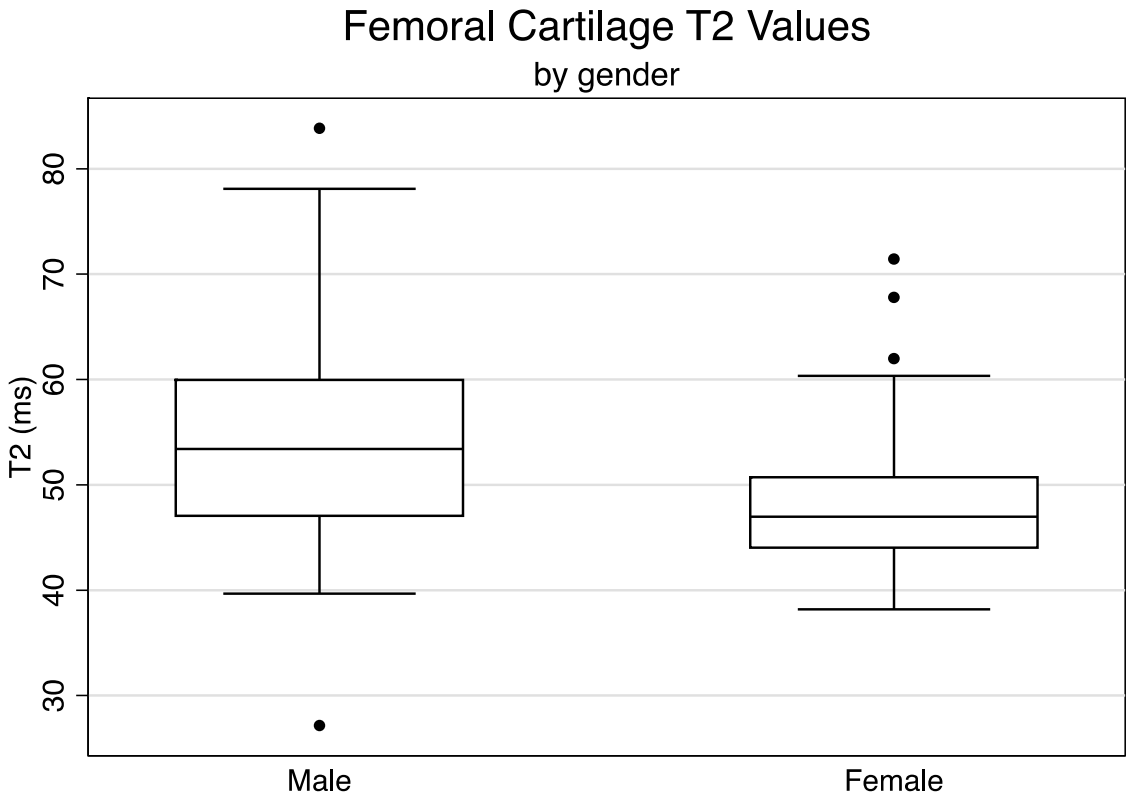
Elite level football players had significantly greater acetabular cartilage T2 values than controls. Adjusting for age, elite male footballers had acetabular cartilage T2 values 4.85ms greater than male controls ($p<0.001$) (Figure 6-7) (Table 6-3). No significant difference in femoral cartilage T2 values was seen between elite level footballers and male controls (Table 6-4).

Figure 6-7 – Acetabular Cartilage T2 Values by Cohort. Box and whisker plot



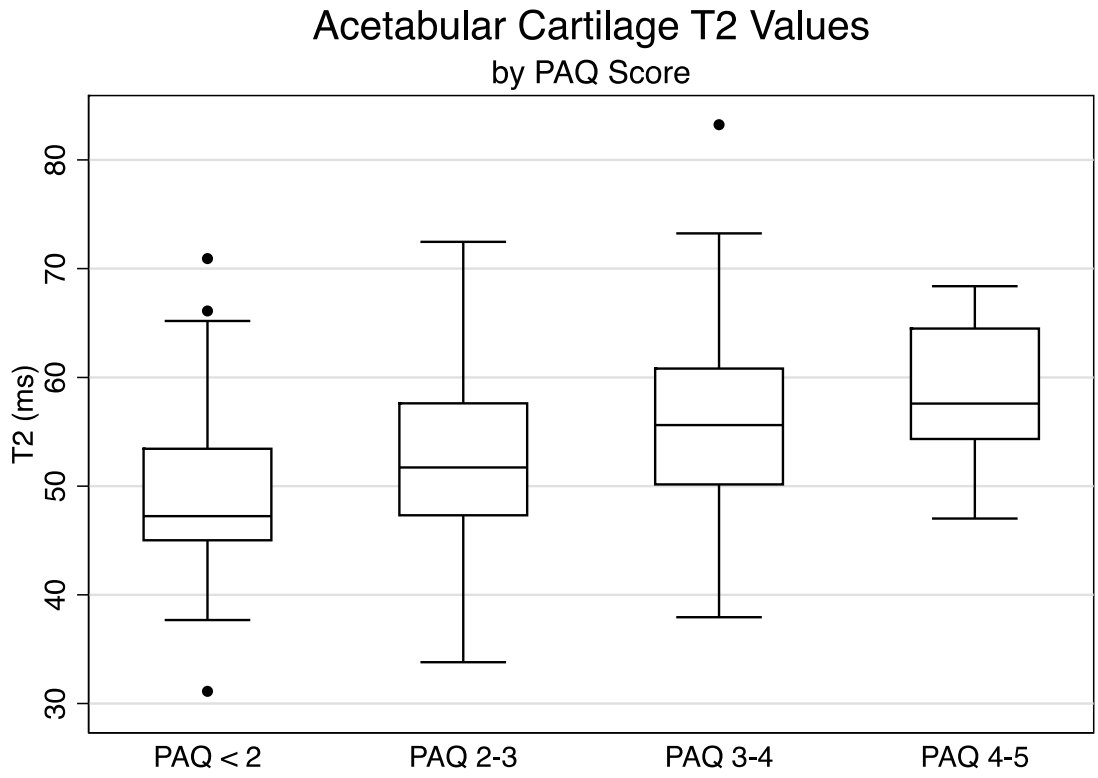
Males had significantly greater acetabular cartilage T2 values than females in a univariate regression analysis, but not in a multivariate regression analysis when controlling for age and activity level (Table 6-3). Males had significantly greater femoral cartilage T2 values than females. Adjusting for age and activity level, males had a femoral cartilage T2 value 6.19ms greater than females ($p<0.001$) (Table 6-4) (Figure 6-8).

Figure 6-8 – Femoral Cartilage T2 Values by Gender. Box and whisker plot



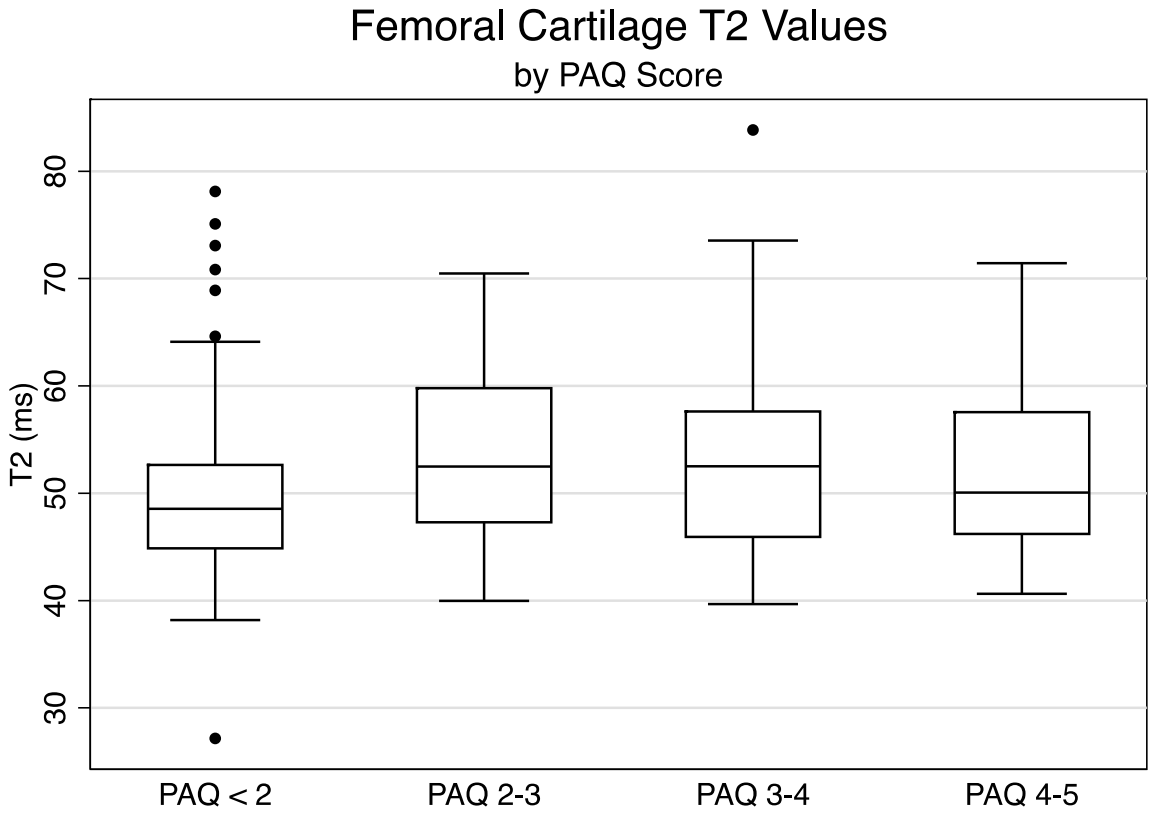
Individuals with high activity levels (PAQ score) had significantly greater acetabular cartilage T2 values than individuals with low activity levels. Adjusting for age and gender in a multivariate linear regression model there was a significant positive linear relationship between PAQ score and acetabular cartilage T2 values (coefficient 1.072, $p<0.001$) (Table 6-3). Adjusting for age and gender individuals with a PAQ score between 4 and 5 had acetabular cartilage T2 values 5.75ms greater than individuals with a PAQ less than 2 ($p<0.001$) (Figure 6-9).

Figure 6-9 – Acetabular Cartilage T2 Values by PAQ Score. Box and whisker plot



Individuals with high activity levels (PAQ score) had significantly greater femoral cartilage T2 values than individuals with low activity levels. Adjusting for age and gender in a multivariate linear regression model there was a significant positive linear relationship between PAQ score and femoral cartilage T2 values (coefficient 0.660, p=0.032) (Table 6-4). Adjusting for age and gender individuals with a PAQ score between 4 and 5 had acetabular cartilage T2 values 9.18ms greater than individuals with a PAQ less than 2 (p<0.001) (Figure 6-10).

Figure 6-10 – Femoral Cartilage T2 Values by PAQ Score. Box and whisker plot



No significant association was seen between leg dominance or BMI and acetabular or femoral cartilage T2 values. (Table 6-3 and Table 6-4)

6.5.4 Effect of Cam Morphology on Cartilage Composition

In this study no correlation was seen between average alpha angle and anterosuperior acetabular cartilage T2 values. Individuals with cam morphology (alpha angle greater than 60 degrees) had lower anterosuperior acetabular cartilage T2 values in a univariate regression model (coefficient -3.23ms, P=0.006), but not in a multivariate regression analysis adjusting for age, gender, and activity level. (Table 6-6)

Table 6-6 – Effect of Cam Morphology on Anterosuperior Acetabular Cartilage Composition. *Age, gender, and activity level (PAQ Score) as covariables.

		Hips	Mean Anterosuperior Acetabular Cartilage T2 Value (±SD)	Univariate regression			Multivariate regression*		
				Coefficient	95% CI	P value	Coefficient	95% CI	P value
Average Alpha Angle	**< 60 degrees**	323	54.422 (±12.958)	-3.235	-5.554 to -0.915	0.006	-1.515	-4.759 to 1.730	0.360
	> 60 degrees	86	51.187 (±8.760)	-	-	-	-	-	-

6.6 Discussion

The aim of this study was to investigate the development of cartilage composition with age, and determine the effects of activity and cam morphology on cartilage composition during adolescence. This study demonstrates that acetabular cartilage composition is affected by activity levels but not by cam morphology, and may change during adolescence in elite athletes but not in controls.

6.6.1 Change in Cartilage Composition with Age

During skeletal growth chondrocytes develop different phenotypes by adapting to local functional requirements within the joint to produce GAG rich areas[204,205]. This would suggest that cartilage composition might change and develop during adolescence. However, no studies exist that have investigated cartilage composition in an adolescent cohort.

Our results demonstrate that acetabular cartilage T2 values decrease with age in elite footballers. In this study elite footballers had a decrease in acetabular T2 values up to 18 years of age, whereas male and female controls did not show any clear pattern of change in acetabular T2 values with age.

T2 relaxation times are believed to be inversely proportional to collage fibre orientation and GAG content[185-187]. Our results would therefore suggest that GAG content in

acetabular cartilage might increase in elite male footballers during adolescence, but not in controls. There was no recognisable pattern of change in femoral cartilage composition. The majority of the acetabulum is involved in weight bearing, whereas weight bearing areas of the femoral head depend on the attitude of the femur to the acetabulum, and change with movement[305]. As joint loading increases with age chondrocytes may respond by increasing the GAG content of the acetabular cartilage to increase resistance to deformation in high activity individuals[203]. The effect may be less in the femoral cartilage due to the more transient nature of its loading in movement. However, by evaluating the femoral cartilage as a whole this study may have missed more localised areas of increased GAG content.

6.6.2 Factors Affecting Cartilage Composition

The effect of exercise on cartilage composition in adolescence has not previously been investigated. Disagreement exists over the effect of exercise on cartilage in healthy adults. Previous compositional MRI studies in adults have reported that increased activity levels both increase GAG levels[209,211] and result in disorientation of collagen fibres and low GAG levels[210].

In this study elite adolescent footballers had significantly greater acetabular cartilage T2 values, but no difference was seen between cohorts in femoral cartilage T2 values. The acetabular cartilage T2 value was 4.85ms greater in elite footballers than male controls.

Higher PAQ scores were also significantly associated with higher T2 values in both acetabular and femoral cartilage.

These results agree with the findings of Stehling et al[210], who reported a difference in patellar cartilage T2 values of 3ms between high and low activity individuals. This would suggest that high activity during adolescence might result in changes to cartilage composition and architecture, such as reduced GAG content and collagen fibre disorientation. However, it should be noted that T2 cartilage values can become transiently raised by loading the cartilage immediately prior to scanning, which elite level footballers would likely be prone to[306]. This could account for some difference seen in T2 relaxation times between high and low activity cohorts. However, T2 relaxation times have been shown to remain stable after 25 minutes of joint unloading prior to T2 scanning in the hip[284]. In this study T2 sequences were performed at the end of the scan session such that joints were unloaded for a minimum of 45 minutes prior to T2 acquisition. The findings from this study contradict those of Tiderius et al[209] and Roos et al[211], who suggested that exercise resulted in increased cartilage GAG content. Tiderius and Roos both used dGEMRIC scanning in healthy adults, which is more sensitive to GAG content than T2 mapping[277]. Although some correlation exists between dGEMRIC and T2 scanning in the hip[284], the use of different compositional sequences between studies likely explains the contradictory findings. This highlights the care that must be taken when interpreting results using MRI sequences as surrogate markers of cartilage composition.

Males had significantly greater femoral cartilage T2 values than females, but no difference was seen between the sexes in acetabular cartilage. This finding may represent measurement noise. Further research is required in adult cohorts before this finding could be interpreted as being clinically significant or consistent in adult cohorts. No difference was found in acetabular or femoral cartilage T2 values between dominant and non-dominant legs. This finding agrees with previous studies that have suggested that the kicking leg does not play an important role in skeletal maturation during adolescence[33].

6.6.3 Effect of Cam Morphology on Cartilage Composition

Cam morphology in healthy adults has been shown to cause GAG loss in the anterosuperior acetabular cartilage that precedes radiographic OA[97]. Cam morphology is thought to develop around 11-14 years of age[52], but the age at which GAG loss first occurs is unknown. In this study cam morphology was not found to affect cartilage composition during adolescence. This would suggest that although cam morphology may be evident from an early age, it does not start to cause irreversible damage until after adolescence. This may offer an important insight into the management of cam-type FAI. If the development of cam morphology cannot be prevented, it may be that intervention after its formation during adolescence can stop it causing cartilage damage and keep cartilage healthy. Further study is required to determine when pathological loss of GAG is first evident.

6.6.4 Limitations

The main limitation of this study is the cross sectional design. It is not possible to comment on the true change in cartilage composition within the individuals over time based on the findings from this study. T2 mapping was not performed in the follow-up scan protocol to reduce MRI scan time to improve participant comfort and retention based on participant feedback. A significant limitation of this study is in using T2 values as a surrogate measure for GAG content and collagen fibre orientation. T2 mapping of the hip is susceptible to error introduced by loading, magic angle effect, and partial volume effect[307,308]. Accordingly the results from this study should be interpreted with care.

6.6.5 Conclusion

Acetabular cartilage T2 values decrease with age in elite footballers and are greater in high physical activity individuals during adolescence, suggesting significant changes to cartilage composition and architecture. Cam morphology is not associated with anterosuperior acetabular cartilage damage during adolescence. Further longitudinal research is required to validate these findings.

Chapter 7 Conclusions

7.1 Summary of Findings

The aim of this thesis was to explore the development of the skeletally immature hip and leg alignment and determine the impact of high activity levels on these during adolescence. This was achieved via a longitudinal prospective observational cohort study in elite level footballers and age matched controls age 9-18 years.

The overarching objective was to identify potentially modifiable predisposing factors and chronology of events for abnormal morphology formation to aid the development of preventative or early interventions. This was addressed through four main objectives;

i. Characterise aetiological factors responsible for cam morphology development
ii. Characterise aetiological factors responsible for abnormal acetabular morphology development
iii. Characterise aetiological factors responsible for varus leg alignment development
iv. Investigate the effect of elite level sport on cartilage composition in adolescence

In addressing the first objective, results from this thesis demonstrate that males undertaking intense sporting activity during adolescence are at greatest risk of developing cam morphology, but there is no significant change in hip morphology after 14 years of age. The longitudinal observational cohort study that was performed is

significantly larger than comparable studies to date. In addition, quantitative assessment of non-osseous morphology using MRI was carried out in order to overcome the limitations of osseous measurements in a skeletally immature hip using radiography based imaging techniques.

Elite football players had a change in average alpha angle 4.83 degrees greater than male controls ($p<0.001$). Individuals with high activity levels (PAQ score) had a significantly greater change in alpha angle than those with lower activity levels. Individuals with a PAQ score between 3 and 4 and between 4 and 5 had a change in average alpha angle 0.58 degrees ($p=0.008$) and 3.20 degrees ($p=0.025$) greater than individuals with a PAQ less than 2 respectively. There was a positive linear relationship between PAQ score and change in average cartilage alpha angle (coefficient 0.79, $p = <0.001$). Male controls had a change in average alpha angle 2.27 degrees greater than female controls ($p =0.016$)

The greatest change in alpha angle in all participants occurred in individuals aged 11-12 years at baseline, with no significant change occurring in individuals older than 14 years at baseline. Individuals with an open physis at baseline and follow-up had a change in average alpha angle 9.29 degrees greater than individuals with a closed physis ($p<0.001$). The salient mechanism of cam formation was soft-tissue hypertrophy and lateral epiphyseal extension. A weak but significant positive correlation was seen between change in average alpha angle and change in average lateral epiphyseal extension (coefficient = 0.002, $p=0.012$). A significant positive correlation was seen between baseline Fibrochondroosseous Tissue area and change in average alpha angle (coefficient

4.09, p = 0.003). A combination of baseline variables consisting of PAQ score, internal rotation range of motion, lateral epiphyseal extension, and Fibrochondroosseous Tissue Area was able to predict the development of cam morphology with an AUC of 0.85 with a sensitivity of 77.33% and specificity of 82.89% where 80.13% of individuals are classified correctly.

The second objective of this thesis was to characterise the risk factors and timing of abnormal acetabular morphology formation. Changes in acetabular morphology and version over the course of adolescent skeletal development have not been well characterised[127]. As such, the aetiology and pathogenesis of abnormal acetabular anatomy during adolescence remains largely unknown. Moreover, the effect of activity on the developing acetabulum has not previously been investigated. The limited studies performed to date have only assessed the bony acetabulum during adolescence retrospectively using ionizing radiation[30,129,214-216]. The prospective longitudinal MRI based study in this thesis reporting changes in acetabular morphology with age comparing elite athletes with controls is the only of its kind within the literature.

This thesis reports that males undertaking intense sporting activity during adolescence, and individuals that develop cam morphology, have an association with the development of abnormal acetabular morphology. Lateral CEA, anterior CEA, and anteversion increased with age. The greatest change in lateral CEA and anterior CEA occurred in individuals aged 11-12 years at baseline. The greatest change in anteversion occurred in individuals aged 13-14 years at baseline. No significant change in lateral

CEA or anteversion occurred in individuals older than 14 years at baseline. The greatest changes in acetabular morphology were seen towards the end of physeal closure.

Elite male footballers had a change in lateral CEA 2.05 degrees less than male controls ($p=0.001$), a change in anterior CEA 4.36 degrees less than male controls ($p<0.001$), and a change in anteversion 1.659 degrees less than male controls ($p=0.040$). A significant negative linear relationship existed between PAQ score and change in lateral CEA (coefficient -0.62, $p = 0.043$), PAQ score and change in anterior CEA (coefficient -3.21, $p = 0.039$), and PAQ score and change in angle of anteversion (coefficient -0.59, $p = 0.048$). Individuals with a PAQ score between 2 and 3, between 3 and 4, and between 4 and 5 had a change in lateral CEA 0.98 degrees ($p <0.001$), 2.54 degrees ($p<0.001$), and 3.49 degrees ($P < 0.001$) less than individuals with a PAQ less than 2 respectively. Individuals with a PAQ score between 3 and 4, and between 4 and 5 had a change in anterior CEA 1.65 degrees ($p <0.001$), and 1.57 degrees ($P < 0.001$) less than individuals with a PAQ less than 2 respectively. Individuals with a PAQ score between 2 and 3, and between 3 and 4 had a change in angle of anteversion 1.20 degrees ($p <0.001$), and 2.03 degrees ($p = 0.006$) less than individuals with a PAQ less than 2 respectively.

Individuals with a larger increase in alpha angle had significantly less change in lateral and anterior CEA. There was a significant negative linear relationship between change in average alpha angle and change in lateral CEA (coefficient -0.08, $p = 0.018$), and change in anterior CEA (coefficient –0.11, $p = 0.014$). The baseline PAQ Score showed some capability for predicting mild dysplasia at follow up with a ROC AUC of 0.68, and a

sensitivity of 66.67% and specificity of 74.19%, where 72.50% of individuals are classified correctly.

The third objective of this thesis was to characterise the risk factors, timing, and pathogenesis of varus leg alignment. The age at which varus alignment develops is unclear with contradictory findings in the literature[135,139,148,153]. Previous studies have shown that athletic activity is associated with greater varus leg alignment in males[135,153]. However, these studies have been based on clinical examination measures. The cross sectional observational cohort study using MRI reported in this thesis is the first of its type in this field of research.

The results from this thesis demonstrate that males undertaking intense exercise during early to mid adolescence are at greatest risk of developing varus leg alignment, which may be secondary to changes at the medial proximal tibial physis. A significant decrease in Hip Knee Angle (HKA) was present in all individuals from 11 years of age, with no significant change in HKA after 15 years of age. Leg alignment was valgus up to 14 years of age and became varus from 15 years. Individuals with an open physis had valgus leg alignment and individuals with a closed physis had varus leg alignment. Individuals with a closed physis had a HKA 1.37 degrees less than individuals with an open physis ($p<0.001$).

Skeletally mature elite male footballers had a HKA 2.28 degrees less than male controls ($p<0.001$). Skeletally mature male controls had a HKA 1.48 degrees less than female controls ($p<0.001$). Individuals with high activity levels (PAQ score) had a significantly more varus leg alignment than individuals with low activity levels. There was a significant negative linear relationship between PAQ score and HKA (coefficient -0.24, $p=0.029$). Individuals with a PAQ score between 2 and 3, between 3 and 4, and between 4 and 5 had HKA 1.40 degrees ($p <0.001$), 0.47 degrees ($p<0.001$), and 1.03 degrees ($P < 0.001$) less than individuals with a PAQ less than 2 respectively.

A significant linear relationship existed between HKA and average alpha angle (coefficient -0.75, $p = 0.003$) and medial tibial proximal physeal angle (coefficient 0.32, $p = 0.008$). Baseline PAQ score showed some capability for predicting varus leg alignment at 3 years. The ROC AUC for PAQ score was 0.69 with a sensitivity of 41.18% and a specificity of 76.05% where 73.93% of individuals are correctly classified.

Based on the findings from this thesis interventions that aim to modify the pathogenesis of cam morphology, acetabular dysplasia and retroversion, and varus leg alignment are most likely to be effective when implemented during early adolescent years, before significant changes to morphology take place. Males participating in high-level sports are at particularly high risk of developing abnormal morphology and possibly subsequent osteoarthritis. It may be possible to screen individuals who are most likely to develop these abnormal morphologies based on their PAQ score, and imaging measures when available, however further research is required to validate these findings.

Avoidance or modification of certain activities during this critical period of hip development offers a potential means of reducing the risk of developing abnormal morphology. However, it is not yet clear what aspect of sporting activity promotes abnormal physeal development, such as extension and hypertrophy. There was no difference in the magnitude of cam morphology or varus alignment between dominant and non-dominant legs. Further studies comparing hip development in individuals from different sports may identify specific loading patterns that predispose to cam formation, acetabular dysplasia and retroversion, and varus leg alignment. An important finding from this thesis is that athletes may warrant surveillance due to their significantly elevated risk of developing these abnormal morphologies that predispose to secondary osteoarthritis.

The final objective of this thesis was to investigate the development of cartilage composition with age, and determine the effects of activity and cam morphology on cartilage composition during adolescence. The development of cartilage composition during adolescence and the effect of exercise on cartilage remain largely unknown. Although cam morphology may be evident from early adolescence it is unknown when associated cartilage damage first occurs.

This thesis reports that acetabular cartilage composition is affected by activity levels but not by cam morphology, and may change during adolescence in elite athletes but not in controls. T2 values were found to decrease with age in the acetabular cartilage of elite footballers but not male or female controls. Individuals with a closed physis had an

acetabular cartilage T2 value 7.86ms less than individuals with an open physis ($p<0.001$). Elite adolescent footballers had significantly greater acetabular cartilage T2 values, but no difference was seen between cohorts in femoral cartilage T2 values. The acetabular cartilage T2 value was 4.85ms greater in elite footballers than male controls. Higher PAQ scores were also significantly associated with higher T2 values in both acetabular and femoral cartilage. There was a significant positive linear relationship between PAQ score and acetabular cartilage T2 values (coefficient 1.072, $p<0.001$). Individuals with a PAQ score between 4 and 5 had acetabular cartilage T2 values 5.75ms greater than individuals with a PAQ less than 2 ($p<0.001$). There was a significant positive linear relationship between PAQ score and femoral cartilage T2 values (coefficient 0.660, $p=0.032$). Individuals with a PAQ score between 4 and 5 had acetabular cartilage T2 values 9.18ms greater than individuals with a PAQ less than 2 ($p<0.001$). No correlation was seen between average alpha angle and anterosuperior acetabular cartilage T2 values.

These findings may offer some important insights into the management of cam morphology, particularly in high-risk cohorts such as elite athletes. Cam morphology may be evident from an early age, however it would appear that it does not start to cause irreversible damage to cartilage until after adolescence, if at all. This finding may help inform the management of cam-type FAI. If the development of cam morphology cannot be prevented, it may be that intervention after its formation during adolescence can stop it causing cartilage damage and keep cartilage healthy. Elite athletes show signs of altered cartilage composition from an early age. This finding may add weight to the argument of reducing load in young athletes, although whether these compositional changes are protective or pathological is unknown. However, at present there remains

insufficient evidence to recommend activity modification during skeletal immaturity and the cardiovascular benefits of exercise are likely to outweigh any potentially detrimental effects on hip morphology

7.2 Future Directions

A valuable cohort was developed during the course of this thesis and continued longitudinal assessment may provide some answers to present and future research questions.

One of the greatest challenges in this field remains the inability to identify individuals at greatest risk of future osteoarthritis. This prevents the implementation of preventative and early intervention joint preserving strategies at a time when they are most likely to be effective. Longitudinal assessment of the FAIM cohort to skeletal maturity and eventual genesis of pathology may inform the development of a risk stratification tool. The results of this thesis would suggest that a predictive model is likely to incorporate activity scores, clinical examination findings, and imaging markers. However, this thesis has also identified that our knowledge of the required component parts of a predictive model are incomplete. A number of areas that remain poorly understood and require further investigation have been identified.

7.2.1 Female athletes

Although participation in female football is growing rapidly worldwide, there is not yet equality with respect to player development. The elite footballer cohort therefore includes only males in this thesis. However, the Premiership Football Club where this study was carried out had their first intake of female academy players during the follow-up period. The well-documented differences in the prevalence of cam morphology

between males and females, and high injury rates reported in adolescent female footballers, is a particular concern and further research may reveal valuable insights into cam pathogenesis[221]. During write up of this thesis, plans have been finalised to extend this study to include female footballers at Southampton Football Club. Investigation and comparison of this cohort with the existing FAIM male elite footballers, male controls, and female controls, may shed further light on the roles of activity and gender on the development of abnormal morphology in the hip.

7.2.2 The role of the Fibrochondroosseous Tissue Area

The mechanism of cam morphology formation remains poorly understood. Evidence to support the pre-eminent theories of sub-clinical SUFE[72,98-101] or lateral epiphyseal extension[102] is limited in the existing literature. Even in this thesis the association between lateral epiphyseal extension and cam development is weak. The mechanism of cam development is likely multifactorial, with genetic, biochemical, and mechanical factors all playing roles. To try and attribute a single abnormal morphological process to cam development is probably too simplistic a view. However, this thesis has identified the area of Fibrochondroosseous tissue at the femoral head neck junction as a potentially important, and previously un-investigated, player in the development of cam morphology.

The results of this thesis allude to a mechanism of cam morphology formation whereby repetitive low energy trauma to the femoral head neck junction through high level

exercise results in soft tissue hypertrophy and eventual ossification of an aspherical femoral head. The strength of the association and predicative value of the Fibrochondroosseous tissue area with cam morphology in this thesis is highly suggestive of a causal relationship, far more so than any other mechanism of cam morphology formation previously proposed. Indeed, the findings in this thesis could lend themselves to form a far more focussed line of investigation into the mechanism of cam morphology development than previously available.

There exists no accepted methodology for investigating the Fibrochondroosseous tissue area, the methodology used was uniquely developed for this thesis. The first step in investigating soft tissue hypertrophy in the Fibrochondroosseous tissue area as a mechanism of cam morphology formation would be to develop and validate a reliable, accurate, and clinically viable measurement tool. The semi-automated segmentation methodology developed for this thesis shows promise, but a significant limitation is its two dimensional representation of a three dimensional structure. Moreover, a volume measure gives little conceptualisation of tissue shape, which in cam morphology may be more important than volume. A gold standard measurement tool would automatically determine the size, shape, and location of the Fibrochondroosseous tissue area. This could be created with further development of our existing software and integration of machine learning on a gold standard dataset.

Validation of this measure would require more extensive follow-up of a cohort from early childhood to full skeletal maturity. Whereas cam morphology becomes evident

from 11-14 years of age, as shown in this thesis, the preceding soft tissue hypertrophy may be evident far earlier than the 9 years of age that was the lower limit in this thesis. A true understanding of the mechanism proposed above would require longitudinal follow-up of a younger cohort over a longer period of time. This may not be feasible, given younger children's compliance issues with MRI scanning, but would certainly be worth investigating.

A further area of research that could provide essential information for the development of cam morphology would be the investigation of the composition and structure of the Fibrochondroosseous tissue area and how this changes during adolescence. Compositional imaging measures are perhaps not extensively validated enough yet to provide meaningful information about tissue composition. The gold standard would be serial tissue harvesting during adolescence with microscopy and assay analysis. However, the ethical issues surrounding this, as a prospective study at least are a significant blockade. Retrospectively analysing surgical samples removed from adolescents for other pathologies may offer a solution, however the logistics and design of any such study would bring significant complications of their own.

Further development and validation of a measurement tool to better define and describe the Fibrochondroosseous tissue area seems the most logical starting point, and at the point of writing this thesis work to develop this is ongoing.

7.2.3 The mechanism of acetabular dysplasia formation

Unlike cam morphology, there are no pre-eminent theories for the cause or mechanism of formation of dysplastic acetabula. An interesting and novel finding from this thesis was the existence of an association between the development of cam morphology and acetabular dysplasia. As the femoral head neck junction becomes more aspherical there is reduced growth of the anterior and lateral acetabula. This thesis found that cam morphology formation might slightly precede acetabular dysplasia formation, suggesting a direct impact of the former upon the latter. This potentially causal relationship warrants further investigation.

A limitation of this thesis is that it was powered specifically for cam morphology development, as not all of the MRI sequences used to investigate morphology outside of the femoral head were available on all scanners at baseline. Accordingly, there were a limited numbers of MRI scans available to investigate acetabula morphology. Future work, as with the female athlete cohort, should be powered to ensure adequate participant numbers to investigate acetabula morphology effectively.

A number of measures exist for numerically describing the physis of long bones, but there exists no validated measure to describe the triradiate cartilage complex of the acetabulum. Until a viable measure is developed investigation of morphological changes in the acetabulum during adolescence will be limited. The development of such a measure would make a sensible starting point moving forward.

7.2.4 The mechanism of varus leg formation

Outside of this thesis there is no imaging studies performed during adolescence investigating the mechanism of varus leg morphology formation. Though previously suggested, this thesis has supplied some evidence to confirm that changes at the medial proximal tibial physis are likely responsible for the development of varus leg morphology. This is a novel and important finding, however, the cross sectional design of the study is a major limitation and places significant restrictions on the conclusions that can be drawn. This was due to the required MRI sequence not being available at baseline. Any true interpretation of change in leg alignment during adolescence requires longitudinal data. Given the significance of the cross-sectional findings in this thesis a strong argument is made for following up the cohort to re-measure leg alignment to determine change in morphology over time.

The MRI sequence used to visualise leg alignment provided limited visualisation of the medial proximal tibial physis due to poor image resolution. This was due to the sequence compromising resolution to gain an increased field of view. Accordingly, only limited measures could be made of the medial proximal tibial physis. For any follow-up work in this cohort a strong argument could be made for including specific anatomical MRI sequences of the proximal tibia to more accurately visualise the physis. This would allow more advanced techniques for visualising the physis. Indeed, collaborative work with a computer science team is on-going at the time of writing this thesis to develop a technique to produce 3D models of long bone physes that can be used for simulating growth models.

7.2.5 Understanding compositional MRI values

Compositional MRI provides an extremely promising method for non-invasively measuring the structure and make-up of chondro-osseous tissues in the human body. It may offer itself as a means to visualise the biological processes taking place in developing tissue for the first time outside of a wet tissue laboratory or microscopy room. Compositional MRI is perhaps one of the most rapidly advancing imaging techniques in the medical field, in part facilitated by the increasing availability of ultra-high field strength MRI[178], and automated image measurement techniques[243]

However, there remains a significant amount of validation work to be done before we can understand exactly what the changes in compositional MRI values mean on a biological level. The majority of tissue imaging correlation work performed to date has been small scale and used animal or cadaveric tissue. Further large-scale human tissue work is required to validate compositional imaging values before the findings from this thesis can be interpreted in a clinical sphere.

7.2.6 Intervention

A driving factor for this thesis was to better understand the abnormal morphologies and conditions that may precede and predict the development of osteoarthritis to inform the development of a risk stratification tool. Further work is almost certainly required before a clinically viable predictive model can be developed. However, a rudimentary tool could be modelled based on the findings from this thesis regarding activity scores,

clinical examination findings, and imaging markers, and validated against future follow-up data from this cohort.

Regardless, the development of a screening tool makes little sense unless there exists a definitive treatment or preventative strategy. With regards to treatment, the jury is still out as to whether surgical intervention in conditions such as cam-type FAI improves symptoms in the long term or reduces the risk of future osteoarthritis. Although, these questions may soon be answered when final follow-up data from the FAIT[309] and FASHIoN[310] trials are released.

Investigating the impact of preventative intervention poses some issues. The results from this thesis would suggest that high activity levels during adolescence predisposes to abnormal morphology formation. Prevention would therefore be to limit exercise. As previously mentioned, not only could this be detrimental to health, but also compliance in active children who enjoy sport and participate to a high level would likely be a major issue. A compromise could be to try to limit intense activity for the sake of intense activity, such as fitness training, in individuals at the age of greatest risk, i.e. 11-12 years. SFC has already made such an intervention where they now focus more on skills training that intense fitness training in their younger cohorts. This move was partially influenced by the results of our work with them. Anecdotally, they have seen positive results, but turning this intervention into a formalised trial would likely be difficult. However, such a trial may be necessary to fill in the missing pieces of the puzzle of how

to predict and prevent cam morphology, acetabular dysplasia and retroversion, and varus leg alignment from developing.

.

Bibliography

1. Woolf AD, Pfleger B. Burden of major musculoskeletal conditions. *Bull World Health Organ* 2003; **81**(9): 646-56.
2. Carr AJ, Robertsson O, Graves S, et al. Knee replacement. *Lancet* 2012; **379**(9823): 1331-40.
3. Pivec R, Johnson AJ, Mears SC, Mont MA. Hip arthroplasty. *Lancet* 2012; **380**(9855): 1768-77.
4. Bijlsma JW, Berenbaum F, Lafeber FP. Osteoarthritis: an update with relevance for clinical practice. *Lancet* 2011; **377**(9783): 2115-26.
5. Learmonth ID, Young C, Rorabeck C. The operation of the century: total hip replacement. *Lancet* 2007; **370**(9597): 1508-19.
6. Powers-Freeling. NJR 12th Annual Report. *National Joint Registry* 2015; **12: 36**.
7. Glyn-Jones S, Palmer AJ, Agricola R, et al. Osteoarthritis. *Lancet* 2015; **386**(9991): 376-87.
8. Lutz W, Sanderson W, Scherbov S. The coming acceleration of global population ageing. *Nature* 2008; **451**(7179): 716-9.
9. Kurtz S, Ong K, Lau E, Mowat F, Halpern M. Projections of primary and revision hip and knee arthroplasty in the United States from 2005 to 2030. *J Bone Joint Surg Am* 2007; **89**(4): 780-5.
10.Sharma L, Chmiel JS, Almagor O, et al. The role of varus and valgus alignment in the initial development of knee cartilage damage by MRI: the MOST study. *Ann Rheum Dis* 2013; **72**(2): 235-40.
11.Felson DT, Niu J, Gross KD, et al. Valgus malalignment is a risk factor for lateral knee osteoarthritis incidence and progression: findings from the Multicenter Osteoarthritis Study and the Osteoarthritis Initiative. *Arthritis Rheum* 2013; **65**(2): 355-62.
12.Klaue K, Durnin CW, Ganz R. The acetabular rim syndrome. A clinical presentation of dysplasia of the hip. *J Bone Joint Surg Br* 1991; **73**(3): 423-9.
13.Murphy SB, Ganz R, Muller ME. The prognosis in untreated dysplasia of the hip. A study of radiographic factors that predict the outcome. *J Bone Joint Surg Am* 1995; **77**(7): 985-9.
14.Mavcic B, Iglic A, Kralj-Iglic V, Brand RA, Vengust R. Cumulative hip contact stress predicts osteoarthritis in DDH. *Clin Orthop Relat Res* 2008; **466**(4): 884-91.
15.Agricola R, Waarsing JH, Arden NK, et al. Cam impingement of the hip: a risk factor for hip osteoarthritis. *Nat Rev Rheumatol* 2013; **9**(10): 630-4.
16.Conaghan PG. Osteoarthritis in 2012: Parallel evolution of OA phenotypes and therapies. *Nat Rev Rheumatol* 2013; **9**(2): 68-70.
17.Drawer S, Fuller CW. Propensity for osteoarthritis and lower limb joint pain in retired professional soccer players. *Br J Sports Med* 2001; **35**(6): 402-8.
18.Klunder KB, Rud B, Hansen J. Osteoarthritis of the hip and knee joint in retired football players. *Acta Orthop Scand* 1980; **51**(6): 925-7.
19.Lindberg H, Roos H, Gardsell P. Prevalence of coxarthrosis in former soccer players. 286 players compared with matched controls. *Acta Orthop Scand* 1993; **64**(2): 165-7.
20.Chantraine A. Knee joint in soccer players: osteoarthritis and axis deviation. *Med Sci Sports Exerc* 1985; **17**(4): 434-9.

21.Kapron AL, Anderson AE, Aoki SK, et al. Radiographic prevalence of femoroacetabular impingement in collegiate football players: AAOS Exhibit Selection. *J Bone Joint Surg Am* 2011; **93**(19): e111(1-10).
22.Agricola R, Waarsing JH, Thomas GE, et al. Cam impingement: defining the presence of a cam deformity by the alpha angle: data from the CHECK cohort and Chingford cohort. *Osteoarthritis Cartilage* 2014; **22**(2): 218-25.
23.Aronson J. Osteoarthritis of the young adult hip: etiology and treatment. *Instr Course Lect* 1986; **35**: 119-28.
24.Harris WH. Etiology of osteoarthritis of the hip. *Clin Orthop Relat Res* 1986; (213): 20-33.
25.Solomon L. Patterns of osteoarthritis of the hip. *J Bone Joint Surg Br* 1976; **58**(2): 176-83.
26.Brouwer GM, van Tol AW, Bergink AP, et al. Association between valgus and varus alignment and the development and progression of radiographic osteoarthritis of the knee. *Arthritis Rheum* 2007; **56**(4): 1204-11.
27.Sharma L, Song J, Felson DT, Cahue S, Shamiyeh E, Dunlop DD. The role of knee alignment in disease progression and functional decline in knee osteoarthritis. *JAMA* 2001; **286**(2): 188-95.
28.Lemaire R. [Osteoarthrosis of the knee joint, a predictable consequence of meniscectomy in patients with angular deformity of the knee (author's transl)]. *Acta Chir Belg* 1977; **76**(3): 355-60.
29.Siebenrock KA, Ferner F, Noble PC, Santore RF, Werlen S, Mamisch TC. The cam-type deformity of the proximal femur arises in childhood in response to vigorous sporting activity. *Clin Orthop Relat Res* 2011; **469**(11): 3229-40.
30.Monazzam S, Bomar JD, Dwek JR, Hosalkar HS, Pennock AT. Development and prevalence of femoroacetabular impingement-associated morphology in a paediatric and adolescent population: a CT study of 225 patients. *Bone Joint J* 2013; **95-B**(5): 598-604.
31.Kienle KP, Keck J, Werlen S, Kim YJ, Siebenrock KA, Mamisch TC. Femoral morphology and epiphyseal growth plate changes of the hip during maturation: MR assessments in a 1-year follow-up on a cross-sectional asymptomatic cohort in the age range of 9-17 years. *Skeletal Radiol* 2012; **41**(11): 1381-90.
32.Carsen S, Moroz PJ, Rakhra K, et al. The Otto Aufranc Award. On the etiology of the cam deformity: a cross-sectional pediatric MRI study. *Clin Orthop Relat Res* 2014; **472**(2): 430-6.
33.Agricola R, Bessems JH, Ginai AZ, et al. The development of Cam-type deformity in adolescent and young male soccer players. *Am J Sports Med* 2012; **40**(5): 1099-106.
34.Demorest RA, Landry GL. Training issues in elite young athletes. *Curr Sports Med Rep* 2004; **3**(3): 167-72.
35.Ericsson KA, Krampe RT, C. T. The Role of Deliberate Practice in the Acquisition of Expert Performance. *Psychol Rev* 1993; **100(3)**: 363-406.
36.Helsen WF, Hodges NJ, Van Winckel J, Starkes JL. The roles of talent, physical precocity and practice in the development of soccer expertise. *J Sports Sci* 2000; **18**(9): 727-36.
37.WF H, JL S, NJ H. Team sports and the theory of deliberate practice. *J Sport Exercise Psy* 1998; **20**(1): 12-34.
38.Maffulli N, Baxter-Jones AD. Common skeletal injuries in young athletes. *Sports Med* 1995; **19**(2): 137-49.
39.Maffulli N, Bruns W. Injuries in young athletes. *Eur J Pediatr* 2000; **159**(1-2): 59-63.
40.Salter R. Textbook of dissorders and injuries of the musculoskeletal system: An introduction to orthopaedics, fractures, and joint injuries, rheumatology, metabolic bone disease, and rehabilitation. *Lippincott Williams &Wilkins* 1999.

41.Dora C, Leunig M, Beck M, Simovitch R, Ganz R. Acetabular dome retroversion: radiological appearance, incidence and relevance. *Hip Int* 2006; **16**(3): 215-22.
42.Mirtz TA, Chandler JP, Eyers CM. The effects of physical activity on the epiphyseal growth plates: a review of the literature on normal physiology and clinical implications. *J Clin Med Res* 2011; **3**(1): 1-7.
43.Kumar R, Madewell JE, Swischuk LE. The normal and abnormal growth plate. *Radiol Clin North Am* 1987; **25**(6): 1133-53.
44.Laor T, Wall EJ, Vu LP. Physeal widening in the knee due to stress injury in child athletes. *AJR Am J Roentgenol* 2006; **186**(5): 1260-4.
45.Savendahl L. Hormonal regulation of growth plate cartilage. *Horm Res* 2005; **64 Suppl 2**: 94-7.
46.Ballock RT, O'Keefe RJ. Physiology and pathophysiology of the growth plate. *Birth Defects Res C Embryo Today* 2003; **69**(2): 123-43.
47.Nilsson O, Marino R, De Luca F, Phillip M, Baron J. Endocrine regulation of the growth plate. *Horm Res* 2005; **64**(4): 157-65.
48.Ulici V, Hoenselaar KD, Gillespie JR, Beier F. The PI3K pathway regulates endochondral bone growth through control of hypertrophic chondrocyte differentiation. *BMC Dev Biol* 2008; **8**: 40.
49.Rauch F. Bone growth in length and width: the Yin and Yang of bone stability. *J Musculoskelet Neuronal Interact* 2005; **5**(3): 194-201.
50.Provot S, Schipani E. Molecular mechanisms of endochondral bone development. *Biochem Biophys Res Commun* 2005; **328**(3): 658-65.
51.Agricola R, Heijboer MP, Ginai AZ, et al. A cam deformity is gradually acquired during skeletal maturation in adolescent and young male soccer players: a prospective study with minimum 2-year follow-up. *Am J Sports Med* 2014; **42**(4): 798-806.
52.Palmer A, Fernquest S, Gimpel M, et al. Physical activity during adolescence and the development of cam morphology: a cross-sectional cohort study of 210 individuals. *Br J Sports Med* 2017; **52**(9): 601-10.
53.Siebenrock KA, Behning A, Mamisch TC, Schwab JM. Growth plate alteration precedes cam-type deformity in elite basketball players. *Clin Orthop Relat Res* 2013; **471**(4): 1084-91.
54.Shapiro F, Holtrop ME, Glimcher MJ. Organization and cellular biology of the perichondrial ossification groove of ranvier: a morphological study in rabbits. *J Bone Joint Surg Am* 1977; **59**(6): 703-23.
55.Parfitt AM. Genetic effects on bone mass and turnover-relevance to black/white differences. *J Am Coll Nutr* 1997; **16**(4): 325-33.
56.Langenskiold A. Role of the ossification groove of Ranvier in normal and pathologic bone growth: a review. *J Pediatr Orthop* 1998; **18**(2): 173-7.
57.Ham AW. Some histophysiological problems peculiar to calcified tissues. *J Bone Joint Surg Am* 1952; **24 A**(3): 701-28.
58.Bucholz RW, Ezaki M, Ogden JA. Injury to the acetabular triradiate physeal cartilage. *J Bone Joint Surg Am* 1982; **64**(4): 600-9.
59.Ponseti IV. Growth and development of the acetabulum in the normal child. Anatomical, histological, and roentgenographic studies. *J Bone Joint Surg Am* 1978; **60**(5): 575-85.
60.Strayer LM, Jr. Embryology of he human hip joint. *Clin Orthop Relat Res* 1971; **74**: 221-40.
61.Fairbank H. Congenital Dislocation of the Hip: With Special Reference to the Anatomy. *British J Surg,* 1930; **17**: 380-416.

62.Harrison TJ. The influence of the femoral head on pelvic growth and acetabular form in the rat. *J Anat* 1961; **95**: 12-24.
63.Fabricant PD, Hirsch BP, Holmes I, et al. A radiographic study of the ossification of the posterior wall of the acetabulum: implications for the diagnosis of pediatric and adolescent hip disorders. *J Bone Joint Surg Am* 2013; **95**(3): 230-6.
64.Juul A. The effects of oestrogens on linear bone growth. *Hum Reprod Update* 2001; **7**(3): 303-13.
65.Kao SC, Smith WL. Skeletal injuries in the pediatric patient. *Radiol Clin North Am* 1997; **35**(3): 727-46.
66.Rais Y, Reich A, Simsa-Maziel S, et al. The growth plate's response to load is partially mediated by mechano-sensing via the chondrocytic primary cilium. *Cell Mol Life Sci* 2015; **72**(3): 597-615.
67.Putz R. [Development and growth of the epiphysis]. *Z Orthop Ihre Grenzgeb* 1996; **134**(5): 391-5.
68.Perron AD, Miller MD, Brady WJ. Orthopedic pitfalls in the ED: pediatric growth plate injuries. *Am J Emerg Med* 2002; **20**(1): 50-4.
69.Loder RT, Skopelja EN. The epidemiology and demographics of slipped capital femoral epiphysis. *ISRN Orthop* 2011; **2011**: 486512.
70.Novais EN, Millis MB. Slipped capital femoral epiphysis: prevalence, pathogenesis, and natural history. *Clin Orthop Relat Res* 2012; **470**(12): 3432-8.
71.Manoff EM, Banffy MB, Winell JJ. Relationship between Body Mass Index and slipped capital femoral epiphysis. *J Pediatr Orthop* 2005; **25**(6): 744-6.
72.Leunig M, Casillas MM, Hamlet M, et al. Slipped capital femoral epiphysis: early mechanical damage to the acetabular cartilage by a prominent femoral metaphysis. *Acta Orthop Scand* 2000; **71**(4): 370-5.
73.Sink EL, Zaltz I, Heare T, Dayton M. Acetabular cartilage and labral damage observed during surgical hip dislocation for stable slipped capital femoral epiphysis. *J Pediatr Orthop* 2010; **30**(1): 26-30.
74.Heesakkers N, van Kempen R, Feith R, Hendriks J, Schreurs W. The long-term prognosis of Legg-Calve-Perthes disease: a historical prospective study with a median follow-up of forty one years. *Int Orthop* 2015; **39**(5): 859-63.
75.Larson AN, Sucato DJ, Herring JA, et al. A prospective multicenter study of Legg-Calve-Perthes disease: functional and radiographic outcomes of nonoperative treatment at a mean follow-up of twenty years. *J Bone Joint Surg Am* 2012; **94**(7): 584-92.
76.Clohisy JC, Dobson MA, Robison JF, et al. Radiographic structural abnormalities associated with premature, natural hip-joint failure. *J Bone Joint Surg Am* 2011; **93 Suppl 2**: 3-9.
77.Yamamura M, Miki H, Nakamura N, Murai M, Yoshikawa H, Sugano N. Open-configuration MRI study of femoro-acetabular impingement. *J Orthop Res* 2007; **25**(12): 1582-8.
78.Fernquest S, Arnold C, Palmer A, et al. Osseous impingement occurs early in flexion in cam-type femoroacetabular impingement: a 4D CT model. *Bone Joint J* 2017; **99-B**(4 Supple B): 41-8.
79.Cobb J, Logishetty K, Davda K, Iranpour F. Cams and pincer impingement are distinct, not mixed: the acetabular pathomorphology of femoroacetabular impingement. *Clin Orthop Relat Res* 2010; **468**(8): 2143-51.
80.Beck M, Kalhor M, Leunig M, Ganz R. Hip morphology influences the pattern of damage to the acetabular cartilage: femoroacetabular impingement as a cause of early osteoarthritis of the hip. *J Bone Joint Surg Br* 2005; **87**(7): 1012-8.

81.Ganz R, Leunig M, Leunig-Ganz K, Harris WH. The etiology of osteoarthritis of the hip: an integrated mechanical concept. *Clin Orthop Relat Res* 2008; **466**(2): 264-72.
82.Agricola R, Heijboer MP, Roze RH, et al. Pincer deformity does not lead to osteoarthritis of the hip whereas acetabular dysplasia does: acetabular coverage and development of osteoarthritis in a nationwide prospective cohort study (CHECK). *Osteoarthritis Cartilage* 2013; **21**(10): 1514-21.
83.Leunig M, Juni P, Werlen S, et al. Prevalence of cam and pincer-type deformities on hip MRI in an asymptomatic young Swiss female population: a cross-sectional study. *Osteoarthritis Cartilage* 2013; **21**(4): 544-50.
84.Siebenrock KA, Schwab JM. The cam-type deformity--what is it: SCFE, osteophyte, or a new disease? *J Pediatr Orthop* 2013; **33 Suppl 1**: S121-5.
85.Reid GD, Reid CG, Widmer N, Munk PL. Femoroacetabular impingement syndrome: an underrecognized cause of hip pain and premature osteoarthritis? *J Rheumatol* 2010; **37**(7): 1395-404.
86.Dickenson E, Wall PD, Robinson B, et al. Prevalence of cam hip shape morphology: a systematic review. *Osteoarthritis Cartilage* 2016; **24**(6): 949-61.
87.Laborie LB, Lehmann TG, Engesaeter IO, Eastwood DM, Engesaeter LB, Rosendahl K. Prevalence of radiographic findings thought to be associated with femoroacetabular impingement in a population-based cohort of 2081 healthy young adults. *Radiology* 2011; **260**(2): 494-502.
88.Frank JM, Harris JD, Erickson BJ, et al. Prevalence of Femoroacetabular Impingement Imaging Findings in Asymptomatic Volunteers: A Systematic Review. *Arthroscopy* 2015; **31**(6): 1199-204.
89.Lievense AM, Bierma-Zeinstra SM, Verhagen AP, Bernsen RM, Verhaar JA, Koes BW. Influence of sporting activities on the development of osteoarthritis of the hip: a systematic review. *Arthritis Rheum* 2003; **49**(2): 228-36.
90.Agricola R, Heijboer MP, Bierma-Zeinstra SM, Verhaar JA, Weinans H, Waarsing JH. Cam impingement causes osteoarthritis of the hip: a nationwide prospective cohort study (CHECK). *Ann Rheum Dis* 2013; **72**(6): 918-23.
91.Thomas GE, Palmer AJ, Batra RN, et al. Subclinical deformities of the hip are significant predictors of radiographic osteoarthritis and joint replacement in women. A 20 year longitudinal cohort study. *Osteoarthritis Cartilage* 2014; **22**(10): 1504-10.
92.Nelson AE, Stiller JL, Shi XA, et al. Measures of hip morphology are related to development of worsening radiographic hip osteoarthritis over 6 to 13 year follow-up: the Johnston County Osteoarthritis Project. *Osteoarthritis Cartilage* 2016; **24**(3): 443-50.
93.Gosvig KK, Jacobsen S, Sonne-Holm S, Palm H, Troelsen A. Prevalence of malformations of the hip joint and their relationship to sex, groin pain, and risk of osteoarthritis: a population-based survey. *J Bone Joint Surg Am* 2010; **92**(5): 1162-9.
94.Doherty M, Courtney P, Doherty S, et al. Nonspherical femoral head shape (pistol grip deformity), neck shaft angle, and risk of hip osteoarthritis: a case-control study. *Arthritis Rheum* 2008; **58**(10): 3172-82.
95.Reichenbach S, Leunig M, Werlen S, et al. Association between cam-type deformities and magnetic resonance imaging-detected structural hip damage: a cross-sectional study in young men. *Arthritis Rheum* 2011; **63**(12): 4023-30.
96.Pollard TC, McNally EG, Wilson DC, et al. Localized cartilage assessment with three-dimensional dGEMRIC in asymptomatic hips with normal morphology and cam deformity. *J Bone Joint Surg Am* 2010; **92**(15): 2557-69.
97.Palmer A, Fernquest S, Rombach I, et al. Diagnostic and prognostic value of delayed Gadolinium Enhanced Magnetic Resonance Imaging of Cartilage (dGEMRIC) in early osteoarthritis of the hip. *Osteoarthritis Cartilage* 2017; **25**(9): 1468-77.

98.Bedi A, Kelly BT. Femoroacetabular impingement. *J Bone Joint Surg Am* 2013; **95**(1): 82-92.
99.Murgier J, Chiron P, Cavaignac E, Espie A, Bayle-Iniguez X, Lepage B. The lateral view head-neck index (LVHNI): a diagnostic tool for the sequelae of slipped capital femoral epiphysis. *Orthop Traumatol Surg Res* 2013; **99**(5): 501-8.
100. Murray RO, Duncan C. Athletic activity in adolescence as an etiological factor in degenerative hip disease. *J Bone Joint Surg Br* 1971; **53**(3): 406-19.
101. Fraitzl CR, Kafer W, Nelitz M, Reichel H. Radiological evidence of femoroacetabular impingement in mild slipped capital femoral epiphysis: a mean follow-up of 14.4 years after pinning in situ. *J Bone Joint Surg Br* 2007; **89**(12): 1592-6.
102. Siebenrock KA, Wahab KH, Werlen S, Kalhor M, Leunig M, Ganz R. Abnormal extension of the femoral head epiphysis as a cause of cam impingement. *Clin Orthop Relat Res* 2004; (418): 54-60.
103. Haider I, Speirs A, Alnabelseya A, Beaule PE, Frei H. Femoral subchondral bone properties of patients with cam-type femoroacetabular impingement. *Osteoarthritis Cartilage* 2016; **24**(6): 1000-6.
104. Caine D, DiFiori J, Maffulli N. Physeal injuries in children's and youth sports: reasons for concern? *Br J Sports Med* 2006; **40**(9): 749-60.
105. Goodman DA, Feighan JE, Smith AD, Latimer B, Buly RL, Cooperman DR. Subclinical slipped capital femoral epiphysis. Relationship to osteoarthrosis of the hip. *J Bone Joint Surg Am* 1997; **79**(10): 1489-97.
106. Nicholls AS, Kiran A, Pollard TC, et al. The association between hip morphology parameters and nineteen-year risk of end-stage osteoarthritis of the hip: a nested case-control study. *Arthritis Rheum* 2011; **63**(11): 3392-400.
107. Bixby SD, Kienle KP, Nasreddine A, Zurakowski D, Kim YJ, Yen YM. Reference values for proximal femoral anatomy in adolescents based on sex, physis, and imaging plane. *Am J Sports Med* 2013; **41**(9): 2074-82.
108. Ecker TM, Tannast M, Puls M, Siebenrock KA, Murphy SB. Pathomorphologic alterations predict presence or absence of hip osteoarthrosis. *Clin Orthop Relat Res* 2007; **465**: 46-52.
109. Cushnaghan J, Dieppe P. Study of 500 patients with limb joint osteoarthritis. I. Analysis by age, sex, and distribution of symptomatic joint sites. *Ann Rheum Dis* 1991; **50**(1): 8-13.
110. Grotle M, Hagen KB, Natvig B, Dahl FA, Kvien TK. Obesity and osteoarthritis in knee, hip and/or hand: an epidemiological study in the general population with 10 years follow-up. *BMC Musculoskelet Disord* 2008; **9**: 132.
111. Wright AA, Cook C, Abbott JH. Variables associated with the progression of hip osteoarthritis: a systematic review. *Arthritis Rheum* 2009; **61**(7): 925-36.
112. Wiberg G. Studies on dysplastic acetabula and congenital subluxation of the hip joint: With special reference to the complications of osteoarthritis. *Acta Chir Scand* 1939; **83**(Suppl 58): 40–138.
113. Murray RO. The aetiology of primary osteoarthritis of the hip. *Br J Radiol* 1965; **38**(455): 810-24.
114. Gala L, Clohisy JC, Beaule PE. Hip Dysplasia in the Young Adult. *J Bone Joint Surg Am* 2016; **98**(1): 63-73.
115. Salter RB, Dubos JP. The first fifteen year's personal experience with innominate osteotomy in the treatment of congenital dislocation and subluxation of the hip. *Clin Orthop Relat Res* 1974; (98): 72-103.

116. Genda E, Iwasaki N, Li G, MacWilliams BA, Barrance PJ, Chao EY. Normal hip joint contact pressure distribution in single-leg standing--effect of gender and anatomic parameters. *J Biomech* 2001; **34**(7): 895-905.
117. Henak CR, Abraham CL, Anderson AE, et al. Patient-specific analysis of cartilage and labrum mechanics in human hips with acetabular dysplasia. *Osteoarthritis Cartilage* 2014; **22**(2): 210-7.
118. Jacobsen S, Sonne-Holm S. Hip dysplasia: a significant risk factor for the development of hip osteoarthritis. A cross-sectional survey. *Rheumatology (Oxford)* 2005; **44**(2): 211-8.
119. Li PL, Ganz R. Morphologic features of congenital acetabular dysplasia: one in six is retroverted. *Clin Orthop Relat Res* 2003; (416): 245-53.
120. Menke W, Schmitz B, Schild H, Koper C. [Transverse skeletal axes of the lower extremity in coxarthrosis]. *Z Orthop Ihre Grenzgeb* 1991; **129**(3): 255-9.
121. Giori NJ, Trousdale RT. Acetabular retroversion is associated with osteoarthritis of the hip. *Clin Orthop Relat Res* 2003; (417): 263-9.
122. Tonnis D, Heinecke A. Acetabular and femoral anteversion: relationship with osteoarthritis of the hip. *J Bone Joint Surg Am* 1999; **81**(12): 1747-70.
123. Mast JW, Brunner RL, Zebrack J. Recognizing acetabular version in the radiographic presentation of hip dysplasia. *Clin Orthop Relat Res* 2004; (418): 48-53.
124. Chan A, McCaul KA, Cundy PJ, Haan EA, Byron-Scott R. Perinatal risk factors for developmental dysplasia of the hip. *Arch Dis Child Fetal Neonatal Ed* 1997; **76**(2): F94-100.
125. Cady RB. Developmental dysplasia of the hip: definition, recognition, and prevention of late sequelae. *Pediatr Ann* 2006; **35**(2): 92-101.
126. Bache CE, Clegg J, Herron M. Risk factors for developmental dysplasia of the hip: ultrasonographic findings in the neonatal period. *J Pediatr Orthop B* 2002; **11**(3): 212-8.
127. Peterson JB, Doan J, Bomar JD, Wenger DR, Pennock AT, Upasani VV. Sex Differences in Cartilage Topography and Orientation of the Developing Acetabulum: Implications for Hip Preservation Surgery. *Clin Orthop Relat Res* 2015; **473**(8): 2489-94.
128. Hingsammer AM, Bixby S, Zurakowski D, Yen YM, Kim YJ. How do acetabular version and femoral head coverage change with skeletal maturity? *Clin Orthop Relat Res* 2015; **473**(4): 1224-33.
129. Weiner LS, Kelley MA, Ulin RI, Wallach D. Development of the acetabulum and hip: computed tomography analysis of the axial plane. *J Pediatr Orthop* 1993; **13**(4): 421-5.
130. Kim SS, Frick SL, Wenger DR. Anteversion of the acetabulum in developmental dysplasia of the hip: analysis with computed tomography. *J Pediatr Orthop* 1999; **19**(4): 438-42.
131. Reikeras O, Bjerkreim I, Kolbenstvedt A. Anteversion of the acetabulum in patients with idiopathic increased anteversion of the femoral neck. *Acta Orthop Scand* 1982; **53**(6): 847-52.
132. Albers CE, Schwarz A, Hanke MS, Kienle KP, Werlen S, Siebenrock KA. Acetabular Version Increases After Closure of the Triradiate Cartilage Complex. *Clin Orthop Relat Res* 2017; **475**(4): 983-94.
133. Lahner M, Jahnke NL, Zirke S, et al. The deviation of the mechanical leg axis correlates with an increased hip alpha angle and could be a predictor of femoroacetabular impingement. *Int Orthop* 2014; **38**(1): 19-25.
134. Palmer JS, Palmer AJ, Jones LD, et al. The failing medial compartment in the varus knee and its association with CAM deformity of the hip. *Knee* 2017; **24**(6): 1383-91.
135. Thijs Y, Bellemans J, Rombaut L, Witvrouw E. Is high-impact sports participation associated with bowlegs in adolescent boys? *Med Sci Sports Exerc* 2012; **44**(6): 993-8.

136. Cahuzac JP, Vardon D, Sales de Gauzy J. Development of the clinical tibiofemoral angle in normal adolescents. A study of 427 normal subjects from 10 to 16 years of age. *J Bone Joint Surg Br* 1995; **77**(5): 729-32.
137. Heath CH, Staheli LT. Normal limits of knee angle in white children--genu varum and genu valgum. *J Pediatr Orthop* 1993; **13**(2): 259-62.
138. Salenius P, Vankka E. The development of the tibiofemoral angle in children. *J Bone Joint Surg Am* 1975; **57**(2): 259-61.
139. Yaniv M, Becker T, Goldwirt M, Khamis S, Steinberg DM, Weintroub S. Prevalence of bowlegs among child and adolescent soccer players. *Clin J Sport Med* 2006; **16**(5): 392-6.
140. Cheema JI, Grissom LE, Harcke HT. Radiographic characteristics of lower-extremity bowing in children. *Radiographics* 2003; **23**(4): 871-80.
141. Espandar R, Mortazavi SM, Baghdadi T. Angular deformities of the lower limb in children. *Asian J Sports Med* 2010; **1**(1): 46-53.
142. Kling TF, Jr. Angular deformities of the lower limbs in children. *Orthop Clin North Am* 1987; **18**(4): 513-27.
143. Bellemans J, Colyn W, Vandenneucker H, Victor J. The Chitranjan Ranawat award: is neutral mechanical alignment normal for all patients? The concept of constitutional varus. *Clin Orthop Relat Res* 2012; **470**(1): 45-53.
144. Chaudhari AM, Andriacchi TP. The mechanical consequences of dynamic frontal plane limb alignment for non-contact ACL injury. *J Biomech* 2006; **39**(2): 330-8.
145. van de Pol GJ, Arnold MP, Verdonschot N, van Kampen A. Varus alignment leads to increased forces in the anterior cruciate ligament. *Am J Sports Med* 2009; **37**(3): 481-7.
146. Lun V, Meeuwisse WH, Stergiou P, Stefanyshyn D. Relation between running injury and static lower limb alignment in recreational runners. *Br J Sports Med* 2004; **38**(5): 576-80.
147. Maffulli N, Bundoc RC, Chan KM, Cheng JC. Paediatric sports injuries in Hong Kong: a seven year survey. *Br J Sports Med* 1996; **30**(3): 218-21.
148. Asadi K, Mirbolook A, Heidarzadeh A, Mardani Kivi M, Emami Meybodi MK, Rouhi Rad M. Association of Soccer and Genu Varum in Adolescents. *Trauma Mon* 2015; **20**(2): e17184.
149. Wen DY, Puffer JC, Schmalzried TP. Injuries in runners: a prospective study of alignment. *Clin J Sport Med* 1998; **8**(3): 187-94.
150. Lewek MD, Rudolph KS, Snyder-Mackler L. Control of frontal plane knee laxity during gait in patients with medial compartment knee osteoarthritis. *Osteoarthritis Cartilage* 2004; **12**(9): 745-51.
151. Laxafoss E, Jacobsen S, Gosvig KK, Sonne-Holm S. The alignment of the knee joint in relationship to age and osteoarthritis: the Copenhagen Osteoarthritis Study. *Skeletal Radiol* 2013; **42**(4): 531-40.
152. Bout-Tabaku S, Shults J, Zemel BS, et al. Obesity is associated with greater valgus knee alignment in pubertal children, and higher body mass index is associated with greater variability in knee alignment in girls. *J Rheumatol* 2015; **42**(1): 126-33.
153. Witvrouw E, Danneels L, Thijs Y, Cambier D, Bellemans J. Does soccer participation lead to genu varum? *Knee Surg Sports Traumatol Arthrosc* 2009; **17**(4): 422-7.
154. Rezende LPM SM, Araujo TL, Matsudo VKR. Does soccer practice stress the degrees of genu varo? *Rev Bras Med Esporte* 2011; **17**: 329-33.
155. Voloc A, Esterle L, Nguyen TM, et al. High prevalence of genu varum/valgum in European children with low vitamin D status and insufficient dairy products/calcium intakes. *Eur J Endocrinol* 2010; **163**(5): 811-7.
156. Bradway JK, Klassen RA, Peterson HA. Blount disease: a review of the English literature. *J Pediatr Orthop* 1987; **7**(4): 472-80.

157. Cook SD, Lavernia CJ, Burke SW, Skinner HB, Haddad RJ, Jr. A biomechanical analysis of the etiology of tibia vara. *J Pediatr Orthop* 1983; **3**(4): 449-54.
158. Johnston CE, 2nd. Infantile tibia vara. *Clin Orthop Relat Res* 1990; (255): 13-23.
159. R V. Impairments of the musculoskeletal system. *In Pitha, Billroth, editors Handbook for Common and Special Surgery Stuttgart: Ferdinand Enkle* 1869: 845-920.
160. Hueter C. Anatomical study of the limb joints of newborns and adults. *Virchows Arch* 1862; **25**: 572-99.
161. Frost HM. A chondral modeling theory. *Calcif Tissue Int* 1979; **28**(3): 181-200.
162. Segesser B, Morscher E, Goesele A. [Lesions of the growth plate caused by sports stress]. *Orthopade* 1995; **24**(5): 446-56.
163. Lipp EJ. Athletic physeal injury in children and adolescents. *Orthop Nurs* 1998; **17**(2): 17-22.
164. Salminen JJ, Oksanen A, Maki P, Pentti J, Kujala UM. Leisure time physical activity in the young. Correlation with low-back pain, spinal mobility and trunk muscle strength in 15-year-old school children. *Int J Sports Med* 1993; **14**(7): 406-10.
165. Darling EM, Athanasiou KA. Biomechanical strategies for articular cartilage regeneration. *Ann Biomed Eng* 2003; **31**(9): 1114-24.
166. Siebenrock KA, Kaschka I, Frauchiger L, Werlen S, Schwab JM. Prevalence of cam-type deformity and hip pain in elite ice hockey players before and after the end of growth. *Am J Sports Med* 2013; **41**(10): 2308-13.
167. Gerhardt MB, Romero AA, Silvers HJ, Harris DJ, Watanabe D, Mandelbaum BR. The prevalence of radiographic hip abnormalities in elite soccer players. *Am J Sports Med* 2012; **40**(3): 584-8.
168. Johnson AC, Shaman MA, Ryan TG. Femoroacetabular impingement in former high-level youth soccer players. *Am J Sports Med* 2012; **40**(6): 1342-6.
169. McDermott ID, Amis AA. The consequences of meniscectomy. *J Bone Joint Surg Br* 2006; **88**(12): 1549-56.
170. MacMahon EB, Carmines DV, Irani RN. Physiologic bowing in children: an analysis of the pendulum mechanism. *J Pediatr Orthop B* 1995; **4**(1): 100-5.
171. Colyn W, Agricola R, Arnout N, Verhaar JA, Bellemans J. How does lower leg alignment differ between soccer players, other athletes, and non-athletic controls? *Knee Surg Sports Traumatol Arthrosc* 2016; **24**(11): 3619-26.
172. Venn M, Maroudas A. Chemical composition and swelling of normal and osteoarthrotic femoral head cartilage. I. Chemical composition. *Annals of the rheumatic diseases* 1977; **36**(2): 121-9.
173. Maroudas A, Bayliss MT, Venn MF. Further studies on the composition of human femoral head cartilage. *Annals of the rheumatic diseases* 1980; **39**(5): 514-23.
174. Weiss C, Rosenberg L, Helfet AJ. An ultrastructural study of normal young adult human articular cartilage. *J Bone Joint Surg Am* 1968; **50**(4): 663-74.
175. Jeffery AK, Blunn GW, Archer CW, Bentley G. Three-dimensional collagen architecture in bovine articular cartilage. *J Bone Joint Surg Br* 1991; **73**(5): 795-801.
176. Buckwalter JA, Mankin HJ. Articular cartilage: degeneration and osteoarthritis, repair, regeneration, and transplantation. *Instructional course lectures* 1998; **47**: 487-504.
177. Akizuki S, Mow VC, Muller F, Pita JC, Howell DS, Manicourt DH. Tensile properties of human knee joint cartilage: I. Influence of ionic conditions, weight bearing, and fibrillation on the tensile modulus. *Journal of orthopaedic research : official publication of the Orthopaedic Research Society* 1986; **4**(4): 379-92.
178. Palmer AJ, Brown CP, McNally EG, et al. Non-invasive imaging of cartilage in early osteoarthritis. *Bone Joint J* 2013; **95-B**(6): 738-46.

179. Bashir A, Gray ML, Burstein D. Gd-DTPA2- as a measure of cartilage degradation. *Magnetic resonance in medicine* 1996; **36**(5): 665-73.
180. Zilkens C, Miese F, Herten M, et al. Validity of gradient-echo three-dimensional delayed gadolinium-enhanced magnetic resonance imaging of hip joint cartilage: a histologically controlled study. *Eur J Radiol* 2013; **82**(2): e81-6.
181. Kim SD, Jessel R, Zurakowski D, Millis MB, Kim YJ. Anterior delayed gadolinium-enhanced MRI of cartilage values predict joint failure after periacetabular osteotomy. *Clinical orthopaedics and related research* 2012; **470**(12): 3332-41.
182. Bellin MF, Van Der Molen AJ. Extracellular gadolinium-based contrast media: an overview. *Eur J Radiol* 2008; **66**(2): 160-7.
183. Heverhagen JT, Krombach GA, Gizewski E. Application of extracellular gadolinium-based MRI contrast agents and the risk of nephrogenic systemic fibrosis. *Rofo* 2014; **186**(7): 661-9.
184. Gulani V, Calamante F, Shellock FG, Kanal E, Reeder SB, International Society for Magnetic Resonance in M. Gadolinium deposition in the brain: summary of evidence and recommendations. *Lancet Neurol* 2017; **16**(7): 564-70.
185. Nieminen MT, Rieppo J, Toyras J, et al. T2 relaxation reveals spatial collagen architecture in articular cartilage: a comparative quantitative MRI and polarized light microscopic study. *Magnetic resonance in medicine* 2001; **46**(3): 487-93.
186. Xia Y, Moody JB, Burton-Wurster N, Lust G. Quantitative in situ correlation between microscopic MRI and polarized light microscopy studies of articular cartilage. *Osteoarthritis and cartilage / OARS, Osteoarthritis Research Society* 2001; **9**(5): 393-406.
187. Wong CS, Yan CH, Gong NJ, Li T, Chan Q, Chu YC. Imaging biomarker with T1rho and T2 mappings in osteoarthritis - in vivo human articular cartilage study. *European journal of radiology* 2013; **82**(4): 647-50.
188. Chapple CM, Nicholson H, Baxter GD, Abbott JH. Patient characteristics that predict progression of knee osteoarthritis: a systematic review of prognostic studies. *Arthritis care & research* 2011; **63**(8): 1115-25.
189. Kijowski R, Blankenbaker DG, Munoz Del Rio A, Baer GS, Graf BK. Evaluation of the articular cartilage of the knee joint: value of adding a T2 mapping sequence to a routine MR imaging protocol. *Radiology* 2013; **267**(2): 503-13.
190. Crema MD, Roemer FW, Marra MD, et al. Articular cartilage in the knee: current MR imaging techniques and applications in clinical practice and research. *Radiographics* 2011; **31**(1): 37-61.
191. Van Ginckel A, Verdonk P, Victor J, Witvrouw E. Cartilage status in relation to return to sports after anterior cruciate ligament reconstruction. *Am J Sports Med* 2013; **41**(3): 550-9.
192. Luke AC, Stehling C, Stahl R, et al. High-field magnetic resonance imaging assessment of articular cartilage before and after marathon running: does long-distance running lead to cartilage damage? *Am J Sports Med* 2010; **38**(11): 2273-80.
193. Wong M, Carter DR. Articular cartilage functional histomorphology and mechanobiology: a research perspective. *Bone* 2003; **33**(1): 1-13.
194. Saamanen AM, Tammi M, Jurvelin J, Kiviranta I, Helminen HJ. Proteoglycan alterations following immobilization and remobilization in the articular cartilage of young canine knee (stifle) joint. *J Orthop Res* 1990; **8**(6): 863-73.
195. Saamanen AM, Tammi M, Kiviranta I, Helminen HJ. Running exercise as a modulatory of proteoglycan matrix in the articular cartilage of young rabbits. *Int J Sports Med* 1988; **9**(2): 127-33.

196. Kiviranta I, Tammi M, Jurvelin J, Saamanen AM, Helminen HJ. Moderate running exercise augments glycosaminoglycans and thickness of articular cartilage in the knee joint of young beagle dogs. *J Orthop Res* 1988; **6**(2): 188-95.
197. Saamanen AM, Tammi M, Kiviranta I, Jurvelin J, Helminen HJ. Levels of chondroitin-6-sulfate and nonaggregating proteoglycans at articular cartilage contact sites in the knees of young dogs subjected to moderate running exercise. *Arthritis Rheum* 1989; **32**(10): 1282-92.
198. Palmer JL, Bertone AL, Malemud CJ, Carter BG, Papay RS, Mansour J. Site-specific proteoglycan characteristics of third carpal articular cartilage in exercised and nonexercised horses. *Am J Vet Res* 1995; **56**(12): 1570-6.
199. Arokoski JP, Hyttinen MM, Helminen HJ, Jurvelin JS. Biomechanical and structural characteristics of canine femoral and tibial cartilage. *J Biomed Mater Res* 1999; **48**(2): 99-107.
200. Athanasiou KA, Rosenwasser MP, Buckwalter JA, Malinin TI, Mow VC. Interspecies comparisons of in situ intrinsic mechanical properties of distal femoral cartilage. *J Orthop Res* 1991; **9**(3): 330-40.
201. Slowman SD, Brandt KD. Composition and glycosaminoglycan metabolism of articular cartilage from habitually loaded and habitually unloaded sites. *Arthritis Rheum* 1986; **29**(1): 88-94.
202. Grodzinsky AJ, Levenston ME, Jin M, Frank EH. Cartilage tissue remodeling in response to mechanical forces. *Annu Rev Biomed Eng* 2000; **2**: 691-713.
203. Lyyra T, Arokoski JP, Oksala N, et al. Experimental validation of arthroscopic cartilage stiffness measurement using enzymatically degraded cartilage samples. *Phys Med Biol* 1999; **44**(2): 525-35.
204. Little CB, Ghosh P. Variation in proteoglycan metabolism by articular chondrocytes in different joint regions is determined by post-natal mechanical loading. *Osteoarthritis Cartilage* 1997; **5**(1): 49-62.
205. Brama PA, TeKoppele JM, Bank RA, Barneveld A, van Weeren PR. Development of biochemical heterogeneity of articular cartilage: influences of age and exercise. *Equine Vet J* 2002; **34**(3): 265-9.
206. Muhlbauer R, Lukasz TS, Faber TS, Stammberger T, Eckstein F. Comparison of knee joint cartilage thickness in triathletes and physically inactive volunteers based on magnetic resonance imaging and three-dimensional analysis. *Am J Sports Med* 2000; **28**(4): 541-6.
207. Eckstein F, Faber S, Muhlbauer R, et al. Functional adaptation of human joints to mechanical stimuli. *Osteoarthritis Cartilage* 2002; **10**(1): 44-50.
208. Eckstein F, Hudelmaier M, Putz R. The effects of exercise on human articular cartilage. *J Anat* 2006; **208**(4): 491-512.
209. Tiderius CJ, Svensson J, Leander P, Ola T, Dahlberg L. dGEMRIC (delayed gadolinium-enhanced MRI of cartilage) indicates adaptive capacity of human knee cartilage. *Magn Reson Med* 2004; **51**(2): 286-90.
210. Stehling C, Liebl H, Krug R, et al. Patellar cartilage: T2 values and morphologic abnormalities at 3.0-T MR imaging in relation to physical activity in asymptomatic subjects from the osteoarthritis initiative. *Radiology* 2010; **254**(2): 509-20.
211. Roos EM, Dahlberg L. Positive effects of moderate exercise on glycosaminoglycan content in knee cartilage: a four-month, randomized, controlled trial in patients at risk of osteoarthritis. *Arthritis Rheum* 2005; **52**(11): 3507-14.
212. Notzli HP, Wyss TF, Stoecklin CH, Schmid MR, Treiber K, Hodler J. The contour of the femoral head-neck junction as a predictor for the risk of anterior impingement. *J Bone Joint Surg Br* 2002; **84**(4): 556-60.

213. Dudda M, Albers C, Mamisch TC, Werlen S, Beck M. Do normal radiographs exclude asphericity of the femoral head-neck junction? *Clin Orthop Relat Res* 2009; **467**(3): 651-9.
214. Dimeglio A. Growth in pediatric orthopaedics. *J Pediatr Orthop* 2001; **21**(4): 549-55.
215. Fredensborg N. The CE angle of normal hips. *Acta Orthop Scand* 1976; **47**(4): 403-5.
216. Meszaros T, Kery L. Quantitative analysis of the growth of the hip joint. A radiological study. *Acta Orthop Scand* 1980; **51**(2): 275-83.
217. Chegini S, Beck M, Ferguson SJ. The effects of impingement and dysplasia on stress distributions in the hip joint during sitting and walking: a finite element analysis. *J Orthop Res* 2009; **27**(2): 195-201.
218. Yeung M, Kowalczuk M, Simunovic N, Ayeni OR. Hip arthroscopy in the setting of hip dysplasia: A systematic review. *Bone Joint Res* 2016; **5**(6): 225-31.
219. Anderson M, Green WT, Messner MB. Growth and predictions of growth in the lower extremities. *J Bone Joint Surg Am* 1963; **45-A**: 1-14.
220. Sun SS, Schubert CM, Chumlea WC, et al. National estimates of the timing of sexual maturation and racial differences among US children. *Pediatrics* 2002; **110**(5): 911-9.
221. Clausen MB, Zebis MK, Moller M, et al. High injury incidence in adolescent female soccer. *Am J Sports Med* 2014; **42**(10): 2487-94.
222. Pfirrmann CW, Mengiardi B, Dora C, Kalberer F, Zanetti M, Hodler J. Cam and pincer femoroacetabular impingement: characteristic MR arthrographic findings in 50 patients. *Radiology* 2006; **240**(3): 778-85.
223. Wall PD, Fernandez M, Griffin DR, Foster NE. Nonoperative treatment for femoroacetabular impingement: a systematic review of the literature. *PM&R* 2013; **5**(5): 418-26.
224. Crocker PR, Bailey DA, Faulkner RA, Kowalski KC, McGrath R. Measuring general levels of physical activity: preliminary evidence for the Physical Activity Questionnaire for Older Children. *Med Sci Sports Exerc* 1997; **29**(10): 1344-9.
225. Welk GJ, Corbin CB, Dale D. Measurement issues in the assessment of physical activity in children. *Res Q Exerc Sport* 2000; **71**(2 Suppl): S59-73.
226. Beaule PE, Hynes K, Parker G, Kemp KA. Can the alpha angle assessment of cam impingement predict acetabular cartilage delamination? *Clin Orthop Relat Res* 2012; **470**(12): 3361-7.
227. Yamasaki T, Yasunaga Y, Shoji T, Izumi S, Hachisuka S, Ochi M. Inclusion and Exclusion Criteria in the Diagnosis of Femoroacetabular Impingement. *Arthroscopy* 2015; **31**(7): 1403-10.
228. Gosvig KK, Jacobsen S, Palm H, Sonne-Holm S, Magnusson E. A new radiological index for assessing asphericity of the femoral head in cam impingement. *J Bone Joint Surg Br* 2007; **89**(10): 1309-16.
229. Ito K, Minka MA, 2nd, Leunig M, Werlen S, Ganz R. Femoroacetabular impingement and the cam-effect. A MRI-based quantitative anatomical study of the femoral head-neck offset. *J Bone Joint Surg Br* 2001; **83**(2): 171-6.
230. Lohan DG, Seeger LL, Motamedi K, Hame S, Sayre J. Cam-type femoral-acetabular impingement: is the alpha angle the best MR arthrography has to offer? *Skeletal Radiol* 2009; **38**(9): 855-62.
231. Clohisy JC, Carlisle JC, Beaule PE, et al. A systematic approach to the plain radiographic evaluation of the young adult hip. *J Bone Joint Surg Am* 2008; **90 Suppl 4**: 47-66.

232. Pollard TC, Villar RN, Norton MR, et al. Femoroacetabular impingement and classification of the cam deformity: the reference interval in normal hips. *Acta Orthop* 2010; **81**(1): 134-41.
233. Meyer DC, Beck M, Ellis T, Ganz R, Leunig M. Comparison of six radiographic projections to assess femoral head/neck asphericity. *Clin Orthop Relat Res* 2006; **445**: 181-5.
234. Kim C, Nevitt MC, Niu J, et al. Association of hip pain with radiographic evidence of hip osteoarthritis: diagnostic test study. *BMJ* 2015; **351**: h5983.
235. Barton C, Salineros MJ, Rakhra KS, Beaule PE. Validity of the alpha angle measurement on plain radiographs in the evaluation of cam-type femoroacetabular impingement. *Clin Orthop Relat Res* 2011; **469**(2): 464-9.
236. Young M, Dempsey M, Rocha Ade L, Podeszwa DA. The cross-table lateral radiograph results in a significantly increased effective radiation dose compared with the Dunn and single frog lateral radiographs. *J Pediatr Orthop* 2015; **35**(2): 157-61.
237. Clohisy JC, Nunley RM, Otto RJ, Schoenecker PL. The frog-leg lateral radiograph accurately visualized hip cam impingement abnormalities. *Clin Orthop Relat Res* 2007; **462**: 115-21.
238. Konan S, Rayan F, Haddad FS. Is the frog lateral plain radiograph a reliable predictor of the alpha angle in femoroacetabular impingement? *J Bone Joint Surg Br* 2010; **92**(1): 47-50.
239. Domayer SE, Ziebarth K, Chan J, Bixby S, Mamisch TC, Kim YJ. Femoroacetabular cam-type impingement: diagnostic sensitivity and specificity of radiographic views compared to radial MRI. *Eur J Radiol* 2011; **80**(3): 805-10.
240. Rakhra KS, Sheikh AM, Allen D, Beaule PE. Comparison of MRI alpha angle measurement planes in femoroacetabular impingement. *Clin Orthop Relat Res* 2009; **467**(3): 660-5.
241. Beaule PE, Zaragoza E, Motamedi K, Copelan N, Dorey FJ. Three-dimensional computed tomography of the hip in the assessment of femoroacetabular impingement. *J Orthop Res* 2005; **23**(6): 1286-92.
242. Rivas R, Shapiro F. Structural stages in the development of the long bones and epiphyses: a study in the New Zealand white rabbit. *J Bone Joint Surg Am* 2002; **84-A**(1): 85-100.
243. Fernquest S, Park D, Marcan M, Palmer A, Voiculescu I, Glyn-Jones S. Segmentation of hip cartilage in compositional magnetic resonance imaging: A fast, accurate, reproducible, and clinically viable semi-automated methodology. *J Orthop Res* 2018; **36**(8): 2280-7.
244. Lequesne M, de S. [False profile of the pelvis. A new radiographic incidence for the study of the hip. Its use in dysplasias and different coxopathies]. *Rev Rhum Mal Osteoartic* 1961; **28**: 643-52.
245. Heyman CH, Herndon CH. Legg-Perthes disease; a method for the measurement of the roentgenographic result. *J Bone Joint Surg Am* 1950; **32 A**(4): 767-78.
246. Lequesne M. [Coxometry. Measurement of the Basic Angles of the Adult Radiographic Hip by a Combined Protractor]. *Rev Rhum Mal Osteoartic* 1963; **30**: 479-85.
247. Saberi Hosnijeh F, Zuiderwijk ME, Versteeg M, et al. Cam Deformity and Acetabular Dysplasia as Risk Factors for Hip Osteoarthritis. *Arthritis Rheumatol* 2017; **69**(1): 86-93.
248. Wyles CC, Heidenreich MJ, Jeng J, Larson DR, Trousdale RT, Sierra RJ. The John Charnley Award: Redefining the Natural History of Osteoarthritis in Patients With Hip Dysplasia and Impingement. *Clin Orthop Relat Res* 2017; **475**(2): 336-50.

249. Cooperman DR, Wallensten R, Stulberg SD. Acetabular dysplasia in the adult. *Clin Orthop Relat Res* 1983; (175): 79-85.
250. Mayer SW, Abdo JC, Hill MK, Kestel LA, Pan Z, Novais EN. Femoroacetabular Impingement Is Associated With Sports-Related Posterior Hip Instability in Adolescents: A Matched-Cohort Study. *Am J Sports Med* 2016; **44**(9): 2299-303.
251. Armand M, Lepisto J, Tallroth K, Elias J, Chao E. Outcome of periacetabular osteotomy: joint contact pressure calculation using standing AP radiographs, 12 patients followed for average 2 years. *Acta Orthop* 2005; **76**(3): 303-13.
252. Hipp JA, Sugano N, Millis MB, Murphy SB. Planning acetabular redirection osteotomies based on joint contact pressures. *Clin Orthop Relat Res* 1999; (364): 134-43.
253. Michaeli DA, Murphy SB, Hipp JA. Comparison of predicted and measured contact pressures in normal and dysplastic hips. *Med Eng Phys* 1997; **19**(2): 180-6.
254. Meunier P, Lefevre C, Le Saout J, et al. [A simple method for measuring anteversion of the acetabulum from a frontal radiograph of the hip]. *J Radiol* 1987; **68**(12): 799-804.
255. Jamali AA, Mladenov K, Meyer DC, et al. Anteroposterior pelvic radiographs to assess acetabular retroversion: high validity of the "cross-over-sign". *J Orthop Res* 2007; **25**(6): 758-65.
256. Tannast M, Zheng G, Anderegg C, et al. Tilt and rotation correction of acetabular version on pelvic radiographs. *Clin Orthop Relat Res* 2005; **438**: 182-90.
257. Siebenrock KA, Kalbermatten DF, Ganz R. Effect of pelvic tilt on acetabular retroversion: a study of pelves from cadavers. *Clin Orthop Relat Res* 2003; (407): 241-8.
258. Abel MF, Sutherland DH, Wenger DR, Mubarak SJ. Evaluation of CT scans and 3-D reformatted images for quantitative assessment of the hip. *J Pediatr Orthop* 1994; **14**(1): 48-53.
259. Anda S, Svenningsen S, Grontvedt T, Benum P. Pelvic inclination and spatial orientation of the acetabulum. A radiographic, computed tomographic and clinical investigation. *Acta Radiol* 1990; **31**(4): 389-94.
260. Hoiseth A, Reikeras O, Fonstelien E. Lack of correlation between femoral neck anteversion and acetabular orientation. Radiography and computed tomography in cadavers and in vivo. *Acta Orthop Scand* 1989; **60**(1): 93-6.
261. Anda S, Terjesen T, Kvistad KA. Computed tomography measurements of the acetabulum in adult dysplastic hips: which level is appropriate? *Skeletal Radiol* 1991; **20**(4): 267-71.
262. Edelson JG, Hirsch M, Weinberg H, Attar D, Barmeir E. Congenital dislocation of the hip and computerised axial tomography. *J Bone Joint Surg Br* 1984; **66**(4): 472-8.
263. Jacquemier M, Jouve JL, Bollini G, Panuel M, Migliani R. Acetabular Anteversion in Children. *J Pediatr Orthoped* 1992; **12**(3): 373-5.
264. Visser JD, Jonkers A, Hillen B. Hip joint measurements with computerized tomography. *J Pediatr Orthop* 1982; **2**(2): 143-6.
265. Clohisy JC, Carlisle JC, Trousdale R, et al. Radiographic evaluation of the hip has limited reliability. *Clin Orthop Relat Res* 2009; **467**(3): 666-75.
266. Dandachli W, Kannan V, Richards R, Shah Z, Hall-Craggs M, Witt J. Analysis of cover of the femoral head in normal and dysplastic hips: new CT-based technique. *J Bone Joint Surg Br* 2008; **90**(11): 1428-34.
267. Dugdale TW, Noyes FR, Styer D. Preoperative planning for high tibial osteotomy. The effect of lateral tibiofemoral separation and tibiofemoral length. *Clin Orthop Relat Res* 1992; (274): 248-64.

268. Andrews M, Noyes FR, Hewett TE, Andriacchi TP. Lower limb alignment and foot angle are related to stance phase knee adduction in normal subjects: a critical analysis of the reliability of gait analysis data. *J Orthop Res* 1996; **14**(2): 289-95.
269. Iseki Y, Takahashi T, Takeda H, et al. Defining the load bearing axis of the lower extremity obtained from anterior-posterior digital radiographs of the whole limb in stance. *Osteoarthritis Cartilage* 2009; **17**(5): 586-91.
270. Coventry MB, Ilstrup DM, Wallrichs SL. Proximal tibial osteotomy. A critical long-term study of eighty-seven cases. *J Bone Joint Surg Am* 1993; **75**(2): 196-201.
271. Cooke TD, Sled EA, Scudamore RA. Frontal plane knee alignment: a call for standardized measurement. *J Rheumatol* 2007; **34**(9): 1796-801.
272. Yoshioka Y, Siu D, Cooke TD. The anatomy and functional axes of the femur. *J Bone Joint Surg Am* 1987; **69**(6): 873-80.
273. Yoshioka Y, Siu DW, Scudamore RA, Cooke TD. Tibial anatomy and functional axes. *J Orthop Res* 1989; **7**(1): 132-7.
274. Parratte S, Pagnano MW, Trousdale RT, Berry DJ. Effect of postoperative mechanical axis alignment on the fifteen-year survival of modern, cemented total knee replacements. *J Bone Joint Surg Am* 2010; **92**(12): 2143-9.
275. Petersen TL, Engh GA. Radiographic assessment of knee alignment after total knee arthroplasty. *J Arthroplasty* 1988; **3**(1): 67-72.
276. Nishii T, Shiomi T, Tanaka H, Yamazaki Y, Murase K, Sugano N. Loaded cartilage T2 mapping in patients with hip dysplasia. *Radiology* 2010; **256**(3): 955-65.
277. Stubendorff JJ, Lammentausta E, Struglics A, Lindberg L, Heinegard D, Dahlberg LE. Is cartilage sGAG content related to early changes in cartilage disease? Implications for interpretation of dGEMRIC. *Osteoarthritis Cartilage* 2012; **20**(5): 396-404.
278. Eckstein F, Ateshian G, Burgkart R, et al. Proposal for a nomenclature for magnetic resonance imaging based measures of articular cartilage in osteoarthritis. *Osteoarthritis Cartilage* 2006; **14**(10): 974-83.
279. Squires GR, Okouneff S, Ionescu M, Poole AR. The pathobiology of focal lesion development in aging human articular cartilage and molecular matrix changes characteristic of osteoarthritis. *Arthritis Rheum* 2003; **48**(5): 1261-70.
280. Subburaj K, Valentinitsch A, Dillon AB, et al. Regional variations in MR relaxation of hip joint cartilage in subjects with and without femoralacetabular impingement. *Magn Reson Imaging* 2013; **31**(7): 1129-36.
281. Ilizaliturri VM, Jr., Byrd JW, Sampson TG, et al. A geographic zone method to describe intra-articular pathology in hip arthroscopy: cadaveric study and preliminary report. *Arthroscopy* 2008; **24**(5): 534-9.
282. Philippon MJ, Stubbs AJ, Schenker ML, Maxwell RB, Ganz R, Leunig M. Arthroscopic management of femoroacetabular impingement: osteoplasty technique and literature review. *Am J Sports Med* 2007; **35**(9): 1571-80.
283. Griffin D. Inter-Observer Reliability of an Arthroscopic Hip Mapping System. *The Journal of bone and joint surgery British* 2011; **93**(B(SUPP II):149).
284. Fernquest S, Palmer A, Gammer B, et al. Compositional MRI of the Hip: Reproducibility, Effect of Joint Unloading, and Comparison of T2 Relaxometry with Delayed Gadolinium-Enhanced Magnetic Resonance Imaging of Cartilage. *Cartilage* 2019: 1947603519841670.
285. Surowiec RK, Lucas EP, Ho CP. Quantitative MRI in the evaluation of articular cartilage health: reproducibility and variability with a focus on T2 mapping. *Knee surgery, sports traumatology, arthroscopy : official journal of the ESSKA* 2014; **22**(6): 1385-95.
286. Mansournia MA, Altman DG. Inverse probability weighting. *BMJ* 2016; **352**: i189.

287. Dam EB, Loog M, Christiansen C, et al. Identification of progressors in osteoarthritis by combining biochemical and MRI-based markers. *Arthritis Res Ther* 2009; **11**(4): R115.
288. Albers CE, Steppacher SD, Haefeli PC, et al. Twelve percent of hips with a primary cam deformity exhibit a slip-like morphology resembling sequelae of slipped capital femoral epiphysis. *Clin Orthop Relat Res* 2015; **473**(4): 1212-23.
289. Carballido-Gamio J, Link TM, Li X, et al. Feasibility and reproducibility of relaxometry, morphometric, and geometrical measurements of the hip joint with magnetic resonance imaging at 3T. *J Magn Reson Imaging* 2008; **28**(1): 227-35.
290. Nemeth A, Di Marco L, Boutitie F, et al. Reproducibility of in vivo magnetic resonance imaging T1 rho and T2 relaxation time measurements of hip cartilage at 3.0T in healthy volunteers. *J Magn Reson Imaging* 2017; **47**(4): 1022-33.
291. Glaser C, Mendlik T, Dinges J, et al. Global and regional reproducibility of T2 relaxation time measurements in human patellar cartilage. *Magnetic resonance in medicine* 2006; **56**(3): 527-34.
292. Watanabe A, Boesch C, Siebenrock K, Obata T, Anderson SE. T2 mapping of hip articular cartilage in healthy volunteers at 3T: a study of topographic variation. *Journal of magnetic resonance imaging : JMRI* 2007; **26**(1): 165-71.
293. Mosher TJ, Zhang Z, Reddy R, et al. Knee articular cartilage damage in osteoarthritis: analysis of MR image biomarker reproducibility in ACRIN-PA 4001 multicenter trial. *Radiology* 2011; **258**(3): 832-42.
294. van Klij P, Heijboer MP, Ginai AZ, Verhaar JAN, Waarsing JH, Agricola R. Cam morphology in young male football players mostly develops before proximal femoral growth plate closure: a prospective study with 5-year follow-up. *Br J Sports Med* 2018; **53**(9): 532-8.
295. Griffin DR, Dickenson EJ, O'Donnell J, et al. The Warwick Agreement on femoroacetabular impingement syndrome (FAI syndrome): an international consensus statement. *Br J Sports Med* 2016; **50**(19): 1169-76.
296. Tak I, Weir A, Langhout R, et al. The relationship between the frequency of football practice during skeletal growth and the presence of a cam deformity in adult elite football players. *Br J Sports Med* 2015; **49**(9): 630-4.
297. Carson WG, Jr., Gasser SI. Little Leaguer's shoulder. A report of 23 cases. *Am J Sports Med* 1998; **26**(4): 575-80.
298. Wedge JH, Wasylenko MJ. The natural history of congenital disease of the hip. *J Bone Joint Surg Br* 1979; **61-B**(3): 334-8.
299. Stasikelis PJ, Sullivan CM, Phillips WA, Polard JA. Slipped capital femoral epiphysis. Prediction of contralateral involvement. *J Bone Joint Surg Am* 1996; **78**(8): 1149-55.
300. Kang AC, Gooding AJ, Coates MH, Goh TD, Armour P, Rietveld J. Computed tomography assessment of hip joints in asymptomatic individuals in relation to femoroacetabular impingement. *Am J Sports Med* 2010; **38**(6): 1160-5.
301. Murtha PE, Hafez MA, Jaramaz B, DiGioia AM, 3rd. Variations in acetabular anatomy with reference to total hip replacement. *J Bone Joint Surg Br* 2008; **90**(3): 308-13.
302. Hetsroni I, Dela Torre K, Duke G, Lyman S, Kelly BT. Sex differences of hip morphology in young adults with hip pain and labral tears. *Arthroscopy* 2013; **29**(1): 54-63.
303. Clohisy JC, Nunley RM, Carlisle JC, Schoenecker PL. Incidence and characteristics of femoral deformities in the dysplastic hip. *Clin Orthop Relat Res* 2009; **467**(1): 128-34.
304. Besier TF, Lloyd DG, Cochrane JL, Ackland TR. External loading of the knee joint during running and cutting maneuvers. *Med Sci Sports Exerc* 2001; **33**(7): 1168-75.

305. Greenwald AS, Haynes DW. Weight-bearing areas in the human hip joint. *J Bone Joint Surg Br* 1972; **54**(1): 157-63.
306. Grunder W, Kanowski M, Wagner M, Werner A. Visualization of pressure distribution within loaded joint cartilage by application of angle-sensitive NMR microscopy. *Magn Reson Med* 2000; **43**(6): 884-91.
307. Levitt MH. Symmetry constraints on spin dynamics: Application to hyperpolarized NMR. *J Magn Reson* 2016; **262**: 91-9.
308. Shao H, Pauli C, Li S, et al. Magic angle effect plays a major role in both T1rho and T2 relaxation in articular cartilage. *Osteoarthritis Cartilage* 2017; **25**(12): 2022-30.
309. Palmer AJR, Ayyar Gupta V, Fernquest S, et al. Arthroscopic hip surgery compared with physiotherapy and activity modification for the treatment of symptomatic femoroacetabular impingement: multicentre randomised controlled trial. *BMJ* 2019; **364**: l185.
310. Griffin DR, Dickenson EJ, Wall PDH, et al. Hip arthroscopy versus best conservative care for the treatment of femoroacetabular impingement syndrome (UK FASHIoN): a multicentre randomised controlled trial. *Lancet* 2018; **391**(10136): 2225-35.
311. Bland JM, Altman DG. Applying the right statistics: analyses of measurement studies. *Ultrasound Obstet Gynecol* 2003; **22**(1): 85-93.
312. Shrout PE, Fleiss JL. Intraclass correlations: uses in assessing rater reliability. *Psychol Bull* 1979; **86**(2): 420-8.
313. Dunn G. Statistical methods in laboratory medicine. *Stat Methods Med Res* 1999; **8**(2): 91.
314. Bland JM, Altman DG. Statistical methods for assessing agreement between two methods of clinical measurement. *Lancet* 1986; **1**(8476): 307-10.
315. Gluer CC, Blake G, Lu Y, Blunt BA, Jergas M, Genant HK. Accurate assessment of precision errors: how to measure the reproducibility of bone densitometry techniques. *Osteoporos Int* 1995; **5**(4): 262-70.

Appendix Contents

Appendix A - Methods 358

A.1 Physical Activity Questionnaire for Children and Adolescents 358

A.1.1 Scoring 358

A.2 Validity, Reliability, and Reproducibility 365

A.2.1 Measurement Error 365

A.2.2 Reproducibility Statistics 365

A.3 Bland-Altman Plots for Imaging Outcome Measures 368

Appendix Tables and Figures

Appendix A-1 – Physical Activity Questionnaire Score for Children.....359

Appendix A-2 – Physical Activity Questionnaire Score for Adolescents.....362

Appendix A-3 - Bland-Altman Plot for Average Alpha Angle Intra-Observer Reproducibility 368

Appendix A-4 - Bland-Altman Plot for Average Alpha Angle Inter-Observer Reproducibility.....369

Appendix A-5 - Bland-Altman Plot for Lateral Epiphyseal Extension Intra-Observer Reproducibility.....369

Appendix A-6 - Bland-Altman Plot for Lateral Epiphyseal Extension Inter-Observer Reproducibility.....370

Appendix A-7 - Bland-Altman Plot for Fibro-chondro-osseous Tissue Area Intra-Observer Reproducibility 370

Appendix A-8 - Bland-Altman Plot for Fibro-chondro-osseous Tissue Area Inter-Observer Reproducibility 371

Appendix A-9 - Bland-Altman Plot for Lateral Centre Edge Angle Intra-Observer Reproducibility 371

Appendix A-10 - Bland-Altman Plot for Lateral Centre Edge Angle Inter-Observer Reproducibility 372

Appendix A-11 - Bland-Altman Plot for Anterior Centre Edge Angle Intra-Observer Reproducibility.....372

Appendix A-12 - Bland-Altman Plot for Anterior Centre Edge Angle Inter-Observer Reproducibility.....373

Appendix A-13 - Bland-Altman Plot for Anteversion Intra-Observer Reproducibility 373

Appendix A-14 - Bland-Altman Plot for Anteversion Inter-Observer Reproducibility 374

Appendix A-15 - Bland-Altman Plot for Hip Knee Angle Intra-Observer Reproducibility 374

Appendix A-16 - Bland-Altman Plot for Hip Knee Angle Inter-Observer Reproducibility.....375

Appendix A-17 - Bland-Altman Plot for Weight Bearing Ratio Intra-Observer Reproducibility 375

Appendix A-18 - Bland-Altman Plot for Weight Bearing Ratio Inter-Observer Reproducibility 376

Appendix A-19 - Bland-Altman Plot for Mean Neck Shaft Angle Intra-Observer Reproducibility 376

Appendix A-20 - Bland-Altman Plot for Mean Neck Shaft Angle Inter-Observer Reproducibility 377

Appendix A-21 - Bland-Altman Plot for Medial Proximal Femoral Angle Intra-Observer Reproducibility.377

Appendix A-22 - Bland-Altman Plot for Medial Proximal Femoral Angle Inter-Observer Reproducibility.378

Appendix A-23 - Bland-Altman Plot for Lateral Proximal Femoral Angle Intra-Observer Reproducibility.378

Appendix A-24 - Bland-Altman Plot for Lateral Proximal Femoral Angle Inter-Observer Reproducibility.379

Appendix A-25 - Bland-Altman Plot for Mechanical Lateral Distal Femoral Angle Intra-Observer Reproducibility.....379

Appendix A-26 - Bland-Altman Plot for Mechanical Lateral Distal Femoral Angle Inter-Observer Reproducibility.....380

Appendix A-27 - Bland-Altman Plot for Anatomical Lateral Distal Femoral Angle Intra-Observer Reproducibility.....380

Appendix A-28 - Bland-Altman Plot for Anatomical Lateral Distal Femoral Angle Inter-Observer Reproducibility.....381

Appendix A-29 - Bland-Altman Plot for Joint Line Congruence Angle Intra-Observer Reproducibility.....381

Appendix A-30 - Bland-Altman Plot for Joint Line Congruence Angle Inter-Observer Reproducibility.....382

Appendix A-31 - Bland-Altman Plot for Mechanical Medial Proximal Tibial Angle Intra-Observer Reproducibility.....382

Appendix A-32 - Bland-Altman Plot for Mechanical Medial Proximal Tibial Angle Inter-Observer Reproducibility.....383

Appendix A-33 - Bland-Altman Plot for Anatomical Medial Proximal Tibial Angle Intra-Observer Reproducibility.....383

Appendix A-34 - Bland-Altman Plot for Anatomical Medial Proximal Tibial Angle Inter-Observer Reproducibility.....384

Appendix A-35 - Bland-Altman Plot for Mechanical Lateral Distal Tibial Angle Intra-Observer Reproducibility.....384

Appendix A-36 - Bland-Altman Plot for Mechanical Lateral Distal Tibial Angle Inter-Observer Reproducibility.....385

Appendix A-37 - Bland-Altman Plot for Anatomical Lateral Distal Tibial Angle Intra-Observer Reproducibility.....385

Appendix A-38 - Bland-Altman Plot for Anatomical Lateral Distal Tibial Angle Inter-Observer Reproducibility.....386

Appendix A-39 - Bland-Altman Plot for Leg Length Discrepancy Intra-Observer Reproducibility.....386

Appendix A-40 - Bland-Altman Plot for Leg Length Discrepancy Inter-Observer Reproducibility.....387

Appendix A-41 - Bland-Altman Plot for Medial Proximal Tibial Physis Angle Intra-Observer Reproducibility.....387

Appendix A-42 - Bland-Altman Plot for Medial Proximal Tibial Physis Angle Inter-Observer Reproducibility.....388

Appendix A-43 - Bland-Altman Plot for Lateral Distal Femoral Physis Angle Intra-Observer Reproducibility 388

Appendix A-44 - Bland-Altman Plot for Lateral Distal Femoral Physis Angle Inter-Observer Reproducibility 389

Appendix A-45 - Bland-Altman Plot for Compositional MRI (T2) Intra-Observer Reproducibility 389

Appendix A-46 - Bland-Altman Plot for Compositional MRI (T2) Inter-Observer Reproducibility 390

Appendix A-47 - Intra and inter observer reproducibility of T2 image analysis for each region. 391

Appendix A-48 - Kernel Density Plot of Residuals for Regression of Change in Average Alpha Angle with Age.....392

Appendix A-49 - Residuals Versus Fitted Values for Regression of Change in Average Alpha Angle with Age.....392

Appendix A-50 - Kernel Density Plot of Residuals for Regression of Change in Lateral Centre Edge Angle with Age.....393

Appendix A-51 - Residuals Versus Fitted Values for Regression of Change in Lateral Centre Edge Angle with Age.....393

Appendix A-52 - Kernel Density Plot of Residuals for Regression of Change in Anterior Centre Edge Angle with Age.....394

Appendix A-53 - Residuals Versus Fitted Values for Regression of Change in Anterior Centre Edge Angle with Age.....394

Appendix A-54 - Kernel Density Plot of Residuals for Regression of Change in Anteversion with Age 395

Appendix A-55 - Residuals Versus Fitted Values for Regression of Change in Anteversion with Age.....395

Appendix A-56 - Kernel Density Plot of Residuals for Regression of Hip Knee Angle with Age 396

Appendix A-57 - Residuals Versus Fitted Values for Regression of Hip Knee Angle with Age.....396

Appendix A - Methods

A.1 Physical Activity Questionnaire for Children and Adolescents

A.1.1 Scoring

Item 1 – take the mean of all activities ('no" activity being a 1, "7 times or more" being a %) o the activity checklist to form a composite score for item 1.

Items 2 to 8 – the answers for each item start from the lowest activity response and progress to the highest activity response. Use the reported value that is checked off for each item (the lowest activity response being a 1 and the highest activity response being a 5).

Item 9 – take the mean of all days of the week ('none' being a 1, "very often" being a 5) to form a composite score for item 9

Item 10 – can be used to identify children who had unusual activity during the previous week, but this question is not used as part of the summary activity score

Calculate final score – take the mean score (1 to 5) for each of the 9 items. A score of 1 indicates low physical activity, whereas a score of 5 indicates high physical activity

Appendix A-1 – Physical Activity Questionnaire Score for Children

Physical Activity Questionnaire (Elementary School)

Name:_____ Age:_____

Sex: M_____ F_____ Grade:_____

Teacher:_____

We are trying to find out about your level of physical activity from *the last 7 days* (in the last week). This includes sports or dance that make you sweat or make your legs feel tired, or games that make you breathe hard, like tag, skipping, running, climbing, and others.

Remember:
1. There are no right and wrong answers — this is not a test.
2. Please answer all the questions as honestly and accurately as you can — this is very important.

---

1. Physical activity in your spare time: Have you done any of the following activities in the past 7 days (last week)? If yes, how many times? (Mark only one circle per row.)

	No	1-2	3-4	5-6	7 times or more
Skipping	❍	❍	❍	❍	❍
Rowing/canoeing	❍	❍	❍	❍	❍
In-line skating	❍	❍	❍	❍	❍
Tag	❍	❍	❍	❍	❍
Walking for exercise	❍	❍	❍	❍	❍
Bicycling	❍	❍	❍	❍	❍
Jogging or running	❍	❍	❍	❍	❍
Aerobics	❍	❍	❍	❍	❍
Swimming	❍	❍	❍	❍	❍
Baseball, softball	❍	❍	❍	❍	❍
Dance	❍	❍	❍	❍	❍
Football	❍	❍	❍	❍	❍
Badminton	❍	❍	❍	❍	❍
Skateboarding	❍	❍	❍	❍	❍
Soccer	❍	❍	❍	❍	❍
Street hockey	❍	❍	❍	❍	❍
Volleyball	❍	❍	❍	❍	❍
Floor hockey	❍	❍	❍	❍	❍
Basketball	❍	❍	❍	❍	❍
Ice skating	❍	❍	❍	❍	❍
Cross-country skiing	❍	❍	❍	❍	❍
Ice hockey/ringette	❍	❍	❍	❍	❍
Other:					
_____	❍	❍	❍	❍	❍
_____	❍	❍	❍	❍	❍

2. In the last 7 days, during your physical education (PE) classes, how often were you very active (playing hard, running, jumping, throwing)? (Check one only.)

I don't do PE ..... ❍
Hardly ever ..... ❍
Sometimes ..... ❍
Quite often ..... ❍
Always ..... ❍

3. In the last 7 days, what did you do most of the time *at recess*? (Check one only.)

Sat down (talking, reading, doing schoolwork)..... ❍
Stood around or walked around ..... ❍
Ran or played a little bit ..... ❍
Ran around and played quite a bit ..... ❍
Ran and played hard most of the time ..... ❍

4. In the last 7 days, what did you normally do *at lunch* (besides eating lunch)? (Check one only.)

Sat down (talking, reading, doing schoolwork)..... ❍
Stood around or walked around ..... ❍
Ran or played a little bit ..... ❍
Ran around and played quite a bit ..... ❍
Ran and played hard most of the time ..... ❍

5. In the last 7 days, on how many days *right after school*, did you do sports, dance, or play games in which you were very active? (Check one only.)

None ..... ❍
1 time last week ..... ❍
2 or 3 times last week ..... ❍
4 times last week ..... ❍
5 times last week ..... ❍

6. In the last 7 days, on how many *evenings* did you do sports, dance, or play games in which you were very active? (Check one only.)

None ..... ❍
1 time last week ..... ❍
2 or 3 times last week ..... ❍
4 or 5 last week ..... ❍
6 or 7 times last week ..... ❍

7. *On the last weekend*, how many times did you do sports, dance, or play games in which you were very active? (Check one only.)

None ..... ❍
1 time ..... ❍
2 — 3 times ..... ❍
4 — 5 times ..... ❍
6 or more times ..... ❍

8. Which *one* of the following describes you best for the last 7 days? Read *all five* statements before deciding on the *one* answer that describes you.

A. All or most of my free time was spent doing things that involve little physical effort ..... ❍

B. I sometimes (1 — 2 times last week) did physical things in my free time (e.g. played sports, went running, swimming, bike riding, did aerobics) ..... ❍

C. I often (3 — 4 times last week) did physical things in my free time ..... ❍

D. I quite often (5 — 6 times last week) did physical things in my free time ..... ❍

E. I very often (7 or more times last week) did physical things in my free time ..... ❍

9. Mark how often you did physical activity (like playing sports, games, doing dance, or any other physical activity) for each day last week.

	None	Little bit	Medium	Often	Very often
Monday	❍	❍	❍	❍	❍
Tuesday	❍	❍	❍	❍	❍
Wednesday	❍	❍	❍	❍	❍
Thursday	❍	❍	❍	❍	❍
Friday	❍	❍	❍	❍	❍
Saturday	❍	❍	❍	❍	❍
Sunday	❍	❍	❍	❍	❍

10. Were you sick last week, or did anything prevent you from doing your normal physical activities? (Check one.)

Yes ..... ❍
No ..... ❍

If Yes, what prevented you? _____

Appendix A-2 – Physical Activity Questionnaire Score for Adolescents

Physical Activity Questionnaire (High School)

Name:_____ Age:_____

Sex: M_____ F_____ Grade:_____

Teacher:_____

We are trying to find out about your level of physical activity from *the last 7 days* (in the last week). This includes sports or dance that make you sweat or make your legs feel tired, or games that make you breathe hard, like tag, skipping, running, climbing, and others.

Remember:

3. There are no right and wrong answers — this is not a test.
4. Please answer all the questions as honestly and accurately as you can — this is very important.

---

1. Physical activity in your spare time: Have you done any of the following activities in the past 7 days (last week)? If yes, how many times? (Mark only one circle per row.)

	No	1-2	3-4	5-6	7 times or more
Skipping	❍	❍	❍	❍	❍
Rowing/canoeing	❍	❍	❍	❍	❍
In-line skating	❍	❍	❍	❍	❍
Tag	❍	❍	❍	❍	❍
Walking for exercise	❍	❍	❍	❍	❍
Bicycling	❍	❍	❍	❍	❍
Jogging or running	❍	❍	❍	❍	❍
Aerobics	❍	❍	❍	❍	❍
Swimming	❍	❍	❍	❍	❍
Baseball, softball	❍	❍	❍	❍	❍
Dance	❍	❍	❍	❍	❍
Football	❍	❍	❍	❍	❍
Badminton	❍	❍	❍	❍	❍
Skateboarding	❍	❍	❍	❍	❍
Soccer	❍	❍	❍	❍	❍
Street hockey	❍	❍	❍	❍	❍
Volleyball	❍	❍	❍	❍	❍
Floor hockey	❍	❍	❍	❍	❍
Basketball	❍	❍	❍	❍	❍
Ice skating	❍	❍	❍	❍	❍
Cross-country skiing	❍	❍	❍	❍	❍
Ice hockey/ringette	❍	❍	❍	❍	❍
Other:					
_____	❍	❍	❍	❍	❍
_____	❍	❍	❍	❍	❍

2. In the last 7 days, during your physical education (PE) classes, how often were you very active (playing hard, running, jumping, throwing)? (Check one only.)

I don't do PE ..... ❍
Hardly ever ..... ❍
Sometimes ..... ❍
Quite often ..... ❍
Always ..... ❍

3. In the last 7 days, what did you normally do *at lunch* (besides eating lunch)? (Check one only.)

Sat down (talking, reading, doing schoolwork)..... ❍
Stood around or walked around ..... ❍
Ran or played a little bit ..... ❍
Ran around and played quite a bit ..... ❍
Ran and played hard most of the time ..... ❍

4. In the last 7 days, on how many days *right after school*, did you do sports, dance, or play games in which you were very active? (Check one only.)

None ..... ❍
1 time last week ..... ❍
2 or 3 times last week ..... ❍
4 times last week ..... ❍
5 times last week ..... ❍

5. In the last 7 days, on how many *evenings* did you do sports, dance, or play games in which you were very active? (Check one only.)

None ..... ❍
1 time last week ..... ❍
2 or 3 times last week ..... ❍
4 or 5 last week ..... ❍
6 or 7 times last week ..... ❍

6. *On the last weekend*, how many times did you do sports, dance, or play games in which you were very active? (Check one only.)

None ..... ❍
1 time ..... ❍
2 — 3 times ..... ❍
4 — 5 times ..... ❍
6 or more times ..... ❍

7. Which *one* of the following describes you best for the last 7 days? Read *all five* statements before deciding on the *one* answer that describes you.

F. All or most of my free time was spent doing things that involve little physical effort ..... ❍

G. I sometimes (1 — 2 times last week) did physical things in my free time (e.g. played sports, went running, swimming, bike riding, did aerobics) ..... ❍

H. I often (3 — 4 times last week) did physical things in my free time ..... ❍

I. I quite often (5 — 6 times last week) did physical things in my free time ..... ❍

J. I very often (7 or more times last week) did physical things in my free time ..... ❍

8. Mark how often you did physical activity (like playing sports, games, doing dance, or any other physical activity) for each day last week.

	None	Little bit	Medium	Often	Very often
Monday	❍	❍	❍	❍	❍
Tuesday	❍	❍	❍	❍	❍
Wednesday	❍	❍	❍	❍	❍
Thursday	❍	❍	❍	❍	❍
Friday	❍	❍	❍	❍	❍
Saturday	❍	❍	❍	❍	❍
Sunday	❍	❍	❍	❍	❍

9. Were you sick last week, or did anything prevent you from doing your normal physical activities? (Check one.)

Yes ..... ❍
No ..... ❍

If Yes, what prevented you? _____

A.2 Validity, Reliability, and Reproducibility

A.2.1 Measurement Error

Measurements are prone to errors that may arise from many sources and may pertain to the observer, the measurement tool, or physiological variation. The performance of a measurement may be viewed in terms of accuracy and precision. Accuracy reflects the degree to which measured values deviate from true values, hence validity. In imaging studies, it is difficult to establish true values, and measurements are usually compared with an existing gold-standard technique.

Precision errors describe the repeatability and reproducibility of a measurement, which is critical when assessing longitudinal change. Repeatability describes the variation in repeat measurements made on the same subject under identical conditions, where all variability represents measurement error. Reproducibility describes the variation in repeat measurements under changing conditions. Examples of changing conditions are when the same measurement is performed by different observers, or by the same observer but after a period of time.

A.2.2 Reproducibility Statistics

Precision errors may be quantified using several statistical methods and those most frequently used are Intraclass Correlation Coefficient (ICC), Coefficients of Variation (CV), Standard Error Measurement (SEM), and Limits of Agreement (LA). ICCs and CVs assess reliability, which determines the ability to discriminate between subjects after taking measurement error into account. LAs assess agreement, which is the absolute

difference between values after repeated measurements and can be used to determine the smallest difference that is detectable within a cohort.

Correlation coefficients evaluate relative reliability and assess the magnitude of measurement error relative to the underlying variability of the true values. As the correlation coefficient of two measurements on the same subject increases, it suggests that less of the variability is derived from measurement error. A coefficient of 1 suggests perfect correlation between readings with no measurement error, whereas a coefficient of 0 suggests no correlation between readings. There are no predefined limits of acceptability for a measurement tool. Interclass Correlation Coefficients (Pearson's Correlation) does not account for systematic differences in values and looks for association rather than agreement[311]. Systematic bias can be detected using a paired t-test, although this is influenced by the amount of random variation between tests. Intraclass Correlation Coefficients (ICC) can be used in a way that is sensitive to

systematic bias[312], and also has the advantage of being a univariate rather than bivariate test, which allows the assessment of repeated measures. However, all correlation coefficients are influenced by the range and distribution of the data and are only relevant to other cohorts when data is of equal heterogeneity. Correlation coefficients should therefore not be reported alone.

CV and SEM measure absolute reliability by assessing the variation between

measurements in relation to the mean value of all the measurements. CV is expressed as a percentage and is often used to supplement ICCs, since it is unaffected by the range

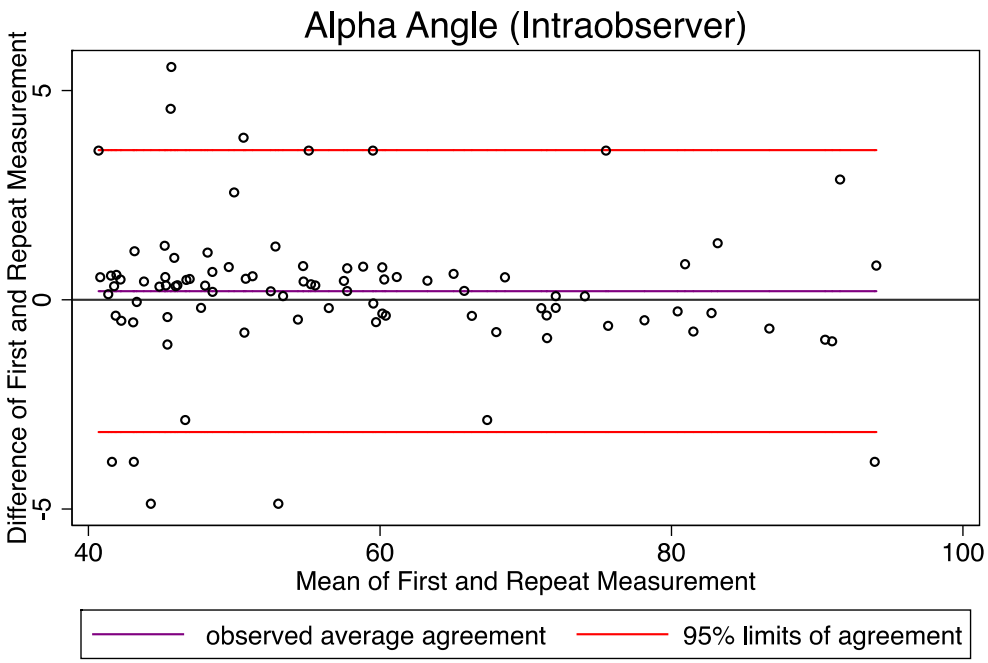
and distribution of data and accounts for heteroscedasticity. It only has a useful interpretation if the measurement scale is positive with zero as the minimum value. Careful interpretation is essential, as CV of 10% means that 68% of the differences between tests lie within 10% of the mean[313]. An alternative method of assessing absolute reliability is the SEM, but in addition to similar limitations as for CVs, it is affected by heteroscedasticity and does not carry the advantage of providing a dimensionless statistic to compare performance between measurement tools. Furthermore, the many different methods used to calculate this statistic are often a source of confusion. LAs quantify the absolute disparity between two measurements in relation to the mean value of all the measurements[314]. This accounts for systematic bias that is not considered with ICCs or CVs. Assuming the mean difference between readings is zero and values are normally distributed, the limits of agreement are defined as -1.96*SD and +1.96*SD, where SD is the standard deviation of the differences between measurements. This defines the range in which 95% of values will agree and is often used to determine the Smallest Detectable Difference (SDD) in measurements.

When performing the above calculations, the root of mean squares (rather than the arithmetic mean) is used to calculate standard deviation and the degrees of freedom is correct for the dataset in order to avoid underestimation of imprecision by up to 25% and 41%, respectively[315]. With the exception of CV, when there is evidence of heteroscedasticity, data should be logarithmically transformed prior to reliability and agreement testing. All of the above measures of precision are estimates and it is therefore necessary to calculate Confidence Intervals (CIs).

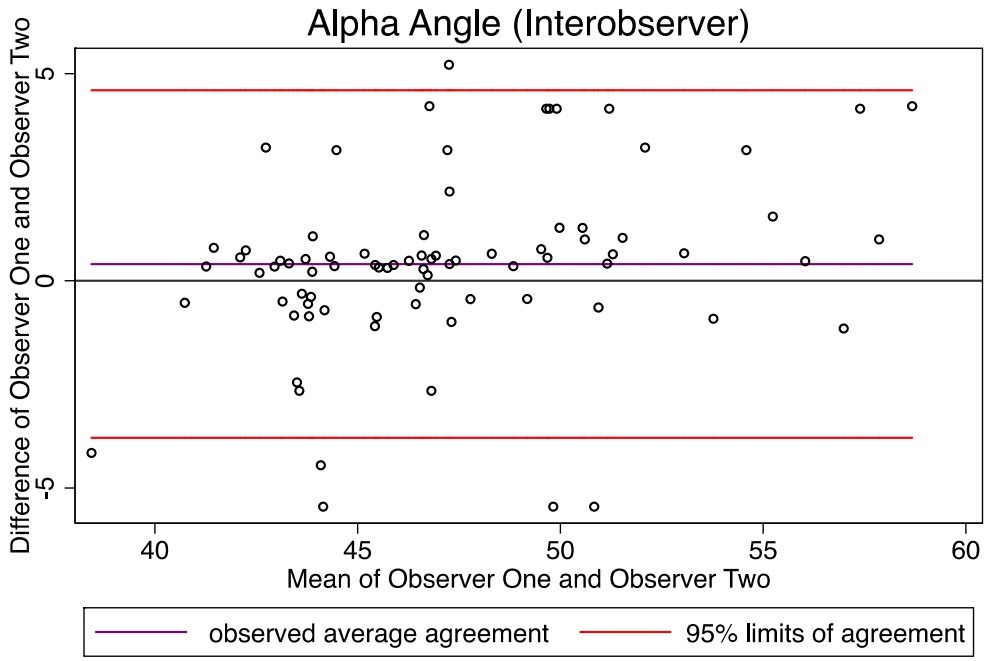
A.3 Bland-Altman Plots for Imaging Outcome Measures

Bland-Altman plots have been produced to illustrate intra-observer and inter-observer reproducibility for each of the imaging outcome measures. Plots include the mean difference between the two measurements and 95% limits of agreements calculated as 1.96 * standard deviation.

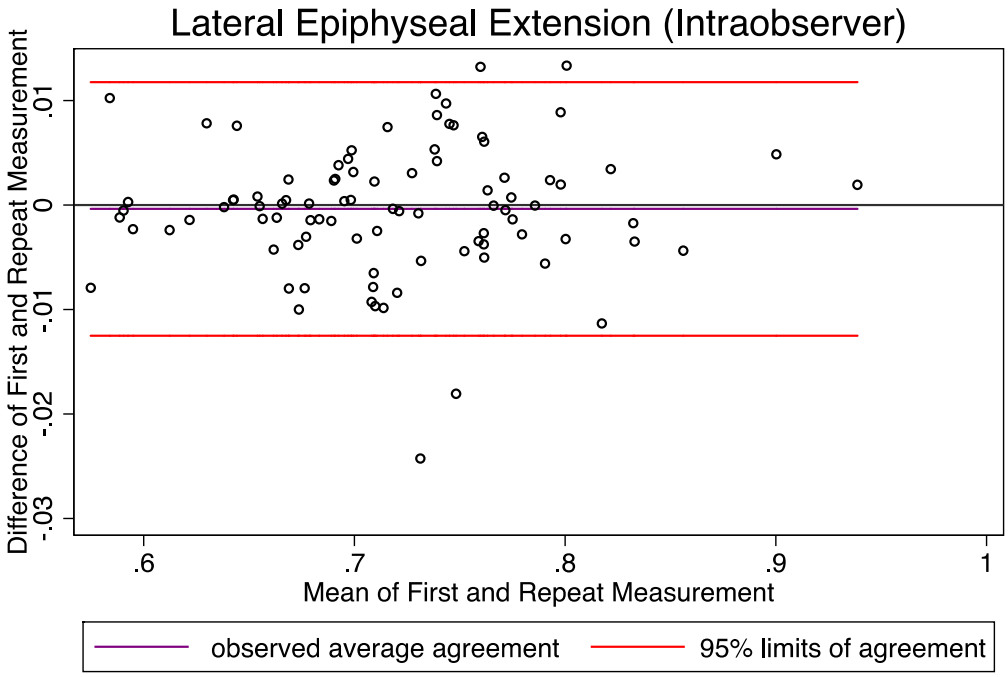
Appendix A-3 - Bland-Altman Plot for Average Alpha Angle Intra-Observer Reproducibility



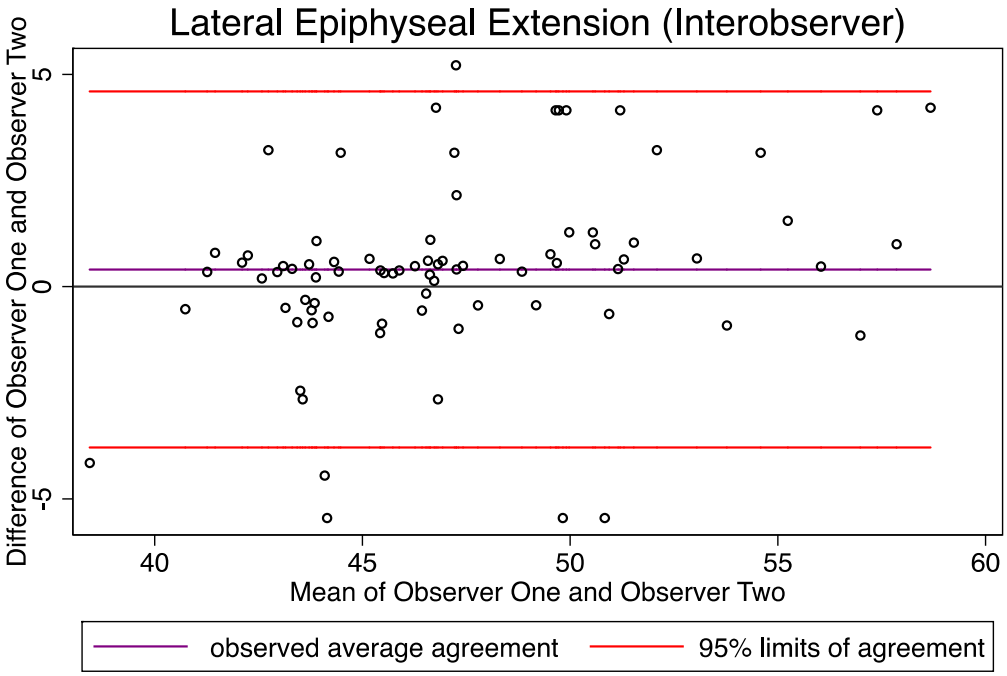
Appendix A-4 - Bland-Altman Plot for Average Alpha Angle Inter-Observer Reproducibility



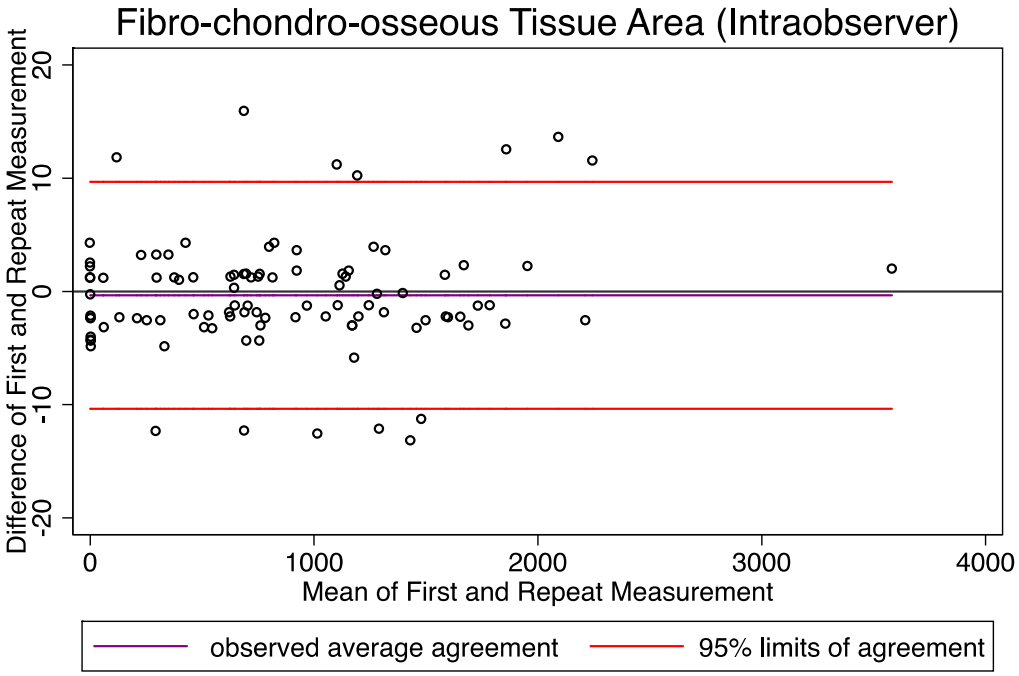
Appendix A-5 - Bland-Altman Plot for Lateral Epiphyseal Extension Intra-Observer Reproducibility



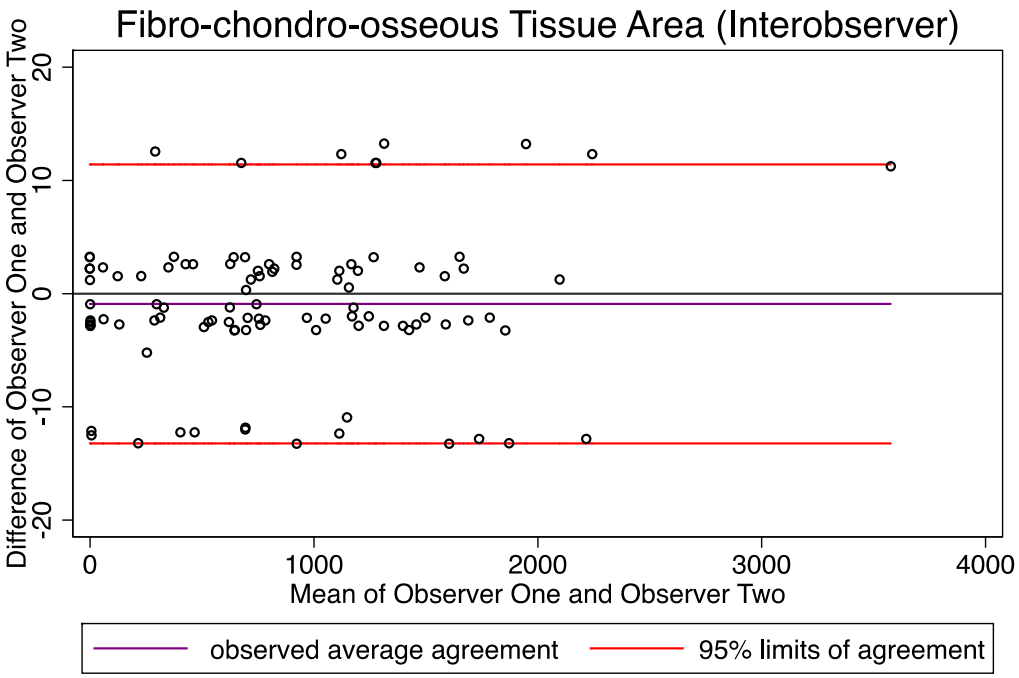
Appendix A-6 - Bland-Altman Plot for Lateral Epiphyseal Extension Inter-Observer Reproducibility



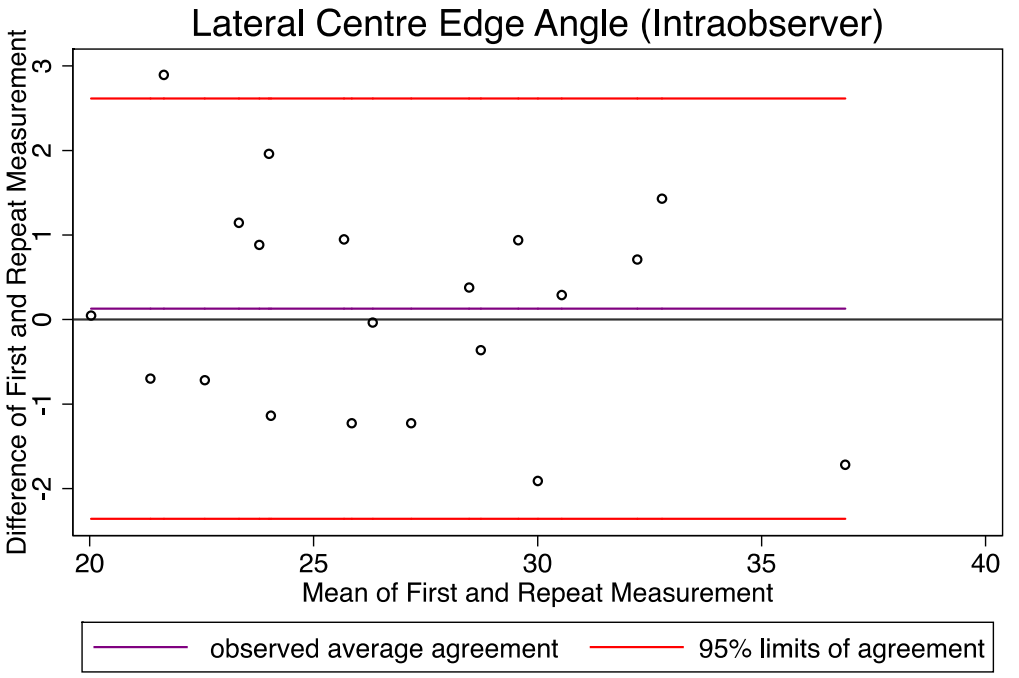
Appendix A-7 - Bland-Altman Plot for Fibro-chondro-osseous Tissue Area Intra-Observer Reproducibility



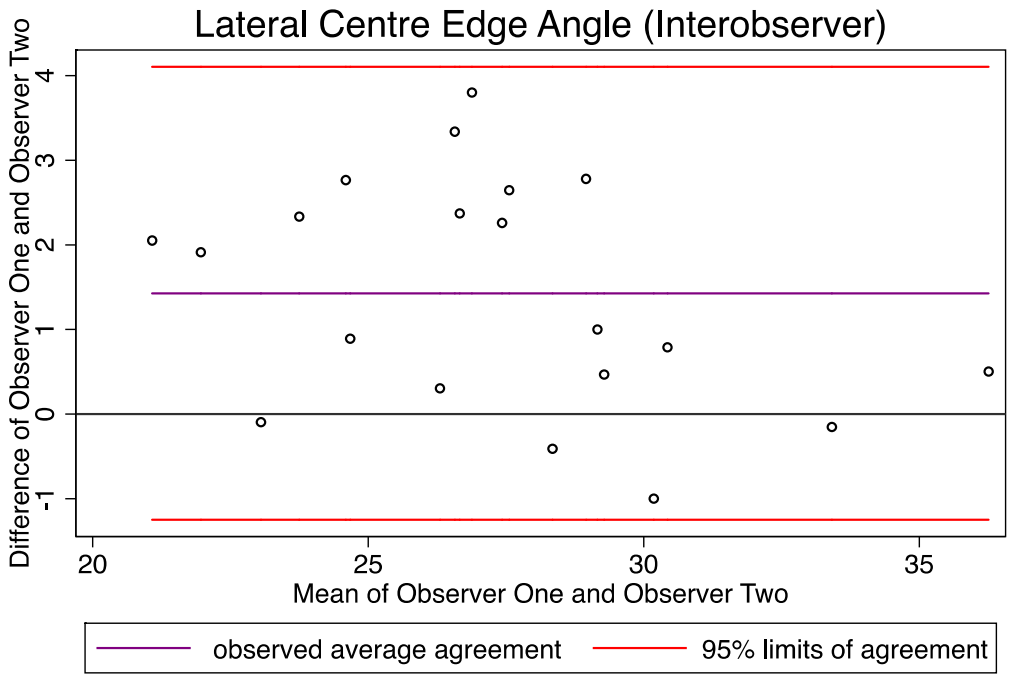
Appendix A-8 - Bland-Altman Plot for Fibro-chondro-osseous Tissue Area Inter-Observer Reproducibility



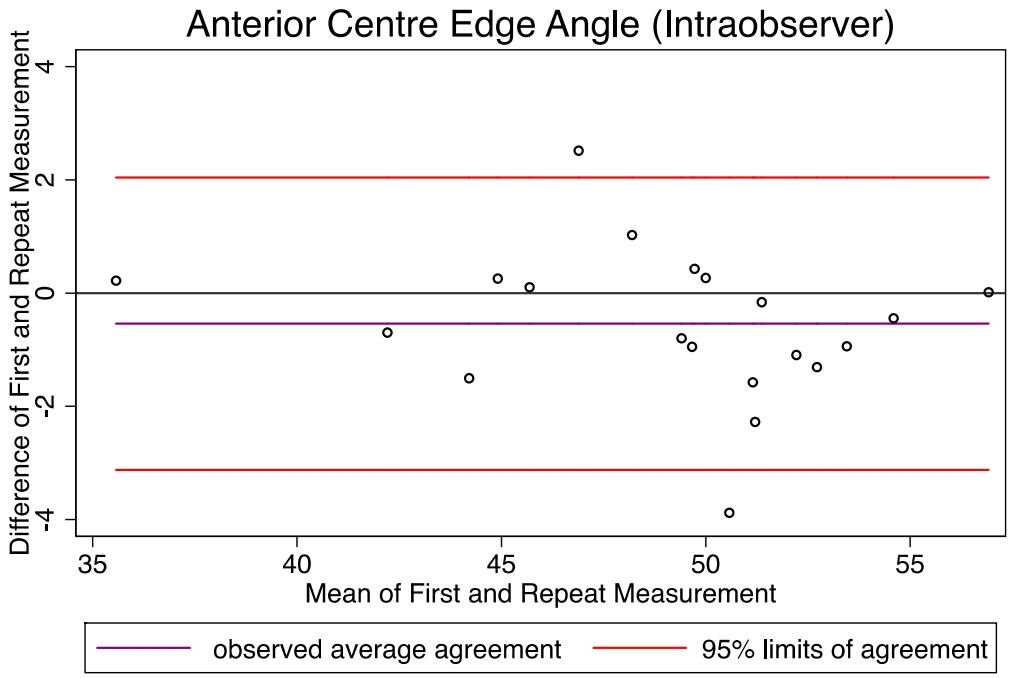
Appendix A-9 - Bland-Altman Plot for Lateral Centre Edge Angle Intra-Observer Reproducibility



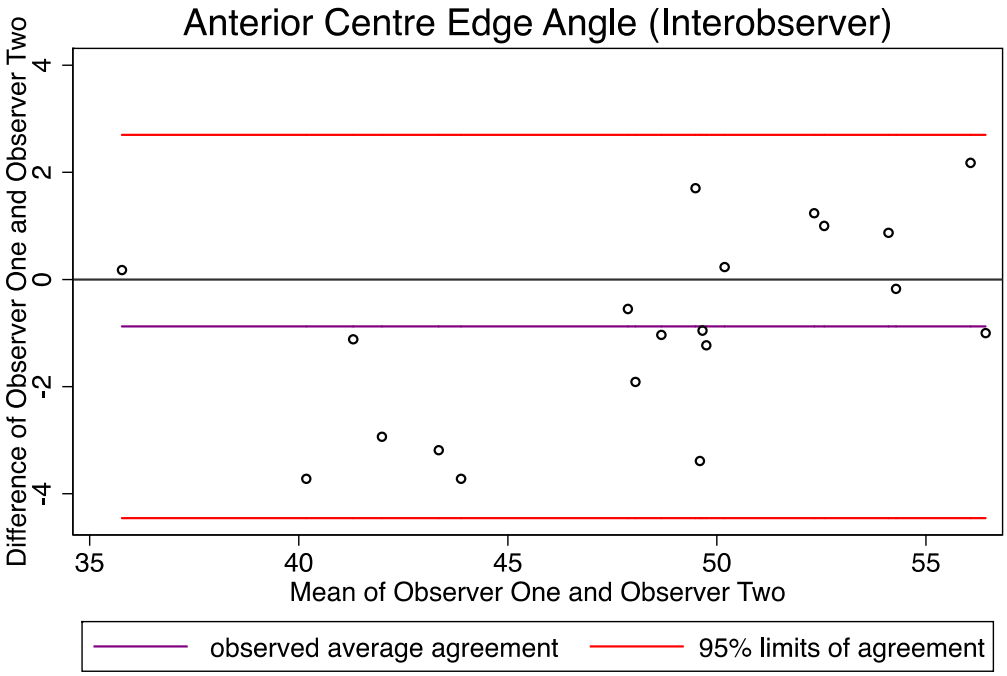
Appendix A-10 - Bland-Altman Plot for Lateral Centre Edge Angle Inter-Observer Reproducibility



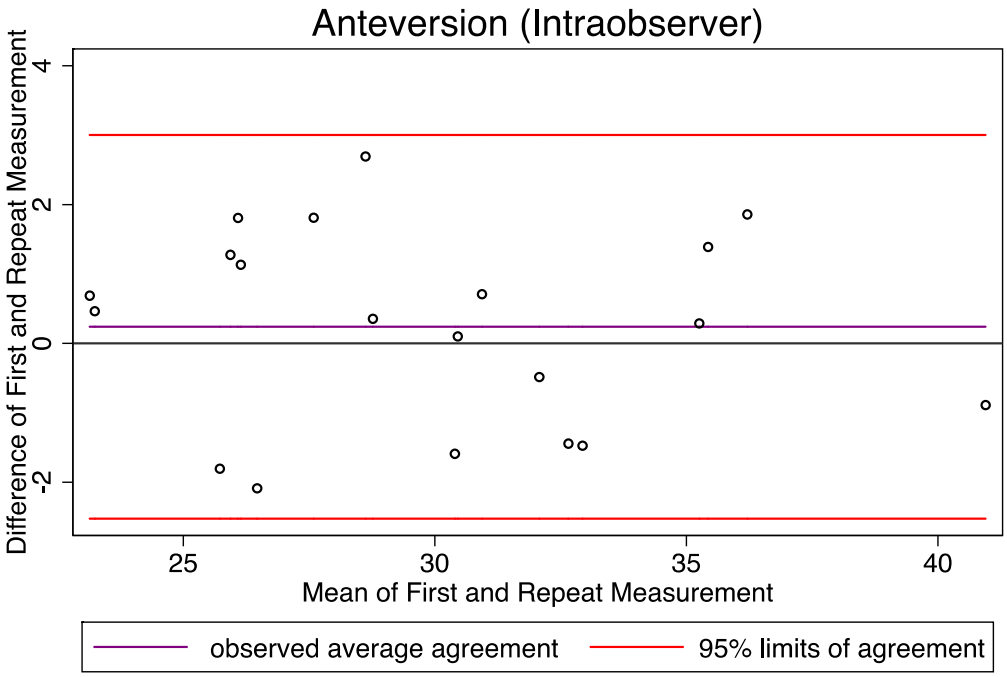
Appendix A-11 - Bland-Altman Plot for Anterior Centre Edge Angle Intra-Observer Reproducibility



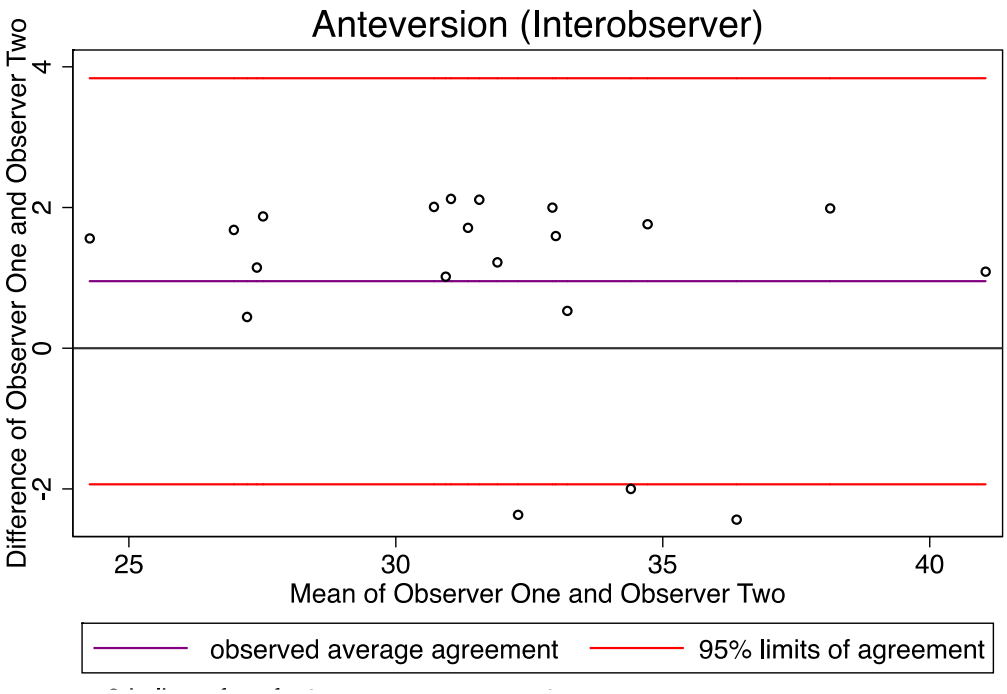
Appendix A-12 - Bland-Altman Plot for Anterior Centre Edge Angle Inter-Observer Reproducibility



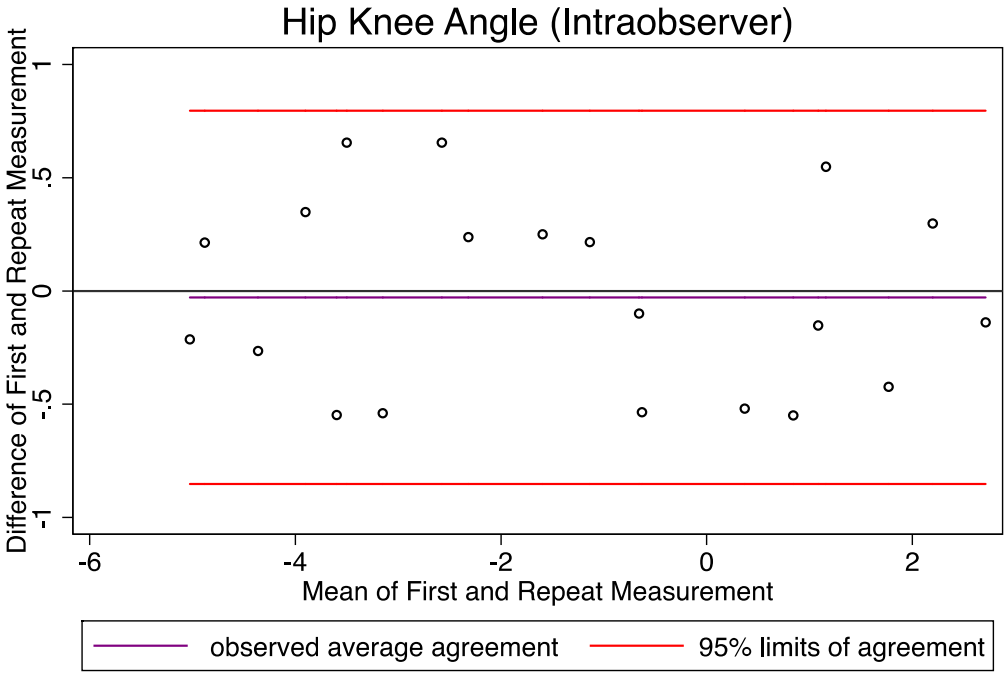
Appendix A-13 - Bland-Altman Plot for Anteversion Intra-Observer Reproducibility



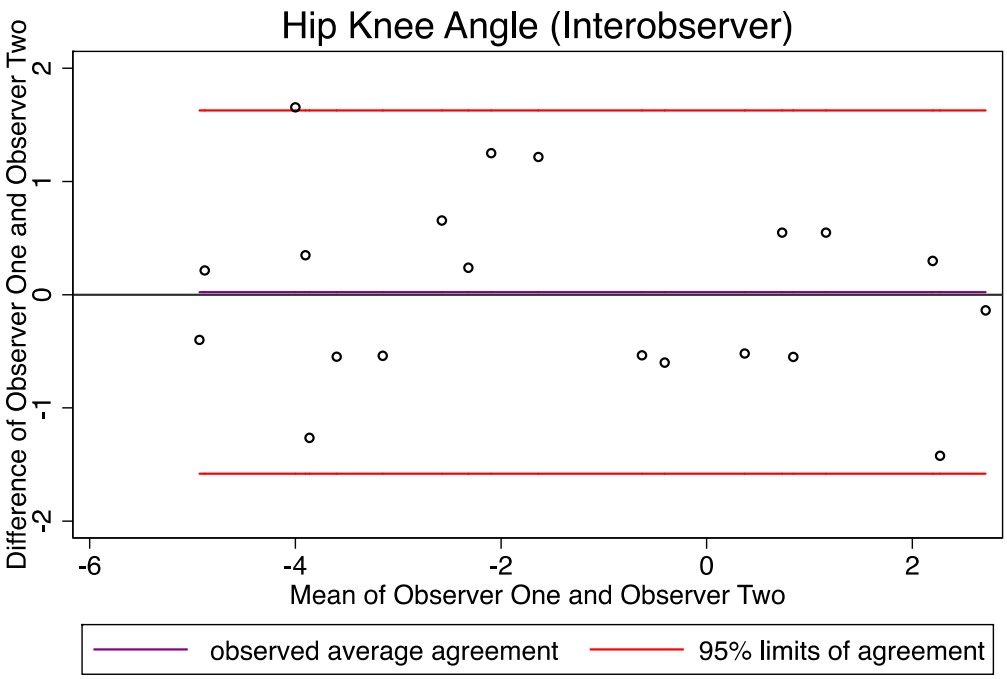
Appendix A-14 - Bland-Altman Plot for Anteversion Inter-Observer Reproducibility



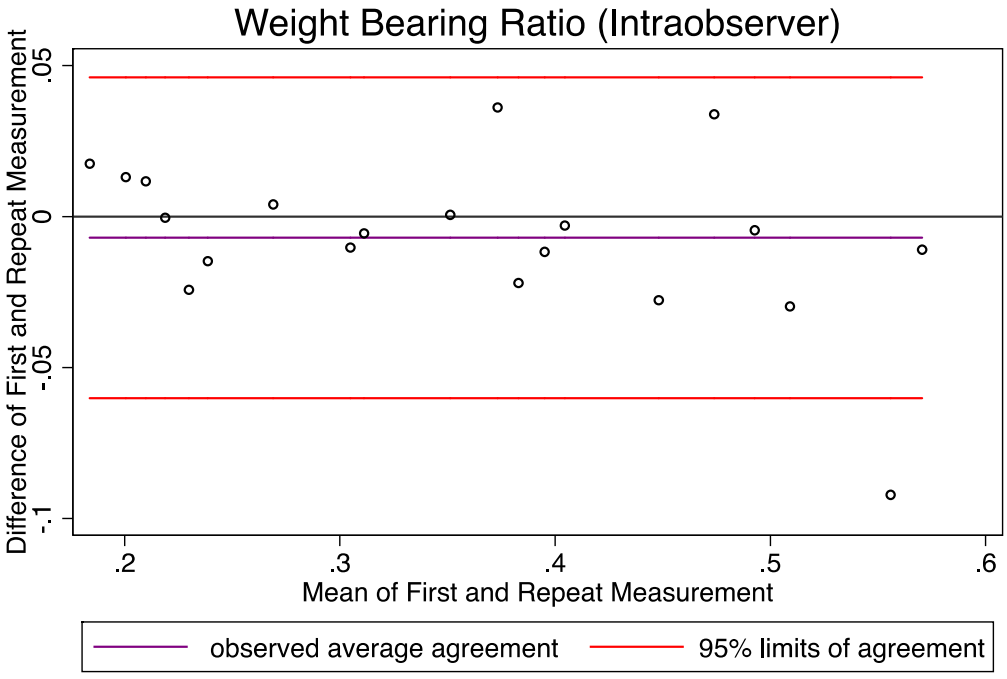
Appendix A-15 - Bland-Altman Plot for Hip Knee Angle Intra-Observer Reproducibility



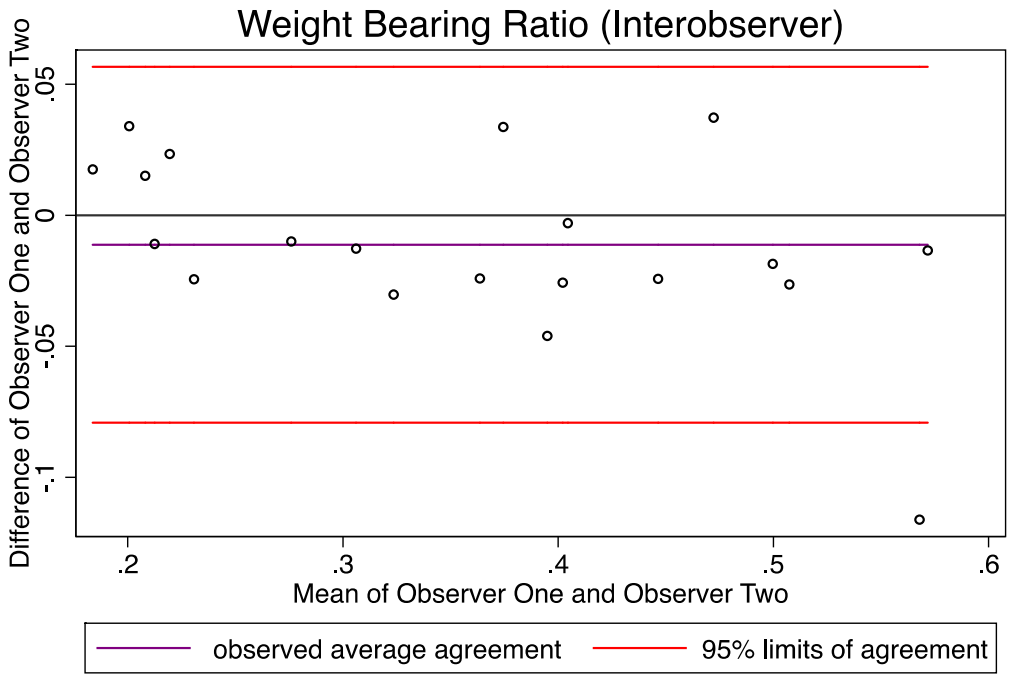
Appendix A-16 - Bland-Altman Plot for Hip Knee Angle Inter-Observer Reproducibility



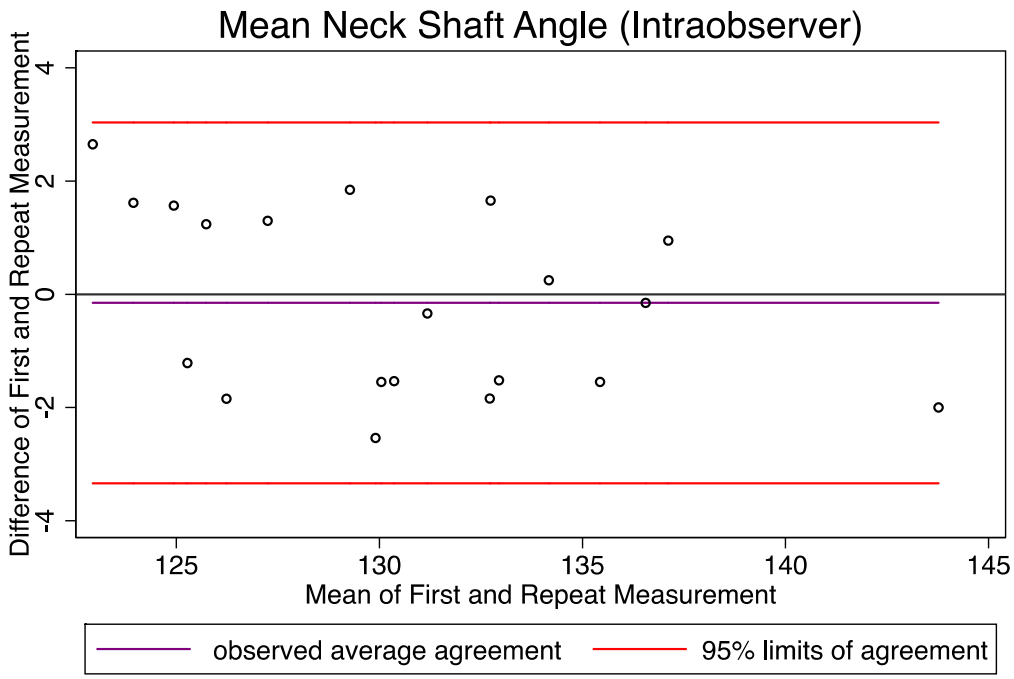
Appendix A-17 - Bland-Altman Plot for Weight Bearing Ratio Intra-Observer Reproducibility



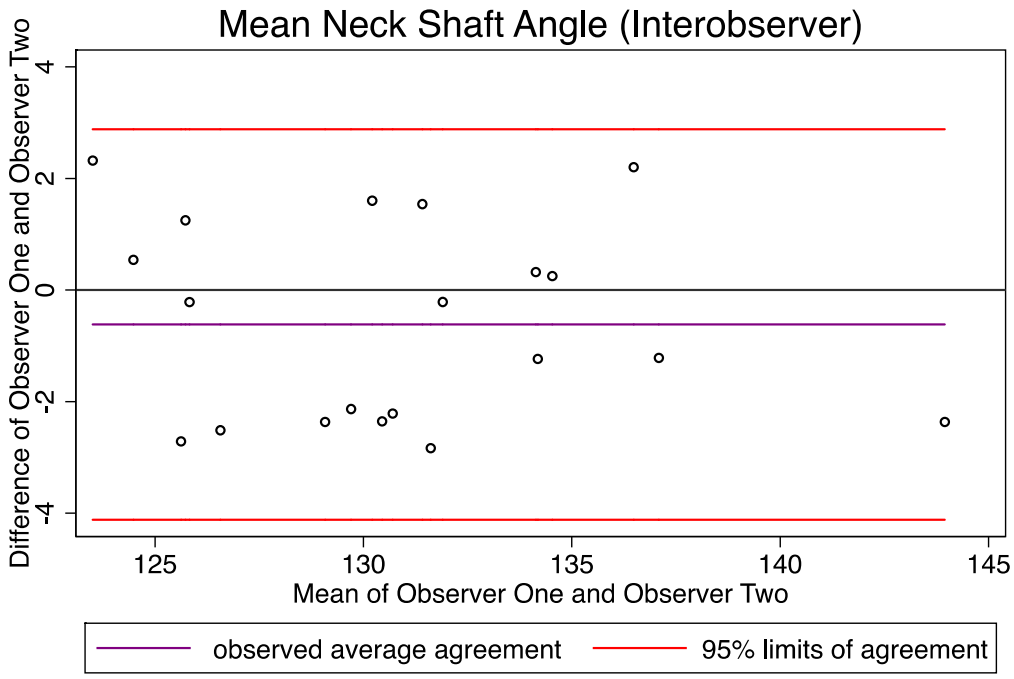
Appendix A-18 - Bland-Altman Plot for Weight Bearing Ratio Inter-Observer Reproducibility



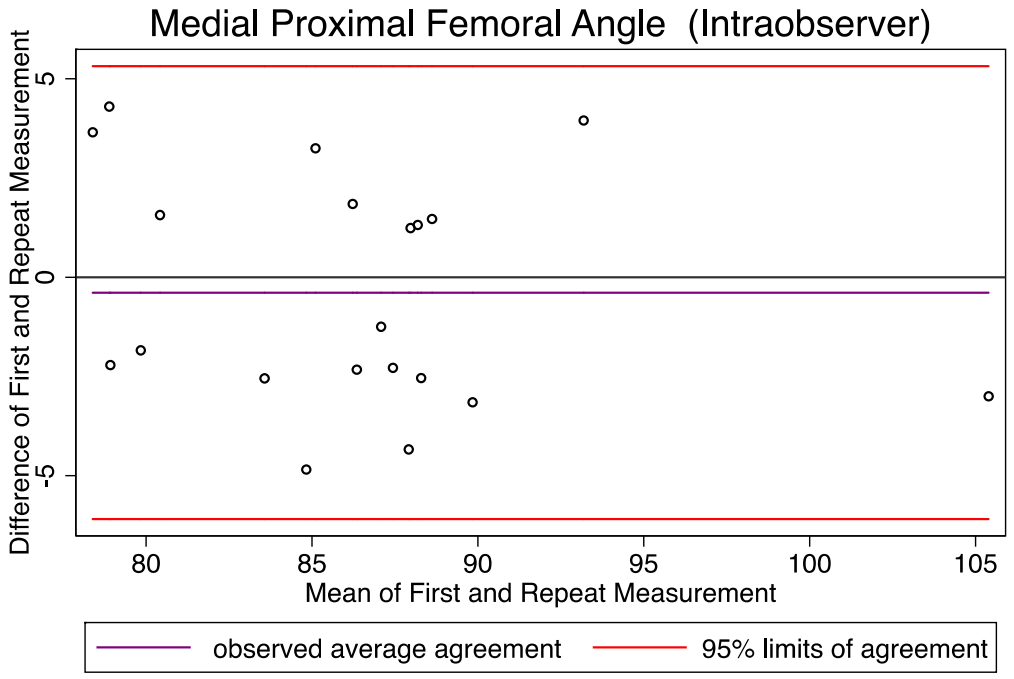
Appendix A-19 - Bland-Altman Plot for Mean Neck Shaft Angle Intra-Observer Reproducibility



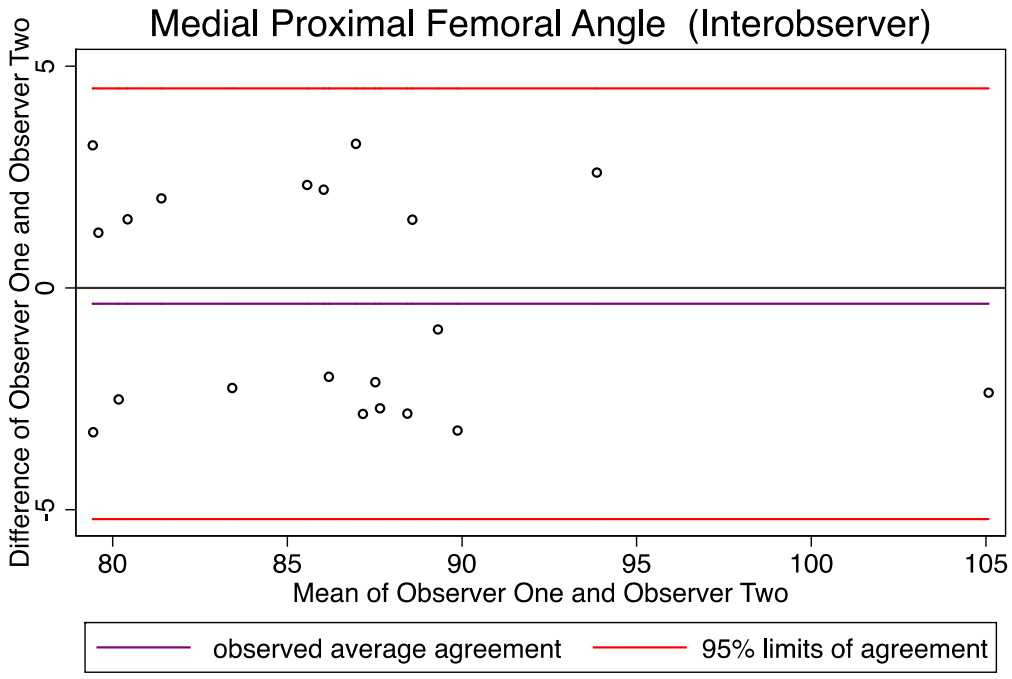
Appendix A-20 - Bland-Altman Plot for Mean Neck Shaft Angle Inter-Observer Reproducibility



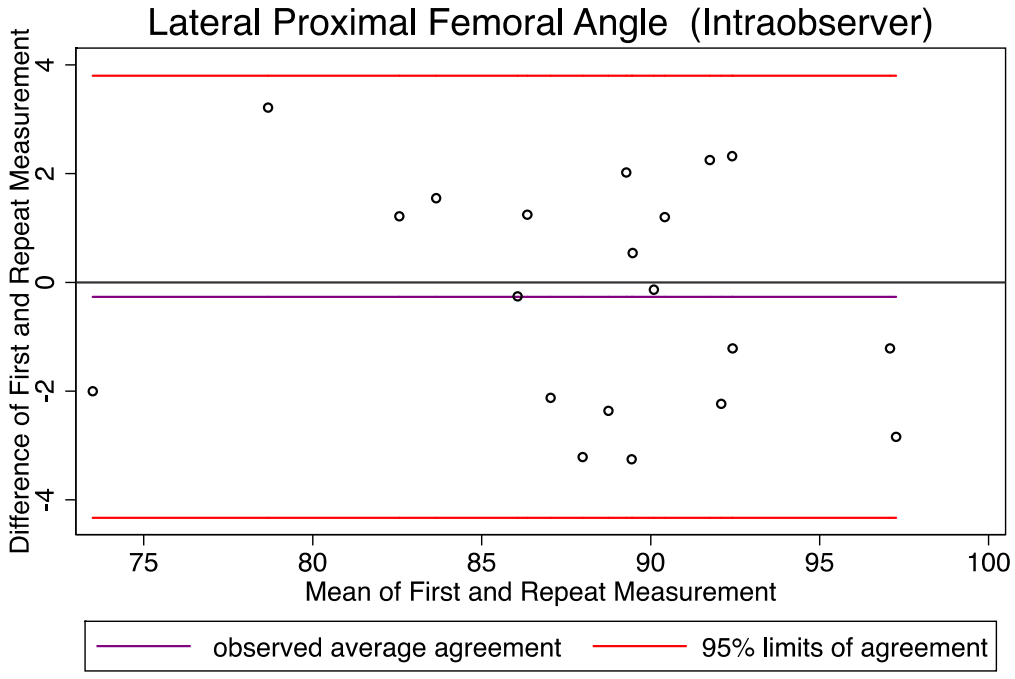
Appendix A-21 - Bland-Altman Plot for Medial Proximal Femoral Angle Intra-Observer Reproducibility



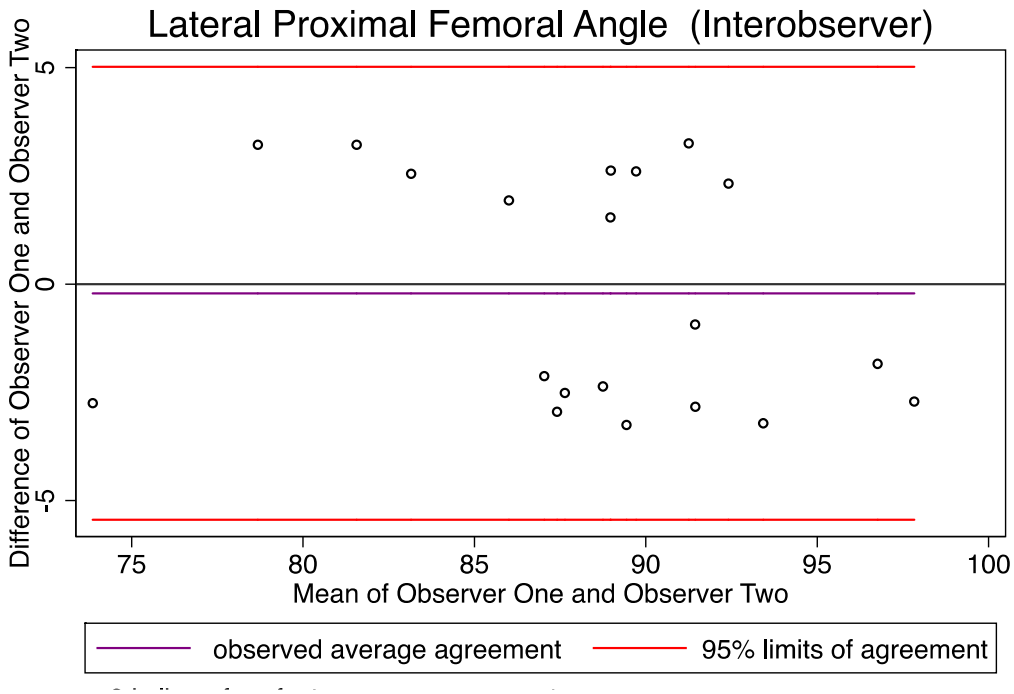
Appendix A-22 - Bland-Altman Plot for Medial Proximal Femoral Angle Inter-Observer Reproducibility



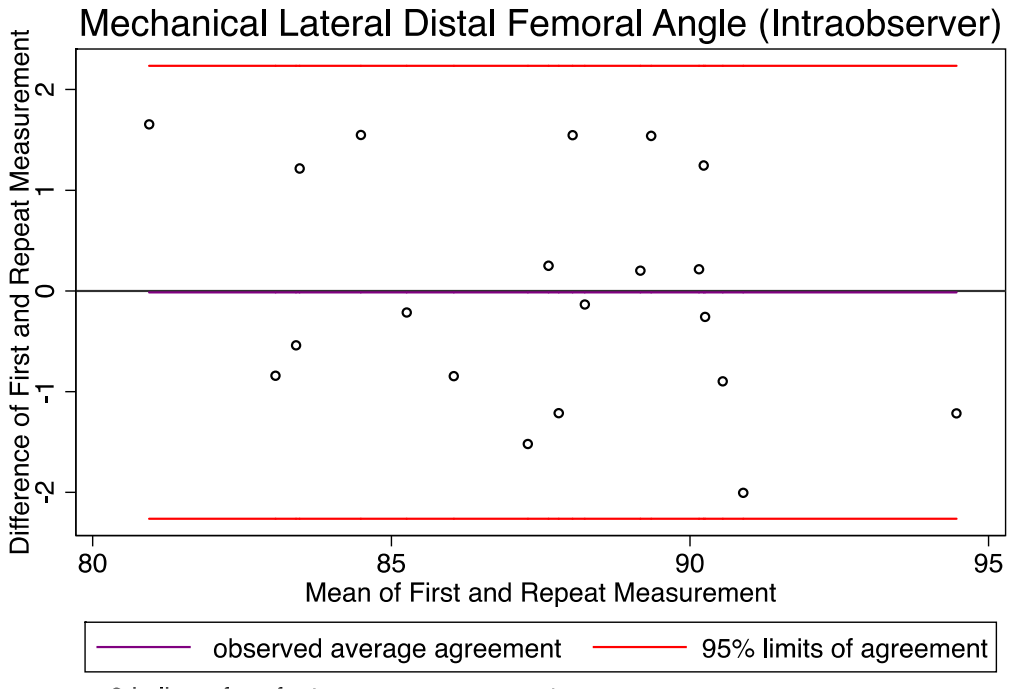
Appendix A-23 - Bland-Altman Plot for Lateral Proximal Femoral Angle Intra-Observer Reproducibility



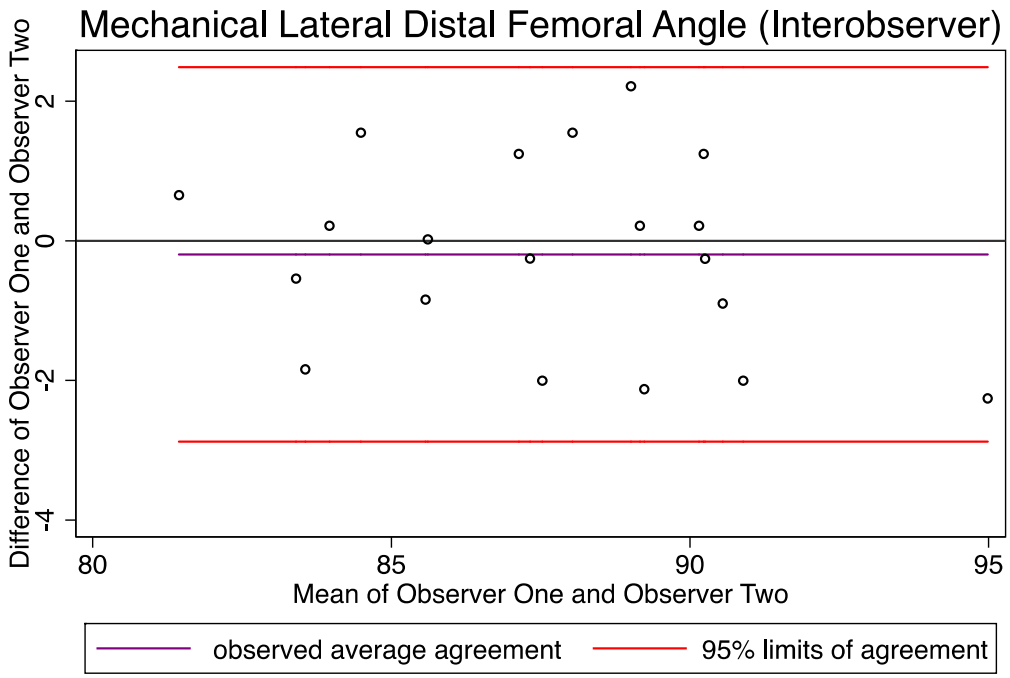
Appendix A-24 - Bland-Altman Plot for Lateral Proximal Femoral Angle Inter-Observer Reproducibility



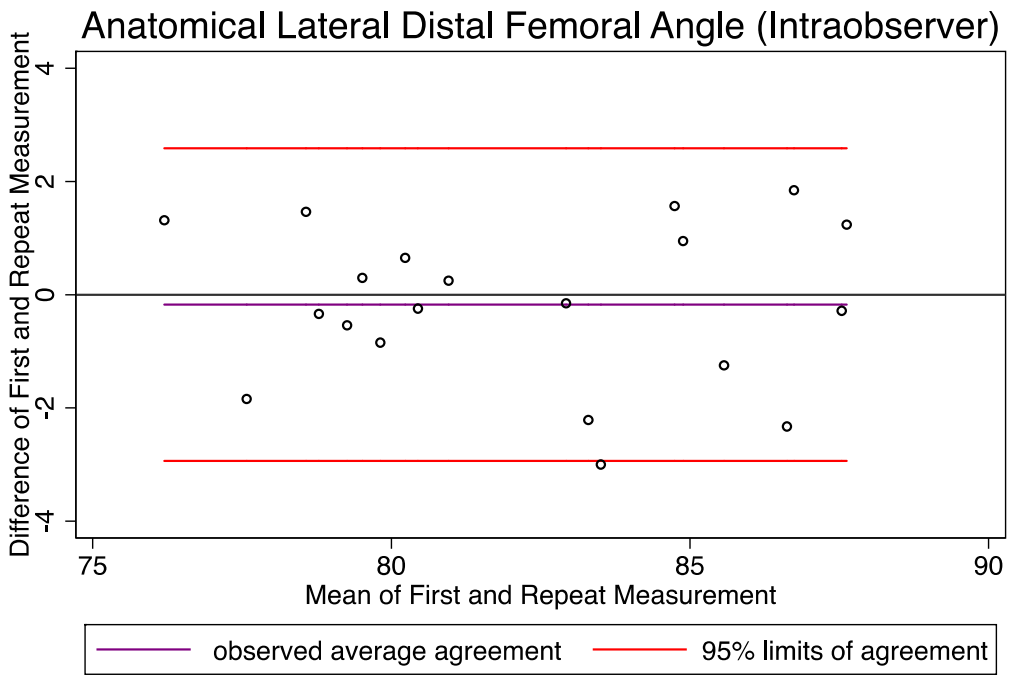
Appendix A-25 - Bland-Altman Plot for Mechanical Lateral Distal Femoral Angle Intra-Observer Reproducibility



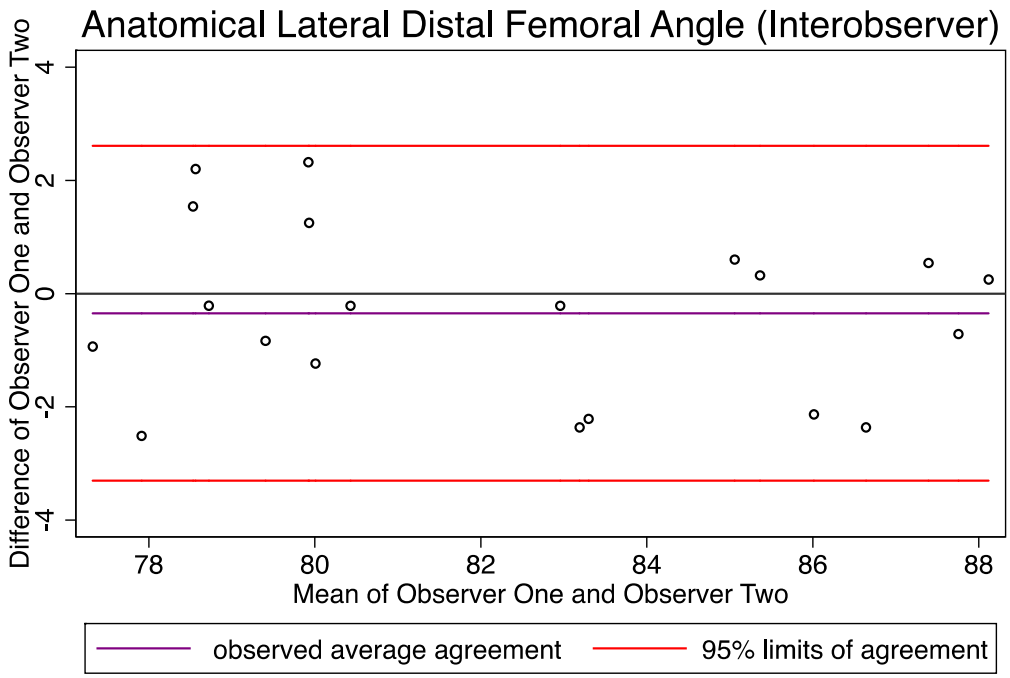
Appendix A-26 - Bland-Altman Plot for Mechanical Lateral Distal Femoral Angle Inter-Observer Reproducibility



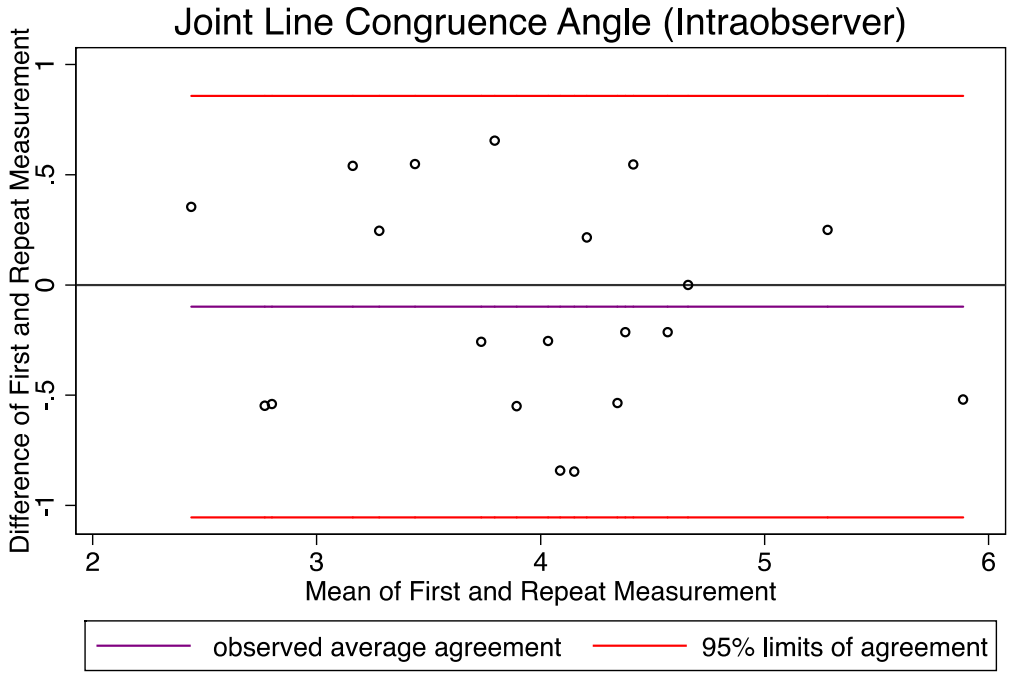
Appendix A-27 - Bland-Altman Plot for Anatomical Lateral Distal Femoral Angle Intra-Observer Reproducibility



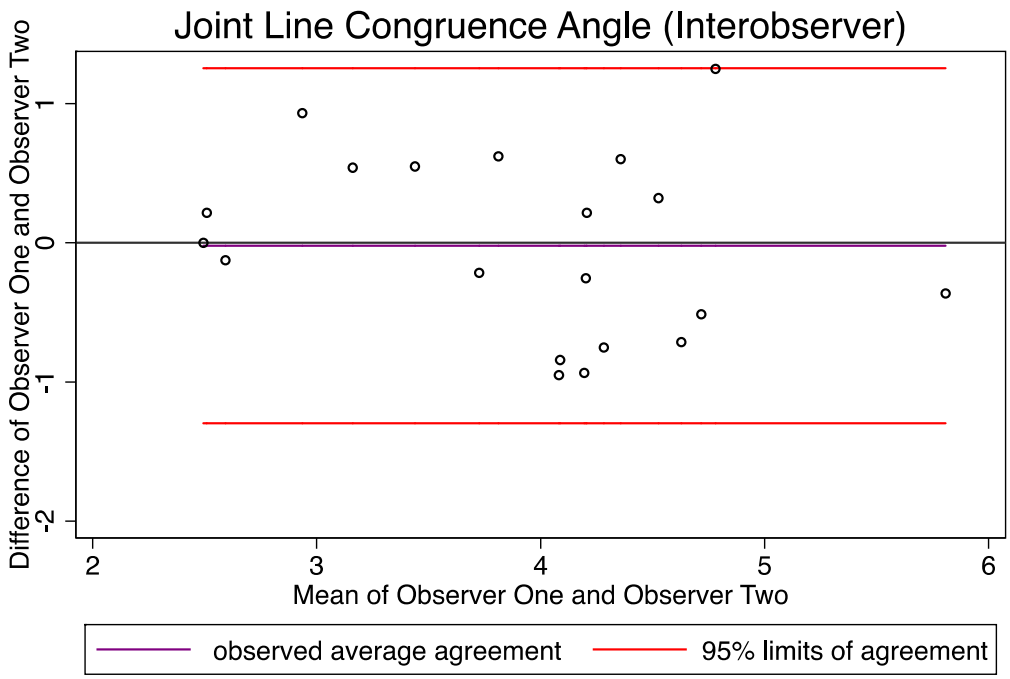
Appendix A-28 - Bland-Altman Plot for Anatomical Lateral Distal Femoral Angle Inter-Observer Reproducibility



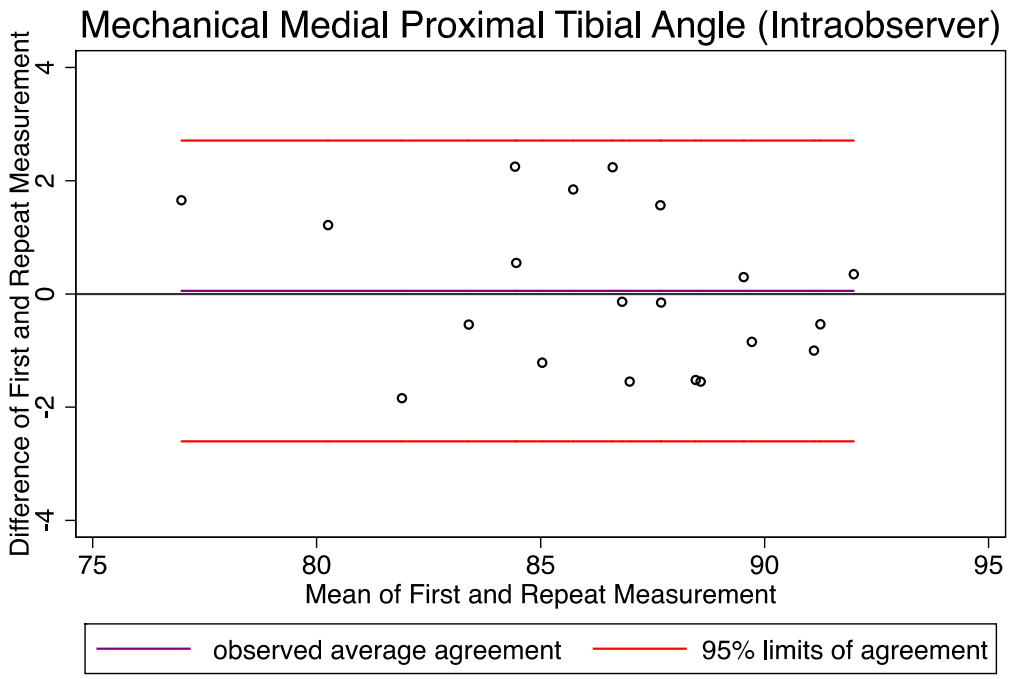
Appendix A-29 - Bland-Altman Plot for Joint Line Congruence Angle Intra-Observer Reproducibility



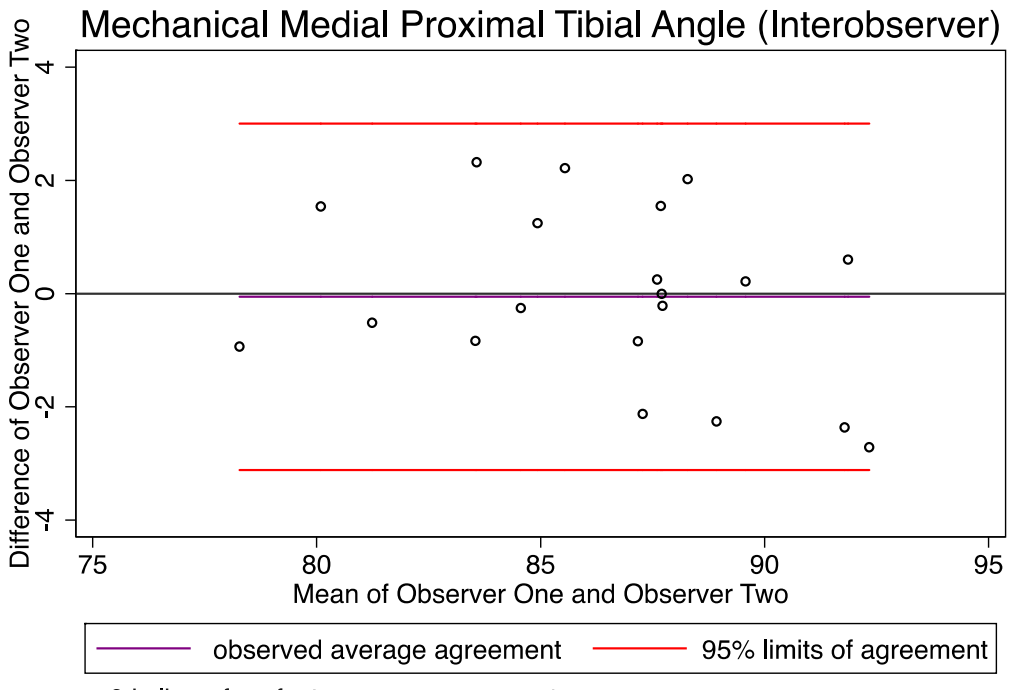
Appendix A-30 - Bland-Altman Plot for Joint Line Congruence Angle Inter-Observer Reproducibility



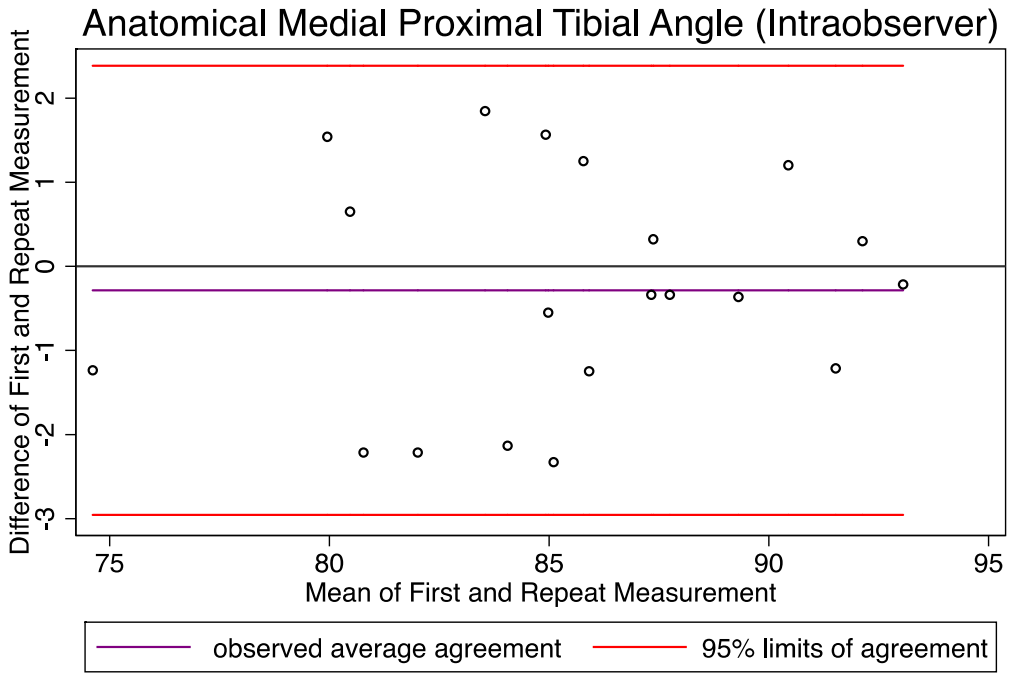
Appendix A-31 - Bland-Altman Plot for Mechanical Medial Proximal Tibial Angle Intra-Observer Reproducibility



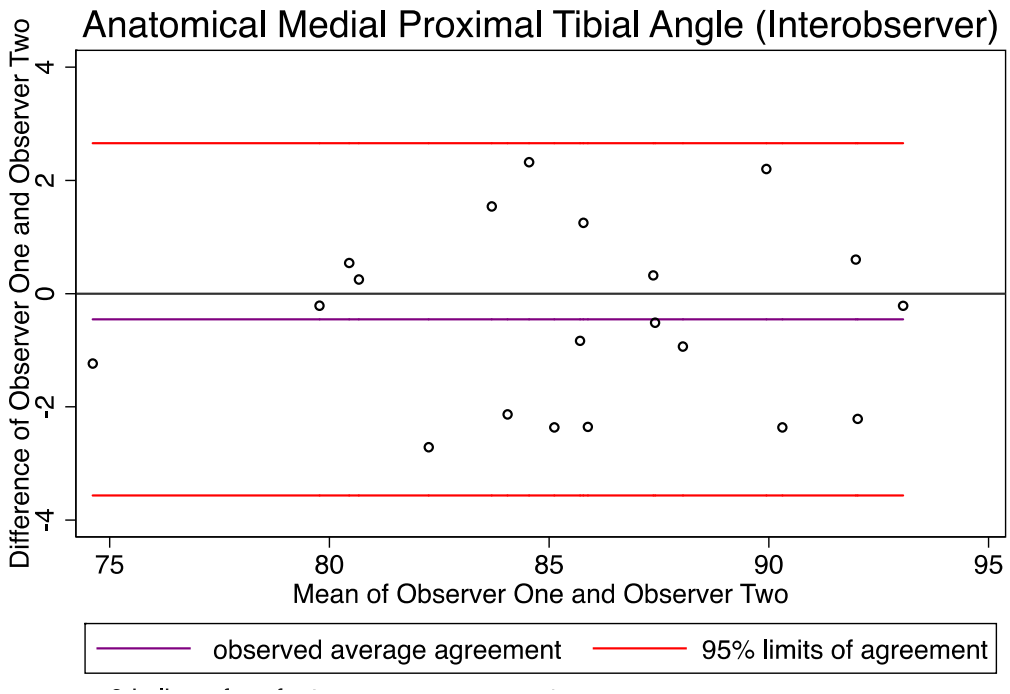
Appendix A-32 - Bland-Altman Plot for Mechanical Medial Proximal Tibial Angle Inter-Observer Reproducibility



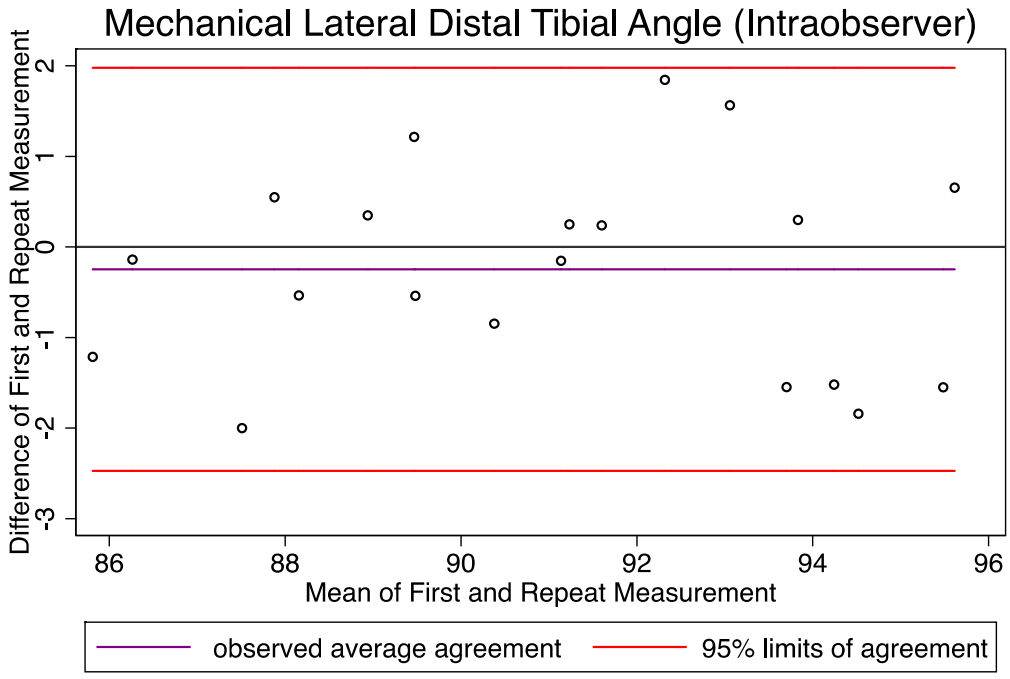
Appendix A-33 - Bland-Altman Plot for Anatomical Medial Proximal Tibial Angle Intra-Observer Reproducibility



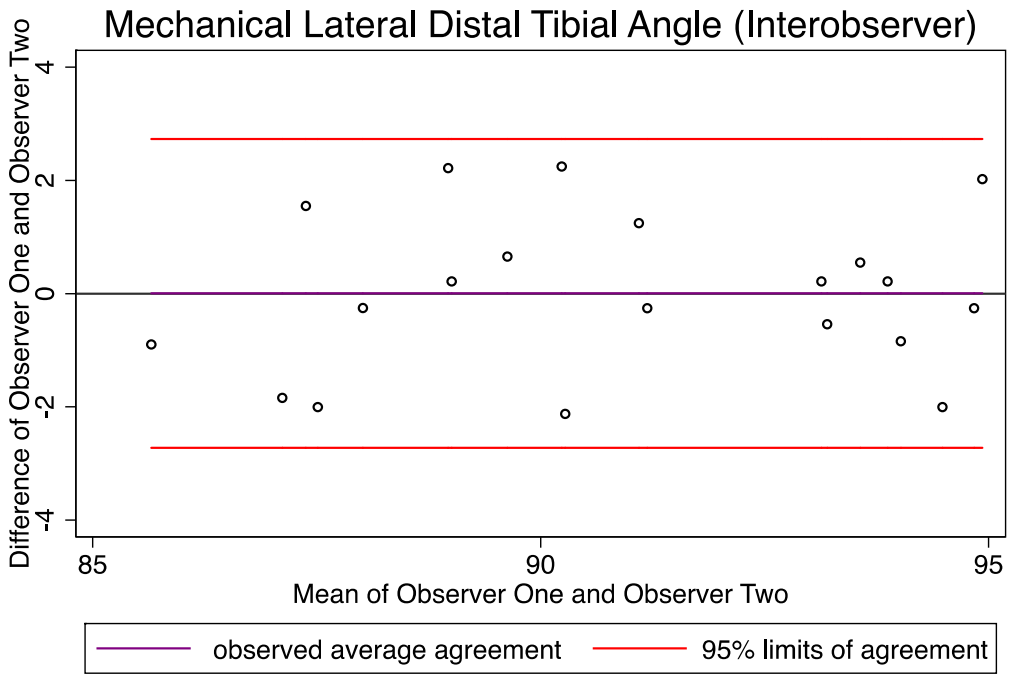
Appendix A-34 - Bland-Altman Plot for Anatomical Medial Proximal Tibial Angle Inter-Observer Reproducibility



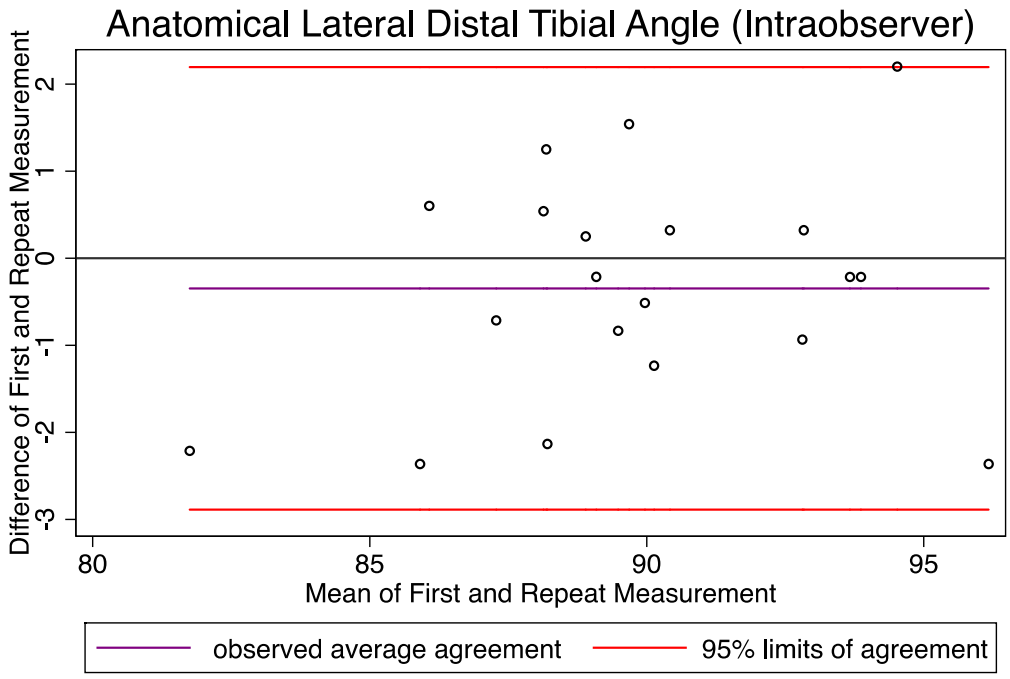
Appendix A-35 - Bland-Altman Plot for Mechanical Lateral Distal Tibial Angle Intra-Observer Reproducibility



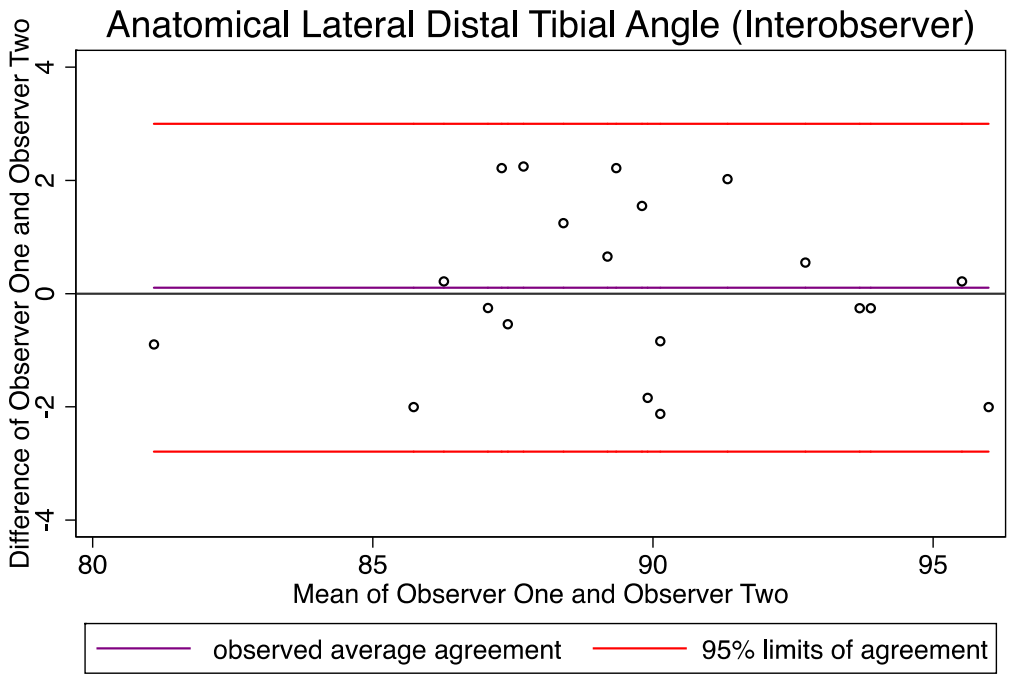
Appendix A-36 - Bland-Altman Plot for Mechanical Lateral Distal Tibial Angle Inter-Observer Reproducibility



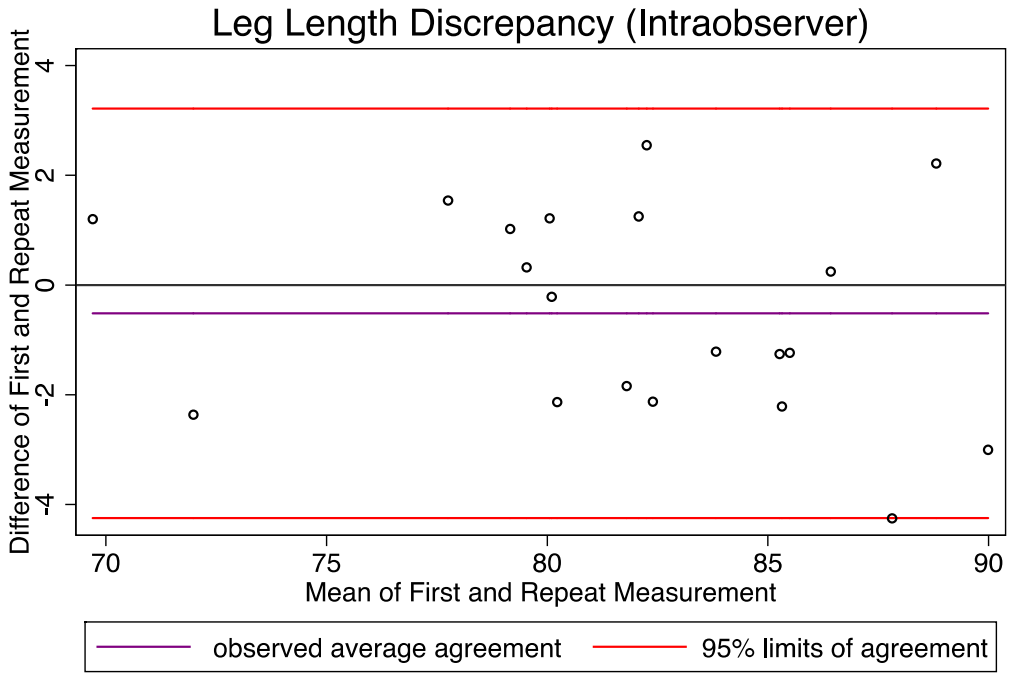
Appendix A-37 - Bland-Altman Plot for Anatomical Lateral Distal Tibial Angle Intra-Observer Reproducibility



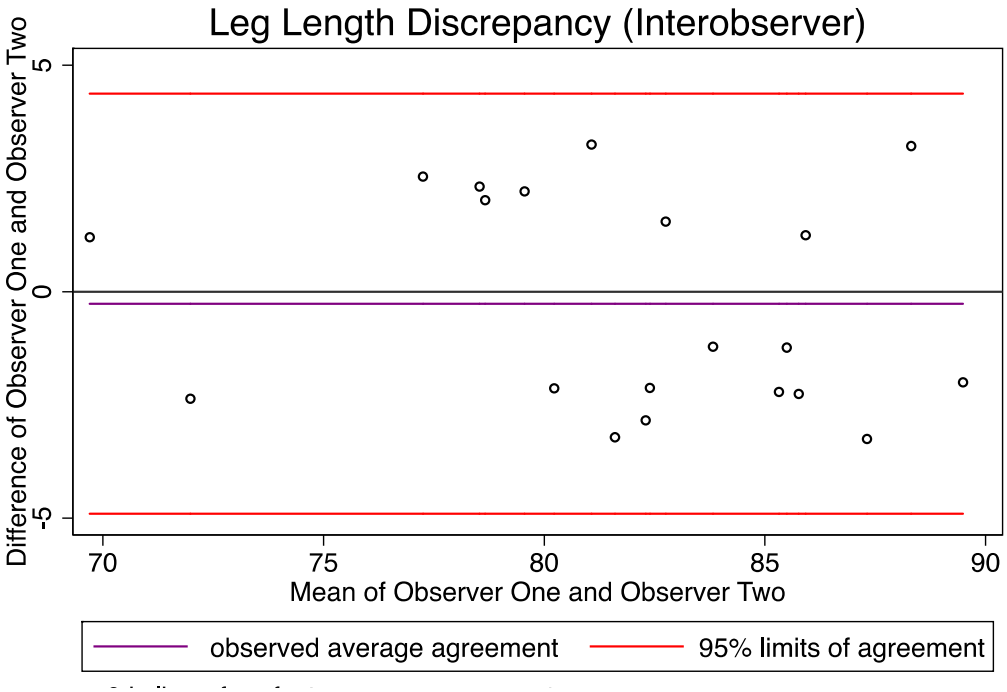
Appendix A-38 - Bland-Altman Plot for Anatomical Lateral Distal Tibial Angle Inter-Observer Reproducibility



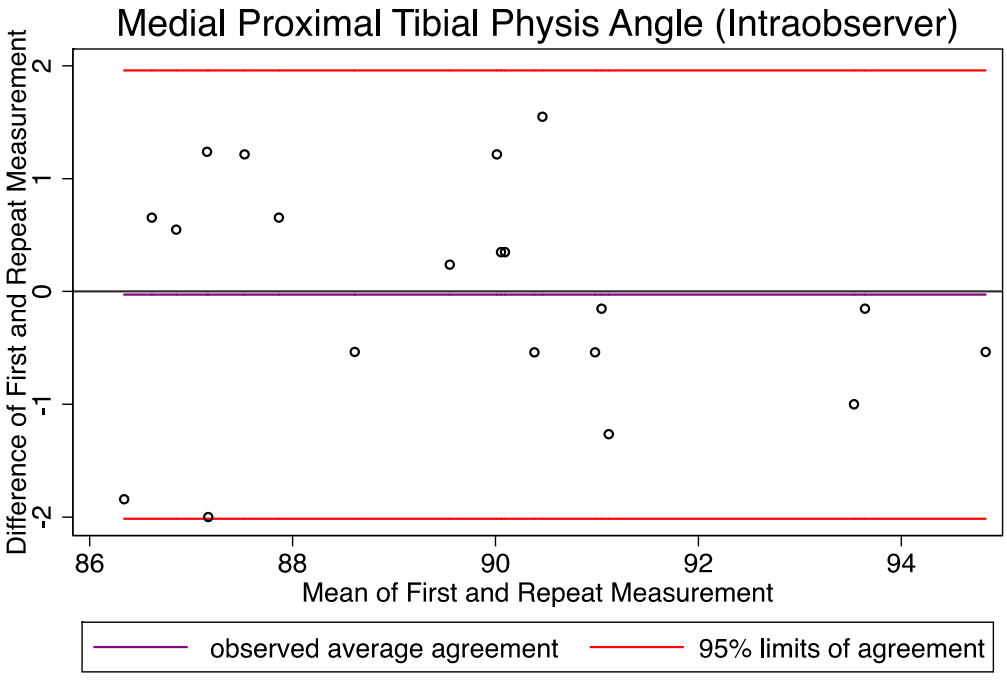
Appendix A-39 - Bland-Altman Plot for Leg Length Discrepancy Intra-Observer Reproducibility



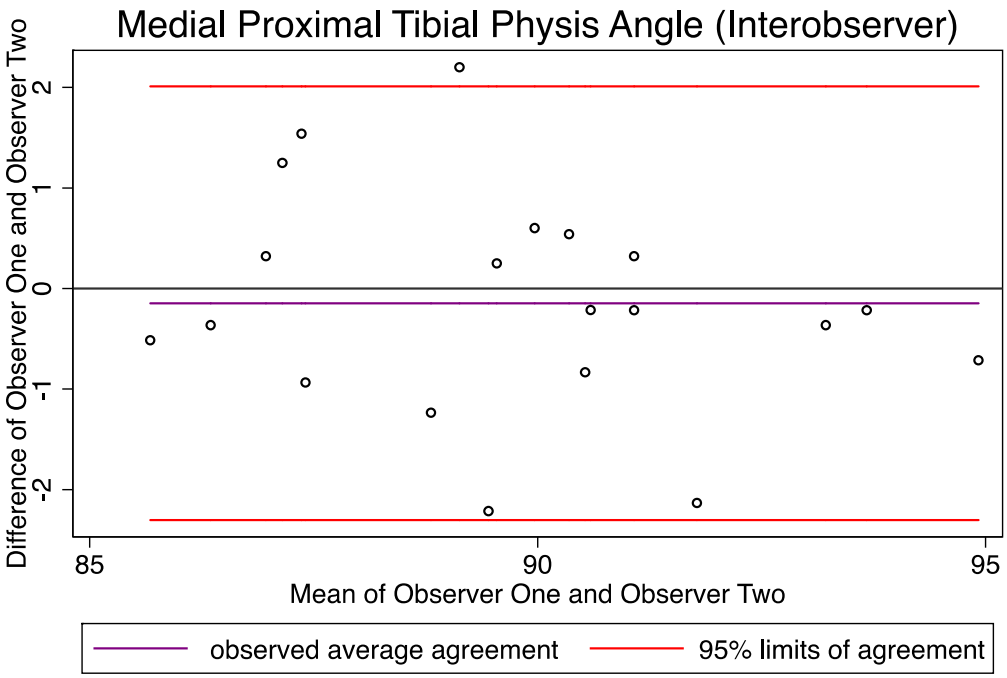
Appendix A-40 - Bland-Altman Plot for Leg Length Discrepancy Inter-Observer Reproducibility



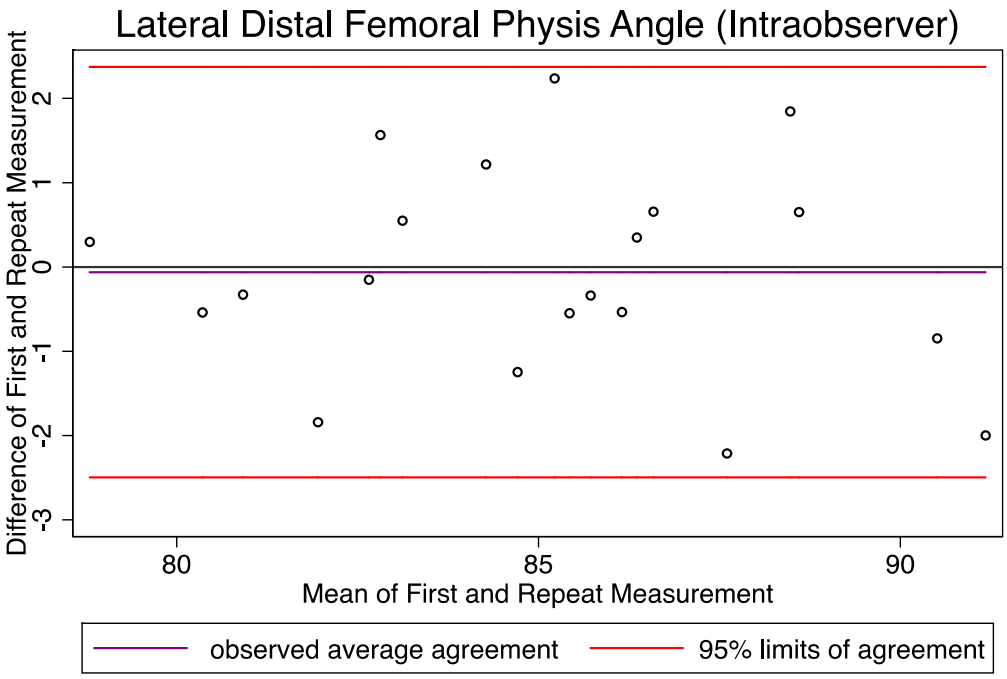
Appendix A-41 - Bland-Altman Plot for Medial Proximal Tibial Physis Angle Intra-Observer Reproducibility



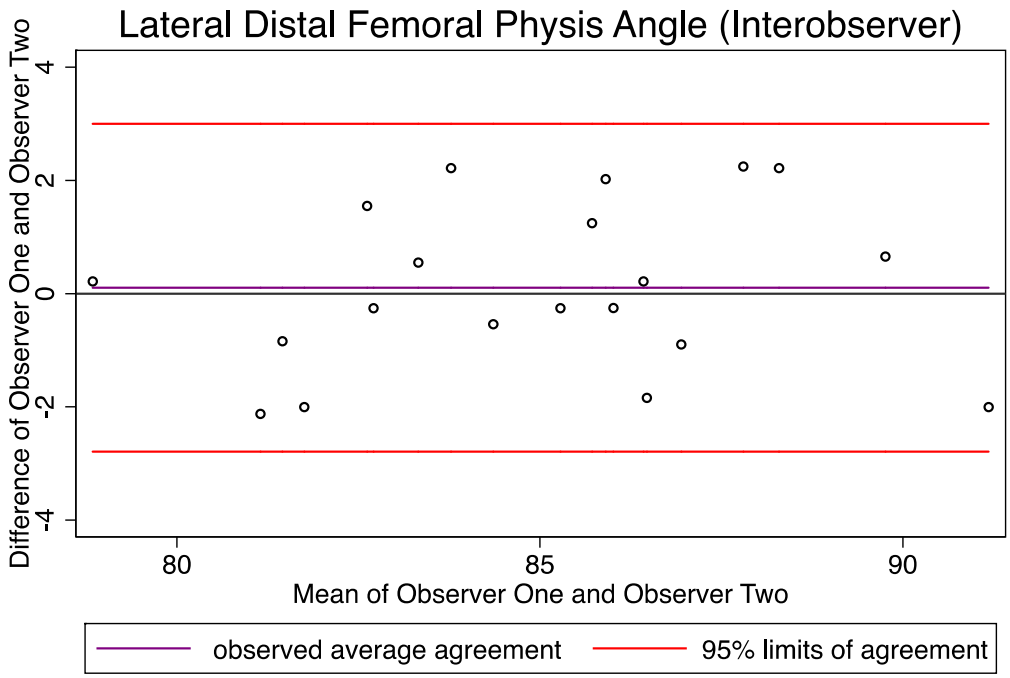
Appendix A-42 - Bland-Altman Plot for Medial Proximal Tibial Physis Angle Inter-Observer Reproducibility



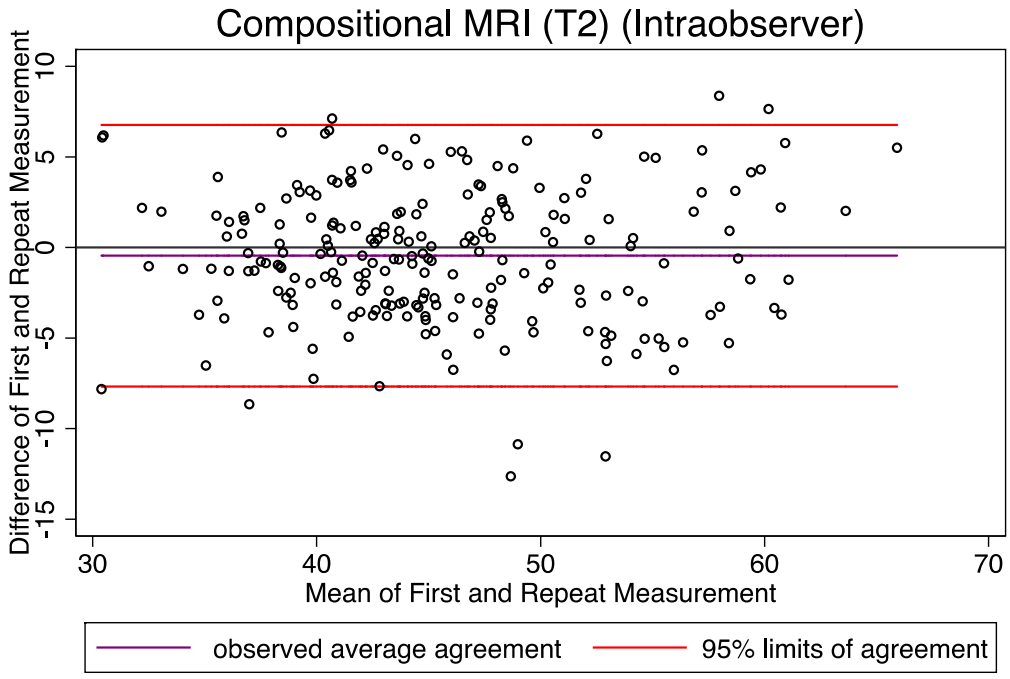
Appendix A-43 - Bland-Altman Plot for Lateral Distal Femoral Physis Angle Intra-Observer Reproducibility



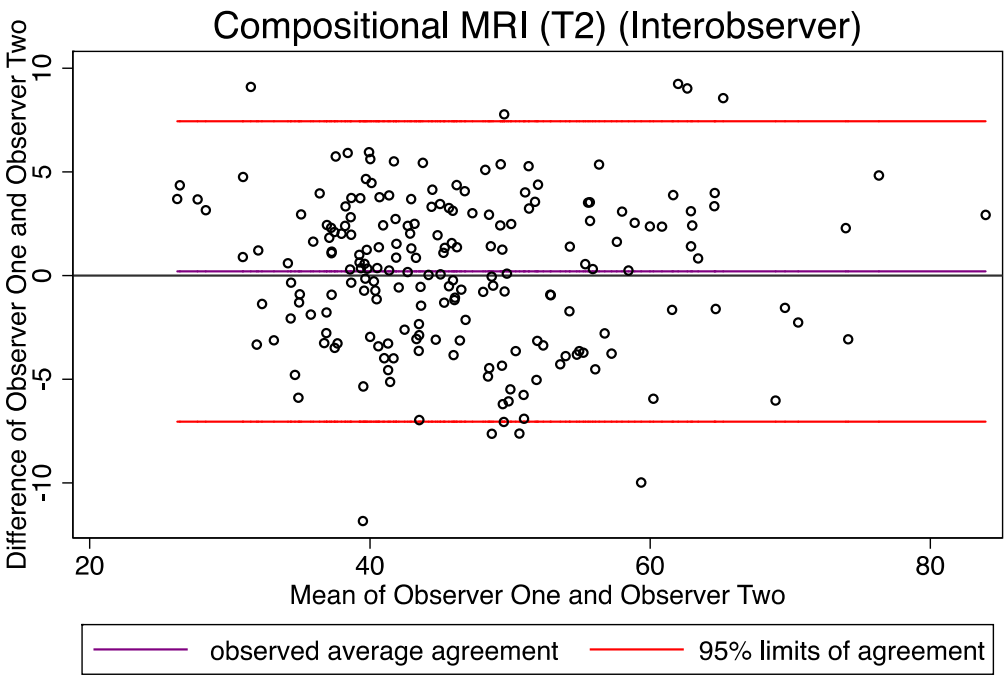
Appendix A-44 - Bland-Altman Plot for Lateral Distal Femoral Physis Angle Inter-Observer Reproducibility



Appendix A-45 - Bland-Altman Plot for Compositional MRI (T2) Intra-Observer Reproducibility



Appendix A-46 - Bland-Altman Plot for Compositional MRI (T2) Inter-Observer Reproducibility



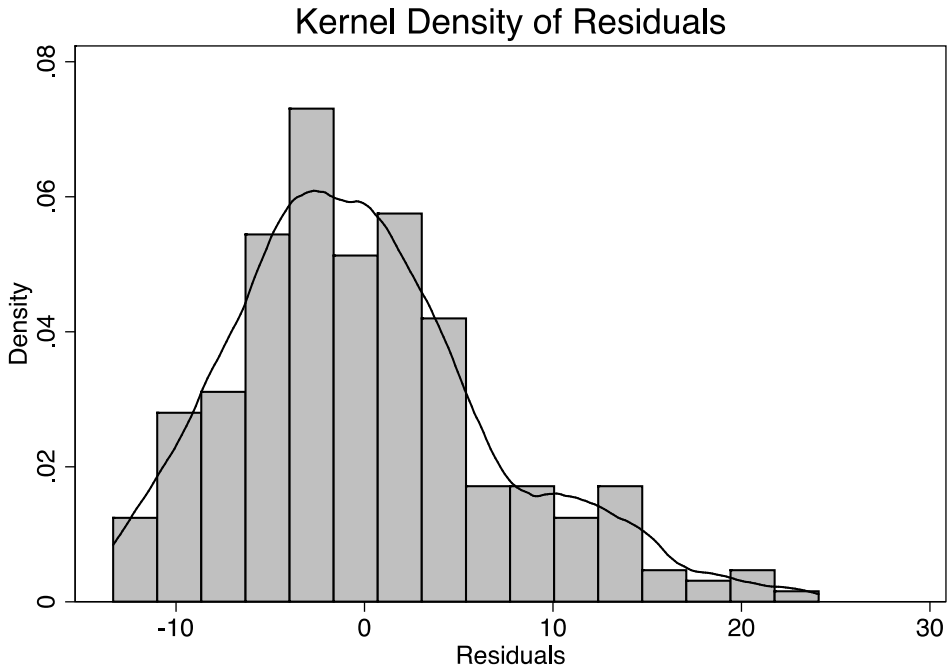
Appendix A-47 - Intra and inter observer reproducibility of T2 image analysis for each region.

	Intra Observer Reproducibility						Inter Observer Reproducibillity					
	Mean T2 Relaxation Time (ms) (±SD)						Mean T2 Relaxation Time (ms)					
	Observation 1	Observation 2	Difference	ICC	RMSCoV	SDD	Observer 1	Observer 2	Difference	ICC	RMSCoV	SDD
ASa	44.1 (±7.0)	43.0 (±7.4)	1.1 (±0.8)	0.98	3.0	1.5	43.7 (±7.5)	45.0 (±7.1)	1.3 (±1.6)	0.96	4.7	3.2
SAa	43.8 (±6.3)	42.1 (±7.1)	1.7 (±1.4)	0.95	5.2	2.7	44.2 (±7.5)	45.7 (±6.9)	1.6 (±1.4)	0.96	4.7	2.8
SPa	47.9 (±5.6)	46.6 (±6.5)	1.3 (±1.5)	0.95	4.2	2.9	48.7 (±7.4)	49.8 (±6.6)	1.1 (±1.5)	0.97	3.7	2.8
PSa	50.9 (±6.4)	50.3 (±6.9)	0.6 (±0.7)	0.99	1.9	1.5	51.3 (±7.1)	52.0 (±6.6)	0.7 (±1.3)	0.98	2.8	2.5
Pa	43.1 (±9.7)	41.8 (±11.2)	1.4 (±2.3)	0.97	6.1	4.5	44.1 (±9.4)	45.3 (±8.6)	1.2 (±2.4)	0.96	6.0	4.7
ASf	46.3 (±4.7)	45.8 (±4.7)	0.5 (±0.4)	0.99	1.4	0.7	46.2 (±4.7)	46.7 (±4.7)	0.4 (±0.4)	0.99	1.3	0.8
SAf	41.1 (±4.9)	39.5 (±5.2)	1.6 (±1.0)	0.93	4.8	2.0	39.4 (±5.4)	41.0 (±4.9)	1.6 (±1.0)	0.94	4.5	1.9
SPf	40.9 (±3.2)	39.8 (±3.6)	1.2 (±0.6)	0.93	3.3	1.3	39.8 (±4.4)	41.1 (±3.9)	1.4 (±1.1)	0.93	4.3	2.2
PSf	43.8 (±3.4)	43.1 (±3.4)	0.7 (±0.4)	0.97	1.9	0.8	42.7 (±3.9)	44.0 (±3.4)	1.3 (±1.6)	0.92	4.8	3.2
Pf	39.6 (±6.3)	38.6 (±6.8)	1.0 (±0.7)	0.98	3.1	1.3	37.9 (±6.1)	40.0 (±5.5)	2.2 (±1.5)	0.85	8.4	4.8
Global	44.365 (±6.551)	43.3 (±7.1)	1.1 (±1.1)	0.98 (0.97 - 0.98)	3.5 (2.6-6.1)	2.2 (1.5-2.9)	43.8 (±7.6)	45.1 (±7.0)	1.2 (±1.8)	0.96 (0.95-0.96)	5.2 (4.0-6.3)	3.5 (2.8-4.2)

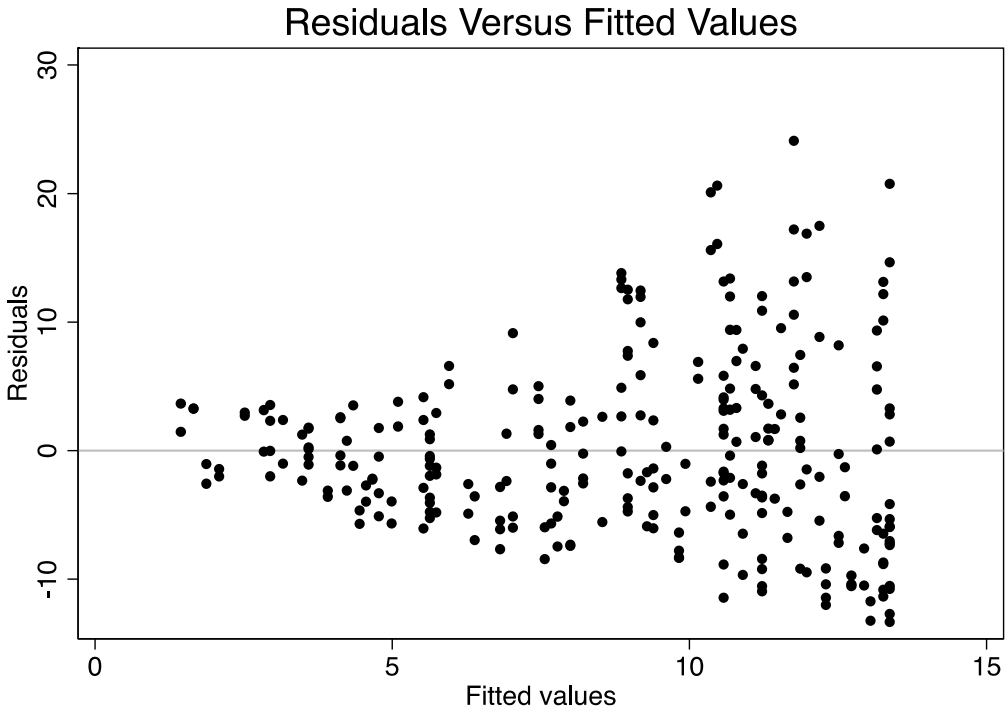
Text modified from:

- Fernquest S, Palmer A, Gammer B, et al. Compositional MRI of the Hip: Reproducibility, Effect of Joint Unloading, and Comparison of T2 Relaxometry with Delayed Gadolinium-Enhanced Magnetic Resonance Imaging of Cartilage. Cartilage. 2019:1947603519841670. PMID: 30971110

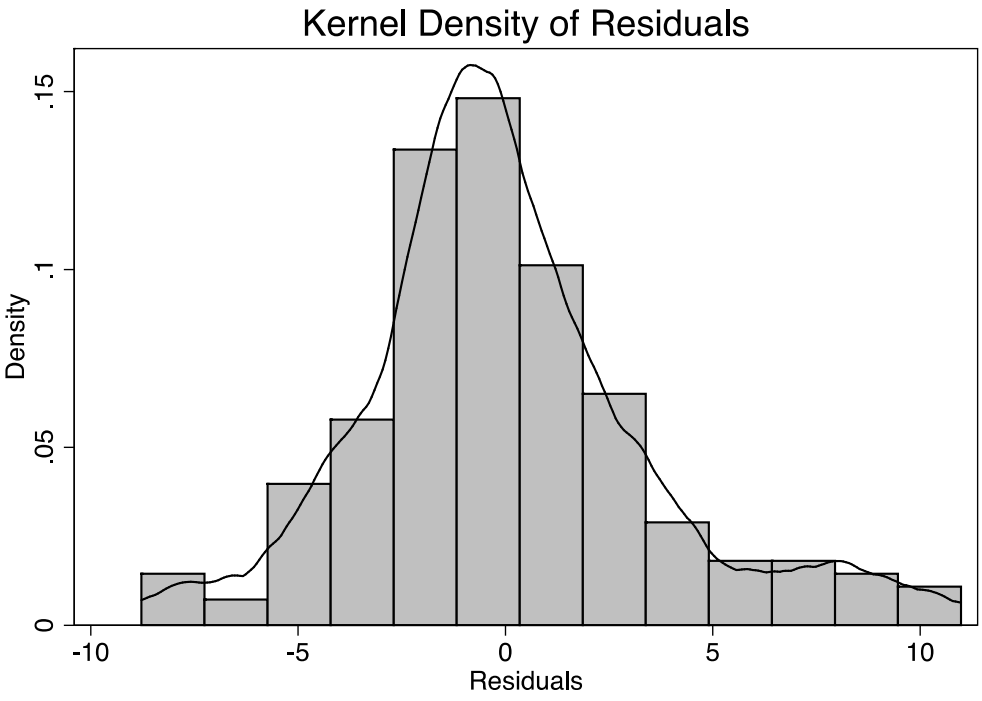
Appendix A-48 - Kernel Density Plot of Residuals for Regression of Change in Average Alpha Angle with Age



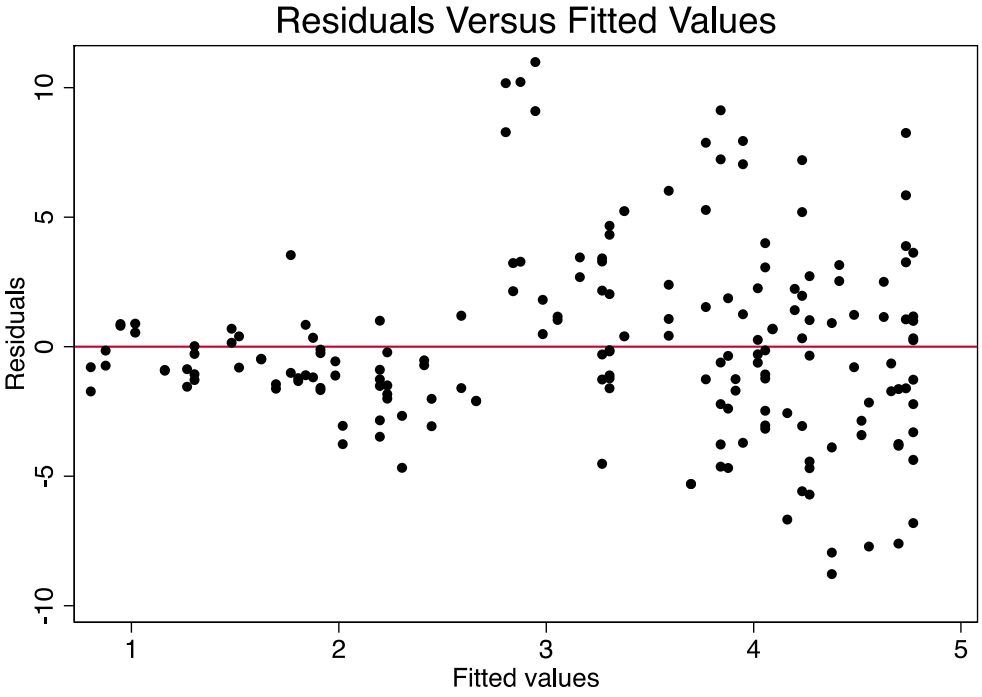
Appendix A-49 - Residuals Versus Fitted Values for Regression of Change in Average Alpha Angle with Age



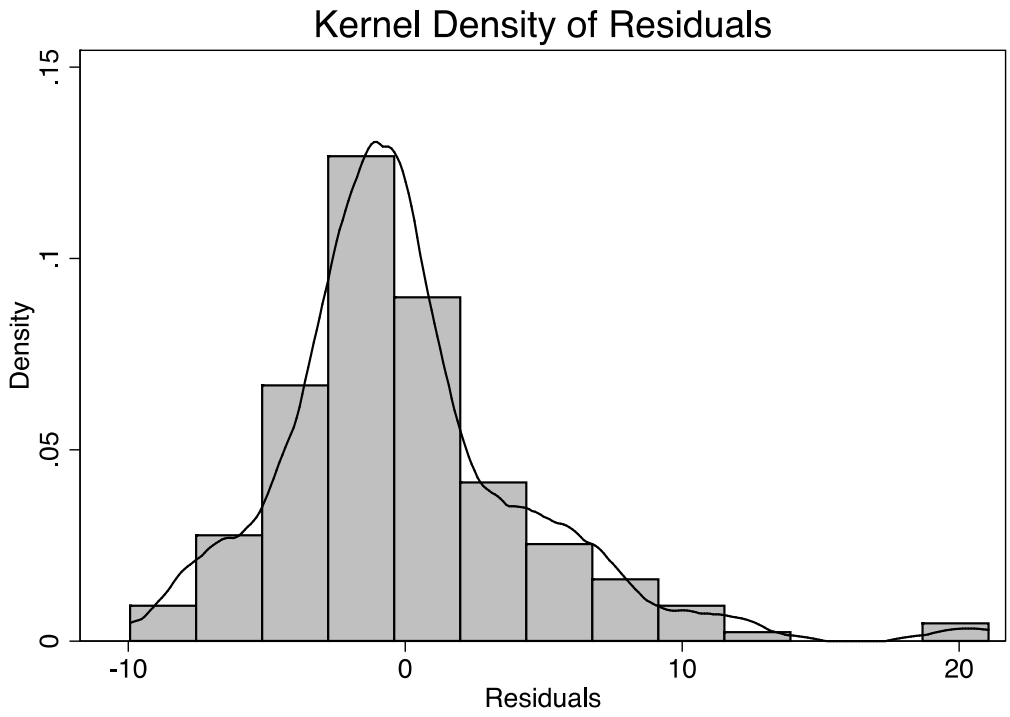
Appendix A-50 - Kernel Density Plot of Residuals for Regression of Change in Lateral Centre Edge Angle with Age



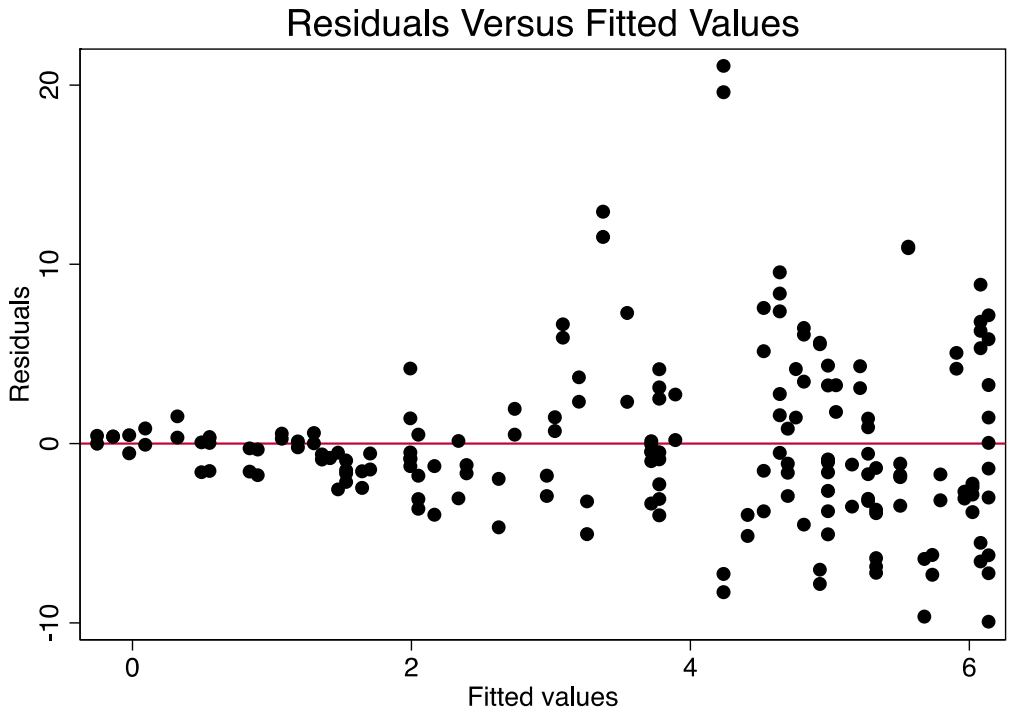
Appendix A-51 - Residuals Versus Fitted Values for Regression of Change in Lateral Centre Edge Angle with Age



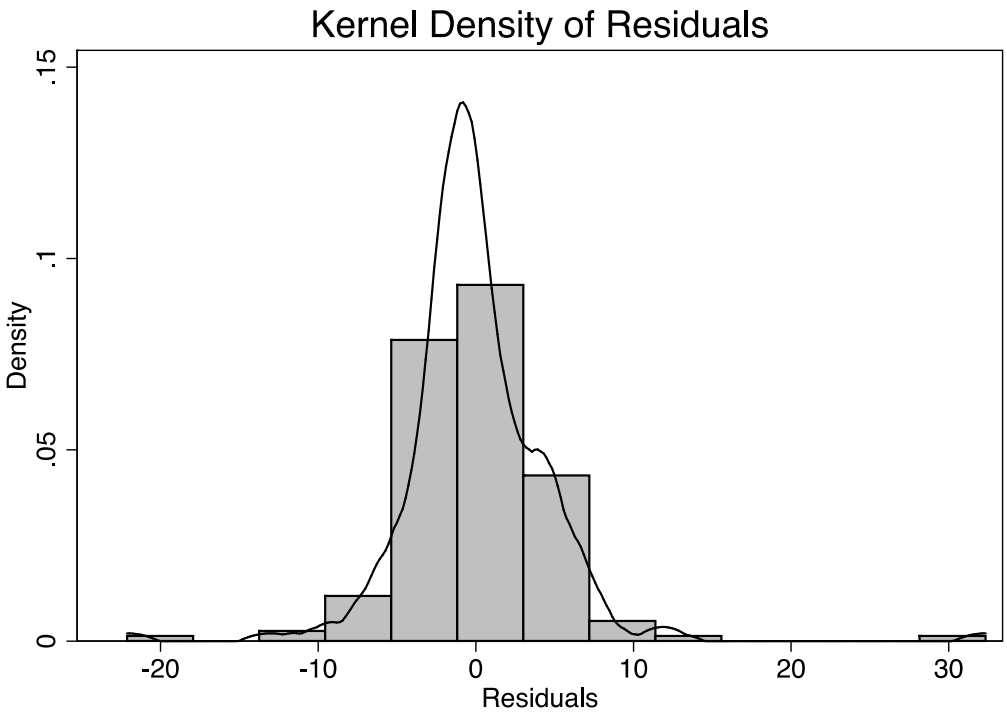
Appendix A-52 - Kernel Density Plot of Residuals for Regression of Change in Anterior Centre Edge Angle with Age



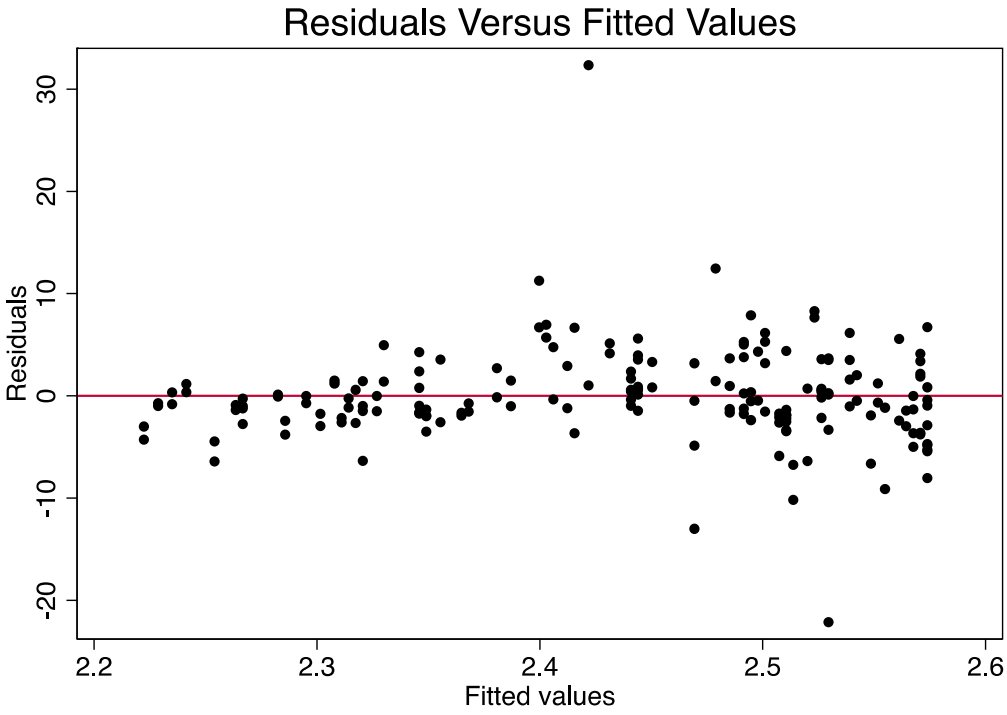
Appendix A-53 - Residuals Versus Fitted Values for Regression of Change in Anterior Centre Edge Angle with Age



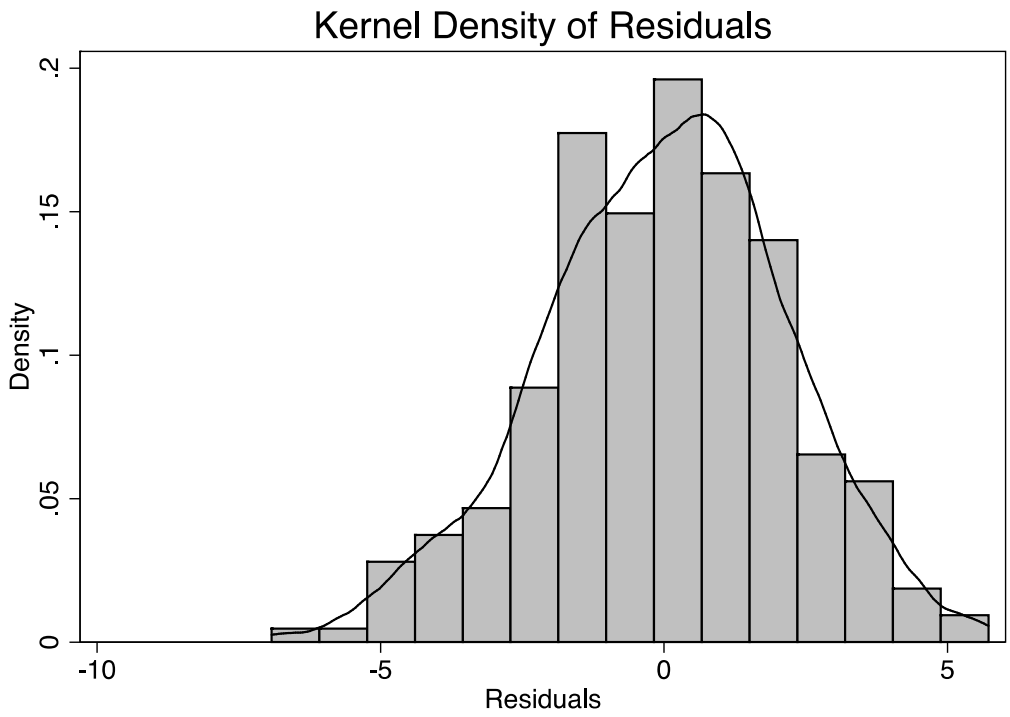
Appendix A-54 - Kernel Density Plot of Residuals for Regression of Change in Anteversion with Age



Appendix A-55 - Residuals Versus Fitted Values for Regression of Change in Anteversion with Age



Appendix A-56 - Kernel Density Plot of Residuals for Regression of Hip Knee Angle with Age



Appendix A-57 - Residuals Versus Fitted Values for Regression of Hip Knee Angle with Age

